NASA CONTRACTOR REPORT

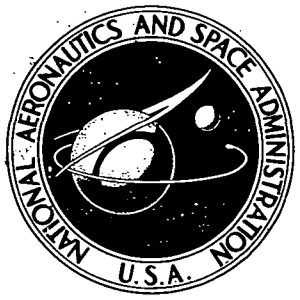

NASA CR-2358

NASA CR-2358

CALCULATION OF THE LONGITUDINAL AERODYNAMIC CHARACTERISTICS OF STOL AIRCRAFT WITH EXTERNALLY-BLOWN JET-AUGMENTED FLAPS

by Marnix F. E. Dillenius, Michael R. Mendenhall, and S. B. Spangler

Prepared by
NIELSEN ENGINEERING & RESEARCH, INC.
Mountain View, Calif. 94043
for Ames Research Center

NATIONAL AERONAUTICS AND SPACE ADMINISTRATION • WASHINGTON, D. C. • FEBRUARY 1974

1. Report No.	2. Government Accession No.	3. Recipient's Catalog No.
NASA CR-2358		

4. Title and Subtitle	5. Report Date
"Calculation of the Longitudinal Aerodynamic Characteristics of STOL Aircraft with Externally-Blown Jet-Augmented Flaps"	February 1974
	6. Performing Organization Code
7. Author(s)	8. Performing Organization Report No.
Marnix F.E. Dillenius, Michael R. Mendenhall, and S.B. Spangler	
	10. Work Unit No.
9. Performing Organization Name and Address	11. Contract or Grant No.
Nielsen Engineering and Research, Inc. 510 Clyde Avenue Mountain View, California 94043	NAS 2-5247
	13. Type of Report and Period Covered
12. Sponsoring Agency Name and Address	Contractor Report/Final Rept.
National Aeronautics & Space Administration Washington, D.C. 20546	14. Sponsoring Agency Code

15. Supplementary Notes

16. Abstract

A theoretical investigation was made to develop methods for predicting the longitudinal aerodynamic characteristics of externally-blown, jet-augmented wing-flap combinations. A potential flow analysis was used to develop two models: a wing-flap lifting surface model and a high-bypass-ratio turbofan engine wake model. The wing-flap model uses a vortex-lattice approach to represent a wing of arbitrary planform, camber, and twist, and a multiply-slotted flap which can be large and highly deflected. The engine wake model consists of a series of closely spaced vortex rings normal to a wake centerline which is permitted to have vertical and lateral curvature to accommodate the local perturbed flow under the wing. Use of these two models in sequence provides for calculation of the wing-flap load distribution including the influence of the engine wake. The method can accommodate multiple engines per wing panel and part-span flaps but is limited to the case where the flow and geometry of the configuration are symmetric about a vertical plane containing the wing root chord.

Comparisons of predicted and measured lift and pitching moment on unswept and swept wings with one and two engines per panel and with various flap deflection angles indicate satisfactory prediction of lift and moment for flap deflections up to 30 to 40 degrees. At higher flap angles with and without power, the method begins to overpredict lift, due probably to the appearance of flow separation on the flaps.

17. Key Words (Suggested by Author(s))	18. Distribution Statement
Externally Blown Flaps STOL	UNCLASSIFIED-UNLIMITED

19. Security Classif. (of this report)	20. Security Classif. (of this page)	21. No. of Pages	22. Price*
UNCLASSIFIED	UNCLASSIFIED	195	Domestic, $5.25 Foreign, $7.75

*For sale by the Clearinghouse for Federal Scientific and Technical Information
Springfield, Virginia 22151

TABLE OF CONTENTS

CALCULATION OF THE LONGITUDINAL AERODYNAMIC CHARACTERISTICS OF STOL AIRCRAFT WITH EXTERNALLY-BLOWN JET-AUGMENTED FLAPS

By Marnix F. E. Dillenius, Michael R. Mendenhall, and S. B. Spangler
Nielsen Engineering & Research, Inc.

SUMMARY

A theoretical investigation was made to develop methods for predicting the lift and pitching moment characteristics of externally-blown, jet-augmented wing-flap combinations. A potential flow analysis was used to develop two models: a wing-flap lifting surface model and a high-bypass-ratio turbofan engine wake model. The wing-flap model uses a vortex-lattice approach to represent a wing of arbitrary planform, camber, and twist, and a multiply-slotted flap which can be large and highly deflected. In order to handle the large angles that appear in the flow-tangency condition applied to the surfaces, trigonometric functions are used instead of the usual linearizations. The horseshoe vortices on the flap are laid out on a surface inclined to the wing at the average flap angle, with the trailing vortex legs lying on an extension of this flap surface. The engine wake model consists of a series of closely spaced vortex rings normal to a wake centerline which is permitted to have vertical and lateral curvature to accommodate the local perturbed flow under the wing. The ring diameters and strengths are determined from the engine thrust such that the resulting potential flow "wake" has essentially the same mass, momentum and spreading rate as the appropriate turbulent, coflowing wake. Use of these two models in sequence provides for calculation of the wing-flap load distribution including the influence of the engine wake. The method can accommodate multiple engines per wing panel and part-span flaps but is limited to the case where the flow and geometry of the configuration are symmetric about a vertical plane containing the wing root chord.

Comparisons of predicted and measured lift and pitching moment on unswept and swept wings with one and two engines per panel and with flaps having a combined chord as large as the basic wing chord indicate

satisfactory prediction of lift and moment for flap deflections up to 30 to 40 degrees. At higher flap angles with and without power, the method begins to overpredict lift, due probably to the appearance of flow separation on the flaps. The agreement on moments is least satisfactory for swept wings, probably as a result of the particular vortex-lattice layout used in the calculations.

INTRODUCTION

The development of high-bypass-ratio turbofan engines with their relatively cool exhaust has generated great interest in the use of external-flow jet-augmented flaps as a means of achieving high lift coefficients for STOL operation. In this concept, the jet efflux from pod-mounted engines is made to impinge on a large, highly deflected, multiply slotted flap system which induces a large amount of additional lift through engine wake deflection. A number of experimental investigations have confirmed the capability of the externally-blown jet-augmented flap to produce high lift coefficients (refs. 1-4).

Most of the work that has been published on externally-blown jet-augmented flaps has been experimental in nature. In addition to the work on complete configurations such as that of references 1-4, experimental work has also been done on a semispan wing-flap-engine model (ref. 5). A wide range of configuration variables have been tested, including swept and unswept wings, partial and full span flaps, various numbers of flap segments, and variations in engine position and incidence relative to the wing. The results of this work are available in the form of overall lift and pitching moment over a range of flap angles and thrust coefficients.

Early analysis of the behavior of a wing with externally-blown jet-augmented flaps considered the lift to be made up of the lift of the wing-flap alone, the lift due to the vertical component of jet momentum, and a circulation lift induced by the jet-flap interaction (ref. 1). While theoretical values of the first two could be obtained, no method was developed to estimate the last. Recently, jet flap theory developed for the jet flap and augmentor wings was applied to a jet-augmented flap (ref. 6). Although good agreement was indicated, empirically determined momentum coefficients, jet turning angles, and jet spreading factors were

used. Thus, no rational, analytical method existed for predicting the performance of an arbitrary jet-augmented flap and wing combination.

The objective of the present work is to develop an engineering method for predicting the characteristics of such a configuration. A potential flow approach was adopted involving the combination of two flow models: a wing-flap lifting surface model and a jet wake model. Because of the size and large deflection angles of flaps required for STOL performance, a nonplanar, nonlinear lifting surface method is required for the wing-flap model. A vortex-lattice approach was selected. The jet wake model required a potential flow approximation to a turbulent, coflowing jet. The jet characteristics used were those of Abramovich (ref. 7). The potential flow approximation was derived from the basic ring vortex model of reference 8. These models must be combined in such a fashion that all the boundary conditions are satisfied. An iterative approach was selected. The development of the models, comparisons of predicted results with data, and a user's description of the resulting computer programs are presented in this report. The computer source programs are available from COSMIC.

SYMBOLS

A_f	fan exit flow area
A_j	jet-wake cross sectional area at beginning of the wake
b	wing span
c	chord of area element on the wing; or basic wing root chord
c_{ave}	average wing chord, S_{REF}/b, used as reference length by wing-flap program
c_ℓ	section lift coefficient, based on local chord
c_{ℓ_i}	design section lift coefficient
C_D	induced drag coefficient, $-F_s/qS_{REF}$
C_L	lift coefficient, L/qS_{REF}
C_μ	thrust coefficient, T/qS_{REF}
C_m	pitching moment coefficient, $M/qS_{REF}C_{ave}$

E	complete elliptic integral of second kind
F_u, F_v, F_w	backwash, sidewash, and downwash influence coefficient for a horseshoe vortex on the wing
$F_{f,u}, F_{f,v}, F_{f,w}$	backwash, sidewash, and downwash influence coefficient for horseshoe vortex on the flap
F_s	streamwise force
k	argument of elliptic integral
K	complete elliptic integral of first kind
L	lift force
ℓ_c	length of initial region in jet-wake
M	pitching moment; or momentum in jet; or number of vortices or control points on wing
MF	number of vortices or control points on flap
m	mass flow in jet
q	free stream dynamic pressure, $\frac{1}{2}\rho_\infty V^2$
R	radius of jet-wake
R_o	radius of jet-wake at beginning of jet wake
r	radial distance given by $\sqrt{\eta^2 + \zeta^2}$ for the jet
s	horseshoe vortex semi-width measured in chordal plane; or distance along jet wake centerline
S_{REF}	wing planform area used as reference area by wing-flap program
T	engine thrust
u,v,w	perturbation velocities in x, y and z directions, respectively, induced by horseshoe vortices on the wing
u_f, v_f, w_f	perturbation velocities in x_f, y_f and z_f directions, respectively, induced by horseshoe vortices on the flap
u_i, v_i, w_i	perturbation velocities in x, y and z directions, respectively, induced on wing-flap by other airframe components
u'_Γ	axial velocity induced by a single vortex ring

v_r'	radial velocity induced by a single vortex ring
V_j	jet velocity directed along the geometric engine centerline at beginning of wake (includes free stream velocity)
$\overline{V}_j$	average jet velocity at a station along the jet (includes free stream velocity)
V_f	fan exit velocity
v_1	perturbation velocity along y direction at the bound leg midpoint of a horseshoe vortex on the wing
v_2	perturbation velocity along y direction at the 3/4 chord of the left side of an area element on the wing
V	free stream velocity
x,y,z	coordinates with origin located at the midspan of a horseshoe vortex on the wing and with same directions as X, Y, Z coordinate system, figure 2; or jet wake coordinate system fixed at beginning of jet, figure 9(a)
x_f, y_f, z_f	coordinates with origin located at the midspan of a horseshoe vortex on the flap, y_f direction same as y and Y directions. Directions of x_f and z_f rotated from x and z through angle δ_{XZ} (positive down), figure 2
X,Y,Z	coordinates with origin located at the wing root chord nose, figure 2. X axis coincident with wing root chord, Z axis positive in downward direction
α	angle of attack of wing root chord with respect to free stream, degrees
α_ℓ	angle between tangent to mean camber surface of the wing and X direction, degrees
Γ	vortex strength of a horseshoe vortex
Γ_j	vortex strength of vortex rings used to model expanding jet wake
γ	vortex strength of vortex cylinder used to model straight jet wake
δ_f	flap deflection angle measured perpendicular to the hingeline, positive downward, degrees
δ_{XZ}	streamwise flap deflection angle measured in a plane parallel to the X-Z plane, positive downwards, degrees

δ_ℓ	angle between tangent to mean camber surface of the flap and the x_f direction, degrees
ϵ_y	angle whose tangent equals the slope of the jet-wake centerline in the X-Y plane, degrees
ϵ_z	angle whose tangent equals the slope of the jet-wake centerline in the X-Z plane, degrees
η	non-dimensional spanwise coordinate, Y/(b/2)
θ	angle of inclination of jet wake centerline, relative to X-direction, degrees
ξ,η,ζ	vortex ring rectangular coordinate system with origin located at the center of the vortex ring, figure 9(b)
ρ_∞	free stream density
ϕ	dihedral of wing, degrees
ϕ_f	dihedral of flap calculated by wing flap program, degrees
ψ	sweep angle of the bound leg of a wing horseshoe vortex (positive for swept back vortices), degrees
ψ_f	sweep angle of the bound leg of a horseshoe vortex on the deflected flap calculated by wing flap program from undeflected flap sweep, degrees
ψ_P	sweep angles measured in the plane of the wing planform, degrees

Subscripts

f	flap
ℓ	left; or local
o	initial
P	field point
Q	center of engine inlet
r	right
S	center of vortex ring
W	wing
LE	leading edge
TE	trailing edge

THEORETICAL ANALYSIS

Wing-Flap Model

In order to appraise aerodynamic interaction effects between a jet-wake and a wing-flap configuration, a method is required to determine aerodynamic loadings on the wing flap surfaces. Furthermore, the method must be able to predict wing-flap induced perturbation velocities at field points in the vicinity of the configuration. For these purposes, a three-dimensional horseshoe vortex lattice is used as the distribution of singularities representing the lifting surfaces. The flow tangency boundary condition, including all wing-flap interference effects, is applied at a finite number of control points on the wing-flap surfaces, which results in a set of simultaneous equations from which the vortex strengths are determined. Wing angle of attack and flap deflection angles are accounted for in terms of trigonometric functions instead of linear terms because the magnitudes of the angles can be large. The jet-wake is considered an external source of perturbation velocities which are included in the wing-flap flow tangency condition as part of the jet wing-flap aerodynamic interference calculation.

The method is developed for flow in the pitch plane; yaw effects are not included. Since large flap deflections are used only at low speeds, compressibility effects are not included. Finally, since potential flow theory is used, the methods cannot account for flow separation or other viscous effects.

Configuration characteristics.- The configuration of interest is a wing with large, deflected flaps attached to the trailing edges of the wing panel. The various configuration parameters included in the method are listed below.

Wing Panels:

Mean camber surface: May have both twist and camber
Leading-edge shape: Straight line which may be swept
Trailing-edge shape: Same as for leading edge
Taper: Linear
Tips: Parallel to wing root chord
Dihedral: Arbitrary but constant over the semispan
Thickness: Assumed small (thickness effects neglected)

Flaps:

Type: Single surface. Multiple flaps are idealized as a single flap with camber to account for the effects of individual flap components.

Location: At or near wing trailing edge with the flap leading edge situated in or off the plane of the wing. (In actuality, the flap can be located anywhere provided certain precautions are followed in the layout of the wing vortex-lattice and the flap control points.)

Mean camber surface: May have camber. Also see remarks regarding flap type.

Span: Full or partial span.

Leading-edge shape: Straight line which may be swept.

Trailing-edge shape: Same as for leading edge.

Taper: Linear

Thickness: Assumed small (thickness effects neglected).

Description of the method.- The three-dimensional horseshoe vortex lattice that is used to represent the wing-flap lifting surfaces is an extension of the vortex-lattice methods and programs developed in references 8, 9, and 10. Specifically, the approach described in reference 8 has been extensively modified to treat a wing-flap system with mutual interference between the wing and flap.

The vortex-lattice arrangement and the coordinate system for a swept wing with trailing edge flaps deflected are shown in figures 1 and 2. The wing panel and flap are divided into trapezoidal area elements. A horseshoe vortex is placed in each area element such that the spanwise bound leg lies along the element quarter chord and its trailing legs along the chordwise sides of the element. The trailing legs are assumed to lie in the plane of the area element. The wing vortex trailing legs consequently extend back to infinity in the plane of the wing. The flap vortex trailing legs extend downwards to infinity in the plane of the flap. Both wing and flap vortex trailing legs lie in planes parallel to the X-Z plane. The angle subtended by the two trailing leg directions equals the streamwise flap angle, δ_{XZ}, whereas the actual flap δ_f is understood to be measured perpendicular to the hingeline.

On the wing, the area elements have a uniform chordwise length at any spanwise station; in the spanwise direction the area element widths need not be equal to allow for closer spacing where large spanwise loading gradients

exist. The flap area elements are arranged likewise although the chordwise and spanwise dimensions need not be the same as those used for the wing area elements.

The flow tangency boundary condition is applied at a finite set of control points given by the midpoint of the 3/4 chord of each area element located in the chordal planes of the wing and the flap. The wing chordal plane is the plane containing the wing root chord and making angle ϕ with the $Z = 0$ plane, see figure 2. The flap chordal plane is the plane containing the flap leading- and trailing-edges and the flap root and tip chords. The boundary condition states that there is no flow through the wing and flap surfaces at each control point. The condition is illustrated in figure 3 for the wing. The velocities normal to the wing consist of a component of the free stream, perturbation velocities u, v and w induced by the wing-flap horseshoe system, and externally induced perturbation velocities u_i, v_i and w_i. The latter velocities may be generated by a turbofan wake as described in a later section. The velocities normal to the flap are categorized in the same manner.

With M control points on the wing and MF on the flap, the boundary condition for the left wing panel is formulated as follows.

$$\sum_{n=1}^{M} \frac{\Gamma_n}{4\pi V}\left(F_{w_{\nu,n}} \cos\phi_\nu - F_{v_{\nu,n}} \sin\phi_\nu\right) + \sum_{n=M+1}^{M+MF} \frac{\Gamma_n}{4\pi V}\left(F_{f,w_{\nu,n}} \cos\phi_\nu \cos\delta_{XZ} - F_{f,u_{\nu,n}} \cos\phi_\nu \sin\delta_{XZ} - F_{f,v_{\nu,n}} \sin\phi_\nu\right)$$

$$= \sin\left(\alpha + \alpha_{\ell_\nu}\right)\cos\phi_\nu + \frac{v_{i,\nu}}{V}\sin\phi_\nu - \left(\frac{u_{i,\nu}}{V}\alpha_{\ell,\nu} + \frac{w_{i,\nu}}{V}\right)\cos\phi_\nu$$

$$\nu = 1,\ldots M \qquad (1)$$

With the flap deflected downwards, the flap boundary condition is written for MF points as

$$\sum_{n=1}^{M} \frac{\Gamma_n}{4\pi V} \left[F_{w_{\nu,n}} \cos \phi_{f,\nu} \cos \left(\delta_{XZ} + \delta_{\ell_\nu} \right) + F_{u_{\nu,n}} \cos \phi_{f,\nu} \sin \left(\delta_{XZ} + \delta_{\ell_\nu} \right) \right.$$

$$\left. - F_{v_{\nu,n}} \sin \phi_{f,\nu} \cos \left(\delta_{XZ} + \delta_{\ell_\nu} \right) \right]$$

$$+ \sum_{n=M+1}^{M+MF} \frac{\Gamma_n}{4\pi V} \left[F_{f,w_{\nu,n}} \cos \phi_{f,\nu} \cos \delta_{\ell_\nu} - F_{f,v_{\nu,n}} \sin \phi_{f,\nu} \cos \delta_{\ell_\nu} \right]$$

$$= \sin \left(\alpha + \delta_{XZ} + \delta_{\ell_\nu} \right) \cos \phi_{f,\nu} + \frac{v_{i,\nu}}{V} \sin \phi_{f,\nu} \cos \left(\delta_{XZ} + \delta_{\ell_\nu} \right)$$

$$- \left[\frac{u_{i,\nu}}{V} \sin \left(\delta_{XZ} + \delta_{\ell_\nu} \right) + \frac{w_{i,\nu}}{V} \cos \left(\delta_{XZ} + \delta_{\ell_\nu} \right) \right] \cos \phi_{f,\nu}$$

$$\nu = M + 1, \ldots M + MF \qquad (2)$$

The wing angle of attack α, the streamwise flap angle δ_{XZ} (positive downwards) and the local flap angle δ_ℓ due to flap camber are accounted for in a nonlinear manner; for example, $\sin \alpha$ instead of α. This allows the method to be used with large magnitudes for these angles. The validity of the wing-flap loading results at high angles will, however, be limited by viscous effects such as flow separation on the flap not accounted for in the present theory. Local wing angles α_ℓ due to wing camber and twist are assumed to have small magnitudes.

The right-hand sides of equations (1) and (2) represent the free-stream component and the externally induced perturbation velocities normal to the wing and flap chordal planes. The first summation on the left-hand sides of the equations represents the perturbation velocities induced by the left and right wing surfaces. The second summation represents the perturbation velocities induced by the left and right flap surfaces. The functions inside the summations will be discussed next.

The functions F_u, F_v, F_w and $F_{f,u}, F_{f,v}, F_{f,w}$ are influence functions relating the perturbation velocity components induced at some point by a wing and flap horseshoe vortex, respectively, to the circulation strength and the coordinates of the point relative to the origin of the vortex coordinate system (x,y,z). This relationship is obtained

from the Biot-Savart law, (ref. 11). The origin of the vortex coordinate system is located at the bound leg midpoint and its directions are aligned with the wing root chord coordinate system (X,Y,Z), (fig. 2). The effect of vortices laid out on the left and the right wing and flap panels must be included in the influence functions shown in equations (1) and (2). The functions F_u, F_v and F_w for the left wing panel are described completely in Appendix A of reference 8 and are repeated below together with other necessary relations. The same functions are used in connection with the flap vortices as described later. The bound leg sweep angle ψ measured in the wing chordal plane is related to the sweep angle ψ_p in the wing planform by the dihedral angle ϕ:

$$\tan \psi = \tan \psi_p \cos \phi \tag{3}$$

The backwash influence coefficient is

$$F_u(x,y,z,s,\psi,\phi)$$

$$= \frac{(z \cos \phi - y \sin \phi) \cos \psi}{\left[x \cos \psi - (y \cos \phi + z \sin \phi) \sin \psi\right]^2 + (z \cos \phi - y \sin \phi)^2}$$

$$\cdot \left\{ \frac{(x + s \tan \psi) \sin \psi + (y + s \cos \phi) \cos \psi \cos \phi + (z + s \sin \phi) \cos \psi \sin \phi}{\left[(x + s \tan \psi)^2 + (y + s \cos \phi)^2 + (z + s \sin \phi)^2\right]^{1/2}} \right.$$

$$\left. - \frac{(x - s \tan \psi) \sin \psi + (y - s \cos \phi) \cos \psi \cos \phi + (z - s \sin \phi) \cos \psi \sin \phi}{\left[(x - s \tan \psi)^2 + (y - s \cos \phi)^2 + (z - s \sin \phi)^2\right]^{1/2}} \right\} \tag{4}$$

The sidewash influence coefficient is

$$F_v(x,y,z,s,\psi,\phi)$$

$$= \frac{-z\sin\psi + x\cos\psi\sin\phi}{\left[x\cos\psi - (y\cos\phi + z\sin\phi)\sin\psi\right]^2 + (z\cos\phi - y\sin\phi)^2}$$

$$\cdot \left\{ \frac{(x + s\tan\psi)\sin\psi + (y + s\cos\phi)\cos\psi\cos\phi + (z + s\sin\phi)\cos\psi\sin\phi}{\left[(x + s\tan\psi)^2 + (y + s\cos\phi)^2 + (z + s\sin\phi)^2\right]^{1/2}} \right.$$

$$\left. - \frac{(x - s\tan\psi)\sin\psi + (y - s\cos\phi)\cos\psi\cos\phi + (z - s\sin\phi)\cos\psi\sin\phi}{\left[(x - s\tan\psi)^2 + (y - s\cos\phi)^2 + (z - s\sin\phi)^2\right]^{1/2}} \right\}$$

$$+ \frac{(z - s\sin\phi)}{(y - s\cos\phi)^2 + (z - s\sin\phi)^2}$$

$$\cdot \left\{ 1 - \frac{(x - s\tan\psi)}{\left[(x - s\tan\psi)^2 + (y - s\cos\phi)^2 + (z - s\sin\phi)^2\right]^{1/2}} \right\}$$

$$- \frac{(z + s\sin\phi)}{(y + s\cos\phi)^2 + (z + s\sin\phi)^2}$$

$$\cdot \left\{ 1 - \frac{(x + s\tan\psi)}{\left[(x + s\tan\psi)^2 + (y + s\cos\phi)^2 + (z + s\sin\phi)^2\right]^{1/2}} \right\}$$

(5)

The downwash influence coefficient is

$$F_w(x,y,z,s,\psi,\phi)$$

$$= \frac{-x\cos\psi\cos\phi + y\sin\psi}{\left[x\cos\psi - (y\cos\phi + z\sin\phi)\sin\psi\right]^2 + (z\cos\phi - y\sin\phi)^2}$$

$$\cdot \left\{ \frac{(x + s\tan\psi)\sin\psi + (y + s\cos\phi)\cos\psi\cos\phi + (z + s\sin\phi)\cos\psi\sin\phi}{\left[(x + s\tan\psi)^2 + (y + s\cos\phi)^2 + (z + s\sin\phi)^2\right]^{1/2}} \right.$$

$$\left. - \frac{(x - s\tan\psi)\sin\psi + (y - s\cos\phi)\cos\psi\cos\phi + (z - s\sin\phi)\cos\psi\sin\phi}{\left[(x - s\tan\psi)^2 + (y - s\cos\phi)^2 + (z - s\sin\phi)^2\right]^{1/2}} \right\}$$

(Continued on next page)

$$- \frac{(y - s\cos\phi)}{(y - s\cos\phi)^2 + (z - s\sin\phi)^2} \cdot \left\{1 - \frac{(x - s\tan\psi)}{\left[(x - s\tan\psi)^2 + (y - s\cos\phi)^2 + (z - s\sin\phi)^2\right]^{1/2}}\right\}$$

$$+ \frac{(y + s\cos\phi)}{(y + s\cos\phi)^2 + (z + s\sin\phi)^2} \cdot \left\{1 - \frac{(x + s\tan\psi)}{\left[(x + s\tan\psi)^2 + (y + s\cos\phi)^2 + (z + s\sin\phi)^2\right]^{1/2}}\right\} \quad (6)$$

The contribution from a vortex situated in the right panel is obtained by changing the signs on the vortex bound leg sweep angle ψ and the dihedral ϕ. In addition, the term y_r stands for the coordinate in the y direction of the point relative to a vortex on the right wing panel. Summing up the contributions from left and right wing panels results in:

$$F_u = F_u(x,y_\ell,z,s,\psi,\phi) + F_u(x,y_r,z,s,-\psi,-\phi) \quad (7)$$

The same expressions hold for F_v and F_w. These functions are substituted in the wing induced effects indicated by the first summations on the left-hand side of equations (1) and (2).

Flap induced effects are obtained in the following manner. First, the wing vortex coordinate system (x,y,z) is rotated about the y-axis through angle δ_{XZ} which is the streamwise flap angle (positive downwards). This transformation relocates the vortex coordinate system such that the transformed x-axis lies in the plane of the flap. The transformed y-axis is parallel to the wing vortex y-axis and the transformed z-axis is perpendicular to the transformed x and y axis. Thus the flap vortices bear the same relationship to the transformed or flap vortex coordinate system (x_f,y_f,z_f) as the wing vortices to the wing vortex coordinates (x,y,z). Flap vortex bound leg sweeps, ψ_f, are calculated by the program in the chordal plane of the deflected flap. The dihedral angle, ϕ_f, associated with the deflected flap is the angle the flap chordal plane makes with the transformed or flap x_f,y_f plane and is

also computed by the program. It is to be observed that the flap vortex y_f-axis is parallel to the wing vortex y-axis as well as the Y-axis of the wing root chord coordinate system.

The coordinates of a point relative to a horseshoe vortex on the flap are specified in the same way as the coordinates (x,y,z) of a point relative to a wing horseshoe vortex. Then, to compute perturbation velocities induced by the flap horseshoe vortex, the following transformations are performed.

$$\left.\begin{aligned} x_f &= x \cos \delta_{XZ} - z \sin \delta_{XZ} \\ y_{f_\ell} &= y_\ell \\ y_{f_r} &= y_r \\ z_f &= x \sin \delta_{XZ} + z \cos \delta_{XZ} \end{aligned}\right\} \qquad (8)$$

Substituting x_f, y_f, z_f and angles ψ_f and ϕ_f in equations (4) through (7) allows for the determination of influence functions $F_{f,u}, F_{f,v}, F_{f,w}$. The flap-vortex-induced perturbation velocity components associated with these functions are consequently aligned with the flap vortex coordinate system (x_f, y_f, z_f). These velocities must therefore be transformed back in the wing coordinate system for inclusion in the boundary conditions expressed by equations (1) and (2). The result is a set of M + MF simultaneous equations in which the unknowns are the M + MF values of circulation strengths, Γ. The values can therefore be obtained from a matrix solution for a given wing angle of attack, α, flap angle δ_f and a specified set of perturbation velocities u_i, v_i, w_i induced by an external source such as the turbofan wake.

Once the circulation values have been calculated, the load distribution on the wing and flap can be obtained by means of the Kutta-Joukowski law for aerodynamic force on a vortex filament. The force per unit length on the vortex filament is obtained as the product of density, velocity and circulation strength. The line of action is perpendicular to the velocity vector and the vortex line. For a given area element on the left wing panel, the lift and streamwise force components are calculated

as the sum of two contributions: lift and streamwise force acting on the bound leg plus lift and streamwise force acting on that part of the trailing legs within the area element. The forces on the bound leg are obtained by first computing the perturbation velocity and free-stream components in the wing coordinate system (X,Y,Z) at the bound-leg midpoint and applying the Kutta-Joukowski law to each velocity component. The force components are then resolved into the lift direction, and the streamwise direction. The forces on the vortex trailing legs are computed at the 3/4 chord of the left side of an area element. According to the Kutta-Joukowski law, the product of the net circulation $\Delta\Gamma$ of the coincident legs along the chordwise sides of the area elements, the sidewash at the element 3/4 chord and the density equals the aerodynamic force per unit length on the vortex trailing legs. The line of action of this force is perpendicular to the plane formed by the sidewash vector (parallel to Y-axis) and the vortex trailing legs (parallel to X-axis). This force is then resolved into the lift and streamwise directions. The expression for lift, made non-dimensional by the dynamic head and reference area, acting on an area element of the left wing panel is specified as

$$\frac{L}{qS_{REF}} = \frac{2\Gamma}{S_{REF}V}\,2s\left[\left(1 - \frac{u}{V}\cos\alpha\right)\cos\phi + \frac{v_1}{V}\left(\tan\psi\cos\alpha + \sin\phi\sin\alpha\right) - \frac{w}{V}\cos\phi\sin\alpha\right] + \frac{2\Delta\Gamma v_2}{S_{REF}V^2}\,c\cos\alpha \qquad (9)$$

The non-dimensional streamwise force acting on a left wing area element is given by

$$\frac{F_s}{qS_{REF}} = \frac{2\Gamma}{S_{REF}V}\,2s\left[\frac{u}{V}\cos\phi\sin\alpha - \frac{v_1}{V}\left(\tan\psi\sin\alpha - \sin\phi\cos\alpha\right) - \frac{w}{V}\cos\phi\cos\alpha\right] - \frac{2\Delta\Gamma v_2}{S_{REF}V^2}\,c\sin\alpha \qquad \text{(positive forwards)} \qquad (10)$$

Backwash u, sidewash v_1 and downwash w are calculated at the mid-point of the vortex bound leg swept at angle ψ. Sidewash v_2 is computed at the 3/4 point of the left side of the element with chord, c. The perturbation velocities u, v_1, v_2, w include flap and wing vorticity effects. Engine jet-wake induced perturbation velocities are also included when determining wake-wing-flap interference.

Aerodynamic forces on the flap are determined in a manner similar to the procedure described above. However, forces due to sidewash have not been included in accordance with the following considerations. The trailing legs of the wing vortices aft of the hinge line should lie in or close to the flap plane rather than the wing plane. Were they to lie in the flap plane, they would induce no sidewash in the flap plane. An an approximation to this condition, the sidewash induced forces have not been included. With this assumption, the expression for lift made nondimensional by the dynamic head and reference area and acting on an area element of the left flap is written as:

$$\frac{L}{qS_{REF}} = \frac{2\Gamma}{S_{REF}V}\, 2s \left\{ \left[1 - \frac{u_f}{V} \cos\,(\alpha + \delta_{XZ}) \right] \cos\,\phi_f - \frac{w_f}{V} \cos\,\phi_f \sin\,(\alpha + \delta_{XZ}) \right\} \tag{11}$$

The specification of the non-dimensional streamwise force acting on a left flap area element is

$$\frac{F_s}{qS_{REF}} = \frac{2\Gamma}{S_{REF}V}\, 2s \left[\frac{u_f}{V} \cos\,\phi_f \sin\,(\alpha + \delta_{XZ}) - \frac{w_f}{V} \cos\,\phi_f \cos\,(\alpha + \delta_{XZ}) \right] \tag{12}$$

(positive forwards)

The perturbation velocities u_f, w_f are computed in the flap or (x_f, y_f, z_f) coordinate system and include contributions from the wing vorticity as well as the flap vorticity. If a jet wake-wing-flap interference calculation is performed, wake induced velocities are also included.

For purposes of computing span loadings on the wing and flap, equations (9) and (11) are summed over the chordwise rows on the wing and flap vortices respectively. The vortex trailing leg contribution, represented by the second term in equation (9) is averaged over the left and right sides of the wing area element. The total lift is then calculated by summing over the semispan and the result is multiplied by two to include the right wing and flap panels.

The pitching moment is calculated by summing the products of the appropriate moment arms with the lift and streamwise forces acting on the area elements on the wing and flap.

Perturbation velocities at points in the vicinity of the wing-flap surfaces are determined by adding the effects of all horseshoe vortices distributed on the wing and the flap as follows. The coordinates (x,y,z) of the point relative to the bound leg midpoint of each horseshoe vortex are first computed. Then the appropriate influence functions are calculated according to equations (4) through (7). The influence functions are then combined with the circulation strengths to calculate the perturbation velocities. For example, the wash velocities at a point (x,y,z) induced by a horseshoe vortex on the left wing panel are

$$\left.\begin{aligned} u(x,y,z) &= \frac{\Gamma}{4\pi} F_u(x,y,z,s,\psi,\phi) \\ v(x,y,z) &= \frac{\Gamma}{4\pi} F_v(x,y,z,s,\psi,\phi) \\ w(x,y,z) &= \frac{\Gamma}{4\pi} F_w(x,y,z,s,\psi,\phi) \end{aligned}\right\} \qquad (13)$$

Transformations indicated by equation (8) are necessary to compute the effects of a horseshoe vortex on the flap. The location of the point relative to the midpoint of the bound leg in the flap vortex coordinate system (x_f,y_f,z_f) is determined first. The perturbation wash velocities induced by a horseshoe vortex on the left flap are then given by

$$
\left.
\begin{aligned}
u(x,y,z) &= \frac{\Gamma}{4\pi} F_u(x_f,y_f,z_f,s_f,\psi_f,\phi_f) \cos \delta_{XZ} \\
&\quad + F_w(x_f,y_f,z_f,s_f,\psi_f,\phi_f) \sin \delta_{XZ} \\
v(x,y,z) &= \frac{\Gamma}{4\pi} F_v(x_f,y_f,z_f,\psi_f,\phi_f) \\
w(x,y,z) &= \frac{\Gamma}{4\pi} F_w(x_f,y_f,z_f,s_f,\psi_f,\phi_f) \cos \delta_{XZ} \\
&\quad - F_u(x_f,y_f,z_f,s_f,\psi_f,\phi_f) \sin \delta_{XZ}
\end{aligned}
\right\} \qquad (14)
$$

The transformations indicated in equation (14) align the directions of the perturbation velocities with the wing vortex coordinate system (x,y,z). The influence functions in equations (13) and (14) are constructed such that they also include the effects of the right wing panel and flap horseshoe vortex as per equation (7). Finally, the process is repeated for all horseshoe vortices distributed on the left wing panel and flap.

Jet Wake Model

A potential flow model of a high-bypass-ratio turbofan engine and its wake is needed which will yield the velocity field both inside and outside the jet wake. The jet shape should behave according to known spreading rates for jets in a coflowing stream and the model should simulate the entrainment effect exhibited by jet wakes. Attention was directed toward the region of the wake within 10 or 12 radii downstream of the engine since this is the region of greatest interaction between the wake and the wing-flap. For the same reason, no attempt was made to model the fan and engine ducts, since their contributions to the engine wake induced flow field are very small compared to those of the wake.

A wake model developed for a turbofan engine in a cruise condition is described in reference 8. In this model, the wake is represented by a constant diameter, constant strength, semi-infinite vortex cylinder. The wake velocity profile inherent with a vortex cylinder is a uniform axial velocity across the wake whose magnitude becomes essentially invariant with axial distance along the wake three radii or so downstream of the origin of the wake. This model has constant momentum inside the jet, but it also has constant mass flow in the jet which indicates that

entrainment of the free stream is not included in the model. The approach used for the cruise fan wake is retained, but the analytical model is modified according to some empirical observations to better approximate the actual turbulent jet in a coflowing stream.

Model description.- The description of an axisymmetric turbulent jet in a coflowing stream as given in reference 7 is used as basis for the needed potential flow model. In this reference, experimental data is used to develop an analytical representation of a coflowing jet. The jet is divided into two separate regions for analysis: the initial region in which the jet velocity does not decay within the confines of a central core, and the main region in which the velocity decays with distance along the jet centerline (fig. 4). With assumptions on the form of the velocity profile and constant momentum within the wake, the spreading rate of an incompressible turbulent jet can be defined. Spreading rates are shown in figure 4 for various jet velocity ratios. The characteristics of the initial region as a function of jet velocity ratio are shown in figure 5.

The development of the potential flow model proceeds in the following manner. Instead of maintaining a constant radius along the jet as in reference 8, a vorticity distribution is placed on the specified expanding jet boundary. This is carried out by replacing the continuous vorticity distribution of the cylinder with a series of vortex rings coaxial with the jet centerline. Each ring represents a finite increment of length of the jet wake boundary and the vortex strength of each ring is equal to the net vorticity on the incremental length of the boundary. This model is shown schematically in figure 6 for a particular jet velocity ratio. The semi-infinite length of the jet wake is replaced with a finite length model of vortex rings. The length is specified such that the difference between induced velocities calculated with a finite length cylinder and those calculated with the semi-infinite cylinder is acceptably small (less than 1 percent) in the near wake.

The strength of the vortex ring at any point along the jet is

$$\frac{\Gamma_j}{V} = \frac{\gamma}{V}\left(\frac{R_o}{R}\right)\Delta s \tag{15}$$

where γ/V is the strength of the constant radius vortex cylinder corresponding to the specified engine thrust coefficient. This vortex cylinder strength is

$$\frac{\gamma}{V} = \frac{V_j}{V} - 1 \tag{16}$$

where V_j is a uniform velocity across the initial jet area, A_j, and can be calculated in terms of the thrust coefficient C_μ as follows. Assuming an incompressible jet, the velocity ratio at the fan exit based on momentum considerations is approximately

$$\frac{V_f}{V} = \frac{1}{2}\left[1 + \sqrt{1 + 2\left(\frac{S_{REF}C_\mu}{A_f}\right)}\right] \tag{17}$$

which when expanded over the entire wake area results in the needed jet velocity ratio:

$$\frac{V_j}{V} = \frac{V_f}{V}\left(\frac{A_f}{A_j}\right) \tag{18}$$

Equations (17) and (18) have been applied to a cold-gas turbine-driven model of a high-bypass-ratio turbofan engine on which the thrust coefficient and the fan exit velocity are known from measurements. This simple method predicted the fan exit velocity within 5 percent of the experimental average value.

From equation (15), the strength of the initial vortex ring is $\Gamma_{j_o} = \gamma\Delta s$. As the radius of the successive rings increases, their circulation strength is decreased proportionally such that the product of Γ_j and the ring circumference remains constant. The induced velocity at any point in the field is calculated by summing the effects of all the vortex rings making up the jet model. The induced velocity equations are described in the next section.

Predicted jet velocity profiles at several stations along a jet centerline are shown in figure 6 for a jet velocity ratio $V_j/V = 6$. The average velocity inside the wake boundary decreases with axial distance along the centerline in almost inverse proportion with the jet radius. The vortex ring model theoretically should give a constant velocity profile across the jet radius; however, the finite-step summation procedure results in a rounded profile near the wake boundary.

The expanding vortex ring model in the absence of a free-stream velocity satisfies the requirement of constant momentum inside the jet which is in agreement with the Abramovich model. When an external flow is superimposed on the vortex ring model, the momentum is no longer constant in the jet. The change in momentum in the initial region of a jet is shown in figure 7 for a range of typical jet velocity ratios. The vortex ring model of the jet shows a small increase in momentum in the initial region of the jet in contrast with the Abramovich model. An estimate of the effect of this momentum change on the externally induced flow field can be made by comparing the mass flows of the two models. This is done in figure 8, where it is shown that the vortex ring model has a larger increase in mass in the initial region of the jet than does the Abramovich model. The implication of this result is that the vortex ring model will predict more inflow to the jet and thus show a larger entrainment effect than the Abramovich model. In the region of interest within 10 radii of the engine exit, the differences are small and should not lead to any appreciable error in the interference calculation.

It is desirable in subsequent interference calculations to permit the jet wake to deflect under the influence of the wing-induced sidewash and downwash and the cross flow component of the free stream. Accordingly, provision has been made in developing the equation for the velocity induced by the wake to place the vortex rings normal to the local wake centerline. A limitation is thereby placed on the centerline curvature, in that numerical problems may arise if two adjacent rings intersect.

Velocities induced by jet wake model.- The wake model is made up of a series of vortex rings lying along the prescribed centerline of the jet as shown in figure 9(a). The details of a single ring and its relative position with respect to an arbitrary field point, P, are shown in figure 9(b). The velocity induced at point P by a single vortex ring is calculated as follows.

The coordinates of point P in the wing coordinate system are transformed to the jet coordinate system according to

$$\left.\begin{aligned} x_P &= -x_P + X_Q \\ y_P &= y_P - y_Q \\ z_P &= -z_P + Z_Q \end{aligned}\right\} \tag{19}$$

where point Q denotes the center of the origin of the jet (fig. 9(a)). Coordinates of P transformed to a ring-centered coordinate system become

$$\left.\begin{aligned} \xi_P &= (x_P - x_S)\cos\theta + (z_P - z_S)\sin\theta \\ \eta_P &= -(y_P - y_S) \\ \zeta_P &= (x_P - x_S)\sin\theta - (z_P - z_S)\cos\theta \end{aligned}\right\} \tag{20}$$

where the point S denotes the location of the center of the vortex ring. From reference 12, the induced axial velocity is

$$\frac{u'_\Gamma}{V} = \left(\frac{1}{2\pi}\right) \frac{\Gamma/V}{\left[\left(\frac{\xi_P}{R_o}\right)^2 + \left(\frac{r_P}{R_o} + \frac{R}{R_o}\right)^2\right]^{1/2}} \left\{K(k) - \left[1 + \frac{2\left(\frac{R}{R_o}\right)\left(\frac{r_P}{R_o} - \frac{R}{R_o}\right)}{\left(\frac{\xi_P}{R_o}\right)^2 + \left(\frac{r_P}{R_o} - \frac{R}{R_o}\right)^2}\right] E(k)\right\} \tag{21}$$

where the radial distance to point P is

$$r_P = \sqrt{(\eta_P)^2 + (\zeta_P)^2} \tag{22}$$

and the argument of the elliptic integrals is

$$k^2 = \frac{r\left(\frac{r_P}{R_o}\right)\left(\frac{R}{R_o}\right)}{\left(\frac{\xi_P}{R_o}\right)^2 + \left(\frac{r_P}{R_o} + \frac{R}{R_o}\right)^2} \tag{23}$$

The induced radial velocity is

$$\frac{v'_\Gamma}{V} = \frac{-\Gamma/V}{2} \frac{\frac{\xi_P}{R_o}}{\left(\frac{r_P}{R_o}\right)\left[\left(\frac{\xi_P}{R_o}\right)^2 + \left(\frac{r_P}{R_o} + \frac{R}{R_o}\right)^2\right]^{1/2}} \left\{ K(k) - \left[1 + \frac{2\left(\frac{r_P}{R_o}\right)\left(\frac{R}{R_o}\right)}{\left(\frac{\xi_P}{R_o}\right)^2 + \left(\frac{r_P}{R_o} - \frac{R}{R_o}\right)^2}\right] E(k) \right\} \tag{24}$$

These velocity components, when resolved into components in the wing coordinate system, become

$$\left.\begin{aligned} \frac{u_i}{V} &= -\frac{u'_\Gamma}{V}\cos\theta - \frac{v'_\Gamma}{V}\left(\frac{\zeta_P}{r_P}\right)\sin\theta \\ \frac{v_i}{V} &= -\frac{v'_P}{V}\left(\frac{\eta_P}{r_P}\right) \\ \frac{w_i}{V} &= -\frac{u'_\Gamma}{V}\sin\theta + \frac{v'_\Gamma}{V}\left(\frac{\zeta_P}{r_P}\right)\cos\theta \end{aligned}\right\} \tag{25}$$

The total velocity induced at the point P by the entire jet wake model is obtained by summing the velocities induced by all the rings forming the wake.

Interference Calculation

In order to calculate the aerodynamic loading of a wing-flap configuration under the influence of the jet wake of a turbofan engine, it is necessary to combine the two potential flow models just described. The wing-flap loading is not considered to affect the engine thrust or the basic velocity distribution in the engine wake. However, the component of the free stream velocity normal to the engine centerline (if any) and the velocity field induced by the wing-flap are considered to deflect the engine wake ahead of the point where it impinges on the wing and flap. Because of this interaction, either a simultaneous solution using both flow models or an iterative solution is required. The latter choice was selected. The general approach evolved is as follows.

The aerodynamic loading on the wing-flap at an angle of attack in a uniform flow (without engine wake) is calculated first. As a part of this solution, the flow field beneath the wing in the region where the engine and its wake would be introduced is calculated. The specific region selected is the engine centerline and its extension aft to a point approximately one chord length aft of the wing. Sufficient points are selected along this line to obtain the induced downwash and sidewash distribution. At this point, the w and v velocities are combined vectorily with V (neglecting the u) to obtain the flow directions along the engine centerline extension. Finally, the streamline passing through the center of the exhaust of the as yet unintroduced engine is defined approximately by laying off a series of straight line segments aft from the engine exhaust, where each segment has the local flow direction as calculated above.[1]

An iteration procedure appropriate to the information noted above would consist of laying the jet wake centerline along the approximate streamline, computing the velocity components induced through the wing-flap at the control points by the wake, recomputing the wing-flap vorticity, and recomputing the streamline by now combining the new wash velocities with V and V_j. Since the coordinates of this streamline would be somewhat different from those of the initial streamline, further iterations would be performed until the streamline coordinates no longer changed by more than some acceptable amount. It should be noted that in the first iteration, the initial streamline would not intersect the wing or flap surfaces, but when the jet model is laid on the streamline, the jet wake generally will pass through portions of the wing and flap surfaces. At the end of the first iteration, however, sufficient additional bound and trailing vorticity has been placed on the wing and flap to cause the combined free stream and jet wake flow (including the effects of induced v and w, V and V_j) to be tangent to the wing and flap surfaces at all control points. The additional vorticity is a measure of the wake-induced interference.

The actual procedure adopted was somewhat different than that just described in order to increase the convergence rate of the iteration

[1] The streamline is approximate in that as the streamline departs from the engine centerline extension, the wash velocities induced at points along this streamline are slightly different from those computed on the extension.

procedure. The down- and sidewash velocities are generally small compared to V, but V_j is perhaps three to six times the value of V. If one examines the changes in the flow field between the wing-flap alone at the beginning of the first iteration and the wing-flap-jet at the end of the first iteration, the largest effect on flow angles is caused by the inclusion of V_j rather than the changes in induced v and w velocities due to wake interaction with the wing-flap. Therefore, the addition of V_j to the flow field underneath the wing-flap alone in order to get the initial wake centerline will decrease the differences between the initial wake centerline and the "engine wake" streamline computed at the end of the first iteration, which should cause more rapid convergence. The procedure is as follows. The induced down- and sidewash velocities due to the wing-flap in a uniform flow are computed as before, to start the first iteration. These are then combined with V and V_j to construct the straight line segments leaving the engine exhaust. This line at this point is no longer a streamline, but will be closer to the streamline calculated at the end of the first iteration than was the case previously. Note again that the total flow at the end of the first iteration will be tangent to the wing and flap surfaces at all control points.

The results presented in this report were obtained after the first iteration. It is felt that with the modified procedure just described, there should be little change in wing-flap loadings between the first and second iterations. Although downwash and sidewash velocity results are shown in the results for the beginning and end of the first iteration, no second iteration calculations were carried out to verify this point. As an additional comment on the convergence issue, it should be noted that the degree of convergence will be dependent on the lattice arrangement used. If a coarse lattice is used, small changes in wake displacement, principally vertically, will affect relatively large areas on the flap and wing, and the solution will oscillate with perhaps undesirably large amplitudes. Thus, the above comments on the improvement in convergence would apply to relatively fine lattice arrangements.

COMPARISON OF THEORY WITH EXPERIMENT

In order to evaluate the methods previously described, calculations were made for a number of configurations for which data exist. For

comparison purposes, the number of investigations providing useful data are quite limited for several reasons. The models in many cases are complete configurations which have tail and fuselage effects in addition to the flap and engine effects. In most cases, the engine thrust is not measured directly and, in particular, the engine wake velocities are not measured. Finally, in many cases it is difficult to obtain sufficient detail on the configuration to accurately model the wing camber and twist and the flap size and location.

Five sets of data were identified and used for comparison purposes. The data consist of overall lift and pitching moment and in two cases chordwise pressure distributions on the wing and flap. The discussion is divided into wing-flap comparisons and jet-wing-flap comparisons and finally discussion of the theoretical methods in light of the comparisons.

Wing-Flap

Lift and pitching moment and chordwise pressure distributions are available on an aspect ratio 6 rectangular wing with a slotted, Fowler-type flap having a chord 24 percent of the wing-flap chord with flaps up (ref. 13). The wing was supported by a small cylindrical "fuselage" which should have a negligible influence on the wing lift. The comparison of predicted and measured lift and moment is shown in figure 10(a) for flaps off and flaps deflected 40°. The vortex-lattice arrangement used was 6 chordwise by 20 spanwise on the wing semispan and 2 by 20 on the flap.

For flaps off, the lift and moment agree very well with the data. With flaps deflected, the lift curve slope is well predicted but the lift magnitude is high by about 5 percent. The moment is also overpredicted (i.e., too negative). Since both the predicted lift and moment are high, the indication is that the flap lift is being overpredicted. This is verified in the results for chordwise variation of pressure difference, shown in figure 10(b). The predicted values were obtained by calculating the circulation on each chordwise area element, computing the pressure difference associated with the circulation strength, and considering that pressure difference to exist at the panel quarter chord. The results indicate that the loading on the flap is overpredicted for both angles of attack shown,

whereas the loading on the wing is reasonably well predicted. The chordwise distribution of area elements for this calculation was chosen so that the elements on both the wing and flap have about the same chordwise length. According to the results of Appendix A, this arrangement for this size flap should give good results. It is possible that a larger chordwise number on the flap (greater than 2) would change the predicted loadings, although this was not investigated.

The second set of results was obtained on a semispan model of a rectangular cambered wing of aspect ratio 5.3 with a double slotted flap system (ref. 14). The flap chord length (sum of both segments) is about 39 percent of the chord of the wing-flap combination with flaps up. The comparison is shown in figure 11 for three flap angles. The predicted results were obtained using a 6 by 20 lattice on the wing semispan and a 3 by 20 lattice on the flaps. The agreement on lift and pitching moment is good for the zero and 20/40 degrees deflection angles. With the 30/60 deflection angle, the lift curve slope agreement is still good but the magnitude is overpredicted by approximately 10 percent. The predicted pitching moment is too negative for this angle. It is probable that some separation existed on the flap at the largest deflection angle, which could cause the measured lift and pitching moment to be lower than the predicted results.

The third set of results consists of chordwise pressure distributions on a swept wing with a partial span flap. The configuration, illustrated in the sketch in figure 12, has a 35° leading-edge sweep angle and a flap occupying approximately half of the semispan. Loading calculations were made at zero angle of attack with a 10° flap deflection at a Mach number of 0.6. A Prandtl-Glauert correction was used to account for compressibility effects, as described in reference 8. The lattice arrangement was 8 chordwise by 15 spanwise (so that there are 2 chordwise on the flap). The results shown in figure 12 are the chordwise variation of pressure difference near the midspan of the flap. The pressure difference was computed in the same manner as was described above in connection with figure 10.

The agreement of ΔC_p is quite good over the entire chord. In this model there was essentially no gap between the flap and wing, unlike figure 10, and there is a loading peak at the wing-flap junction, which is also well predicted.

Jet-Wing-Flap

Data are available in reference 4 on a STOL model with a rectangular, cambered wing with a leading-edge slat, double-slotted flaps, and two engines on the semispan. The model engines are cold-gas-turbine-driven fans which model quite well the wake of a high-bypass-ratio turbofan engine. The engines were mounted at 3° incidence to the wing in order to direct their exhaust upwards towards the flap. Their static thrust was measured over a range of engine speeds and these data were used to obtain thrust coefficients at the flight condition of interest. The model had no tail surfaces and the influence of the fuselage was neglected, which is felt to be a reasonable assumption because of its small size with respect to the wing. The slat has a chord equal to 19 percent of the wing flap and the two flaps have a combined chord equal to 33 percent of the wing-flap with flaps up. The slat was treated as a highly cambered leading edge.

The wing and flap system were modeled with a 10 chordwise by 15 spanwise lattice on the wing and a 2 by 24 lattice on the flaps. The area element layout for the left wing panel and flap is illustrated in figure 13. Several features are noteworthy. First, the area elements locally are symmetric with respect to each engine centerline. Since the wing has no sweep, the sidewash under the wing is small and the engine wakes tend to move straight aft. Maintaining local symmetry provides that panels both inboard and outboard of the wake are affected equally as the wake spreads. The shaded areas represent the area elements within the undeflected jet wake boundary. Secondly, the area elements have smaller spanwise dimensions in the region of the jet wake. By using smaller elements in this region, the area of the wing and flap impinged upon by the jet wake changes more smoothly as the wake spreading changes or as the wake moves vertically due to the effects of the flow field under the wing-flap surfaces. By the same reasoning, it is desirable to have small chordwise spacings on the area elements of the wing in the region of the wake.

Results for lift and moment on this wing are given in figure 14. The lower two curves represent an engine-off condition for zero flap deflection and 17.5/35 degrees flap deflection. The zero deflection data and theory agree very well whereas the 17.5/35 degree results do not.

In view of the agreement obtained at moderate flap angles in figure 10 and the irregularity of the data points, the lack of agreement is not considered significant. The upper three curves represent two different power settings with flaps deflected 17.5/35 degrees. For the full power case (C_μ = 5.5), calculations were made assuming the wake remained coaxial with the engine (dashed curve) and assuming the engine wake was deflected in accordance with the downwash field under the wing (solid curve). In the latter case, at small α, the induced downwash deflects the wake downward and thus reduces the effect of the wake on the wing and flap loading over the undeflected wake case. At high α, the α-induced upwash drives the wake into the wing and flap and increases the wake-induced effects. The net result is to improve the agreement for the case where downwash-induced wake deflection is included. For the intermediate power case (C_μ = 2.75), the slope (which includes downwash effects) is good but the predicted magnitude is low. The reason for the discrepancy is not known but may be due to the use of an incorrect engine wake velocity, since the slope agrees well. The moments are in reasonable agreement in all cases.

The final set of results are for a semispan model with one engine per panel (ref. 5). The tests were quite systematic in that the same wing-engine combination was tested unswept and swept 30° with three different flap configurations. The wing is an untapered, cambered wing with aspect ratio of about 3.5 in the unswept configuration and 3 in the swept configuration, based on the span and the wing without flap. The engine is a 1.02 pressure-ratio ducted fan mounted on a long, large centerbody, as illustrated in the sketch on figure 15(a). Fan wake measurements were made to determine the engine wake velocity profile (the only such measurements made in all the data examined). Since the theoretical turbofan engine model does not allow for a centerbody aft of the engine, the assumption was made that the fan exit flow expands to fill the entire area within the duct trailing edge. The wing-flap was modeled with a 4 by 20 lattice on the wing and the flap lattice arrangement was dependent on the flap size. The spanwise lattice spacing was uniform on both wing and flap.

Figure 15(a) shows results for an unswept wing with a thrust coefficient of 2.3 and a double-slotted flap with 10/30 degrees flap deflection. The flap chord (both flaps) is 47 percent of the wing-flap

chord with flaps up. The lattice arrangement used on the flaps was a 4 chordwise by 20 spanwise layout. The agreement on lift and moment is excellent in this case. The engine wake was assumed to remain coaxial with the fan in this calculation, since it was felt that the centerbody would tend to "guide" the wake flow under the wing. In addition, the predicted downwash distribution for the wing-flap in uniform flow, shown in figure 15(b), was relatively small in the region where it could influence the wake vertical deflection (the $V \sin \alpha$ component, which is negative, tends to offset the w to get the net angle of the jet flow).

Figures 16(a) and (b) show similar comparisons for the same configuration and thrust coefficient but a considerably larger flap deflection angle. Two theoretical curves are shown. The dashed one is for the case of the engine wake coaxial with the engine centerbody. The solid curve is based on vertical deflection of the wake in accordance with the wing-flap-induced downwash distribution of figure 16(b). Both curves are higher than the data by 25 and 10 percent, respectively.

The comparison of the undeflected wake curve given by the dashed line in figure 16(a), with the upper curve of figure 15(a) indicates the predicted lift to vary approximately linearly with flap deflection angle for the same thrust coefficient. However, the wing loading increases due to increasing flap deflection and therefore the induced downwash below the wing increases, as shown by comparing figures 15(b) and 16(b). The result is a slightly higher upwash below the leading edge and a higher downwash below the aft part of the wing and the flap. The effect of deflecting the wake according to this downwash (ignoring any "guiding" effect the centerbody might have), is to lower the lift coefficient considerably near zero α because of the flap-induced downwash and lower it less at high α because the $V_\infty \sin \alpha$ component tends to drive the wake up into the flap and wing. The net effect is to increase the lift-curve slope so it agrees with the data and to reduce the magnitude of the lift coefficient towards that of the experimental values. The 30/60 degrees experimental data do not show the linear range indicated by the 10/30 degrees data. Some powered static test results for this wing-flap configuration presented in reference 5 indicate little loss in flap effectiveness at 10/30 degrees but a considerable loss at

30/60 degrees. Consequently, it is probable that some separation is occurring for the 30/60 degrees case, which would account for the overprediction.

The moment predictions in figure 16(a) are consistent with the lift results. The moment is overpredicted (i.e., more negative) without inclusion of the downwash, and its inclusion improves the agreement on magnitude and provides a moment curve slope that agrees with the data for low angles of attack.

Figure 17(a) shows lift and moment results for the 30° swept wing with a triple slotted flap. The combined flap chord is about 58 percent of the chord of the wing-flap combination with the flap undeflected. A 5 chordwise by 20 spanwise vortex element arrangement was used to represent the flap system. The lift and moment curves for the engine-off, flaps-up case agree reasonably well with the data. The lift curve slope for 10/20/30 degrees flap deflection with engine off agrees well and the overprediction on lift is mostly due to the camber problem. The moment, however, is considerably underpredicted. The data indicate a slight shift forward in center of pressure with angle of attack whereas the theory predicts a large forward shift. The calculation of moments on a swept wing is much more sensitive to the spanwise and chordwise load distribution than is the case on an unswept wing. It is possible that a different vortex layout would more adequately represent the loading distribution on the wing and flap, but such calculations were not made.

Two sets of curves are shown for the case of 10/20/30 degrees flap and wing loading with power. The dashed one represents the predicted results with an engine wake coaxial with the centerbody and considerably overpredicts the measured lift although the slope is reasonably good. In order to assess the influence of wake deflection on the calculated results, the downwash and sidewash velocities induced by the wing and flap in uniform flow were computed along the (absent) engine centerline and are shown in figure 17(b). In addition to the downwash distribution, there is some sidewash due to wing sweep which tends to move the wake outboard. Using these results, a calculation was made with a wake deflected both vertically and laterally and the upper solid

curve was obtained. The magnitude of the lift is considerably improved, although it is still about 12 percent high. The predicted moment results are not affected greatly by the wake deflection and still show too low a nose down moment.

Discussion of Results

Insofar as the results described above are concerned, there are three aspects of the method that should be discussed. These are the subjects of iteration, lattice layout, and jet wake deflection.

The description of the interference calculation indicated that an iterative scheme involving sequential use of the wing-flap and jet wake models was employed. Since the only "interference" of the wing-flap on the jet wake is the deflection of the wake centerline, the iteration is on the centerline location. All of the data comparisons just described are based on results obtained at the end of the first iteration. At this point, the wake position has been based on a line determined by the free-stream velocity, the induced flow from the wing-flap in uniform flow, and the jet velocity. Also at this point, a streamline leaving the engine exit can be calculated using the free stream, the induced flow from the wing-flap as interfered upon by the jet wake, and the jet velocity. The changes to be expected between iterations are determined by the differences between these two line locations.

Although no complete second iteration has been calculated, wing-induced downwash comparisons have been made before and after jet-induced loadings have been included in the wing circulation distribution. As an example, figure 18 illustrates these two downwash and sidewash distributions for the swept wing-flap configuration described in connection with figure 17 at zero angle of attack. The curves are very similar from the engine exit aft to approximately the midchord of the three segment flap. Thereafter, the velocities calculated with jet-wake interference differ from the wing-flap alone values, particularly for downwash. Thus wake centerlines with and without jet-wake interference placed on a streamline under the wing would not differ significantly until the wake has reached the midchord of the flap, and the wake would strike the same area elements on the wing and the forward half of the flap. On the basis of these results, it is anticipated that the second iteration would not produce a significant change in the lift and moment on the wing.

It is known that the number of area elements used on the wing and flap affects the calculated lift and moment for a vortex-lattice method (ref. 10). The general guides of reference 10 with respect to the ratio of spanwise to chordwise area elements and the spanwise number of elements were used initially to minimize the errors from this source. However, with jet impingement on a portion of the wing and flap, an additional difficulty arises with regard to the element arrangement. Initially, a uniform spanwise spacing was used in calculating wake-induced loadings. It was found that the results were sensitive to those factors determining the wing-flap area on which the jet impinged, such as wake spreading angle, wake deflection, and engine incidence. Finer lattice arrangements improved this situation. The scope of the contract was subsequently increased to permit the systematic lattice investigation described in Appendix A. On the basis of these results, it is felt that many of the calculated results presented here are essentially converged in terms of changes with increasingly fine lattice arrangements. However, it is desirable that some additional work on lattice arrangement be done with wake augmentation, particularly in conjunction with consideration of wake deflection.

Finally, it should be noted that very little data are available for use as a guide in estimating the accuracy with which the wake centerline is modeled. A relatively simple streamline model consisting of 3 or 4 points axially to define the slope and deflection of the wake center streamline was used in the comparisons presented herein. On the basis of results obtained with this model, the general approach of fitting a wake profile to a centerline which is permitted to change with the wing-flap-induced flow field appears to yield the proper behavior for the wake-flap interaction. It was felt however that a more detailed calculation of the streamline was not justified until additional flow field data were available for comparison with predictions.

WING-FLAP VORTEX-LATTICE PROGRAM

The purpose of this section is to describe the vortex-lattice computer program in sufficient detail to permit understanding and use of the program. This program computes span loadings, overall lift and pitching moment coefficients for a wing-flap configuration. Perturbation velocities induced by the wing-flap lifting surfaces at prescribed field points can also be computed. The wing is considered the main surface and the flap

is an optional item. The influence of an engine jet-wake or other source of externally induced perturbation velocities can be included in the loading calculation.

Configuration parameters taken into consideration by the program are listed in the section concerned with the theoretical analysis of the vortex-lattice lifting-surface model.

Fundamentally, the program is based on representing the wing and flap surfaces by horseshoe vortices. The circulation strengths are determined from a set of simultaneous equations provided by the flow tangency boundary condition applied at a finite set of control points distributed over the wing and flap surfaces. The boundary conditions, expressed by equations (1) and (2), feature the optional inclusion of interference velocities induced by an external component such as the jet-wake of a turbofan engine.

Sample cases described at the end of this section illustrate how the program handles a wing-flap combination with and without engine jet-wake interference.

Program Description

Calculation procedure.- The computer program proceeds through various stages as follows. After run identification and input of certain control variables, the wing-flap geometry is read in. This includes information such as wing leading- and trailing-edge sweep angles measured in the wing planform plane, root chord, semispan, and dihedral. The same parameters are specified for the undeflected flap except dihedral but with the addition of the flap root chord leading-edge location in the wing root chord coordinate system.

The vortex lattice to be laid out on the wing and flap is specified next in terms of the chordwise and spanwise numbers of vortices on the left wing panel and flap. Associated with the spanwise specifications are the spanwise coordinates of the left trailing legs of the horseshoe vortices. The distances along the semispan from the plane of symmetry (X-Z plane) to the left legs are predetermined by the user and read in separately for the wing and the flap.

After reading in the local wing and flap angles due to wing camber and twist and flap camber, respectively, the program proceeds to calculate the tangents of the wing and undeflected flap leading- and trailing-edge sweep angles in the wing chordal plane. The next optional input consists of coordinates of field points at which wing-flap vortex-lattice induced perturbation velocities are to be calculated. This is followed by the specification of wing angle of attack, flap deflection angle measured perpendicular to the hingeline, and some more control variables.

The program then computes angles necessary for the layout of vortices on the deflected flap. The set of externally induced perturbation velocities is optionally read in as the last item of input.

After displaying most of the geometry and vortex-lattice specifications in output, the program proceeds to lay out the wing and deflected flap with one horseshoe vortex assigned to an area element. The wing vortex trailing legs extend downstream to infinity while the flap vortex trailing legs extend downward at the streamwise flap angle, δ_{XZ}, relative to the wing vortex trailing legs. This section of the program also calculates the coordinates of the control points at which the flow tangency boundary conditions are to be satisfied.

Upon completion of the wing and flap vortex layout computations, Subroutine INFWW determines the influence functions required by the main program and given by equations (4) through (7) for the construction of the influence coefficient matrix defined by the left-hand side of equations (1) and (2). The next step is to build up the array defined by the right-hand side of the equations. Subroutine INVERS then solves the set of simultaneous equations by a Gaussian elimination method to obtain the unknown circulation strengths, Γ/V.

After the circulation strengths are known, wing-flap vorticity-induced perturbation velocities at field points specified by the user are computed as an option. Next, the program calls on Subroutine LOAD1 to calculate overall lift and pitching moments as well as spanwise loadings on the wing and the flap. This calculation is based on equations (9) through (12) for the aerodynamic forces acting on wing and flap area elements. These loadings are due to vorticity on the wing and flap with or without the interference effects of externally induced velocities,

such as produced by an engine jet wake. If an engine is present, the direct contribution to lift and pitching moment must be separately determined by the user and added to the program calculated lift and pitching moment which include the effects of jet wake-wing-flap interference.

The remainder of the program arranges for the output of control point coordinates, vortex-lattice arrangement and circulation strengths. Overall lift and pitching moment and spanwise loadings are printed. Lastly, the optionally determined wing-flap induced velocities at user prescribed field points are listed.

For a given wing-flap configuration, the computer program can treat a maximum of 10 flow condition cases. The flow conditions are given by the wing angle of attack and the set of externally induced velocities (if applicable), both of which appear on the right hand side of equations (1) and (2). In addition, the program is arranged to read in consecutively as many sets of wing-flap configuration data as the user desires.

Program operation.- The wing-flap vortex-lattice computer program is written in Fortran IV language and has been run on the IBM 360/67 TSS batch system at the Ames Research Laboratory. With this machine 220 control points can be used, although this number is not necessarily a maximum. This program also makes use of the ability of the TSS system to generate, store, and read from data sets. This feature is used as an option and the items treated this way are the control point coordinates and the externally induced velocities. As an alternative, the latter are read in via cards. If the program is to be run on a different computer with smaller storage, dimension statements need to be changed to permit operation on that machine.

No tapes are required other than the standard input and output. For a configuration employing 160 control points, the running time on the TSS batch system to calculate loadings and wing-flap induced perturbation velocities at about 10 field points requires approximately 4 minutes for one angle of attack.

Program limitations and precautions.- There are problems that could arise in the use of the program. The first has to do with the layout of the vortices. The velocity induced at a point by a vortex filament becomes singular as the point approaches the filament. For each influence function,

Subroutine INFWW avoids the singularity by examining a function which contains the distance between the point and the filament. If the value of this function is less than 225×10^{-10} times the square of the wing semispan (also used in ref. 10), that influence coefficient is set equal to zero.

Some care must be taken in selecting the spanwise widths of adjacent area elements and selecting field point locations for calculating wing-flap induced velocities. As a general rule, the spanwise widths of two adjacent area elements should not differ by more than half of the smaller width. Use of the program has indicated that wing-flap induced velocities can be computed at locations as close to the wing and/or flap as one-half of the width of the nearest horseshoe vortex. At smaller distances, the influence of the nearest bound vortex filament is unduly large and causes unrealistic velocities. The same reasons preclude the positioning of a flap such that the wing trailing vortex legs cut through the flap surfaces close to the flap control points. The input specification of the chordwise number of flap vortices fixes the number of area elements on the flap in the chordwise direction. In a cross section of the wing with the flap deflected, the user should compute the 3/4 chord of the area elements on the flap. He should then make sure that the wing trailing vortices are at least one-half of the wing vortex-width removed from the nearest flap control points.

Description of Input

This section describes the input for the wing-flap computer program. In the following discussion, the content of all input cards is described and, where appropriate, instructions on generating the input quantities are given. All input variables are listed at the end of this section in the order of appearance in the input deck, except that the first four variables listed do not appear in the input deck but are needed for program input preparation. The input format for all cards is shown in figure 19, and the item numbers refer to figure 19.

Item 1

The first card serves as identification and may contain any alphanumeric information desired. This information is printed on the first page of the output.

Item 2

The second card contains several control variables which govern certain geometric parameter input options as indicated in the table at the end of this section. The option concerning the specification of the flap root chord is discussed in connection with Item 4 below.

Item 3

The third card contains wing geometry data specified in the wing planform plane. The necessary parameters are the leading- and trailing-edge sweep angles, root chord, semispan and dihedral. The sign conventions for the sweep and dihedral angles are shown in figure 2 and follow the usual convention where positive sweep is aft, positive dihedral corresponds to wing tips above the wing root chord. The wing root chord, semispan, and all other lengths shown in figure 2, are dimensional and should have consistent units of length.

Item 4

The fourth card contains the following geometry data for the flap: leading- and trailing-edge sweep angles, flap root chord, semispan, and the coordinates of the flap root chord leading edge. The flap root chord is defined for the undeflected or deflected flap as follows. The leading and trailing edges of the flap are extended inboard until they intersect the symmetry plane. The line connecting the two intersection points lies in the plane of symmetry and is defined as the flap root chord measured in that plane.

The flap geometry parameters are specified for the undeflected flap except for the flap root chord which may be specified for either the deflected or undeflected flap in accordance with the value of the control variable MFSPEC in Item 2. This choice depends on the manner in which the flap details are specified to the user: cross section with the flap deflected or undeflected. This distinction is not applicable to unswept wing-flap combinations. The undeflected flap lies in or is parallel to the wing chordal plane and has its planform and dimensions determined

by rotating the deflected flap into the wing chordal plane or a plane parallel to it. In this way, flap sweep angles are specified in the wing planform plane as are the wing sweep angles.

At this point it should be noted that the vortex-lattice program performs certain geometrical transformations while in the process of laying out the vortex lattice in the chordal plane of the deflected flap In doing so, the innermost and the outermost horseshoe vortex trailing legs on the flap, which lie in planes parallel to the X-Z plane, are made to originate from the leading edge of the deflected flap inboard and outboard chords. The effective span of the deflected flap is therefore determined by the innermost and outermost locations of the flap vortex trailing legs. This in effect changes the aerodynamically loaded area of the flap by a small amount which should be of little consequence in the lift and pitching moment calculation.

Multiple slotted flaps are idealized as a single flap with its chordal plane defined by the leading edge of the most forward flap component and the trailing edge of the aft flap component. The camber of the idealized flap is determined from the individual flap component angles.

If no flap is present, a blank card is inserted for this item.

Item 5

The fifth card specifies the number of chordwise and spanwise vortices on the left wing panel and flap. The accuracy of the predicted lift and moment depends on the number of layout of vortices used.

A number of calculations were made to investigate the sensitivity of the predicted loading distribution to the vortex-lattice layout. These calculations are described in Appendix A. From these calculations, recommendations have been determined for the optimum vortex-lattice layout for a variety of wing-flap configurations. The user should consult the appendix for guidance on the layout.

While the vortex layout associated with this computer program is very flexible, it is limited by the maximum allowable number of vortices (or control points) specified in the DIMENSION statements. The sum of the products of chordwise and spanwise vortices on the wing and flap should not exceed 220.

Item 6

The sixth and following cards comprising Item 6 list the spanwise location Y(I) of the outboard trailing legs of each chord row of vortices on the wing. The input quantities are dimensional spanwise distances which should have the same units as the wing and flap semispan and chord input values. All distances are input as positive quantities. The input starts at the root chord and proceeds outward towards the tip, according to the index I. An index value I = 1 is assigned to the trailing legs on the root chord with spanwise location Y(I = 1) = 0.0. This is the first quantity on the first card for this item. The second quantity is the distance from the root chord to the outboard trailing legs of the innermost chordwise row of horseshoe vortices.

Since there are MSW vortices, spanwise, on the wing, the maximum value of I (which is IMAX) is MSW + 1. IMAX is limited to 50 in the program, so the maximum number of vortices, spanwise, on the wing is limited to 49. The last value of Y to be entered, Y(IMAX), must be equal to the value of the semispan; that is, Y(IMAX) = SSPAN.

Item 7

This is the first optional set of input necessary only if a flap is presented (MFLAP = 1). The quantities required are the distances from the plane of symmetry to the outboard trailing legs of each chordwise row of vortices on the flap. The trailing legs lie in planes parallel to the plane of symmetry (X-Z plane). These positive input quantites are dimensional spanwise distances which should have the same units as the wing and flap semispan and chord input values. All distances are input as positive quantities. The input starts at the plane of symmetry for a flap with its inboard chord lying in that plane. For a partial span flap with its inboard chord not in the plane of symmetry, the input starts with the spanwise distance from the symmetry plane to the inboard chord of the flap. An index value of IF = 1 is assigned to the

flap vortex trailing legs either in the plane of symmetry with spanwise location YF(IF = 1) = 0.0 or in a plane parallel to that plane with spanwise location YF(IF = 1) ≠ 0.0. One of these is the first quantity on the first card for this item. The second quantity is the distance from the symmetry plane to the outboard trailing legs of the innermost row of horseshoe vortices on the flap.

Since there are MSF vortices, spanwise, on the flap, the maximum value of IF (which is IFMAX) is MSF + 1. IFMAX is limited to 50 in the program, so the maximum number of vortices, spanwise, on the flap is limited to 49. The last value of YF to be entered, YF(IFMAX), must equal the value of the flap semispan; that is, YF(IMAX) = FSSPAN.

If no flap is present (MFLAP = 0), no cards are required for Item 7.

Item 8

The card of this input contains the coordinates of the center of moments. These are dimensional quantities, whose units should be consistent with those of the wing-flap dimensions and whose signs must be consistent with the wing coordinate system. The Y coordinate, YM, must be input as zero.

Item 9

This optional set of input is necessary only if the wing has camber and twist (ALPHLC = 1.0). The specification of the vortex-lattice through Item 5 fixes the layout of the area elements on both wing and flap in their respective chordal planes. In particular, the chordwise specification allows the á priori determination of the chordwise location of control points since they are given by the midpoint of the 3/4 chord of each area element. This is done in a wing-flap cross section (parallel to the X-Z plane). The quantities specified in this set of cards are the tangents of the local angles of attack, ALPHAL, of the cambered and twisted wing mean surface measured in the streamwise direction at each control point relative to the wing coordinate system. The first card in this item contains these values for the chordwise row of elemental panels nearest the root chord, starting with the element nearest the leading edge. In the event that there are more than eight chordwise elements on the wing, the second card would have the values for the ninth,

tenth, etc., elements in that first row. Otherwise, the second card has the values for the chordwise row next outboard of the first row, and so on. The ALPHAL value for the leading edge wing area element in each chordwise row must start on a new card. Thus, there are MSW (or possibly 2 MSW) cards in this item.

The values of ALPHAL are obtained as follows. Consider the sketch in figure 20(a) which shows the cambered and twisted section of the lifting surface at some spanwise station η, for α wing angle of attack. At a point P, corresponding to a control point in the wing chordal plane, a tangent to the wing mean surface is constructed, which makes an angle α_ℓ with the wing root chord (the X-axis). The positive sense of α_ℓ is shown. The input value required is ALPHAL = tan α_ℓ.

Item 10

This optional set of input is required only if a flap is present, MFLAP = 1, and has camber, DELLC = 1.0, Item 2. The quantities specified in this set of cards are the local angles in radians, DELL, of the cambered flap at the control points measured in the streamwise direction. The first card in this item contains these values for the chordwise row of area elements on the flap nearest the plane of symmetry, starting with the area element nearest the flap leading edge. If there are more than eight chordwise elements on the flap, the second card has the values for the ninth, tenth, etc., elements in the first row. Otherwise the second card has the values for the chordwise row next outboard of the first row, and so on. The DELL value for the leading edge flap area element in each chordwise row must start on a new card. Therefore, there are MSF (or possibly 2 MSF) cards in this item.

The values of DELL are obtained as follows. First the case of a single flap with camber will be discussed; then the case of multiple flaps idealized as a single flap with camber will be treated. The top half of figure 20(b) shows the former and the bottom half the latter. Both are in combination with an unswept, untwisted, untapered wing with dihedral which has its trailing edge cut off to accommodate the trailing edge flaps. The dashed lines represent the thickness envelopes of the wing and flap. Consider the single flap case. At a point P, corresponding to a control point in the flap chordal plane, a tangent to the flap mean surface is constructed, which makes a positive angle δ_ℓ with

the flap root chord as shown. The input value required is DELL = δ_ℓ, radians. Consider the multiple flap case next. Connect the leading edge of the flap component nearest the wing trailing edge to the trailing edge of the aft flap component. This line is the local chord of the idealized flap representing the multiple flaps system. This local chord also lies in the chordal plane of the idealized flap. The chordal plane also contains the root chord of the idealized flap. At a point P, corresponding to a control point in the idealized flap chordal plane, a tangent to the mean surface of the flap component is drawn, which makes positive angle δ_ℓ with the flap root chord as shown. The input value required is DELL = δ_ℓ, radians.

If no flap is presented (MFLAP = 0) or the flap does not have camber (DELLC = 0.0), no cards are required for Item 10.

Item 11

This optional set of data is required only if induced velocities are to be computed at field points adjacent to the wing-flap (MMM $\neq$ 0 in Item 2). The number of cards in this item is MMM. Each card has X, Y, and Z coordinates of a point where the induced velocities are desired. The points need not be in any particular order, although an order might be dictated by the subsequent use of the output in, for instance, an engine-wing-flap interference calculation. If no induced velocities are to be computed (MMM = 0, Item 2), no cards are required for Item 11.

Item 12

The single card of this item contains several quantities. The first is the flap deflection angle, DELD, which must be measured perpendicular to the flap hinge line. If only the streamwise flap angle DLXD is known, angle DELD may be estimated through the average sweep angle of the flap:

$$\tan \text{DELD} = (\tan \text{DLXD})/\cos \psi_{f_{ave}} \qquad (26)$$

Control integer variables KEI and KCP govern options regarding the method of input of the externally induced velocities and the output of control points associated with the vortex lattice, respectively. Control variable NRHS equals the number of cases to be run successively for a given wing

flap combination without recalculating the influence coefficient matrix. For each case, an angle of attack and a set of induced velocities (if applicable) will be specified in Items 13 and 14. A maximum of 10 cases can be treated in this manner.

Item 13

This item specifies the wing angle of attack, ALPHAD, for each of the NRHS cases specified in Item 12 above.

Item 14

The input quantities in this optional item are externally induced perturbation velocities at the control points on the left wing panel and flap. Cards with this input are required only if KEI of Item 12 is different from zero. For each of the cases specified in Item 12, these velocities are read in via cards if KEI = 5; if KEI = 8 a data set generated by the jet-wake program is called and velocities are read in from it. The signs of the perturbation velocity components must be consistent with the wing root chord coordinate system.

The externally induced perturbation velocities must be input in the same order as the control point layout: the first is nearest the wing leading edge and root chord, the succeeding points proceed aft chordwise to the wing trailing edge, then from the leading edge of the next outboard chordwise row aft towards the trailing edge of this row and so forth. The last point on the wing is the control point nearest the tip and wing trailing edge. There are M cards for the wing, where $M = MSW \times NCW$. On the flap, if present, the first point is nearest the flap leading edge and inboard chord, the succeeding points proceed aft chordwise to the flap trailing edge and then from the leading edge of the next outboard chordwise row aft towards the flap trailing edge and so on. As on the wing, the last point is the control point nearest the flap outboard chord and flap trailing edge.

Again, if no external velocities are considered (KEI = 0) no cards are required for this item.

This completes the description of the input and its preparation. The program variables with algebraic symbol and comments are listed below in the order in which they appear in the input deck.

Program Variable	Algebraic Symbol (if applicable)	Comment
M	M	number of control points on wing M = NCW × MSW
MF	MF	number of control points on flap MF = NCF × MSF
J		running index of control points on wing 1 < J < M, also used as overall running index 1 < J < M + MF in Item 13 of the input and also in the output
JF		running index of control points on flap 1 < JF < MF
N		running index of successive cases 1 ≤ N ≤ NRHS
Item 1		any alphanumeric information may be put on this card for identification of the calculation
Item 2		
ALPHLC		ALPHLC = 0.0: wing without camber and twist ALPHLC = 1.0: wing with camber and twist
DELLC		DELLC = 0.0: flap without camber DELLC = 1.0: flap with camber
MMM		number of locations in vicinity of wing-flap at which wing-flap induced velocities are determined (MMM ≤ 50). If MMM = 0, induced velocities are not calculated
MFLAP		MFLAP = 0: flap not present, i.e., wing only MFLAP = 1: flap included
MFSPEC		MFSPEC = 0: flap root chord CRF specified for undeflected flap in Item 4 MFSPEC = 1: flap root chord CRF specified for deflected flap in Item 4. This differentiation is applicable to swept wing-flap combinations only
Item 3		
PSIWLE	$\psi_{W_{LE}}$	wing leading-edge sweep angle measured in the wing planform, positive for sweep back, deg.

Program Variable	Algebraic Symbol (if applicable)	Comment
PSIWTE	$\psi_{w_{TE}}$	wing trailing-edge sweep angle measured in the wing planform, positive for sweep back, degrees
CRW	c	wing root chord, dimensional
SSPAN	b/c	wing semispan, dimensional
PHID	ϕ	wing dihedral, positive for wing tips above root chord, degrees
Item 4		
PSIFLE	$\psi_{f_{LE}}$	flap leading-edge sweep angle measured in the wing planform for the undeflected flap, positive for sweep back, degrees (this angle normally equals $\psi_{w_{TE}}$)
PSIFTE	$\psi_{f_{TE}}$	flap trailing-edge sweep angle measured in the wing planform for the undeflected flap, positive for sweep back, degrees
CRF	c_f	flap root chord measured in the plane of symmetry, dimensional. According to Item 2: if MFSPEC = 0, CRF specified for undeflected flap, if MFSPEC = 1, CRF specified for deflected flap. See the earlier discussion under Item 4
FSSPAN		flap semispan defined as the distance from the plane of symmetry to the flap outboard span, dimensional
XF		X-coordinate in wing coordinate system of the leading edge of the flap root chord, dimensional
ZF		Z-coordinate in wing coordinate system of the leading edge of the flap root chord, dimensional
Item 5		
NCW		number of chordwise vortices on wing, $1 \leq NCW \leq 10$
MSW		number of spanwise vortices on left wing panel, $1 \leq MSW \leq 49$

Program Variable	Algebraic Symbol (if applicable)	Comment
NCF		number of chordwise vortices on flap, $1 \leq NCF \leq 10$
MSF		number of spanwise vortices on left flap $1 \leq MSF \leq 49$
Item 6		
Y(I)	Y(1),Y(2),..., Y(IMAX)	distance parallel to Y-axis from plane of symmetry to outboard trailing leg of I'th wing horseshoe vortex, dimensional ($1 \leq I \leq IMAX$, IMAX = MSW + 1)
Item 7		
YF(IF)	YF(1),YF(2),..., YF(IFMAX)	distance parallel to Y-axis from plane of symmetry to outboard trailing leg of IF'th flap horseshoe vortex, dimensional ($1 \leq IF \leq IFMAX$, IFMAX = MSF + 1). If MFLAP = 0, no input cards necessary
Item 8		
XM YM ZM		coordinates of pitching-moment center in wing coordinate system, dimensional
Item 9		
ALPHAL(J)	$\tan \alpha_\ell(1)$, $\tan \alpha_\ell(2)$, ..., $\tan \alpha_\ell(M)$	tangent of local angle of wing mean surface at J'th control point due to wing twist and camber. See figure 20 for sign convention. $1 \leq J \leq M$, $M \leq 150$. (If ALPHLC = 0.0, no input cards are necessary)
Item 10		
DELL(JF)	$\delta_\ell(1)$, $\delta_\ell(2)$, ..., $\delta_\ell(MF)$	local angle in radians of flap mean surface at JF'th control point due to flap camber. See figure 20 for sign convention. $1 \leq JF \leq MF$, $MF \leq 100$. (If DELLC = 0.0, no input cards necessary)
Item 11		
PMX(MM) PMY(MM) PMZ(MM)		coordinates of locations at which wing-flap induced velocities are computed. $1 \leq MM \leq MMM$, $MMM \leq 50$. If MMM = 0, no input cards are required.

Program Variable	Algebraic Symbol (if applicable)	Comment
Item 12		
DELD	δ_f	flap deflection angle measured perpendicular to hingeline, positive downwards, degrees, see figure 1
KEI		KEI = 0: no externally induced velocities KEI = 5: externally induced velocities read in via cards KEI > 6: externally induced velocities read in from a data set. $(7 \leq KEI \leq 98)$
KCP		KCP = 0: control point coordinates in program output KCP > 6: control point coordinates in program output and data set. $(7 \leq KCP \leq 98)$ NOTE: $KEI \neq KCP$
NRHS		number of successive cases to be treated for the same wing-flap configuration. $1 \leq NRHS \leq 10$
Item 13		
ALPHAD(N)	$\alpha(1), \alpha(2), \ldots, \alpha(NRHS)$	wing root chord angle of attack relative to free stream, degrees, see figure 1. $(1 \leq N \leq NRHS)$
Item 14		
UEI(J,N) VEI(J,N) WEI(J,N)	$\frac{u_i}{V}(1,N), \frac{v_i}{V}(1,N), \frac{w_i}{V}(1,N), \ldots$ $\frac{u_i}{V}(M,N), \frac{v_i}{V}(M,N), \frac{w_i}{V}(M,N)$	this input is read in only if $KEI \neq 0$. The first card contains any alphanumeric information for identification of these data. These are externally induced velocity components at wing control points J, $1 \leq J \leq M$, $M \leq 150$.

Program Variable	Algebraic Symbol (if applicable)	Comment
	$\frac{u_i}{V}(M+1,N)$,	this input required only if MFLAP = 1 and KEI $\neq$ 0. These are externally induced velocity components at flap control points J. $M+1 \leq J \leq M+MF$ (NOTE: $M \leq 150$, $MF \leq 150$ but $M+MF \leq 220$.) For these data, if KEI = 5, input via cards; if KEI = 8, input via data set. There will be N sets of these data for the N successive cases. $1 \leq N \leq NRHS$.
	$\frac{v_i}{V}(M+1,N)$,	
	$\frac{w_i}{V}(M+1,N)$,...	
	$\frac{u_i}{V}(M+MF,N)$,	
	$\frac{v_i}{V}(M+MF,N)$,	
	$\frac{w_i}{V}(M+MF,N)$	

Samples of two input decks are shown in figure 21 illustrating the options concerning externally induced perturbation velocities and flow-field determination. The first input deck shown is for a swept wing with full span, triple slotted flaps and without externally induced velocities. The configuration is shown in figure 22. The vortex lattice on the wing is made up of 20 spanwise rows with 4 vortices on the chord. On the flap there are 20 spanwise rows with 5 vortices on the chord. The 30° swept-back wing is untapered and has zero dihedral. The full span, triple slotted flap system is idealized to a single flap with camber, as shown in figure 22(c). One of the desired results of the calculation is the perturbation flow field determined at eight specified field points for 0° angle of attack. The points lie along a line colinear with a typical centerline location of a turbofan engine that could be hung under the wing.

The second input deck shown in figure 21 concerns the same configuration, but includes perturbation velocities induced by a high-bypass-ratio turbofan engine. The determination of these velocities is described in the jet wake section.

Description of Output

This section describes the output from the wing-flap program. In the following, all items of output are enumerated and the contents briefly described. Two sample outputs are shown in figure 23.

The first page identifies the run and prints the wing-flap geometry data, vortex-lattice layout and the pitching moment center as specified in the input. The flap deflection angle, DELD, is the specified angle perpendicular to the hingeline whereas the streamwise flap deflection angle, DLXD, is calculated by the program. All length dimensions in the output are the same as in input.

The second page shows the wing angle of attack and the identification of the set of externally induced velocities (when applicable) for the flow condition case under consideration. Both are specified in the input. In the first sample case, figure 23(a), the flow conditions only include the wing angle of attack. In the second case, the wing angle of attack and identification of a set of induced velocities are printed under the flow condition heading.

On the next pages of the output, program-computed control point coordinates are listed for the wing and the flap together with mean surface streamwise slopes specified in input as tangents at the control points. The coordinate system associated with the control point locations is the wing coordinate system shown in figure 2. This part of the output also prints the externally induced perturbation velocities. In the first sample case, figure 23(a), these velocities appear as zeros. In the second case, figure 23(b), non-zero values were read in. The order of the output in this item and the next is as follows. J = 1 corresponds to the area element on the left wing panel closest to the wing root chord and nearest the wing leading edge. This starts the first chordwise row. The sequence proceeds towards the wing trailing edge (J = NCW) and then back up to the wing leading edge (J = NCW + 1) for the next chordwise row. This process continues along the semispan for each chordwise row of area elements on the wing until the wing tip is reached. There, the aft element of the last chordwise row on the wing is located closest to the wing tip and nearest the wing trailing edge. On the flap, the sequence starts in a manner analogous to the wing with the first element (J = M + 1) closest to the inboard span of the flap and nearest the flap leading edge.

The process then continues towards the outboard tip of the flap. The aft area element (J = M + MF) of the last chordwise row on the flap is located closest to the flap outboard span and nearest the flap trailing edge.

The next item starts on a new page and provides information concerning the computed horseshoe vortex characteristics. This output includes bound leg midpoint coordinates, bound leg sweep angles and horseshoe vortex half-widths, together with the calculated vortex strengths. Wing angle of attack, ALPHAD, and flap deflection angle, DELD, are again listed in the heading of this output. The output sequence is described above and the coordinates are expressed in the wing root chord coordinate system of figure 2.

The following new page contains aerodynamic performance parameters computed by the program. The wing and flap lift coefficients, and the sum of the two, C_L, are referenced with respect to the wing planform area, SREF. The pitching moment coefficient, C_m, is referenced with respect to SREF and the wing average chord, CAVE. Both reference quantities are listed in this output also. The spanload coefficient, $c_\ell c/c_L c_{ave}$, is referenced with respect to the wing lift coefficient and CAVE for spanloads on the wing. Spanloads on the flap are referenced with respect to the flap lift coefficient and CAVE. These values of spanloads are listed for each chordwise row of area elements on the wing and flap starting nearest the wing root chord and flap inboard span respectively. The last line provides a breakdown of the pitching moment and induced drag in terms of the wing and flap contributions. The total induced drag, C_D, is also listed by itself and in combination with the total lift, C_L. Both parameters are calculated on the basis of equations (9) and (10).

The last and optional output item is called for by MMM $\neq$ 0 in Item 2 of the input and starts on a new page. This output includes coordinates of the locations at which the components of wing-flap induced velocities are computed and the induced velocity components. The sequence of this output is dictated by the sequence of the specified field point coordinates in Item 11 of the input.

Program Listing

The wing-flap vortex-lattice program is written in Fortran IV language for the IBM 360/67 computer. The computer consists of the main program and three subroutines.

Program	Identification	Page No.
MAINP1	WF01	53
LOAD1	WF02	65
INFWW	WF03	73
INVERS	WF04	75

```
C                                                                       WF01 001
C     THIS PROGRAM CALLS FOR SUBROUTINES LOAD1, INFWW, INVERS           WF01 002
C                                                                       WF01 003
C     WING-FLAP VORTEX LATTICE PROGRAM                                  WF01 004
C                                                                       WF01 005
C                                                                       WF01 006
      DIMENSION          SLDCO(50),SECLIF(50),FSLDCO(50),FECLIF(50),    WF01 007
     1TITLE(10,20),        TALK(20),ALPHAL(150),DELL(150)               WF01 008
C                                                                       WF01 009
      DIMENSION CIR(220,10),UEI(220,10),VEI(220,10),WEI(220,10),        WF01 010
     1          ALPHAD(10),ALPHA(10)                                    WF01 011
C                                                                       WF01 012
      DIMENSION                          UI(50),VI(50),WI(50),FVN(220,WF01 013
     1230),FUW(2),FVW(2),FWW(2),FUF(2),FVF(2),FWF(2)                   WF01 014
C                                                                       WF01 015
      DIMENSION PTLX(150),PTLY(150),PTLZ(150),PVX(150),PCX(150),PVY(150)WF01 016
     1,PVZ(150),PVFX(150),PCFX(150),PVFY(150),PVFZ(150),PCFZ(150),PTLFX(WF01 017
     2150),PTLFY(150),PTLFZ(150),PMX(50),PMY(50),PMZ(50)               WF01 018
C                                                                       WF01 019
      DIMENSION SWPVVP(150),SWPVVF(150),SWPC(10),SWPCF(10),SWPV(150),   WF01 020
     1SF(150),SW(150),Y(50),YF(50),YFC(50),YLOC(50),YLOCF(50),SUMY(50), WF01 021
     2SUMYF(50),CHLOCB(50),FCHLOB(50)                                  WF01 022
C                                                                       WF01 023
      DIMENSION YWW(2),YWF(2),YWFP(2),YFW(2),YFF(2),YFFP(2),YWM(2),YFM(2WF01 024
     1),YFMP(2)                                                        WF01 025
C                                                                       WF01 026
C                                                                       WF01 027
      COMMON CIR,SUMLIF,FUMLIF,CLTOT,TOTMOM,SLDCO,SECLIF,FSLDCO,FECLIF  WF01 028
C                                                                       WF01 029
      COMMON WMOM,FMOM,SUMDRG,FUMDRG,DRGTOT,CDOCLS                      WF01 030
C                                                                       WF01 031
      COMMON PTLX,PTLY,PTLZ,PVX,PVY,PVZ,PVFX,PVFY,PVFZ,PTLFX,PTLFY,PTLFZWF01 032
C                                                                       WF01 033
      COMMON SWPWLE,SWPWTE,SWPFLE,SWPFTE,SWPVVP,SWPVVF,SF,SW,Y,YF       WF01 034
C                                                                       WF01 035
      COMMON CRW,SSPAN,CRF,FSSPAN,PHI,PHIF,CSPHIF,CSPHI,ALPHA,DLX,COS+LXWF01 036
     1,SINDLX,SREF,CAVE,XM,ZM,SPHIF,SPHI                               WF01 037
C                                                                       WF01 038
      COMMON NCW,M,MP1,MF,MPMF,IFMAX,IMAX,NCF,MFLAP                     WF01 039
C                                                                       WF01 040
      COMMON AE,YFC,TANTH8,TANTH7                                       WF01 041
C                                                                       WF01 042
      COMMON UEI,VEI,WEI                                                WF01 043
C                                                                       WF01 044
      COMMON/INF/BOT                                                    WF01 045
C                                                                       WF01 046
C                                                                       WF01 047
C                                                                       WF01 048
C                                                                       WF01 049
    1 FORMAT (1H1,27X,32HHORSESHOE VORTEX CHARACTERISTICS//10X,17HBOUNDLWF01 050
     1EG MIDPOINT,35X,24HVORTEX STRENGTHS,GAMMA/V/13X,11HCOORDINATES/3X,WF01 051
     21HJ,5X,1HX,9X,1HY,9X,1HZ,5X,10HSWEEP,DEG.,1X,9HSEMIWIDTH,7X,7HALPHWF01 052
     3AD=,F8.4,1H,,5HDELD=,F8.4/2X,13HWING VORTICES/)                   WF01 053
    6 FORMAT (7I5)                                                      WF01 054
    7 FORMAT (8F10.5)                                                   WF01 055
    8 FORMAT (4X,23HTE SWEEP,DEG.          ,F8.4,7X,F8.4)               WF01 056
   13 FORMAT (I4,1X,F9.4,2X,F9.4,2X,F8.4,2X,F8.4,2X,F8.4,12X,F8.4)      WF01 057
   14 FORMAT (1H1, 20A4/)                                               WF01 058
   15 FORMAT(20A4)                                                      WF01 059
   17 FORMAT (1H1, 25H      DETERMINANT IS ZERO)                       WF01 060
   18 FORMAT(/9X,25HTOTAL LIFT COEFFICIENT,CL,10X,30HPITCHING MOMENT COEWF01 061
     1FFICIENT,CM/)                                                     WF01 062
   19 FORMAT ( 10X,F8.4,30X,F8.4)                                       WF01 063
   21 FORMAT (4X,23HDIHEDRAL,DEG.          ,F8.4,7X,F8.4)               WF01 064
```

```
   22 FORMAT (4X,23HCHORD AT WING ROOT      ,F8.4,7X,F8.4)                  WF01 065
   23 FORMAT (3X,I3,7X,F8.4,6X,F8.4,10X,F8.4,15X,F8.4)                      WF01 066
   24 FORMAT ( 3X,4HWING/)                                                  WF01 067
   25 FORMAT (4X,23HSEMISPAN                ,F8.4,7X,F8.4/)                 WF01 068
   28 FORMAT (/24X,20HREFERENCE QUANTITIES//5X,11HWING SPAN,B,4X,23HWINGWF01 069
     1 PLANFORM AREA,SREF,4X,19HWING AVE.CHORD,CAVE)                        WF01 070
   29 FORMAT (7X,F8.4,8X,F12.4,14X,F8.4)                                    WF01 071
   30 FORMAT (4X,23HLE SWEEP,DEG.           ,F8.4,7X,F8.4)                  WF01 072
   31 FORMAT (/4X,29HUNDEFLECTED FLAP INBOARD SPAN,8X,F8.4)                 WF01 073
   32 FORMAT (2F5.1 ,3I5)                                                   WF01 074
   33 FORMAT (3F10.3)                                                       WF01 075
   34 FORMAT (1H1,4X,36HCONTROL POINT COORDINATES AND SLOPES,11X,           WF01 076
     1 29HEXTERNALLY INDUCED VELOCITIES)                                    WF01 077
   35 FORMAT (I4,1X,F9.4,2X,F9.4,2X,F8.4,2X,F8.4,6X,F9.5,1X,F9.5,1X,F9.5WF01 078
     1,1X,F9.4,2X,F9.4,2X,F8.4)                                             WF01 079
   36 FORMAT (1H1,9X,66HVELOCITIES INDUCED AT SPECIFIED POINTS IN THE VIWF01 080
     1CINITY OF THE WING//3X,1HN,6X,1HX,9X,1HY,9X,1HZ,13X,3HU/V,7X,3HV/VWF01 081
     2,7X,3HW/V/)                                                           WF01 082
   37 FORMAT (4X,30HUNDEFLECTED FLAP OUTBOARD SPAN,7X,F8.4//)               WF01 083
   38 FORMAT (4X,30HPITCHING MOMENT CENTER      ,2X,F8.4,2X,F8.4,2X,F8WF01 084
     1.4)                                                                   WF01 085
   39 FORMAT (2X,I2,3X,F8.4,2X,F8.4,2X,F8.4,7X,F8.5,2X,F8.5,2X,F8.5)        WF01 086
   43 FORMAT (3E13.6)                                                       WF01 087
   47 FORMAT (/2X,19HWING CONTROL POINTS/)                                  WF01 088
   51 FORMAT (34X,12HMEAN SURFACE/3X,1HJ,5X,1HX,9X,1HY,9X,1HZ,7X,5HSLOPEWF01 089
     1,10X,3HU/V,7X,3HV/V,7X,3HW/V)                                         WF01 090
   58 FORMAT (4X,23HCHORDWISE VORTICES      ,2X,I3,12X,I3)                  WF01 091
   59 FORMAT (//34X,13HGEOMETRY DATA//28X,4HWING,11X,4HFLAP/)               WF01 092
   60 FORMAT (4X,23HSPANWISE VORTICES       ,2X,I3,12X,I3)                  WF01 093
   64 FORMAT (/3X,4HFLAP)                                                   WF01 094
   65 FORMAT(/24X,26HSPANWISE LOAD DISTRIBUTION//2X,7HSTATION,5X,7HY/(B/WF01 095
     12),5X,13HLOCAL CHORD,C,6X,12HCL*C/CL*CAVE,14X,10HCL*C/(2*B)//)        WF01 096
   66 FORMAT (4X,27HANGLE OF ATTACK,ALPHA ,DEG.,15X,F8.4//)                 WF01 097
   67 FORMAT (//4X,27HFLAP ANGLE,DELD,DEG.        ,15X,F8.4)                WF01 098
   68 FORMAT (4X,37HCALC. STREAMWISE FLAP ANGLE,DLXD,DEG.,5X,F8.4)          WF01 099
   72 FORMAT (1H1,15X,39HAERODYNAMIC LOADING RESULTS FOR ALPHA =,F10.5,     WF01 100
     11X,4HDEG.                                        ///9X,21HWING LIFT CWF01 101
     1OEFFICIENT,20X,21HFLAP LIFT COEFFICIENT/)                             WF01 102
   73 FORMAT (//39X,21HX         Y         Z)                               WF01 103
   74 FORMAT (/2X,19HFLAP CONTROL POINTS)                                   WF01 104
   76 FORMAT (/2X,13HFLAP VORTICES/)                                        WF01 105
   78 FORMAT(1H1,20X,26HFLOW CONDITIONS FOR CASE ,I3//)                     WF01 106
   79 FORMAT (/4X,63HCOORDS. OF ROOTCHORD NOSE OF FLAP EXTENDED TO PLANEWF01 107
     1 OF SYMMETRY/39X,                                                     WF01 108
     2         21HX                    Z/36X,F8.4,12X,F8.4)                WF01 109
   81 FORMAT (1F10.5,3I10)                                                  WF01 110
   83 FORMAT (///2X,7HCM,WING,8X,7HCM,FLAP,8X,7HCD,WING,8X,7HCD,FLAP,9X,WF01 111
     12HCD,11X,8HCD/CL*CL/)                                                 WF01 112
   84 FORMAT (F10.5,5X,F10.5,5X,F10.5,5X,F10.5,5X,F10.5,5X,F10.5)           WF01 113
   85 FORMAT (////20A4//)                                                   WF01 114
C                                                                           WF01 115
C     INITIALIZE                                                            WF01 116
C                                                                           WF01 117
      DO 3008 J=1,150                                                       WF01 118
 3008 ALPHAL(J)=0.0                                                         WF01 119
      DO 3080 JF=1,100                                                      WF01 120
 3080 DELL(JF)=0.0                                                          WF01 121
C                                                                           WF01 122
 1010 READ (5,15) TALK                                                      WF01 123
C                                                                           WF01 124
C     CONTROL VARIABLES READ IN                                             WF01 125
C                                                                           WF01 126
      READ (5,32) ALPHLC,DELLC,MMM,MFLAP,MFSPEC                             WF01 127
C                                                                           WF01 128
C     WING GEOMETRY SPECIFIED IN WING PLATFORM PLANE                        WF01 129
C                                                                           WF01 130
```

```
      READ (5,7) PSIWLE,PSIWTE,CRW,SSPAN,PHID                          WF01 131
      BOT= SSPAN                                                       WF01 132
C                                                                      WF01 133
C     FLAP GEOMETRY SPECIFIED IN UNDEFLECTED FLAP PLANFORM PLANE       WF01 134
C     UNDEFLECTED FLAP PLANFORM PLANE IS THE WING PLANFORM PLANE       WF01 135
C                                                                      WF01 136
      READ (5,7) PSIFLE,PSIFTE,CRF,FSSPAN,XF,ZF                        WF01 137
C                                                                      WF01 138
C     SPECIFY VORTEX LATTICE ON WING AND FLAP                          WF01 139
C                                                                      WF01 140
      READ (5,6) NCW,MSW,NCF,MSF                                       WF01 141
C                                                                      WF01 142
      IMAX=MSW+1                                                       WF01 143
      IFMAX=MSF+1                                                      WF01 144
      M=MSW*NCW                                                        WF01 145
      MF=MSF*NCF                                                       WF01 146
      MP1=M+1                                                          WF01 147
      MPMF=M+MF                                                        WF01 148
C                                                                      WF01 149
C     LAY OUT WING VORTEX TAILS ALONG WING SEMISPAN                    WF01 150
C     POSITIVE VALUES FOR LEFT PANEL                                   WF01 151
C                                                                      WF01 152
      READ (5,7) (Y(I),I=1,IMAX)                                       WF01 153
C                                                                      WF01 154
C     LAY OUT FLAP VORTEX TAILS ALONG UNDEFLECTED FLAP SEMI SPAN       WF01 155
C     POSITIVE VALUES FOR LEFT PANEL                                   WF01 156
C                                                                      WF01 157
      IF(MFLAP.EQ.0) GO TO 9912                                        WF01 158
      READ (5,7) (YF(IF),IF=1,IFMAX)                                   WF01 159
 9912 CONTINUE                                                         WF01 160
C                                                                      WF01 161
C     SPECIFY MOMENT CENTER                                            WF01 162
C                                                                      WF01 163
      READ (5,7) XM,YM,ZM                                              WF01 164
C                                                                      WF01 165
C     INPUT LOCAL WING ANGLES DUE TO WING CAMBER AND TWIST             WF01 166
C                                                                      WF01 167
      IF (ALPHLC.EQ.0.0) GO TO 1001                                    WF01 168
      MN=0                                                             WF01 169
      DO 9910 JNW=1,M,NCW                                              WF01 170
      MN=MN+NCW                                                        WF01 171
 9910 READ (5,7) (ALPHAL(J),J=JNW,MN)                                  WF01 172
 1001 CONTINUE                                                         WF01 173
C                                                                      WF01 174
C     INPUT LOCAL FLAP ANGLES DUE TO FLAP CAMBER                       WF01 175
C                                                                      WF01 176
      IF(MFLAP.EQ.0) GO TO 1002                                        WF01 177
      IF (DELLC.EQ.0.0) GO TO 1002                                     WF01 178
      MFN=0                                                            WF01 179
      DO 9911 JNF=1,MF,NCF                                             WF01 180
      MFN=MFN+NCF                                                      WF01 181
 9911 READ (5,7) (DELL(JF),JF=JNF,MFN)                                 WF01 182
 1002 CONTINUE                                                         WF01 183
                                                                       WF01 184
C                                                                      WF01 185
C     DTR=PI/180                                                       WF01 186
      DTR=0.01745329                                                   WF01 187
C                                                                      WF01 188
      SPAN=2.0*SSPAN                                                   WF01 189
      PHI= PHID*DTR                                                    WF01 190
      SPHI=SIN(PHI)                                                    WF01 191
      CSPHI=COS (PHI)                                                  WF01 192
      TANPHI=TAN(PHI)                                                  WF01 193
      SWPWLE=TAN (PSIWLE*DTR)                                          WF01 194
      SWPWTE=TAN (PSIWTE*DTR)                                          WF01 195
```

```
C                                                                       WF01 196
C     FLAP SWEEPS ARE SPECIFIED FOR THE UNDEFLECTED FLAP AND MEASURED   WF01 197
C     IN THE WING PLANFORM PLANE                                        WF01 198
C                                                                       WF01 199
      SWPFLE=TAN (PSIFLE*DTR)                                           WF01 200
      SWPFTE=TAN (PSIFTE*DTR)                                           WF01 201
C                                                                       WF01 202
C     COMPUTE WING L.E. AND WING T.E. SWEEPS IN THE WING CHORDAL PLANE  WF01 203
C                                                                       WF01 204
      SWPWLV=SWPWLE*CSPHI                                               WF01 205
      SWPWTV=SWPWTE*CSPHI                                               WF01 206
      WTV=ATAN(SWPWTV)                                                  WF01 207
      SINWTV=SIN(WTV)                                                   WF01 208
      COSWTV=COS(WTV)                                                   WF01 209
C                                                                       WF01 210
C     COMPUTE UNDEFLECTED FLAP T.E. SWEEP IN WING CHORDAL PLANE         WF01 211
C                                                                       WF01 212
      SWPFTV=SWPFTE*CSPHI                                               WF01 213
      FTE=ATAN(SWPFTV)                                                  WF01 214
C                                                                       WF01 215
C                                                                       WF01 216
C     READ IN COORDINATES OF POINTS AT WHICH  PERTURBATION VELOCITIES   WF01 217
C     INDUCED BY WING FLAP ARE CALCULATED                               WF01 218
C                                                                       WF01 219
      IF(MMM.EQ.0) GO TO 4000                                           WF01 220
      READ (5,33) (PMX(MM),PMY(MM),PMZ(MM),MM=1,MMM)                    WF01 221
 4000 CONTINUE                                                          WF01 222
C                                                                       WF01 223
C     READ IN CERTAIN FIXED QUANTITIES                                  WF01 224
C     DELD= FLAP ANGLE MEASURED PERPENDICULAR TO HINGE LINE,POSITIVE    WF01 225
C     DOWN,DEG.                                                         WF01 226
C     IF KEI=0 NO EXTERNALLY INDUCED VELOCITIES                         WF01 227
C     IF KEI=5 INPUT EXTERNALLY INDUCED VELOCITIES VIA CARDS            WF01 228
C     IF KEI GT.6 INPUT EXTERNALLY INDUCED VELOCITIES VIA DATASET       WF01 229
C     IF KCP=0 CONTROL POINT COORDINATES IN OUTPUT                      WF01 230
C     IF KCP GT.6 CONTROL POINT COORDINATES IN OUTPUT AND IN DATASET    WF01 231
C     NRHS= NUMBER OF SUCCESSIVE CASES TO BE TREATED                    WF01 232
C                                                                       WF01 233
C                                                                       WF01 234
      READ (5,81) DELD,KEI,KCP,NRHS                                     WF01 235
C                                                                       WF01 236
      IF (KEI.LT.0) KEI=0                                               WF01 237
      IF (KCP.LT.7) KCP=0                                               WF01 238
C                                                                       WF01 239
C                                                                       WF01 240
      DO 3081 JC=1,220                                                  WF01 241
      DO 3081 JV=1,230                                                  WF01 242
 3081 FVN(JC,JV)= 0.0                                                   WF01 243
C                                                                       WF01 244
      DO 3082 N=1,NRHS                                                  WF01 245
      DO 3082 JC=1,220                                                  WF01 246
 3082 CIR(JC,N)=0.0                                                     WF01 247
C                                                                       WF01 248
C                                                                       WF01 249
      DEL= DELD*DTR                                                     WF01 250
C                                                                       WF01 251
      SINDEL=SIN(DEL)                                                   WF01 252
      COSDEL=COS(DEL)                                                   WF01 253
      TANDEL=TAN(DEL)                                                   WF01 254
C                                                                       WF01 255
C                                                                       WF01 256
C     CALCULATE ANGLES THETAP NECESSARY FOR THE FLAP DEFLECTION MEASURED WF01 257
C     IN THE X-Z PLANE  DLX, FLAP DIHEDRAL  PHIF, AND FLAP VORTEX LAYOUT WF01 258
C                                                                       WF01 259
```

```
      A1=COSDEL*COSWTV                                                  WF01 260
      C1=-(COSDEL*SINWTV*SPHI+SINDEL*CSPHI)                             WF01 261
      A3=-(SINDEL*COSWTV)                                               WF01 262
      B3=SINDEL*SINWTV*CSPHI+COSDEL*SPHI                                WF01 263
      C3=SINDEL*SINWTV*SPHI-COSDEL*CSPHI                                WF01 264
C                                                                       WF01 265
      THETAP=ARCOS((A3*C1-A1*C3)/((C3*C3+A3*A3)**0.5))                  WF01 266
      SINTHP= SIN(THETAP)                                               WF01 267
      COSTHP= COS(THETAP)                                               WF01 268
C                                                                       WF01 269
C     PIO2=PI/2                                                         WF01 270
      PIO2= 1.57079633                                                  WF01 271
C                                                                       WF01 272
      THETA2=  PIO2-THETAP                                              WF01 273
      THETA7=THETA2-  PIO2+WTV-FTE                                      WF01 274
      THETA8=  PIO2-THETA2                                              WF01 275
      THETA9=THETA2-(  PIO2-WTV)                                        WF01 276
      THET10=  PIO2-THETA9                                              WF01 277
C                                                                       WF01 278
      THETA=  PIO2+THETAP                                               WF01 279
      SINTH=SIN(THETA)                                                  WF01 280
      COSTH=COS(THETA)                                                  WF01 281
C                                                                       WF01 282
C     NOTE, COSTHP=SINTH AND -SINTHP=COSTH                              WF01 283
C                                                                       WF01 284
      DLX= 0.0                                                          WF01 285
      IF (DEL.NE.0.0) DLX= ARCOS(COSTHP*COSDEL*COSWTV+SINTHP*SINWTV)    WF01 286
      SINDLX=SIN(DLX)                                                   WF01 287
      COSDLX=COS(DLX)                                                   WF01 288
      DLXD= DLX*1.0/DTR                                                 WF01 289
C                                                                       WF01 290
      PHIF=ARCOS((A3*A3+C3*C3)/((A3*B3)**2+(A3*A3+C3*C3)**2+(C3*B3)**2)WF01 291
     1**0.5))                                                           WF01 292
      SPHIF=SIN(PHIF)                                                   WF01 293
      CSPHIF=COS(PHIF)                                                  WF01 294
C                                                                       WF01 295
C                                                                       WF01 296
C                                                                       WF01 297
C     GEOMETRY AND VORTEX NUMBERS LAY-OUT OUTPUT                        WF01 298
C                                                                       WF01 299
      WRITE (6,14) TALK                                                 WE01 300
      WRITE (6,59)                                                      WF01 301
      WRITE (6,30) PSIWLE,PSIFLE                                        WF01 302
      WRITE (6,8) PSIWTE,PSIFTE                                         WF01 303
      WRITE (6,21) PHID                                                 WF01 304
      WRITE (6,22) CRW,CRF                                              WF01 305
      WRITE (6,25) SSPAN,FSSPAN                                         WF01 306
      WRITE (6,58) NCW,NCF                                              WF01 307
      WRITE (6,60) MSW,MSF                                              WF01 308
      IF (MFLAP.EQ.0) GO TO 9971                                        WF01 309
      WRITE (6,79) XF,ZF                                                WF01 310
      WRITE (6,31) YF(1)                                                WF01 311
      WRITE (6,37) YF(IFMAX)                                            WF01 312
 9971 CONTINUE                                                          WF01 313
      WRITE (6,73)                                                      WF01 314
      WRITE (6,38) XM,YM,ZM                                             WF01 315
      WRITE (6,67)DELD                                                  WF01 316
      WRITE (6,68) DLXD                                                 WF01 317
C                                                                       WF01 318
C     LAY-OUT VORTEX BOUND LEG MIDPOINTS AND CONTROL POINTS ON THE WING WF01 319
C                                                                       WF01 320
      D=NCW                                                             WF01 321
      DO 701 I=2,IMAX                                                   WF01 322
      SUMY(I)=(Y(I)+Y(I-1))/2.0                                         WF01 323
      YLOC(I)=SUMY(I)/SSPAN                                             WF01 324
```

```
      DO 720 JCW=1,NCW                                                  WF01 325
      A=JCW                                                             WF01 326
      SWPC(JCW)=SWPWLE-((A-0.25)/D)*(SWPWLE-SWPWTE)                     WF01 327
      J=(I-2)*NCW+JCW                                                   WF01 328
      SWPV(J)=  SWPWLE-((A-0.75)/D)*(SWPWLE-SWPWTE)                     WF01 329
C                                                                       WF01 330
C     DISTINCTION BETWEEN SWEEP IN CHORDAL(SWPVVP) AND PLANFORM(SWPV)   WF01 331
C     PLANES                                                            WF01 332
C                                                                       WF01 333
      SWPVVP(J)=SWPV(J)*CSPHI                                           WF01 334
      SWPVVP(J)= ATAN (SWPVVP(J))                                       WF01 335
C                                                                       WF01 336
C     WING VORTEX HALFWIDTH=SW                                          WF01 337
C                                                                       WF01 338
      SW(J)=(Y(I)-Y(I-1))/(2.0*CSPHI)                                   WF01 339
      PVX(J)=-((A-0.75)*(CRW/D))-(SUMY(I)*SWPV(J))                      WF01 340
      PVY(J)=-SUMY(I)                                                   WF01 341
      PVZ(J)=-SUMY(I)*TANPHI                                            WF01 342
      PCX(J)=-((A-0.25)*(CRW/D))-(SUMY(I)*SWPC(JCW))                    WF01 343
C                                                                       WF01 344
C     COORDINATES OF 3/4 CHORD ELEMENTAL PANEL LEFT SIDE POINT,PTL      WF01 345
C                                                                       WF01 346
      PTLX(J)=-((A-0.25)*(CRW/D))-(Y(I)*SWPC(JCW))                      WF01 347
      PTLY(J)=-Y(I)                                                     WF01 348
      PTLZ(J)=-Y(I)*TANPHI                                              WF01 349
  720 CONTINUE                                                          WF01 350
  701 CONTINUE                                                          WF01 351
C                                                                       WF01 352
      IF(MFLAP.EQ.0) GO TO 9913                                         WF01 353
C                                                                       WF01 354
C     LAY-OUT VORTEX BOUNDLEG MID POINTS AND CONTROL POINTS ON THE FLAP WF01 355
C                                                                       WF01 356
C                                                                       WF01 357
      TANTH7=TAN(THETA7)                                                WF01 358
      COSTH8=COS(THETA8)                                                WF01 359
      TANTH8=TAN(THETA8)                                                WF01 360
      COSTH9=COS(THETA9)                                                WF01 361
      COST10=COS(THET10)                                                WF01 362
C                                                                       WF01 363
C     AE IS INTERSECTION OF DEFLECTED FLAP PLANE AND XZ PLANE           WF01 364
C                                                                       WF01 365
      IF (MFSPEC.EQ.1) GO TO 6970                                       WF01 366
      AE=CRF*(COSTH9+COST10*TANTH7)                                     WF01 367
      GO TO 6971                                                        WF01 368
 6970 AE=CRF                                                            WF01 369
 6971 CONTINUE                                                          WF01 370
C                                                                       WF01 371
C     YFC....DISTANCE FROM FLAP X-Z PLANE TO LEFT TRAILING LEG OF       WF01 372
C     HORSE SHOE VORTEX ON DEFLECTED FLAP                               WF01 373
C                                                                       WF01 374
      E=NCF                                                             WF01 375
      YFC(1 )=(YF(1 )*COSTH8)/(CSPHI*COSWTV)                            WF01 376
      DO 702 IF=2,IFMAX                                                 WF01 377
      YFC(IF)=(YF(IF)*COSTH8)/(CSPHI*COSWTV)                            WF01 378
      SUMYF(IF)=(YFC(IF)+YFC(IF-1))/2.0                                 WF01 379
      YLOCF(IF)=SUMYF(IF)/ SSPAN                                        WF01 380
      DO 721 JCF=1,NCF                                                  WF01 381
      B=JCF                                                             WF01 382
      JF=(IF-2)*NCF+JCF                                                 WF01 383
      SWPVVF(JF)= TANTH8-((B-0.75)/E)*(TANTH8+TANTH7)                   WF01 384
      SWPCF(JCF)= TANTH8-((B-0.25)/E)*(TANTH8+TANTH7)                   WF01 385
C                                                                       WF01 386
C     SF IS FLAP VORTEX HALFWIDTH                                       WF01 387
C                                                                       WF01 388
      SF(JF)=(YFC(IF)-YFC(IF-1))/2.0                                    WF01 389
```

```
C                                                                       WF01 390
      PVFX(JF)=XF                                                       WF01 391
     1          -(SUMYF(IF)*SINWTV/COSTH8)-(((B-0.75)/E)*AE+SUMYF(IF)* WF01 392
     1SWPVVF(JF)-SUMYF(IF)*TANTH8)*COSDLX                               WF01 393
      PVFY(JF)=-SUMYF(IF)*(COSWTV*CSPHI/COSTH8)                         WF01 394
      PVFZ(JF)=ZF                                                       WF01 395
     1          -SUMYF(IF)*(COSWTV*SPHI/COSTH8)+(((B-0.75)/E)*AE+SUMYF(IFWF01 396
     1)*SWPVVF(JF)-SUMYF(IF)*TANTH8)*SINDLX                             WF01 397
      PCFX(JF)=XF                                                       WF01 398
     1          -(SUMYF(IF)*SINWTV/COSTH8)-(((B-0.25)/E)*AE+SUMYF(IF)* WF01 399
     1SWPCF(JCF)-SUMYF(IF)*TANTH8)*COSDLX                               WF01 400
      PCFZ(JF)=ZF                                                       WF01 401
     1          -SUMYF(IF)*(COSWTV*SPHI/COSTH8)+(((B-0.25)/E)*AE+SUMYF(IFWF01 402
     1)*SWPCF(JCF)-SUMYF(IF)*TANTH8)*SINDLX                             WF01 403
C                                                                       WF01 404
C     COORDINATES OF FLAP ELEMENTAL PANEL 3/4 CHORD POINT ON THE LEFT   WF01 405
C     SIDE                                                              WF01 406
C                                                                       WF01 407
      PTLFX(JF)= XF                                                     WF01 408
     1          -(YFC(IF)*SINWTV/COSTH8)-(((B-0.25)/E)*AE+YFC(IF)*     WF01 409
     1SWPCF(JCF)-YFC(IF)*TANTH8)*COSDLX                                 WF01 410
      PTLFY(JF)=-YFC(IF)*(COSWTV*CSPHI/COSTH8)                          WF01 411
      PTLFZ(JF)=ZF                                                      WF01 412
     1          -YFC(IF)*(COSWTV*SPHI/COSTH8)+(((B-0.25)/E)*AE+YFC(IF)*SWF01 413
     1WPCF(JCF)-YFC(IF)*TANTH8)*SINDLX                                  WF01 414
C                                                                       WF01 415
      SWPVVF(JF)= ATAN (SWPVVF(JF))                                     WF01 416
  721 CONTINUE                                                          WF01 417
  702 CONTINUE                                                          WF01 418
 9913 CONTINUE                                                          WF01 419
C                                                                       WF01 420
C                                                                       WF01 421
C                                                                       WF01 422
C     GENERATE DATA SET FOR CONTROL POINT COORDINATES                   WF01 423
C                                                                       WF01 424
      IF ( KCP.EQ.0) GO TO 875                                          WF01 425
      DO 876 J=1,M                                                      WF01 426
  876 WRITE (KCP,7) PCX(J),PVY(J),PVZ(J)                                WF01 427
      IF (MFLAP.EQ.0) GO TO 875                                         WF01 428
      DO 877 J=MP1,MPMF                                                 WF01 429
      JF=J-M                                                            WF01 430
  877 WRITE (KCP ,7) PCFX(JF),PVFY(JF),PCFZ(JF)                         WF01 431
  875 CONTINUE                                                          WF01 432
C                                                                       WF01 433
C     BUILD UP L.H.S. OF BOUNDARY CONDITION, THE COEFFICIENT MATRIX     WF01 434
C                                                                       WF01 435
C     CONTROL POINTS ON WING, VORTICES ON WING                          WF01 436
C                                                                       WF01 437
      DO 212 JC=1,M                                                     WF01 438
      DO 212 JV=1,M                                                     WF01 439
      XWW=PCX(JC)-PVX(JV)                                               WF01 440
      YWW(1)=PVY(JC)-PVY(JV)                                            WF01 441
      YWW(2)=PVY(JC)+PVY(JV)                                            WF01 442
      ZWW=PVZ(JC)-PVZ(JV)                                               WF01 443
      DO 261 I=1,2                                                      WF01 444
      CALL INFWW(SWPVVP(JV),PHI,XWW,YWW(I),ZWW,SW(JV),FUW(I),FVW(I),    WF01 445
     1FWW(I))                                                           WF01 446
      SWPVVP(JV)=-SWPVVP(JV)                                            WF01 447
      PHI=-PHI                                                          WF01 448
  261 CONTINUE                                                          WF01 449
      FVN(JC,JV)=(FWW(1)+FWW(2))*CSPHI-(FVW(1)+FVW(2))*SPHI             WF01 450
  212 CONTINUE                                                          WF01 451
C                                                                       WF01 452
C     CONTROL POINTS ON WING, VORTICES ON FLAP                          WF01 453
C                                                                       WF01 454
```

```
      IF (MFLAP.EQ.0) GO TO 9914                                        WF01 455
      DO 312 JC=1,M                                                     WF01 456
      DO 312 JV=MP1,MPMF                                                WF01 457
      JVF=JV-M                                                          WF01 458
      XWF=PCX(JC)-PVFX(JVF)                                             WF01 459
      YWF(1)=PVY(JC)-PVFY(JVF)                                          WF01 460
      YWF(2)=PVY(JC)+PVFY(JVF)                                          WF01 461
      ZWF=PVZ(JC)-PVFZ(JVF)                                             WF01 462
C                                                                       WF01 463
C     TRANSFORM COORDINATES, ROTATION THROUGH -DLX DEGREES              WF01 464
C                                                                       WF01 465
      XWFP=XWF*COSDLX-ZWF*SINDLX                                        WF01 466
      YWFP(1)=YWF(1)                                                    WF01 467
      YWFP(2)=YWF(2)                                                    WF01 468
      ZWFP=XWF*SINDLX+ZWF*COSDLX                                        WF01 469
C                                                                       WF01 470
      DO 262 I=1,2                                                      WF01 471
      CALL INFWW(SWPVVF(JVF),PHIF,XWFP,YWFP(I),ZWFP,SF(JVF),FUF(I),FVF(IWF01 472
     1),FWF(I))                                                         WF01 473
      SWPVVF(JVF)=-SWPVVF(JVF)                                          WF01 474
      PHIF=-PHIF                                                        WF01 475
  262 CONTINUE                                                          WF01 476
      FVN(JC,JV)=(FWF(1)+FWF(2))*CSPHI*COSDLX-(FUF(1)+FUF(2))*CSPHI*SINDWF01 477
     1LX-(FVF(1)+FVF(2))*SPHI                                           WF01 478
  312 CONTINUE                                                          WF01 479
C                                                                       WF01 480
C     CONTROL POINTS ON FLAP, VORTICES ON WING                          WF01 481
C                                                                       WF01 482
      DO 412 JC=MP1,MPMF                                                WF01 483
      JCF=JC-M                                                          WF01 484
      DO 412 JV=1,M                                                     WF01 485
      XFW=PCFX(JCF)-PVX(JV)                                             WF01 486
      YFW(1)=PVFY(JCF)-PVY(JV)                                          WF01 487
      YFW(2)=PVFY(JCF)+PVY(JV)                                          WF01 488
      ZFW=PCFZ(JCF)-PVZ(JV)                                             WF01 489
      DO 263 I=1,2                                                      WF01 490
      CALL INFWW(SWPVVP(JV),PHI,XFW,YFW(I),ZFW,SW(JV),FUW(I),FVW(I),    WF01 491
     1FWW(I))                                                           WF01 492
      SWPVVP(JV)=-SWPVVP(JV)                                            WF01 493
      PHI=-PHI                                                          WF01 494
  263 CONTINUE                                                          WF01 495
      FVN(JC,JV)=(FWW(1)+FWW(2))*COS(DLX+DELL(JCF))*CSPHIF+(FUW(1)+FUW  WF01 496
     1(2))*SIN(DLX+DELL(JCF))*CSPHIF-(FVW(1)+FVW(2))*SPHIF*             WF01 497
     2COS(DLX+DELL(JCF))                                                WF01 498
  412 CONTINUE                                                          WF01 499
C                                                                       WF01 500
C     CONTROL POINTS ON FLAP, VORTICES ON FLAP                          WF01 501
C                                                                       WF01 502
      DO 512 JC=MP1,MPMF                                                WF01 503
      JCF=JC-M                                                          WF01 504
      DO 512 JV=MP1,MPMF                                                WF01 505
      JVF=JV-M                                                          WF01 506
      XFF=PCFX(JCF)-PVFX(JVF)                                           WF01 507
      YFF(1)=PVFY(JCF)-PVFY(JVF)                                        WF01 508
      YFF(2)=PVFY(JCF)+PVFY(JVF)                                        WF01 509
      ZFF=PCFZ(JCF)-PVFZ(JVF)                                           WF01 510
C                                                                       WF01 511
C     TRANSFORM COORDINATES, ROTATION THROUGH -DLX DEGREES              WF01 512
C                                                                       WF01 513
      XFFP=XFF*COSDLX-ZFF*SINDLX                                        WF01 514
      YFFP(1)=YFF(1)                                                    WF01 515
      YFFP(2)=YFF(2)                                                    WF01 516
      ZFFP=XFF*SINDLX+ZFF*COSDLX                                        WF01 517
C                                                                       WF01 518
```

```
      DO 264 I=1,2                                                      WF01 519
      CALL INFWW(SWPVVF(JVF),PHIF,XFFP,YFFP(I),ZFFP,SF(JVF),FUF(I),FVF(IWF01 520
     1),FWF(I))                                                         WF01 521
      SWPVVF(JVF)=-SWPVVF(JVF)                                          WF01 522
      PHIF=-PHIF                                                        WF01 523
  264 CONTINUE                                                          WF01 524
      FVN(JC,JV)=(FWF(1)+FWF(2))*CSPHIF*COS(DELL(JCF))-(FVF(1)+FVF(2))* WF01 525
     1SPHIF*COS(DELL(JCF))                                              WF01 526
  512 CONTINUE                                                          WF01 527
 9914 CONTINUE                                                          WF01 528
C                                                                       WF01 529
C                                                                       WF01 530
C                                                                       WF01 531
C     READ IN ANGLE OF ATTACK,DEG.,FOR SUCCESSIVE CASES                 WF01 532
C                                                                       WF01 533
      DO 1006 N=1,NRHS                                                  WF01 534
      READ (5,7) ALPHAD(N)                                              WF01 535
 1006 ALPHA(N)=ALPHAD(N)*DTR                                            WF01 536
C                                                                       WF01 537
C     READ IN ENGINE INDUCED PERTURBATION VELOCITIES FOR SUCCESSIVE     WF01 538
C    1CASES FROM MULTIPLE DATASETS                                      WF01 539
C                                                                       WF01 540
      IF (KEI) 1004,1004,1005                                           WF01 541
 1005 DO 7011 N=1,NRHS                                                  WF01 542
      READ (KEI,15) (TITLE(N,JI),JI=1,20)                               WF01 543
      DO 7001 J=1,MPMF                                                  WF01 544
 7001 READ (KEI,43) UEI(J,N),VEI(J,N),WEI(J,N)                          WF01 545
      IF (KEI.EQ.5) GO TO 7011                                          WF01 546
      READ (KEI,43,END=7011)                                            WF01 547
 7011 CONTINUE                                                          WF01 548
C                                                                       WF01 549
      GO TO 1003                                                        WF01 550
 1004 DO 7003 N=1,NRHS                                                  WF01 551
      DO 7003 J=1,MPMF                                                  WF01 552
      UEI(J,N)=0.0                                                      WF01 553
      VEI(J,N)=0.0                                                      WF01 554
 7003 WEI(J,N)=0.0                                                      WF01 555
 1003 CONTINUE                                                          WF01 556
C                                                                       WF01 557
C                                                                       WF01 558
C     CONTROL POINTS ON THE WING                                        WF01 559
C                                                                       WF01 560
      DO 2612 N=1,NRHS                                                  WF01 561
      MPMFPN=M+MF+N                                                     WF01 562
      DO 2612 JC=1,M                                                    WF01 563
 2612 FVN(JC,MPMFPN)=12.566371*(SIN(ALPHA(N)+ALPHAL(JC))*CSPHI+         WF01 564
     1VEI(JC,N)*SPHI-(UEI(JC,N)*ALPHAL(JC)+WEI(JC,N))*CSPHI)            WF01 565
C                                                                       WF01 566
C     CONTROL POINTS ON THE FLAP                                        WF01 567
C                                                                       WF01 568
      IF (MFLAP.EQ.0) GO TO 9915                                        WF01 569
      DO 2613 N=1,NRHS                                                  WF01 570
      MPMFPN=M+MF+N                                                     WF01 571
      DO 2613 JC=MP1,MPMF                                               WF01 572
      JCF=JC-M                                                          WF01 573
 2613 FVN(JC,MPMFPN)=12.566371*(SIN(ALPHA(N)+DLX+DELL(JCF))*CSPHIF+     WF01 574
     1VEI(JC,N)*SPHIF*COS(DLX+DELL(JCF))-(UEI(JC,N)*SIN(DLX+DELL(JCF))+ WF01 575
     2WEI(JC,N)*COS(DLX+DELL(JCF)))*CSPHIF)                             WF01 576
 9915 CONTINUE                                                          WF01 577
C                                                                       WF01 578
C     SOLVE FOR UNKNOWN VORTEX STRENGTHS                                WF01 579
C                                                                       WF01 580
C                                                                       WF01 581
C                                                                       WF01 582
      CALL INVERS(FVN,NRHS,MPMF,220,230)                                WF01 583
C                                                                       WF01 584
```

```
      DO 9812 N=1,NRHS                                                  WF01 585
      MPMFPN=M+MF+N                                                     WF01 586
      DO 9812 JC=1,MPMF                                                 WF01 587
 9812 CIR(JC,N)=FVN(JC,MPMFPN)                                          WF01 588
C                                                                       WF01 589
C     ALL OF THE FOLLOWING OPERATIONS PERFORMED FOR EACH SUCCESSIVE CASE WF01 590
C                                                                       WF01 591
      DO 1000 N=1,NRHS                                                  WF01 592
      WRITE (6,78) N                                                    WF01 593
      WRITE (6,66) ALPHAD(N)                                            WF01 594
      IF (KEI.GT.6) WRITE (6,85) (TITLE(N,J),J=1,20)                    WF01 595
C                                                                       WF01 596
      IF (MMM.EQ.0) GO TO 4001                                          WF01 597
C                                                                       WF01 598
C     COMPUTE INDUCED VELOCITIES AT POINTS (PMX,PMY,PMZ) DUE TO WING    WF01 599
C     VORTICES                                                          WF01 600
C                                                                       WF01 601
      DO 5000 JC=1,MMM                                                  WF01 602
      UI(JC)=0.0                                                        WF01 603
      VI(JC)=0.0                                                        WF01 604
      WI(JC)=0.0                                                        WF01 605
      DO 5000 JV=1,M                                                    WF01 606
      XWM=PMX(JC)-PVX(JV)                                               WF01 607
      YWM(1)=PMY(JC)-PVY(JV)                                            WF01 608
      YWM(2)=PMY(JC)+PVY(JV)                                            WF01 609
      ZWM=PMZ(JC)-PVZ(JV)                                               WF01 610
      DO 1261 I=1,2                                                     WF01 611
      CALL INFWW (SWPVVP(JV),PHI,XWM,YWM(I),ZWM,SW(JV),FUW(I),FVW(I),FWWWF01 612
     1(I))                                                              WF01 613
      SWPVVP(JV)=-SWPVVP(JV)                                            WF01 614
      PHI=-PHI                                                          WF01 615
 1261 CONTINUE                                                          WF01 616
      UI(JC)=UI(JC)+((FUW(1)+FUW(2))*CIR(JV,N))/12.566371               WF01 617
      VI(JC)=VI(JC)+((FVW(1)+FVW(2))*CIR(JV,N))/12.566371               WF01 618
      WI(JC)=WI(JC)+((FWW(1)+FWW(2))*CIR(JV,N))/12.566371               WF01 619
 5000 CONTINUE                                                          WF01 620
C                                                                       WF01 621
C     COMPUTE INDUCED VELOCITIES AT POINTS (PMX,PMY,PMZ) DUE TO FLAP    WF01 622
C     VORTICES                                                          WF01 623
C                                                                       WF01 624
      IF(MFLAP.EQ.0) GO TO 9916                                         WF01 625
      DO 5010 JC=1,MMM                                                  WF01 626
      DO 5010 JV=MP1,MPMF                                               WF01 627
      JVF=JV-M                                                          WF01 628
      XFM=PMX(JC)-PVFX(JVF)                                             WF01 629
      YFM(1)=PMY(JC)-PVFY(JVF)                                          WF01 630
      YFM(2)=PMY(JC)+PVFY(JVF)                                          WF01 631
      ZFM=PMZ(JC)-PVFZ(JVF)                                             WF01 632
C                                                                       WF01 633
C     TRANSFORM COORDINATES, ROTATION THROUGH -DLX DEGREES              WF01 634
C                                                                       WF01 635
      XFMP=XFM*COSDLX-ZFM*SINDLX                                        WF01 636
      YFMP(1)=YFM(1)                                                    WF01 637
      YFMP(2)=YFM(2)                                                    WF01 638
      ZFMP=XFM*SINDLX+ZFM*COSDLX                                        WF01 639
      DO 1271 I=1,2                                                     WF01 640
      CALL INFWW (SWPVVF(JVF),PHIF,XFMP,YFMP(I),ZFMP,SF(JVF),FUF(I),    WF01 641
     1FVF(I),FWF(I))                                                    WF01 642
      SWPVVF(JVF)=-SWPVVF(JVF)                                          WF01 643
      PHIF=-PHIF                                                        WF01 644
 1271 CONTINUE                                                          WF01 645
      UI(JC)=UI(JC)+(((FUF(1)+FUF(2))*COSDLX+(FWF(1)+FWF(2))*SINDLX)*CIRWF01 646
     1(JV,N))/12.566371                                                 WF01 647
      VI(JC)=VI(JC)+((FVF(1)+FVF(2))*CIR(JV,N))/12.566371               WF01 648
```

```
      WI(JC)=WI(JC)+(((FWF(1)+FWF(2))*COSDLX-(FUF(1)+FUF(2))*SINDLX)*CIRWF01 649
     1(JV,N))/12.566371                                                 WF01 650
 5010 CONTINUE                                                          WF01 651
 9916 CONTINUE                                                          WF01 652
 4001 CONTINUE                                                          WF01 653
C                                                                       WF01 654
C     LOADING CALCULATIONS FOLLOW                                       WF01 655
C                                                                       WF01 656
C                                                                       WF01 657
      CALL LOAD1(N)                                                     WF01 658
C                                                                       WF01 659
C                                                                       WF01 660
C     CONTROL POINTS COORDINATES, MEAN SURFACE SLOPES AND EXTERNALLY    WF01 661
C     INDUCED VELOCITIES OUTPUT                                         WF01 662
C                                                                       WF01 663
      WRITE (6,34)                                                      WF01 664
      WRITE (6,51)                                                      WF01 665
      WRITE (6,47)                                                      WF01 666
C                                                                       WF01 667
      DO 6001 J=1,M                                                     WF01 668
 6001 WRITE (6,35) J,PCX(J),PVY(J),PVZ(J),ALPHAL(J),UEI(J,N),VEI(J,N),  WF01 669
     1WEI(J,N)                                                          WF01 670
C                                                                       WF01 671
      IF(MFLAP.EQ.0) GO TO 9917                                         WF01 672
      WRITE (6,74)                                                      WF01 673
      DO 6002 J=MP1,MPMF                                                WF01 674
      JF=J-M                                                            WF01 675
 6002 WRITE (6,35) J,PCFX(JF),PVFY(JF),PCFZ(JF),DELL(JF),UEI(J,N),      WF01 676
     1VEI(J,N),WEI(J,N)                                                 WF01 677
 9917 CONTINUE                                                          WF01 678
C                                                                       WF01 679
C                                                                       WF01 680
C                                                                       WF01 681
C     HORSESHOE VORTEX CHARACTERISTICS OUTPUT                           WF01 682
C                                                                       WF01 683
      WRITE (6,1) ALPHAD(N),DELD                                        WF01 684
      DO 550 J=1,M                                                      WF01 685
      SWPVVD=         SWPVVP(J) *57.29578                               WF01 686
  550 WRITE (6,13) J,PVX(J),PVY(J),PVZ(J),SWPVVD   ,SW(J),CIR(J,N)      WF01 687
C                                                                       WF01 688
C                                                                       WF01 689
      IF(MFLAP.EQ.0) GO TO 9918                                         WF01 690
      WRITE (6,76)                                                      WF01 691
C                                                                       WF01 692
      DO 551 J=MP1,MPMF                                                 WF01 693
      JF=J-M                                                            WF01 694
      SWPVVD=           SWPVVF(JF) *57.29578                            WF01 695
  551 WRITE (6,13) J,PVFX(JF),PVFY(JF),PVFZ(JF),SWPVVD    ,SF(JF),      WF01 696
     1CIR(J,N)                                                          WF01 697
C                                                                       WF01 698
C                                                                       WF01 699
 9918 CONTINUE                                                          WF01 700
C                                                                       WF01 701
C                                                                       WF01 702
C     OVERALL LIFT AND MOMENT COEFFICIENT, REFERENCE QUANTITIES, SPAN-  WF01 703
C     WISE LOADINGS OUTPUT                                              WF01 704
C                                                                       WF01 705
C                                                                       WF01 706
      WRITE (6,72)  ALPHAD(N)                                           WF01 707
      WRITE (6,19) SUMLIF,FUMLIF                                        WF01 708
      WRITE (6,18)                                                      WF01 709
      WRITE (6,19) CLTOT,TOTMOM                                         WF01 710
      WRITE (6,28)                                                      WF01 711
      WRITE (6,29) SPAN,SREF,CAVE                                       WF01 712
```

```
      WRITE (6,65)                                                    WF01 713
      WRITE (6,24)                                                    WF01 714
      DO 3000 I=2,IMAX                                                WF01 715
      IM1=I-1                                                         WF01 716
      CHLOCB(I)=CRW-SUMY(I)*(SWPWLE-SWPWTE)                           WF01 717
 3000 WRITE (6,23) IM1,YLOC(I),CHLOCB(I),SLDCO(I),SECLIF(I)           WF01 718
C                                                                     WF01 719
      IF(MFLAP.EQ.0) GO TO 9919                                       WF01 720
      WRITE (6,64)                                                    WF01 721
      DO 3100 IF=2,IFMAX                                              WF01 722
      IFM1=IF-1                                                       WF01 723
      FCHLOB(IF)= AE-SUMYF(IF)*(TANTH8+TANTH7)                        WF01 724
 3100 WRITE (6,23) IFM1,YLOCF(IF),FCHLOB(IF),FSLDCO(IF),FECLIF(IF)    WF01 725
 9919 CONTINUE                                                        WF01 726
C                                                                     WF01 727
      WRITE (6,83)                                                    WF01 728
      WRITE (6,84) WMOM,FMOM,SUMDRG,FUMDRG,DRGTOT,CDOCLS              WF01 729
C                                                                     WF01 730
      IF(MMM.EQ.0) GO TO 9100                                         WF01 731
      WRITE (6,36)                                                    WF01 732
      DO 4002 J=1,MMM                                                 WF01 733
 4002 WRITE (6,39) J,PMX(J),PMY(J),PMZ(J),UI(J),VI(J),WI(J)           WF01 734
 9100 CONTINUE                                                        WF01 735
C                                                                     WF01 736
C                                                                     WF01 737
 1000 CONTINUE                                                        WF01 738
      GO TO 1010                                                      WF01 739
      END                                                             WF01 740
```

```
      SUBROUTINE LOAD1(N)                                                    WF02 001
C                                                                            WF02 002
C                                                                            WF02 003
      DIMENSION          SLDCO(50),SECLIF(50),FSLDCO(50),FECLIF(50),CHLI   WF02 004
     1FT(50),TLLIFT(150),BLLIFT(150),SLDCO1(50),FCHLIF(50),TFLIFT(150),     WF02 005
     2BFLIFT(150),SLDCF1(50),BFLIF1(150),BFLIF2(150),BFLIF3(150),           WF02 006
     3BFLIF4(150),BFLIF5(150),BLLIF1(150),BLLIF2(150),BLLIF3(150),          WF02 007
     4BLLIF4(150),BFDRG2(150),BFDRG3(150),BFDRG4(150),BFDRG5(150),          WF02 008
     5TFDRAG(150),FCDRAG(50),BFDRAG(150),BLDRG2(150),BLDRG3(150),BLDRG4     WF02 009
     6(150), BLDRG5(150),BLDRAG(150),TLDRAG(150),CHDRAG(50),BLLIF5(150)     WF02 010
C                                                                            WF02 011
      DIMENSION V(150),U(150),VB(150),VF(150),UF(150),VBF(150),FUW(2),FWF02 012
     1VW(2),FWW(2),FUF(2),FVF(2),FWF(2),WF(150),WB(150)                     WF02 013
C                                                                            WF02 014
      DIMENSION UEI(220,10),VEI(220,10),WEI(220,10),ALPHA(10),              WF02 015
     1CIR(220,10)                                                           WF02 016
C                                                                            WF02 017
      DIMENSION PTLX(150),PTLY(150),PTLZ(150),PVX(150),PVY(150),PVZ(150)WF02 018
     1,PVFX(150),PVFY(150),PVFZ(150),PTLFX(150),PTLFY(150),PTLFZ(150)       WF02 019
C                                                                            WF02 020
      DIMENSION SWPVVP(150),SWPVVF(150),SF(150),SW(150),Y(50),YF(50),CHLWF02 021
     1OC(50),FCHLOC(50),YFC(50)                                             WF02 022
C                                                                            WF02 023
      DIMENSION YTW(2),YTWP(2),YBWP(2),YTFW(2),YTFP(2),YTFF(2),YBFW(2),YWF02 024
     1BFF(2),YBFP(2),YBW(2),T(150),TF(150),ELPANL(150),FLPANL(150)          WF02 025
C                                                                           WF02 026
C                                                                            WF02 027
      COMMON CIR,SUMLIF,FUMLIF,CLTOT,TOTMOM,SLDCO,SECLIF,FSLDCO,FECLIF      WF02 028
C                                                                            WF02 029
      COMMON WMOM,FMOM,SUMDRG,FUMDRG,DRGTOT,CDOCLS                          WF02 030
C                                                                            WF02 031
      COMMON PTLX,PTLY,PTLZ,PVX,PVY,PVZ,PVFX,PVFY,PVFZ,PTLFX,PTLFY,PTLFZWF02 032
C                                                                            WF02 033
      COMMON SWPWLE,SWPWTE,SWPFLE,SWPFTE,SWPVVP,SWPVVF,SF,SW,Y,YF           WF02 034
C                                                                            WF02 035
      COMMON CRW,SSPAN,CRF,FSSPAN,PHI,PHIF,CSPHIF,CSPHI,ALPHA,DLX,COSDLXWF02 036
     1,SINDLX,SREF,CAVE,XM,ZM,SPHIF,SPHI                                    WF02 037
C                                                                            WF02 038
      COMMON NCW,M,MP1,MF,MPMF,IFMAX,IMAX,NCF,MFLAP                         WF02 039
C                                                                            WF02 040
      COMMON AE,YFC,TANTH8,TANTH7                                           WF02 041
C                                                                            WF02 042
      COMMON UEI,VEI,WEI                                                    WF02 043
C                                                                            WF02 044
      COMMON/INF/BOT                                                        WF02 045
C                                                                            WF02 046
C                                                                            WF02 047
C                                                                            WF02 048
C     COMPUTE REFERENCE WING AREA = PLANFORM AREA = SREF, WING AVERAGE       WF02 049
C     CHORD = CAVE                                                           WF02 050
C                                                                            WF02 051
      SINALP= SIN(ALPHA(N))                                                 WF02 052
      COSALP= COS(ALPHA(N))                                                 WF02 053
      D=NCW                                                                 WF02 054
      CTW=CRW-SSPAN*(SWPWLE-SWPWTE)                                         WF02 055
      SREF=(CRW+CTW)*SSPAN                                                  WF02 056
      CAVE=SREF/(2.0*SSPAN)                                                 WF02 057
      I=1                                                                   WF02 058
      SUMLIF=0.0                                                            WF02 059
      SUMDRG=0.0                                                            WF02 060
  702 I=I+1                                                                 WF02 061
      CHLIFT(I)=0.0                                                         WF02 062
      CHDRAG(I)=0.0                                                         WF02 063
```

```
C                                                                       WF02 064
C     COMPUTE VELOCITIES NEEDED FOR LOADING CALCULATIONS                WF02 065
C                                                                       WF02 066
C     SIDEWASH  V  INDUCED BY WING VORTICES AT THE 3/4 CHORD OF THE LEFTWF02 067
C     TRAILING WING VORTEX LEGS                                         WF02 068
C                                                                       WF02 069
      DO 823 NV=1,NCW                                                   WF02 070
      JT=(I-2)*NCW+NV                                                   WF02 071
C                                                                       WF02 072
C     ADD EXTERNALLY INDUCED VELOCITY VEI                               WF02 073
C                                                                       WF02 074
      V(JT)=VEI(JT,N)                                                   WF02 075
      DO 823 NN=1,M                                                     WF02 076
      XTW=PTLX(JT)-PVX(NN)                                              WF02 077
      YTW(1)=PTLY(JT)-PVY(NN)                                           WF02 078
      YTW(2)=PTLY(JT)+PVY(NN)                                           WF02 079
      ZTW=PTLZ(JT)-PVZ(NN)                                              WF02 080
      DO 271 L=1,2                                                      WF02 081
      CALL INFWW(SWPVVP(NN),PHI,XTW,YTW(L),ZTW,SW(NN),FUW(L),FVW(L),    WF02 082
     1FWW(L))                                                           WF02 083
      SWPVVP(NN)=-SWPVVP(NN)                                            WF02 084
      PHI=-PHI                                                          WF02 085
  271 CONTINUE                                                          WF02 086
      V(JT)=V(JT)+((FVW(1)+FVW(2))*CIR(NN,N))/12.566371                 WF02 087
  823 CONTINUE                                                          WF02 088
C                                                                       WF02 089
C     SIDEWASH  V  INDUCED BY FLAP VORTICES AT THE 3/4 CHORD OF THE LEFTWF02 090
C     TRAILING WING VORTEX LEGS                                         WF02 091
C                                                                       WF02 092
      IF(MFLAP.EQ.0) GO TO 8901                                         WF02 093
      DO 824 NV=1,NCW                                                   WF02 094
      JT=(I-2)*NCW+NV                                                   WF02 095
      DO 824 NN=MP1,MPMF                                                WF02 096
      NNF=NN-M                                                          WF02 097
      XTW=PTLX(JT)-PVFX(NNF)                                            WF02 098
      YTW(1)=PTLY(JT)-PVFY(NNF)                                         WF02 099
      YTW(2)=PTLY(JT)+PVFY(NNF)                                         WF02 100
      ZTW=PTLZ(JT)-PVFZ(NNF)                                            WF02 101
C                                                                       WF02 102
C     TRANSFORM COORDINATES, ROTATION THROUGH -DLX DEGREES              WF02 103
C                                                                       WF02 104
      XTWP=XTW*COSDLX-ZTW*SINDLX                                        WF02 105
      YTWP(1)=YTW(1)                                                    WF02 106
      YTWP(2)=YTW(2)                                                    WF02 107
      ZTWP=XTW*SINDLX+ZTW*COSDLX                                        WF02 108
C                                                                       WF02 109
      DO 272 L=1,2                                                      WF02 110
      CALL INFWW (SWPVVF(NNF),PHIF,XTWP,YTWP(L),ZTWP,SF(NNF),FUF(L),FVF(WF02 111
     1L),FWF(L))                                                        WF02 112
      SWPVVF(NNF)=-SWPVVF(NNF)                                          WF02 113
      PHIF=-PHIF                                                        WF02 114
  272 CONTINUE                                                          WF02 115
      V(JT)=V(JT)+((FVF(1)+FVF(2))*CIR(NN,N))/12.566371                 WF02 116
  824 CONTINUE                                                          WF02 117
 8901 CONTINUE                                                          WF02 118
C                                                                       WF02 119
C     VELOCITIES  U  AND  V  INDUCED AT WING VORTEX BOUND LEG MIDPOINT  WF02 120
C     INDUCED BY WING VORTICES                                          WF02 121
C                                                                       WF02 122
      DO 826 NV=1,NCW                                                   WF02 123
      JB=(I-2)*NCW+NV                                                   WF02 124
C                                                                       WF02 125
C     ADD EXTERNALLY INDUCED VELOCITIES UEI,VEI                         WF02 126
C                                                                       WF02 127
```

```
      U(JB)=UEI(JB,N)                                                   WF02 128
      VB(JB)=VEI(JB,N)                                                  WF02 129
      WB(JB)= WEI(JB,N)                                                 WF02 130
      DO 826 NN=1,M                                                     WF02 131
      XBW=PVX(JB)-PVX(NN)                                               WF02 132
      YBW(1)=PVY(JB)-PVY(NN)                                            WF02 133
      YBW(2)=PVY(JB)+PVY(NN)                                            WF02 134
      ZBW=PVZ(JB)-PVZ(NN)                                               WF02 135
      DO 268 L=1,2                                                      WF02 136
      CALL INFWW(SWPVVP(NN),PHI,XBW,YBW(L),ZBW,SW(NN),FUW(L),FVW(L),    WF02 137
     1FWW(L))                                                           WF02 138
      SWPVVP(NN)=-SWPVVP(NN)                                            WF02 139
      PHI=-PHI                                                          WF02 140
  268 CONTINUE                                                          WF02 141
      U(JB)=U(JB)+((FUW(1)+FUW(2))*CIR(NN,N))/12.566371                 WF02 142
      VB(JB)=VB(JB)+((FVW(1)+FVW(2))*CIR(NN,N))/12.566371               WF02 143
      WB(JB)=WB(JB)+((FWW(1)+FWW(2))*CIR(NN,N))/12.566371               WF02 144
  826 CONTINUE                                                          WF02 145
C                                                                       WF02 146
C     VELOCITIES  U  AND  V  INDUCED AT WING VORTEX BOUND LEG MIDPOINT  WF02 147
C     INDUCED BY FLAP VORTICES                                          WF02 148
C                                                                       WF02 149
      IF(MFLAP.EQ.0) GO TO 8902                                         WF02 150
      DO 827 NV=1,NCW                                                   WF02 151
      JB=(I-2)*NCW+NV                                                   WF02 152
      DO 827 NN=MP1,MPMF                                                WF02 153
      NNF=NN-M                                                          WF02 154
      XBW=PVX(JB)-PVFX(NNF)                                             WF02 155
      YBW(1)=PVY(JB)-PVFY(NNF)                                          WF02 156
      YBW(2)=PVY(JB)+PVFY(NNF)                                          WF02 157
      ZBW=PVZ(JB)-PVFZ(NNF)                                             WF02 158
C                                                                       WF02 159
C     TRANSFORM COORDINATES, ROTATION THROUGH -DLX DEGREES              WF02 160
C                                                                       WF02 161
      XBWP=XBW*COSDLX-ZBW*SINDLX                                        WF02 162
      YBWP(1)=YBW(1)                                                    WF02 163
      YBWP(2)=YBW(2)                                                    WF02 164
      ZBWP=XBW*SINDLX+ZBW*COSDLX                                        WF02 165
C                                                                       WF02 166
      DO 269 L=1,2                                                      WF02 167
      CALL INFWW (SWPVVF(NNF),PHIF,XBWP,YBWP(L),ZBWP,SF(NNF),FUF(L),FVF(WF02 168
     1L),FWF(L))                                                        WF02 169
      SWPVVF(NNF)=-SWPVVF(NNF)                                          WF02 170
      PHIF=-PHIF                                                        WF02 171
  269 CONTINUE                                                          WF02 172
      U(JB)=U(JB)+(((FUF(1)+FUF(2))*COSDLX+(FWF(1)+FWF(2))*SINDLX)*CIR(NWF02 173
     1N,N))/12.566371                                                   WF02 174
      VB(JB)=VB(JB)+((FVF(1)+FVF(2))*CIR(NN,N))/12.566371               WF02 175
      WB(JB)=WB(JB)+((-(FUF(1)+FUF(2))*SINDLX+(FWF(1) +FWF(2))*COSDLX)* WF02 176
     1CIR(NN,N))/12.566371                                              WF02 177
  827 CONTINUE                                                          WF02 178
 8902 CONTINUE                                                          WF02 179
C                                                                       WF02 180
C     CALCULATE LIFT ON CHORDWISE ROW OF ELEMENTAL PANELS ON THE WING   WF02 181
C                                                                       WF02 182
      CHLOC(I)=CRW-Y(I)*(SWPWLE-SWPWTE)                                 WF02 183
      CIRNET=0.0                                                        WF02 184
      DO 829 KCW=1,NCW                                                  WF02 185
      JT=(I-2)*NCW+KCW                                                  WF02 186
      JS=(I-1)*NCW+KCW                                                  WF02 187
      T(JT)=SSPAN/(SW(JT)*CSPHI)                                        WF02 188
      IF (I.EQ.IMAX) GO TO 2010                                         WF02 189
      CIRNET=CIRNET+CIR(JT,N)-CIR(JS,N)                                 WF02 190
      GO TO 2011                                                        WF02 191
```

```
 2010 CIRNET=CIRNET+CIR(JT,N)                                                    WF02 192
 2011 FAC=1.0                                                                   WF02 193
      IF (KCW.EQ.NCW) FAC=0.75                                                  WF02 194
      ELPANL(JT)=CHLOC(I)/D                                                     WF02 195
C                                                                               WF02 196
C     TLLIFT=LIFT ACTING ON LEFT LEG OF WING VORTEX TAIL AT THE 3/4             WF02 197
C     ELEMENTAL PANEL CHORD                                                     WF02 198
C     TLDRAG=FORCE ACTING ON LEFT LEG OF WING VORTEX TAIL AT THE 3/4            WF02 199
C     ELEMENTAL PANEL CHORD,IT ACTS ALONG VINF LINE AND POINTS FORWARD          WF02 200
C                                                                               WF02 201
      TLLIFT(JT)=ELPANL(JT)*FAC*V(JT)*(2.0/SREF)*CIRNET*COSALP                  WF02 202
      TLDRAG(JT)=ELPANL(JT)*FAC*V(JT)*(-2.0/SREF)*CIRNET*SINALP                 WF02 203
C                                                                               WF02 204
C     BLLIFT = LIFT ACTING ON BOUND LEG OF THE WING VORTEX AT THE               WF02 205
C     MIDPOINT                                                                  WF02 206
C     BLDRAG= -DRAG FORCE ACTING AT SAME POINT                                  WF02 207
C                                                                               WF02 208
      SWPVVT= TAN(SWPVVP(JT))                                                   WF02 209
      FACLDW= (2.0/SREF)*2.0*SW(JT)*CIR(JT,N)                                   WF02 210
      BLLIF1(JT)= FACLDW*CSPHI                                                  WF02 211
      BLLIF2(JT)= FACLDW*(-U(JT)*COSALP)*CSPHI                                  WF02 212
      BLLIF3(JT)= FACLDW*VB(JT)*SWPVVT     *COSALP                              WF02 213
      BLLIF4(JT)= FACLDW*VB(JT)*SPHI*SINALP                                     WF02 214
      BLLIF5(JT)= FACLDW*(-WB(JT)) *CSPHI*SINALP                                WF02 215
      BLLIFT(JT)=BLLIF1(JT)+BLLIF2(JT)+BLLIF3(JT)+BLLIF4(JT)+BLLIF5(JT)         WF02 216
C                                                                               WF02 217
      BLDRG2(JT)= FACLDW*U(JT)*SINALP*CSPHI                                     WF02 218
      BLDRG3(JT)= FACLDW*(-VB(JT))*SWPVVT     *SINALP                           WF02 219
      BLDRG4(JT)= FACLDW*VB(JT)*SPHI*COSALP                                     WF02 220
      BLDRG5(JT)= FACLDW*(-WB(JT))*CSPHI*COSALP                                 WF02 221
      BLDRAG(JT)= BLDRG2(JT)+BLDRG3(JT)+BLDRG4(JT)+BLDRG5(JT)                   WF02 222
C                                                                               WF02 223
      IF (I.GT.2) GO TO 2007                                                    WF02 224
      CHLIFT(I)=CHLIFT(I)+(TLLIFT(JT)     )+BLLIFT(JT)                          WF02 225
      CHDRAG(I)= CHDRAG(I)+(TLDRAG(JT)     )+BLDRAG(JT)                         WF02 226
      GO TO 1832                                                                WF02 227
 2007 JU=(I-3)*NCW+KCW                                                          WF02 228
      CHLIFT(I)=CHLIFT(I)+ (TLLIFT(JT)                    )+BLLIFT(JT)         WF02 229
      CHDRAG(I)= CHDRAG(I)+ (TLDRAG(JT)                    )+BLDRAG(JT)        WF02 230
 1832 SLDCO1(I)=T(JT)*CHLIFT(I)                                                 WF02 231
C                                                                               WF02 232
C     SECLIF=(WING SECTION LIFT*WING LOCAL CHORD)/2*SPAN                        WF02 233
C                                                                               WF02 234
      SECLIF(I)=CHLIFT(I)*(SREF/(2.0*SW(JT)*CSPHI*4.0*SSPAN))                   WF02 235
  829 CONTINUE                                                                  WF02 236
C                                                                               WF02 237
C     SPANWISE SUMMING UP OF LIFTS ACTING ON CHORDWISE ROW OF ELEMENTAL         WF02 238
C     PANELS,SUMLIF=CL                                                          WF02 239
C                                                                               WF02 240
      SUMLIF=SUMLIF+2.0*CHLIFT(I)                                               WF02 241
      SUMDRG= SUMDRG-2.0*CHDRAG(I)                                              WF02 242
      IF(I.LT.IMAX) GO TO 702                                                   WF02 243
C                                                                               WF02 244
C     SLDCO=SPANLOAD COEFFICIENT CLC/CLCAVE FOR THE WING                        WF02 245
C                                                                               WF02 246
C                                                                               WF02 247
      DO 3010 I=2,IMAX                                                          WF02 248
      IF(ABS(SUMLIF).LT.1.0E-07) GO TO 3811                                     WF02 249
      SLDCO(I)=SLDCO1(I)/SUMLIF                                                 WF02 250
      GO TO 3010                                                                WF02 251
 3811 SLDCO(I)=0.0                                                              WF02 252
 3010 CONTINUE                                                                  WF02 253
```

```
C                                                                       WF02 254
      IF(MFLAP.EQ.0) GO TO 8903                                         WF02 255
      SINAPD=SIN(ALPHA(N)+DLX)                                          WF02 256
      COSAPD=COS(ALPHA(N)+DLX)                                          WF02 257
C                                                                       WF02 258
C     COMPUTE FLAP LOADINGS                                             WF02 259
C                                                                       WF02 260
      E=NCF                                                             WF02 261
      IF=1                                                              WF02 262
      FUMLIF=0.0                                                        WF02 263
      FUMDRG=0.0                                                        WF02 264
 7020 IF=IF+1                                                           WF02 265
      FCHLIF(IF)=0.0                                                    WF02 266
      FCDRAG(IF)=0.0                                                    WF02 267
C                                                                       WF02 268
C     COMPUTE VELOCITIES NEEDED FOR FLAP LOADING CALCULATIONS           WF02 269
C                                                                       WF02 270
C     SIDEWASH  V  AT 3/4 CHORD OF LEFT TRAILING VORTEX LEGS ON FLAP    WF02 271
C     INDUCED BY WING VORTICES                                          WF02 272
C                                                                       WF02 273
      DO 8230 NV=1,NCF                                                  WF02 274
      JFT=(IF-2)*NCF+NV                                                 WF02 275
C                                                                       WF02 276
C     ADD EXTERNALLY INDUCED VELOCITY VEI                               WF02 277
C                                                                       WF02 278
      JF=JFT+M                                                          WF02 279
      VFT(JFT)=VEI(JF,N)                                                WF02 280
      DO 8230 NN=1,M                                                    WF02 281
      XTFW=PTLFX(JFT)-PVX(NN)                                           WF02 282
      YTFW(1)=PTLFY(JFT)-PVY(NN)                                        WF02 283
      YTFW(2)=PTLFY(JFT)+PVY(NN)                                        WF02 284
      ZTFW=PTLFZ(JFT)-PVZ(NN)                                           WF02 285
      DO 2715 L=1,2                                                     WF02 286
      CALL INFWW (SWPVVP(NN),PHI,XTFW,YTFW(L),ZTFW,SW(NN),FUW(L),FVW(L),WF02 287
     1FWW(L))                                                           WF02 288
      SWPVVP(NN)=-SWPVVP(NN)                                            WF02 289
      PHI=-PHI                                                          WF02 290
 2715 CONTINUE                                                          WF02 291
      VFT(JFT)=VFT(JFT)+((FVW(1)+FVW(2))*CIR(NN,N))/12.566371           WF02 292
 8230 CONTINUE                                                          WF02 293
C                                                                       WF02 294
C     CALCULATE SIDEWASH  V  AT 3/4 CHORD OF LEFT TRAILING VORTEX LEGS  WF02 295
C     ON FLAP INDUCED BY FLAP VORTICES                                  WF02 296
C                                                                       WF02 297
      DO 8240 NV=1,NCF                                                  WF02 298
      JFT=(IF-2)*NCF+NV                                                 WF02 299
      DO 8240 NN=MP1,MPMF                                               WF02 300
      NNF=NN-M                                                          WF02 301
      XTFF=PTLFX(JFT)-PVFX(NNF)                                         WF02 302
      YTFF(1)=PTLFY(JFT)-PVFY(NNF)                                      WF02 303
      YTFF(2)=PTLFY(JFT)+PVFY(NNF)                                      WF02 304
      ZTFF=PTLFZ(JFT)-PVFZ(NNF)                                         WF02 305
C                                                                       WF02 306
C     TRANSFORM COORDINATES, ROTATION THROUGH -DLX DEGREES              WF02 307
C                                                                       WF02 308
      XTFP=XTFF*COSDLX-ZTFF*SINDLX                                      WF02 309
      YTFP(1)=YTFF(1)                                                   WF02 310
      YTFP(2)=YTFF(2)                                                   WF02 311
      ZTFP=XTFF*SINDLX+ZTFF*COSDLX                                      WF02 312
C                                                                       WF02 313
      DO 2660 L=1,2                                                     WF02 314
      CALL INFWW (SWPVVF(NNF),PHIF,XTFP,YTFP(L),ZTFP,SF(NNF),FUF(L),FVF(WF02 315
     1L),FWF(L))                                                        WF02 316
      SWPVVF(NNF)=-SWPVVF(NNF)                                          WF02 317
```

```
      PHIF=-PHIF                                                        WF02 318
 2660 CONTINUE                                                          WF02 319
      VFT(JFT)=VFT(JFT)+((FVF(1)+FVF(2))*CIR(NN,N))/12.566371           WF02 320
 8240 CONTINUE                                                          WF02 321
C                                                                       WF02 322
C     VELOCITIES U,V,W INDUCED AT FLAP VORTEX BOUNDLEG MIDPOINT INDUCED WF02 323
C     BY WING VORTICES                                                  WF02 324
C                                                                       WF02 325
      DO 8260 NV=1,NCF                                                  WF02 326
      JFB=(IF-2)*NCF+NV                                                 WF02 327
C                                                                       WF02 328
C     ADD EXTERNALLY INDUCED VELOCITIES UEI,VEI,WEI                     WF02 329
C                                                                       WF02 330
      JF=JFB+M                                                          WF02 331
      UF(JFB)= UEI(JF,N)*COSDLX-WEI(JF,N)*SINDLX                        WF02 332
      VBF(JFB)= VEI(JF,N)                                               WF02 333
      WF(JFB)= UEI(JF,N)*SINDLX+WEI(JF,N)*COSDLX                        WF02 334
      DO 8260 NN=1,M                                                    WF02 335
      XBFW=PVFX(JFB)-PVX(NN)                                            WF02 336
      YBFW(1)=PVFY(JFB)-PVY(NN)                                         WF02 337
      YBFW(2)=PVFY(JFB)+PVY(NN)                                         WF02 338
      ZBFW=PVFZ(JFB)-PVZ(NN)                                            WF02 339
      DO 2680 L=1,2                                                     WF02 340
      CALL INFWW (SWPVVP(NN),PHI,XBFW,YBFW(L),ZBFW,SW(NN),FUW(L),FVW(L),WF02 341
     1FWW(L))                                                           WF02 342
      SWPVVP(NN)=-SWPVVP(NN)                                            WF02 343
      PHI=-PHI                                                          WF02 344
 2680 CONTINUE                                                          WF02 345
      UF(JFB)= UF(JFB)+(((FUW(1)+FUW(2))*COSDLX-(FWW(1)+FWW(2))*SINDLX)*WF02 346
     1CIR(NN,N))/12.566371                                              WF02 347
      VBF(JFB)=VBF(JFB)+((FVW(1)+FVW(2))*CIR(NN,N))/12.566371           WF02 348
      WF(JFB)=WF(JFB)+(((FUW(1)+FUW(2))*SINDLX+(FWW(1)+FWW(2))*COSDLX)* WF02 349
     1CIR(NN,N))/12.566371                                              WF02 350
 8260 CONTINUE                                                          WF02 351
C                                                                       WF02 352
C     VELOCITIES  U  AND  V  INDUCED AT FLAP VORTEX BOUND LEG MIDPOINT  WF02 353
C     INDUCED BY FLAP VORTICES                                          WF02 354
C                                                                       WF02 355
      DO 8270 NV=1,NCF                                                  WF02 356
      JFB=(IF-2)*NCF+NV                                                 WF02 357
      DO 8270 NN=MP1,MPMF                                               WF02 358
      NNF=NN-M                                                          WF02 359
      XBFF=PVFX(JFB)-PVFX(NNF)                                          WF02 360
      YBFF(1)=PVFY(JFB)-PVFY(NNF)                                       WF02 361
      YBFF(2)=PVFY(JFB)+PVFY(NNF)                                       WF02 362
      ZBFF=PVFZ(JFB)-PVFZ(NNF)                                          WF02 363
C                                                                       WF02 364
C     TRANSFORM COORDINATES, ROTATION THROUGH -DLX DEGREES              WF02 365
C                                                                       WF02 366
      XBFP=XBFF*COSDLX-ZBFF*SINDLX                                      WF02 367
      YBFP(1)=YBFF(1)                                                   WF02 368
      YBFP(2)=YBFF(2)                                                   WF02 369
      ZBFP=XBFF*SINDLX+ZBFF*COSDLX                                      WF02 370
C                                                                       WF02 371
      DO 2690 L=1,2                                                     WF02 372
      CALL INFWW (SWPVVF(NNF),PHIF,XBFP,YBFP(L),ZBFP,SF(NNF),FUF(L),FVF(WF02 373
     1L),FWF(L))                                                        WF02 374
      SWPVVF(NNF)=-SWPVVF(NNF)                                          WF02 375
      PHIF=-PHIF                                                        WF02 376
 2690 CONTINUE                                                          WF02 377
      UF(JFB)= UF(JFB)+((FUF(1)+FUF(2))*CIR(NN,N))/12.566371            WF02 378
      VBF(JFB)=VBF(JFB)+((FVF(1)+FVF(2))*CIR(NN,N))/12.566371           WF02 379
      WF(JFB)= WF(JFB)+((FWF(1)+FWF(2))*CIR(NN,N))/12.566371            WF02 380
```

```
 8270 CONTINUE                                                          WF02 381
C                                                                       WF02 382
C     CALCULATE LIFT ON CHORDWISE ROW OF ELEMENTAL PANELS ON THE FLAP   WF02 383
C                                                                       WF02 384
C                                                                       WF02 385
      FCHLOC(IF)=AE-YFC(IF)*(TANTH8+TANTH7)                             WF02 386
      CIRNET=0.0                                                        WF02 387
      DO 8290 KCF=1,NCF                                                 WF02 388
      JFT=(IF-2)*NCF+KCF+M                                              WF02 389
      JF=JFT-M                                                          WF02 390
      JFS=(IF-1)*NCF+KCF+M                                              WF02 391
      TF(JF )=FSSPAN/(SF(JF )*CSPHIF)                                   WF02 392
      IF(IF.EQ.IFMAX) GO TO 2110                                        WF02 393
      CIRNET=CIRNET+CIR(JFT,N)-CIR(JFS,N)                               WF02 394
      GO TO 2111                                                        WF02 395
 2110 CIRNET=CIRNET+CIR(JFT,N)                                          WF02 396
 2111 FAC=1.0                                                           WF02 397
      IF(KCF.EQ.NCF) FAC=0.75                                           WF02 398
      FLPANL(JF )=FCHLOC(IF)/E                                          WF02 399
C                                                                       WF02 400
C     TELIFT = LIFT ACTING ON LEFT LEG OF FLAP VORTEX TAIL AT THE 3/4   WF02 401
C     ELEMENTAL PANEL CHORD                                             WF02 402
C     TEDRAG= FORCE ACTING ON LEFT LEG OF FLAP VORTEX TAIL AT THE 3/4   WF02 403
C     ELEMENTAL PANEL CHORD,IT ACTS ALONG VINF LINE AND POINTS FORWARD  WF02 404
C                                                                       WF02 405
      TELIFT(JF )=0.0                                                   WF02 406
      TEDRAG(JF)= 0.0                                                   WF02 407
C                                                                       WF02 408
C     BFLIFT = LIFT ACTING ON BOUND LEG OF THE FLAP VORTEX AT THE       WF02 409
C     MIDPOINT                                                          WF02 410
C     BFDRAG=-DRAG FORCE ACTING AT SAME PLACE                           WF02 411
C                                                                       WF02 412
      FACLOD= (2.0/SREF)*2.0*SF(JF)*CIR(JFT,N)                          WF02 413
      BFLIF1(JF)= FACLOD*CSPHIF                                         WF02 414
      BFLIF2(JF)= FACLOD*(-UF(JF)*COSAPD)*CSPHIF                        WF02 415
      BFLIF3(JF)= 0.0                                                   WF02 416
      BFLIF4(JF)= FACLOD*(-WF(JF)*CSPHIF)*SINAPD                        WF02 417
      BFLIF5(JF)= 0.0                                                   WF02 418
      BFLIFT(JF)= BFLIF1(JF)+BFLIF2(JF)+BFLIF3(JF)+BFLIF4(JF)+BFLIF5(JF)WF02 419
C                                                                       WF02 420
      BFDRG2(JF)= FACLOD*UF(JF)*SINAPD*CSPHIF                           WF02 421
      BFDRG3(JF)= 0.0                                                   WF02 422
      BFDRG4(JF)= FACLOD*(-WF(JF)*CSPHIF*COSAPD)                        WF02 423
      BFDRG5(JF)= 0.0                                                   WF02 424
      BFDRAG(JF)= BFDRG2(JF)+BFDRG3(JF)+BFDRG4(JF)+BFDRG5(JF)           WF02 425
      IF(IF.GT.2) GO TO 2107                                            WF02 426
      FCHLIF(IF)=FCHLIF(IF)+ (TFLIFT(JF )     )+BFLIFT(JF )             WF02 427
      FCDRAG(IF)=FCDRAG(IF)+ (TFDRAG(JF)     )+BFDRAG(JF)               WF02 428
      GO TO 8320                                                        WF02 429
 2107 JFU=(IF-3)*NCF+KCF                                                WF02 430
      FCHLIF(IF)=FCHLIF(IF)+ (TFLIFT(JF )                 )+BFLIFT(JF ) WF02 431
      FCDRAG(IF)=FCDRAG(IF)+ (TFDRAG(JF)                 )+BFDRAG(JF)   WF02 432
 8320 SLDCF1(IF)=TF(JF )*FCHLIF(IF)                                     WF02 433
C                                                                       WF02 434
C     FECLIF = (FLAP SECTION LIFT*FLAP LOCAL CHORD)/2*WING SPAN         WF02 435
C                                                                       WF02 436
      FECLIF(IF)=FCHLIF(IF)*(SREF/(2.0*SF(JF )*CSPHIF*4.0*SSPAN))       WF02 437
 8290 CONTINUE                                                          WF02 438
C                                                                       WF02 439
C     SPANWISE SUMMING UP OF LIFTS ACTING ON CHORDWISE ROW OF FLAP      WF02 440
C     ELEMENTAL PANELS, FUMLIF=CL FOR FLAP,FUMDRG=  CD FOR FLAP         WF02 441
C                                                                       WF02 442
```

```
      FUMLIF=FUMLIF+2.0*FCHLIF(IF)                                      WF02 443
      FUMDRG= FUMDRG-2.0*FCDRAG(IF)                                     WF02 444
      IF(IF.LT.IFMAX) GO TO 7020                                        WF02 445
C                                                                       WF02 446
C     FSLDCO = SPANLOAD COEFFICIENT CLC/CLCAVE FOR THE FLAP             WF02 447
C                                                                       WF02 448
      DO 3110 IF=2,IFMAX                                                WF02 449
      IF(ABS(FUMLIF).LT.1.0E-07) GO TO 3821                             WF02 450
      FSLDCO(IF)=SLDCF1(IF)/FUMLIF                                      WF02 451
      GO TO 3110                                                        WF02 452
 3821 FSLDCO(IF)=0.0                                                    WF02 453
 3110 CONTINUE                                                          WF02 454
      GO TO 8906                                                        WF02 455
 8903 FUMLIF=0.0                                                        WF02 456
      FUMDRG=0.0                                                        WF02 457
 8906 CONTINUE                                                          WF02 458
      CLTOT=SUMLIF+FUMLIF                                               WF02 459
      DRGTOT=SUMDRG+FUMDRG                                              WF02 460
      CDOCLS=DRGTOT/(CLTOT*CLTOT)                                       WF02 461
C                                                                       WF02 462
C     PITCHING MOMENT CALCULATION, MOMENTS TAKEN ABOUT POINT  XM,YM,ZM  WF02 463
C     AND DIVIDED BY  Q*SREF*CAVE                                       WF02 464
C                                                                       WF02 465
      WMOM=0.0                                                          WF02 466
      FMOM=0.0                                                          WF02 467
      DO 9109 JT=1,M                                                    WF02 468
 9109 WMOM=WMOM+(2.0*((BLLIFT(JT)*SINALP+BLDRAG(JT)*COSALP)*(PVZ(JT)-ZM)WF02 469
     1+(BLDRAG(JT)*SINALP-BLLIFT(JT)*COSALP)*(XM-PVX(JT)))+(TLLIFT(JT)*  WF02 470
     2SINALP+TLDRAG(JT)*COSALP)*(PTLZ(JT)-ZM)+(TLDRAG(JT)*SINALP         WF02 471
     3-TLLIFT(JT)*COSALP)*(XM-PTLX(JT)))/CAVE)                          WF02 472
      IF(MFLAP.EQ.0) GO TO 8904                                         WF02 473
      DO 9110 JFT=1,MF                                                  WF02 474
 9110 FMOM=FMOM+(2.0*((BFLIFT(JFT)*SINALP+BFDRAG(JFT)*COSALP)*(PVFZ(JFT)WF02 475
     1-ZM)+(BFDRAG(JFT)*SINALP-BFLIFT(JFT)*COSALP)*(XM-PVFX(JFT)))+      WF02 476
     2(TFLIFT(JFT)*SINALP+TFDRAG(JFT)*COSALP)*(PTLFZ(JFT)-ZM)+          WF02 477
     3(TFDRAG(JFT)*SINALP-TFLIFT(JFT)*COSALP)*(XM-PTLFX(JFT)))/CAVE)    WF02 478
      GO TO 8905                                                        WF02 479
 8904 FMOM=0.0                                                          WF02 480
 8905 TOTMOM=WMOM+FMOM                                                  WF02 481
      RETURN                                                            WF02 482
      END                                                               WF02 483
```

```
      SUBROUTINE INFWW (PSII,APHII,XXX,YYY,ZZZ,SNN,FUI,FVI,FWI)          WF03 001
C 50                                                                     WF03 002
C                                                                        WF03 003
      COMMON/INF/BOT                                                     WF03 004
C                                                                        WF03 005
      TOLRNC=(BOT*15.0E-05)**2                                           WF03 006
      DATA PSIID,APHIID/0., 0./ , FS,FC,FPS,FPC/0.,1.,0.,1./             WF03 007
      IF (PSII .EQ. PSIID) GO TO 10                                      WF03 008
      FS = SIN(PSII)                                                     WF03 009
      FC = COS(PSII)                                                     WF03 010
      FT = FS/FC                                                         WF03 011
      PSIID=PSII                                                         WF03 012
   10 CONTINUE                                                           WF03 013
      IF (APHII.EQ.APHIID) GO TO 20                                      WF03 014
      FPS=SIN(APHII)                                                     WF03 015
      FPC=COS(APHII)                                                     WF03 016
      APHIID=APHII                                                       WF03 017
   20 CONTINUE                                                           WF03 018
      DUMY=SNN*FT                                                        WF03 019
      F1=XXX+DUMY                                                        WF03 020
      F4=XXX-DUMY                                                        WF03 021
      DUMY=SNN*FPC                                                       WF03 022
      F2=YYY+DUMY                                                        WF03 023
      F5=YYY-DUMY                                                        WF03 024
      DUMY=SNN*FPS                                                       WF03 025
      F3=ZZZ+DUMY                                                        WF03 026
      F6=ZZZ-DUMY                                                        WF03 027
      DUMY2=YYY*FPS-ZZZ*FPC                                              WF03 028
      FFA=(XXX*FC-(YYY*FPC+ZZZ*FPS)*FS)**2+DUMY2*DUMY2                   WF03 029
      FFE=F2*F2+F3*F3                                                    WF03 030
      FFB=SQRT(F1*F1+FFE)                                                WF03 031
      FFD=F5*F5+F6*F6                                                    WF03 032
      FFC=SQRT(F4*F4+FFD)                                                WF03 033
      DUMY3=FC*FPC                                                       WF03 034
      DUMY4=FC*FPS                                                       WF03 035
      FFF=(F1*FS+F2*DUMY3+F3*DUMY4)/FFB-(F4*FS+F5*DUMY3+F6*DUMY4)/FFC    WF03 036
C                                                                        WF03 037
C                                                                        WF03 038
      IF(ABS(FFA).LT.TOLRNC) GO TO 262                                   WF03 039
      DUMY=FFF/FFA                                                       WF03 040
      FUONE=(ZZZ*FPC-YYY*FPS)*FC*DUMY                                    WF03 041
      FVONE=(XXX*DUMY4-ZZZ*FS)*DUMY                                      WF03 042
      FWONE=(YYY*FS-XXX*DUMY3)*DUMY                                      WF03 043
      GO TO 265                                                          WF03 044
  262 FUONE=0.                                                           WF03 045
      FVONE=0.                                                           WF03 046
      FWONE=0.                                                           WF03 047
  265 IF(ABS(FFD).LT.TOLRNC) GO TO 263                                   WF03 048
C                                                                        WF03 049
      DUMY=(1.-F4/FFC)/FFD                                               WF03 050
      FVTWO=F6*DUMY                                                      WF03 051
      FWTWO=-F5*DUMY                                                     WF03 052
      GO TO 266                                                          WF03 053
  263 FVTWO=0.                                                           WF03 054
      FWTWO=0.                                                           WF03 055
  266 IF(ABS(FFE).LT.TOLRNC) GO TO 264                                   WF03 056
C                                                                        WF03 057
      DUMY=(1.-F1/FFB)/FFE                                               WF03 058
      FVTHRE=-F3*DUMY                                                    WF03 059
      FWTHRE=F2*DUMY                                                     WF03 060
C                                                                        WF03 061
```

```
      GO TO 267
  264 FVTHRE=0.
      FWTHRE=0.
  267 FUI=FUONE
      FVI=FVONE+FVTWO+FVTHRE
      FWI=FWONE+FWTWO+FWTHRE
      RETURN
      END
```

```
WF03 062
WF03 063
WF03 064
WF03 065
WF03 066
WF03 067
WF03 068
WF03 069
```

```
      SUBROUTINE INVERS(A,NSYS,N,NMAX,MMAX)                          WF04 001
C     SUBROUTINE TO SOLVE SIMULTANEOUS EQUATIONS                     WF04 002
      DIMENSION A(NMAX,MMAX),X(300)                                  WF04 003
    5 SIGN=1.0                                                       WF04 004
      NPI=N+1                                                        WF04 005
      NMI=N-1                                                        WF04 006
      NPLSY=N+NSYS                                                   WF04 007
    9 DO 14 I=1,NMI                                                  WF04 008
      IPI=I+1                                                        WF04 009
      MAX=I                                                          WF04 010
      AMAX=ABS(A(I,I))                                               WF04 011
      DO 10 K=IPI,N                                                  WF04 012
      AKMAX=ABS(A(K,I))                                              WF04 013
      IF(AKMAX.LE.AMAX) GO TO 10                                     WF04 014
      MAX=K                                                          WF04 015
      AMAX=AKMAX                                                     WF04 016
   10 CONTINUE                                                       WF04 017
      IF(AMAX.LT.1.0E-12) GO TO 16                                   WF04 018
      IF(MAX.EQ.I) GO TO 12                                          WF04 019
      DO 11 L=I,NPLSY                                                WF04 020
      TEMP=A(I,L)                                                    WF04 021
      A(I,L)=A(MAX,L)                                                WF04 022
   11 A(MAX,L)=TEMP                                                  WF04 023
      SIGN=-SIGN                                                     WF04 024
   12 DO 14 J=IPI,N                                                  WF04 025
      IF (A(J,I)) 30,14,30                                           WF04 026
   30 CONST=-A(J,I)/A(I,I)                                           WF04 027
      DO 13 L=I,NPLSY                                                WF04 028
   13 A(J,L)=A(J,L)+A(I,L)*CONST                                     WF04 029
   14 CONTINUE                                                       WF04 030
      DO 15 I=1,N                                                    WF04 031
      IF (A(I,I)) 15,16,15                                           WF04 032
   15 CONTINUE                                                       WF04 033
      GO TO 18                                                       WF04 034
   16 WRITE(6,100)                                                   WF04 035
  100 FORMAT(5X,18HMATRIX IS SINGULAR)                               WF04 036
      STOP                                                           WF04 037
   18 DO 21 I=NPI,NPLSY                                              WF04 038
      DO 20 KK=1,N                                                   WF04 039
      K=NPI-KK                                                       WF04 040
      X(K)=A(K,I)                                                    WF04 041
      IF(K.EQ.N) GO TO 20                                            WF04 042
      J=K                                                            WF04 043
   19 J=J+1                                                          WF04 044
      X(K)=X(K)-A(K,J)*X(J)                                          WF04 045
      IF(J.NE.N) GO TO 19                                            WF04 046
   20 X(K)=X(K)/A(K,K)                                               WF04 047
      DO 21 J=1,N                                                    WF04 048
   21 A(J,I)=X(J)                                                    WF04 049
      RETURN                                                         WF04 050
      END                                                            WF04 051
```

JET WAKE PROGRAM

The purpose of this section is to describe the jet wake computer program in sufficient detail to permit understanding and use of the program. The program calculates the velocity field induced by the jet wake of a turbofan engine, both inside and outside the boundary of the jet. Since the purpose for which the program was developed is the calculation of interference between the jet wake and the wing-flap, the computer program is oriented principally toward use with the wing-flap program described previously.

The program represents the wake by a series of closely spaced ring vortices on the boundary of the jet. The strength of the vortices is determined from the initial jet velocity in accordance with equations (15) and (16). The ring vortices and jet boundary are centered on a wake centerline that is permitted to have curvature in accordance with the flow field induced in the region of the wake by the wing-flap and the free stream velocity. Once the ring vortex system is defined, induced velocities are computed at points in the vicinity of the jet wake corresponding to the control points on the wing.

Sample cases described in this section illustrate the preparation of the input and the details of the output.

Program Description

Calculation procedure.- The purpose of this program is to calculate the jet-wake induced velocity components at field points corresponding to the control points on the wing and flap. Upon input, the program transforms the coordinates of the field points from the wing coordinate system to the coordinate system of the jet wake. All calculations are carried out in a jet coordinate system and the results transformed back to the wing coordinate system for output.

The program first determines the location of the vortex rings using the specified centerline coordinates and wake boundary shape. Then the position of each field point relative to the nearest vortex ring is examined. If the radial distance from the field point to the ring is Δs or less, where Δs is the axial spacing of the rings, then the field point is moved axially upstream or downstream until it lies in a

plane midway between two adjacent rings. This adjustment was found necessary because if the field point is very close to a ring, unrealistically high velocities are induced at that field point. By moving the field point to the midplane, the induced velocities computed at the point agree with those computed on the basis of a continuous vorticity distribution. In subsequent wing calculations, the induced velocities are considered to act at the original control point location in the wing coordinate system.

The velocities induced by the jet at all the control points are computed. If more than one jet is present, the above procedure is repeated for each jet in turn, and the final result is a sum of all the induced velocities at each control point. These velocities are output and the program returns to the beginning for a new case.

Program operation.- The program is written in Fortran IV for the IBM 360/67 computer at the Ames Research Center, NASA. The input is either by cards only or by a combination of cards and internally stored data sets containing the field point coordinates. The output is printed and the option is available to store the induced velocities in a data set. Typical execution time is approximately 6 minutes for a case with 200 field points and one jet with a maximum length of 150 R_o and a ring spacing of 0.1 R_o. The running time is doubled when a second jet is added. A complete description of the input and output is presented in the following sections.

Description of Input

This section describes the input for the jet-wake program. In the following discussion, the content of all input cards is described and, where appropriate, instructions on generating input quantities are given. The following section then presents a more detailed discussion of how the jet wake parameters are computed. The relationship between the jet wake and the wing-flap is shown in figures 9 and 22(a) for purposes of illustrating the geometry of the configuration.

Card content.- The input quantites on each card are described. All input variables are listed at the end of this section in order of appearance in the input deck. The input form is presented in figure 24.

Item 1

The first card contains identification information which is printed at the top of the first page of output. Any alphanumeric information can be used on this card. If a data set is created for the induced velocities, the information on this card is also printed at the beginning of the data set for identification purposes.

Item 2

The second card contains six indices and the vortex ring spacing DS. The indices and their use are defined in the table at the end of this section. The limit on the number of field points NP is the same as the limit on the number of wing-flap control points. The jet centerline table entries NCYL are discussed further in the following section describing the input for the wake centerline. The print index NPRNT is used to obtain additional printed output if desired. The normal output (NPRNT = 0) contains details of the jet wake boundary specification and the jet wake induced velocities in the wing coordinate system. As optional output (NPRNT = 1), the wake-induced velocities for each jet in its own coordinate system can be printed.

The values of KIN and KOUT define the manner in which the field points are input and the velocities output. This option is presented in order to make use of data blocks in the Ames Research Center TSS system. A value of KIN = 5 corresponds to input of field points by cards. A value of KIN of seven or more (up through 98) indicates input of field points by a data set which, for instance, has been generated by the wing-flap program. The value of KIN must correspond to the number on the appropriate control card which defines the data set containing the field point coordinates. A value of KOUT = 6 indicates printed output only. Values of KOUT of seven or higher (up through 98) indicate both printed output and induced velocities stored in a data set. With the data set, the value of KOUT must correspond to the number on the appropriate control card which defines the data set in which the induced velocities are to be stored. KOUT and KIN should never be equal to each other. More information on the appropriate values of KIN and KOUT is presented at the end of this section.

Finally, DS is the dimensional axial spacing between vortex rings. It is recommended that DS be chosen such that $\Delta s/R_o \approx 0.1$. As the

spacing increases from this value, the accuracy in calculating velocities begins to decrease. Smaller spacings do not provide any appreciable increases in accuracy but increase the running time.

Item 3

This item consists of one or more groups of cards: one group for each jet wake in the calculation (NJET). For each group, the following information is required. The first card contains the initial vortex strength from equation (16), the initial radius of the jet, and the coordinates in the wing coordinate system of the origin of the wake centerline. The radius and origin coordinates are dimensional and all dimensions should be consistent. Note that since the wing-flap calculation is carried out on the left wing panel, the Y-coordinate of the jet origin is negative. The following cards, of which there are NCYL in number, specify the location of the jet centerline and the growth of the jet boundary. On each card, the variables are the three coordinates of the jet centerline in the jet coordinate system, $(x_{CL}/R_o, y_{CL}/R_o, z_{CL}/R_o)$, the ratio of the local jet boundary radius to the initial radius (R/R_o), and the inclination of the centerline in degrees (θ). These variables are described further in a subsequent section concerning input for the wake centerline. The last of these cards defines the downstream end of the wake. This group of cards is repeated for each jet wake. Thus there are NJET groups of cards.

Item 4

This item consists of the field point coordinates, in the wing coordinate system, at which the induced velocities are to be computed. These coordinates are input according to the value of KIN. If KIN = 5, this item is made up of NP cards, on each of which are the coordinates of one field point. If KIN > 6, no cards are required. Since all wing-flap calculations are carried out on the left wing panel, the field point coordinates will generally have negative Y coordinates.

This completes the input for one case. The program input variables are defined as follows:

Program Variable	Algebraic Symbol (if applicable)	Comments
Item 1		any alphanumeric information may be put on this card for identification
Item 2		
NJET		number of jet wakes under the left wing panel to be included in the induced velocity calculation $1 \leq NJET \leq 4$
NP		number of vield points at which induced velocities are to be calculated $1 \leq NP \leq 200$
NCYL		number of entries in table specifying jet centerline $2 \leq NCYL \leq 100$
NPRNT		index controlling optional output NPRNT = 0 for normal output NPRNT = 1 for expanded output
KIN		index controlling input of field points KIN = 5 input via cards KIN > 6 input via data set($7 \leq KIN \leq 98$)
KOUT		index controlling output of induced velocities KOUT = 6 output printed only KOUT > 6 induced velocities stored in data set ($7 \leq KOUT \leq 98$) Note: KOUT $\neq$ KIN
DS	Δs	spacing between vortex rings in appropriate units
Item 3		
GAMVJ(J)	γ/V	vortex cylinder strength of J'th jet
RJET(J)	R_o	initial radius of J'th jet
XQ(J),YQ(J), ZQ(J)	X_Q, Y_Q, Z_Q	coordinates of center of origin of J'th jet wake in wing coordinate system
XCLR(J,N), YCLR(J,N), ZCLR(J,N)	$\frac{x_{CL}}{R_o}, \frac{y_{CL}}{R_o}, \frac{z_{CL}}{R_o}$	N'th set of coordinates specifying centerline of J'th jet in jet coordinate system. N = 1,2,...,NCYL $1 \leq J \leq 4$

Program Variable	Algebraic Symbol (if applicable)	Comments
RGR(J,N)	R/R_o	ratio of local radius of jet wake boundary to initial jet radius at N'th point specified by XCLR(J,N)
THETA(J,N)	θ	inclination in the jet coordinate system of the J'th jet centerline at N'th point, positive upwards, degrees. See figure 9(a)
Item 4		
XW(N),YW(N), ZW(N)	X,Y,Z	coordinates of field points in wing coordinate system $1 \leq N \leq 200$

The last card in the data deck should be a %END card preceeding the LOGOFF command to terminate execution.

Samples of input decks are shown in figure 25 illustrating all of the options discussed previously. In figure 25(a), two complete sets of input are shown for a configuration with one jet per semispan and for two angles of attack. The field point coordinates for both cases are input via the same data set (KIN = 7) and the final induced velocity results are stored in one data set (KOUT = 8 for $\alpha = 0°$ and 10°). The control cards for a run of this type are listed as follows:

Col. 5 10 15 20 25

```
LOGON
DDEF  FT07F001,VS,CPXYZ
DDEF  FT08F001,VS,JETV1
DDEF  FT08F002,VS,JETV2
CALL  JET1$$
```

Notice that the unit number in columns 8 and 9 of the first DDEF card corresponds to the value of KIN on the second card of both input decks. The data set containing the table of field point coordinates is stored under the name CPXYZ and is defined by this DDEF control card. Similarly, the output, which is a table of u/V, v/V, and w/V induced velocity components at the specified field points, is stored under the name JETV1 for $\alpha = 0°$ and JETV2 for $\alpha = 10°$ in the data set defined by FT08 (KOUT = 8). Note that the sequence numbers in columns 11, 12, and 13 of the DDEF card

defining the data set in which the velocities are stored must be different as must the names of each data group (e.g., JETV1 and JETV2). This data set is now available for use as input to the vortex-lattice program. Separate data sets can be generated by changing the DDEF numbers in columns 8 and 9 for each case. The value of KOUT in each case should agree with the appropriate number of the data set.

A second set of input shown in figure 25(b) illustrates a typical case of a wing with two engines on the semispan. The input deck is complete as shown (KIN = 5) and the output is to be printed (KOUT = 6). For purposes of illustration, the control points shown correspond to one inboard chordwise row on the wing and the five outboard rows on the flap. Since no data sets are required, no DDEF control cards are needed.

Calculation of input wake characteristics.- The results obtained from interference calculations on an externally-blown jet-augmented flap have shown that the predicted load distribution is sensitive to the position of the wake relative to the wing-flap. In the method, both the vertical and lateral displacements and the slope of the centerline must be specified. Of these, the most important effect is the vertical displacement, in that by moving the jet vertically, the wake boundary is caused to intersect more or less area element control points on the wing-flap. The objective in defining the jet centerline was to develop a simple rational approach that could be applied equally well to any wing-flap-engine configuration. The approach described below appears to fulfill this objective, although more experience with the method, comparisons with more lift and moment data, or particularly comparisons with wake survey data that may become available may indicate areas of improvement.

The coordinates specifying the jet centerline (x_{CL}/R_o, y_{CL}/R_o, z_{CL}/R_o) are input in the jet coordinate system, figure 9. The x_{CL} values are always positive. The axes of this coordinate system are always taken to be parallel to their respective wing axes, whether or not the engine has incidence relative to the wing root chord. The local inclination of the centerline, θ, is input in degrees, positive when the jet is angled up toward the wing. Experience has shown that the best jet model is obtained when the jet origin is placed at the engine inlet. In the region of the engine nacelle, the jet is not allowed to deflect or expand. At the

fan nacelle exit, the wake then is considered to begin expansion. The reason for this practice is that in a vortex ring (or continuous vortex cylinder) model, the calculated axial jet velocity at the origin is $1/2\ V_j$ and within two diameters or so increases to nearly V_j. Thus, by permitting this adjustment to occur over the nacelle length, the jet has essentially become fully developed at the fan exit station.

After the initial jet velocity ratio, V_j/V, is calculated according to equation (18), the jet boundary is chosen from figure 4. The initial region is fixed by the velocity ratio, and when the total length of the main region is chosen, the variation of radius along the entire length of the jet is specified. Again on the basis of calculations comparing the ring vortex model with a semi-infinite vortex cylinder, it has been found that the rings must be used over a total length of about 150 R_o to have sufficient wake to accurately model the velocities within the first 15 radii of length.

The change in the average jet velocity $\bar{V}_j$ along the jet can be determined approximately from the relation

$$\frac{\bar{V}_j}{V} \simeq \frac{R_o}{R}\left(\frac{V_j}{V} - 1\right) + 1 \qquad (27)$$

This value is needed in calculating the displacement of the jet centerline due to induced downwash and sidewash. The distribution of wing-flap induced downwash and sidewash (with no power effects) along a line colinear with the engine centerline is shown in figure 17(b) for a typical configuration with zero engine incidence. Although a streamline leaving the center of the engine exhaust would deviate from this line, the deviations are small and should not change the computed downwash significantly except near the flap trailing edge, where the resultant changes in wake position would have little effect on the wing-flap area within the wake boundary. Consequently, all the results presented in this report were based on down- and sidewash velocities computed along the jet x-axis. For zero engine incidence, this line is colinear with the engine centerline.

A distribution of points along the wake centerline must be selected in order to define the wake centerline coordinates, the slope of this centerline, and the radius of the wake for Item 3 of the input. The number of points chosen is arbitrary. In accordance with the above discussion, the first point should be the engine inlet and the second the engine exit. The slopes of the wake in the jet coordinate system are given by the engine incidence angles for these first two points, and the wake radius is R_o. The last point should be approximately 150 R_o downstream of the engine. Linear interpolation is used between points defining the wake. The computation procedure is the same for any number of points and will be illustrated for the N'th point along the wake centerline.

At the N'th point, the direction of the flow is first computed relative to the engine coordinate system. An estimate of the average jet velocity $\overline{V}_j$ is obtained from equation (27). If the engine has an incidence ε_{ez} in the vertical plane measured with respect to the x-axis (positive if the wake is directed upward toward the wing), and a toe-in angle ε_{ey} in the horizontal plane measured with respect to the x-axis (positive if the wake is directed outboard under the right wing panel), then the angles made by the velocity vector with respect to the x-axis in the vertical and horizontal planes are, respectively

$$\left.\begin{aligned} \varepsilon_z &\equiv \tan^{-1}\left(\frac{\sin\alpha - \frac{w}{V} + \frac{\overline{V}_j}{V}\sin\varepsilon_{ez}}{\overline{V}_j/V}\right) \\ \varepsilon_y &\equiv \tan^{-1}\left(\frac{\frac{\overline{V}_j}{V}\sin\varepsilon_{ey} + \frac{v}{V}}{\overline{V}_j/V}\right) \end{aligned}\right\} \qquad (28)$$

In the above equations, positive values indicate the velocity vector to be directed upward toward the wing in the positive z direction and outboard under the right wing in the positive y direction, and the cosines of the engine incidence angles are assumed equal to 1. Note that under the left wing panel, which is where the calculations are made, ε_{ey} will have a negative value if the engine is toed-in so that its wake is directed outboard.

The vertical and lateral displacements are then computed separately to get the z_{CL}/R_o and y_{CL}/R_o coordinates at the N'th x_{CL}/R_o, as follows. With all the slopes at the NCYL points known, the displacement in each plane (vertical and horizontal) can be determined by assuming the wake centerline to be divided into straight line segments between each x_{CL}/R_o. The slope of an individual segment is considered the average between the slopes at the two ends of the segment. The line segments are laid out starting at the engine exhaust station and working aft. The wake characteristics aft of the flap trailing edge have a decreasing effect on the induced velocities on the wing and flap with increasing distances; thus the wake centerline can be made a straight line for most of the 150 R_o of length.

The slope of the wake centerline at each point is required in order to tilt the plane of the vortex rings to make them normal locally to the wake centerline. The tilting of the rings has only a very small effect on the induced velocities, and for all practical purposes, the rings could be oriented normal to the x-axis. Provision is made in the program for vertical tilting by specifying values of $\theta(N)$, where θ is equal to ϵ_z at each point, as given by equation (28). One caution should be indicated in calculating θ values. If θ changes sufficiently between adjacent vortex rings, the two rings can intersect and cause numerical problems. Since the slopes are small in practical cases and the program linearly interpolates between input values, it is unlikely that this condition will occur.

The wake radius is obtained at each x_{CL}/R_o from the appropriate curve in figure 4.

For most configurations of interest, the major interference of the wake on the wing-flap occurs in the initial region of the wake, thus it is necessary to describe the initial region more precisely than the main region. Because of the desire to retain simplicity and ease of application of the method and the fact that no appropriate wake survey data exists to use as a guide, the calculations presented in this report were made using only a few points. The main region of the jet was defined by two points: the end of the initial region, which is usually aft of the flap trailing edge, and the 150 R_o point. The initial region was specified by the first two points on the engine, the end of the initial

region, and possibly one or two intermediate points. The procedures are illustrated in the sample cases in a later section.

Description of Output

A sample set of output, shown in figure 26, was generated from the input deck illustrated in figure 25. The entire set of optional output has been obtained for this case.

The identification information from the first card of the input deck is printed at the top of the first page. This is followed immediately by the jet vortex ring spacing and the input and output indices KIN, KOUT. The next block of output describes the geometry of the jet wake(s). Under the major heading JET PARAMETERS are given the nondimensional vortex ring spacing, $\Delta s/R_o$; the initial jet radius, R_o; the coordinates of the origin of the jet in the wing coordinate system, XQ, YQ, ZQ; the initial vortex strength, GAMMA/V; and a table defining the jet centerline. The centerline coordinates in the jet coordinate system x_{CL}/R_o, y_{CL}/R_o, z_{CL}/R_o; vertical inclination, θ, and jet radius, R/R_o are all input quantities. The distance along the centerline, s/R_o, is calculated in the program. If more than one jet is present, the same block of information for the other jets follows.

The next items of output are optional (NPRNT = 1). The induced velocity components at the specified field points are output in the jet coordinate system. The field point coordinates, x_p/R_o, y_p/R_o, z_p/R_o are expressed also in the jet coordinate system. The induced axial velocity, u/V, is positive aft, and the other components v/V and w/V are positive in the direction of increasing jet coordinates y_p and z_p respectively. Note that these velocities are jet wake induced and do not have any free-stream velocity components included. If more than one jet is considered, the same output is given for the second and succeeding jets.

The last block of output is the induced velocity field due to the entire system of jets. The field points in the wing coordinate system X_W, Y_W, Z_W are printed as are the total jet induced velocity components u/V, v/V, and w/V. The velocities are positive in the positive wing coordinate direction as shown in figure 2. If the data set option (KOUT > 6) is requested, this last set of velocity components is also

stored in the specified data set for use as input to the vortex-lattice program.

Program Listing

The jet flow model program is written in Fortran IV for the NASA, Ames Research Center IBM 360/67 computer. The program consists of the main program and three subroutines. The table below will act as a table of contents for the program listing given on the following pages.

```
C      COMPUTE VELOCITY INDUCED BY A SERIES OF CONSTANT STRENGTH      JET1 001
C        VORTEX RINGS WITH VARIABLE RADII LYING ALONG A PRESCRIBED PATHJET1 002
C                                                                     JET1 003
C       ALL FIELD POINT COORDINATES ARE INPUT IN THE WING SYSTEM AND  JET1 004
C        TRANSFORMED TO THE ENGINE SYSTEM FOR CALCULATIONS            JET1 005
C      JET CENTERLINE COORDINATES ARE INPUT IN ENGINE SYSTEM          JET1 006
C      ALL OUTPUT IS IN THE WING SYSTEM,OPTIONAL OUTPUT IN ENGINE SYSTEMJET1 007
C                                                                     JET1 008
C        OPTIONS ... INPUT OF FIELD POINTS MAY BE VIA CARDS OR DATA SET JET1 009
C                ... INDUCED VELOCITY OUTPUT IS BOTH PRINTED AND      JET1 010
C                    STORED IN A DATA SET                             JET1 011
C                                                                     JET1 012
C                                                                     JET1 013
      DIMENSION  XCLR(4,100),ZCLR(4,100),RGR(4,100),SCLR(4,100),      JET1 014
     1   THETA(4,100),YCLR(4,100),GAMVJ(4),RJET(4),XQ(4),YQ(4),ZQ(4)  JET1 015
      DIMENSION  TITLE(20),XPR(220),YPR(220),ZPR(220),U(220),V(220),  JET1 016
     1          W(220),XP(220),YP(220),ZP(220),UP(220),VP(220),WP(220) JET1 017
      COMMON MZZZ                                                     JET1 018
  700 FORMAT (8F10.5)                                                 JET1 019
  701 FORMAT (6I5,5F10.4)                                             JET1 020
  702 FORMAT (20A4)                                                   JET1 021
  710 FORMAT (1H1/10X,20A4)                                           JET1 022
  711 FORMAT (/2H (I1,16H) JET PARAMETERS5X8HD(S/R) =,F7.4/            JET1 023
     110X3HX/R7X3HY/R7X3HZ/R7X3HS/R                                   JET1 024
     2 5X5HTHETA,4X6HRGAM/R, 5X1HR,8X2HXQ,6X2HYQ,6X2HZQ,4X7HGAMMA/V)  JET1 025
  712 FORMAT (3X6F10.2,  F10.4,4F8.3)                                 JET1 026
  713 FORMAT (/5X4HD(S),4X3HKIN,2X4HKOUT)                             JET1 027
  714 FORMAT (F10.4,I5,I6)                                            JET1 028
  715 FORMAT ( 4X1HN,5X2HXW,8X2HYW,8X2HZW8X3HU/V,9X3HV/V,9X3HW/V)     JET1 029
  716 FORMAT (I5,3F10.3,3(1PE12.4))                                   JET1 030
  717 FORMAT (/2X,22HWING COORDINATE SYSTEM)                          JET1 031
  718 FORMAT (/2X,25HVELOCITIES INDUCED BY JET,I2,24H - JET COORDINATE SJET1 032
     1YSTEM/4X1HN,6X4HXP/R,6X4HYP/R,6X4HZP/R,7X3HU/V9X3HV/V9X3HW/V)    JET1 033
  719 FORMAT (3E13.6)                                                 JET1 034
C                                                                     JET1 035
      MZZZ=1                                                          JET1 036
      RAD=180./3.1415926                                              JET1 037
C                                                                     JET1 038
C     INPUT          NOTE ..  IF KIN=5    , INPUT FIELD POINTS VIA CARDS  JET1 039
C                             IF KIN.GT.6, INPUT FIELD POINTS VIA DATA SETJET1 040
C                                                                     JET1 041
C                             IF KOUT=6    , PRINTED OUTPUT ONLY      JET1 042
C                             IF KOUT.GT.6, VELOCITIES OUTPUT IN DATA SET JET1 043
C                              KIN MUST NOT EQUAL KOUT                JET1 044
C                                                                     JET1 045
   10 READ (5,702) TITLE                                              JET1 046
      READ(5,701) NJET,NP,NCYL,NPRNT,KIN,KOUT,DS                     JET1 047
      IF (KIN .LT. 5) KIN=5                                          JET1 048
      IF (KOUT .LT. 6) KOUT=6                                        JET1 049
C                                                                     JET1 050
C       INPUT INDIVIDUAL JET PARAMETERS                               JET1 051
C                                                                     JET1 052
      DO 16 J=1,NJET                                                 JET1 053
      READ (5,700) GAMVJ(J),RJET(J),XQ(J),YQ(J),ZQ(J)                JET1 054
      DO 11 N=1,NCYL                                                 JET1 055
   11 READ (5,700) XCLR(J,N),YCLR(J,N),ZCLR(J,N),RGR(J,N),THETA(J,N) JET1 056
   16 CONTINUE                                                       JET1 057
C                                                                     JET1 058
C       INPUT FIELD POINT COORDINATES                                 JET1 059
C                                                                     JET1 060
      DO 12 N=1,NP                                                   JET1 061
   12 READ (KIN,700) XP(N),YP(N),ZP(N)                               JET1 062
C                                                                     JET1 063
C       SET UP TABLE OF JET CENTERLINE PARAMETERS                     JET1 064
C                                                                     JET1 065
```

```
      DO 14 J=1,NJET                                                    JET1 066
      SCLR(J,1)=0.0                                                     JET1 067
      DO 13 N=2,NCYL                                                    JET1 068
      SR = (XCLR(J,N)-XCLR(J,N-1))**2 + (YCLR(J,N)-YCLR(J,N-1))**2 +    JET1 069
     1     (ZCLR(J,N)-ZCLR(J,N-1))**2                                   JET1 070
   13 SCLR(J,N)=SQRT(SR) + SCLR(J,N-1)                                  JET1 071
   14 CONTINUE                                                          JET1 072
C                                                                       JET1 073
C        PRELIMINARY OUTPUT                                             JET1 074
C                                                                       JET1 075
      WRITE (6,710) TITLE                                               JET1 076
      WRITE (6,713)                                                     JET1 077
      WRITE (6,714) DS,KIN,KOUT                                         JET1 078
      IF (KIN .EQ. KOUT) GO TO 10                                       JET1 079
      DO 15 N=1,NJET                                                    JET1 080
      DSR=DS/RJET(N)                                                    JET1 081
      WRITE (6,711) N,DSR                                               JET1 082
      DO 15 J=1,NCYL                                                    JET1 083
      IF (J-1) 150,150,151                                              JET1 084
  150 WRITE (6,712) XCLR(N,J),YCLR(N,J),ZCLR(N,J),SCLR(N,J),THETA(N,J), JET1 085
     1              RGR(N,J),RJET(N),XQ(N),YQ(N),ZQ(N),GAMVJ(N)        JET1 086
      GO TO 15                                                          JET1 087
  151 WRITE (6,712) XCLR(N,J),YCLR(N,J),ZCLR(N,J),SCLR(N,J),THETA(N,J), JET1 088
     1              RGR(N,J)                                           JET1 089
   15 CONTINUE                                                          JET1 090
      DO 192 J=1,NP                                                     JET1 091
      UP(J)=0.0                                                         JET1 092
      VP(J)=0.0                                                         JET1 093
  192 WP(J)=0.0                                                         JET1 094
      DO 40 M=1,NJET                                                    JET1 095
      IF (NPRNT .NE. 0) WRITE (6,718) M                                 JET1 096
      DO 19 J=1,NP                                                      JET1 097
      U(J)=0.0                                                          JET1 098
      V(J)=0.0                                                          JET1 099
   19 W(J)=0.0                                                          JET1 100
      SREND=SCLR(M,NCYL)                                                JET1 101
      DSR=DS/RJET(M)                                                    JET1 102
C                                                                       JET1 103
C       TRANSFORM FIELD POINT COORDINATES TO ENGINE SYSTEM              JET1 104
C                                                                       JET1 105
  190 DO 191 J=1,NP                                                     JET1 106
      XPR(J)=(-XP(J)+XQ(M))/RJET(M)                                     JET1 107
      YPR(J)=(YP(J)-YQ(M))/RJET(M)                                      JET1 108
  191 ZPR(J)=(-ZP(J)+ZQ(M))/RJET(M)                                     JET1 109
      CALL CORECT (NP,XPR,YPR,ZPR,DSR,M,NCYL,XCLR,YCLR,ZCLR,SCLR,RGR,   JET1 110
     1             THETA)                                             JET1 111
      SR=-DSR/2.0                                                       JET1 112
      JSR=1                                                             JET1 113
   20 SR=SR+DSR                                                         JET1 114
C                                                                       JET1 115
C       LOCATE INDIVIDUAL VORTEX RINGS                                  JET1 116
C                                                                       JET1 117
   21 IF (SR-SCLR(M,JSR)) 23,25,22                                      JET1 118
   22 JSR=JSR+1                                                         JET1 119
      IF(JSR.GT.NCYL) GO TO 51                                          JET1 120
      GO TO 21                                                          JET1 121
   25 XG=XCLR(M,JSR)                                                    JET1 122
      YG=YCLR(M,JSR)                                                    JET1 123
      ZG=ZCLR(M,JSR)                                                    JET1 124
      RG=RGR(M,JSR)                                                     JET1 125
      THG=THETA(M,JSR)/RAD                                              JET1 126
      GO TO 30                                                          JET1 127
   23 DELTA=(SR-SCLR(M,JSR-1))/(SCLR(M,JSR)-SCLR(M,JSR-1))              JET1 128
      XG=XCLR(M,JSR-1)+(XCLR(M,JSR)-XCLR(M,JSR-1))*DELTA                JET1 129
      YG=YCLR(M,JSR-1)+(YCLR(M,JSR)-YCLR(M,JSR-1))*DELTA                JET1 130
      ZG=ZCLR(M,JSR-1)+(ZCLR(M,JSR)-ZCLR(M,JSR-1))*DELTA                JET1 131
```

```
      RG =  RGR(M,JSR-1)+(RGR(M,JSR)-RGR(M,JSR-1))*DELTA                JET1 132
      THG=THETA(M,JSR-1)+(THETA(M,JSR)-THETA(M,JSR-1))*DELTA            JET1 133
      THG=THG/RAD                                                       JET1 134
   30 CONTINUE                                                          JET1 135
      SNTH=SIN(THG)                                                     JET1 136
      CSTH=COS(THG)                                                     JET1 137
      RGAMR=RG                                                          JET1 138
      DO 38 N=1,NP                                                      JET1 139
      XIPR=(XPR(N)-XG)*CSTH + (ZPR(N)-ZG)*SNTH                          JET1 140
      ETAR=-(YPR(N)-YG)                                                 JET1 141
      ZETAR= (XPR(N)-XG)*SNTH - (ZPR(N)-ZG)*CSTH                        JET1 142
      RPR=SQRT(ETAR**2 + ZETAR**2)                                      JET1 143
      CALL VRING(RGAMR,XIPR,RPR,UGAM,VGAM)                              JET1 144
      IF (RPR - 1.0E-05) 33,33,34                                       JET1 145
   33 DUMU=UGAM*CSTH                                                    JET1 146
      DUMV=0.                                                           JET1 147
      DUMW=UGAM*SNTH                                                    JET1 148
      GO TO 35                                                          JET1 149
   34 DUMU=UGAM*CSTH + VGAM*ZETAR/RPR*SNTH                              JET1 150
      DUMV=-VGAM*ETAR/RPR                                               JET1 151
      DUMW=UGAM*SNTH - VGAM*ZETAR/RPR*CSTH                              JET1 152
   35 UGAM=DUMU                                                         JET1 153
      VGAM=DUMV                                                         JET1 154
      WGAM=DUMW                                                         JET1 155
C                                                                       JET1 156
C        CORRECT VORTEX RING STRENGTH FOR RADIUS EFFECT                 JET1 157
C                                                                       JET1 158
      U(N)=U(N)+UGAM*GAMVJ(M)*DSR/RGAMR                                 JET1 159
      W(N)=W(N)+WGAM*GAMVJ(M)*DSR/RGAMR                                 JET1 160
   38 V(N)=V(N)+VGAM*GAMVJ(M)*DSR/RGAMR                                 JET1 161
C                                                                       JET1 162
C        NOTE.. U(N),V(N),W(N) ARE VELOCITIES INDUCED IN ENGINE SYSTEM  JET1 163
C                                                                       JET1 164
      IF (SR.LT.SREND) GO TO 20                                         JET1 165
   51 CONTINUE                                                          JET1 166
      DO 52 N=1,NP                                                      JET1 167
      UP(N)=UP(N)+U(N)                                                  JET1 168
      VP(N)=VP(N)+V(N)                                                  JET1 169
   52 WP(N)=WP(N)+W(N)                                                  JET1 170
      IF (NPRNT.EQ.0) GO TO 40                                          JET1 171
C                                                                       JET1 172
C        OPTIONAL OUTPUT                                                JET1 173
C                                                                       JET1 174
      DO 50 N=1,NP                                                      JET1 175
   50 WRITE (6,716) N,XPR(N),YPR(N),ZPR(N),U(N),V(N),W(N)               JET1 176
   40 CONTINUE                                                          JET1 177
      WRITE (6,717)                                                     JET1 178
      WRITE (6,715)                                                     JET1 179
C                                                                       JET1 180
C        OUTPUT INDUCED VELOCITIES IN WING SYSTEM                       JET1 181
C                                                                       JET1 182
      DO 41 N=1,NP                                                      JET1 183
      UP(N)=-UP(N)                                                      JET1 184
      WP(N)=-WP(N)                                                      JET1 185
   41 WRITE (6,716)N,XP(N),YP(N),ZP(N),UP(N),VP(N),WP(N)                JET1 186
      IF (KOUT .LE. 6) GO TO 60                                         JET1 187
C                                                                       JET1 188
C        GENERATE INDUCED VELOCITIES DATA SET                           JET1 189
C                                                                       JET1 190
      WRITE (KOUT,702) TITLE                                            JET1 191
      DO 42 N=1,NP                                                      JET1 192
   42 WRITE (KOUT,719) UP(N),VP(N),WP(N)                                JET1 193
      END FILE KOUT                                                     JET1 194
   60 IF (KIN .LE. 6) GO TO 10                                          JET1 195
      REWIND KIN                                                        JET1 196
      GO TO 10                                                          JET1 197
      END                                                               JET1 198
```

```
      SUBROUTINE CORECT (NP,XPR,YPR,ZPR,DSR,M,NCYL,XCLR,YCLR,ZCLR,SCLR,  JET2 001
     1                   RGR,THETA)                                     JET2 002
C                                                                       JET2 003
C     CORRECT FIELD POINT LOCATIONS TO AVOID VORTEX RING SINGULARITIES  JET2 004
C                                                                       JET2 005
      DIMENSION XPR(220),YPR(220),ZPR(220),XCLR(4,100),YCLR(4,100),     JET2 006
     1          ZCLR(4,100),RGR(4,100),SCLR(4,100),THETA(4,100),NFP(220)JET2 007
C                                                                       JET2 008
      JSR=1                                                             JET2 009
      SR=-DSR/2.0                                                       JET2 010
      DO 11 J=1,NP                                                      JET2 011
   11 NFP(J)=1                                                          JET2 012
      NCT=0                                                             JET2 013
      RAD=57.2957795                                                    JET2 014
   20 SR=SR+DSR                                                         JET2 015
   21 IF (SR-SCLR(M,JSR)) 23,25,22                                      JET2 016
   22 JSR=JSR+1                                                         JET2 017
      IF (JSR .GT. NCYL) RETURN                                         JET2 018
      GO TO 21                                                          JET2 019
   25 XG=XCLR(M,JSR)                                                    JET2 020
      YG=YCLR(M,JSR)                                                    JET2 021
      ZG=ZCLR(M,JSR)                                                    JET2 022
      RG= RGR(M,JSR)                                                    JET2 023
      THG=THETA(M,JSR)/RAD                                              JET2 024
      GO TO 30                                                          JET2 025
   23 DELTA=(SR-SCLR(M,JSR-1))/(SCLR(M,JSR)-SCLR(M,JSR-1))              JET2 026
      XG=XCLR(M,JSR-1)+(XCLR(M,JSR)-XCLR(M,JSR-1))*DELTA                JET2 027
      YG=YCLR(M,JSR-1)+(YCLR(M,JSR)-YCLR(M,JSR-1))*DELTA                JET2 028
      ZG=ZCLR(M,JSR-1)+(ZCLR(M,JSR)-ZCLR(M,JSR-1))*DELTA                JET2 029
      RG= RGR(M,JSR-1)+( RGR(M,JSR)- RGR(M,JSR-1))*DELTA                JET2 030
      THG=THETA(M,JSR-1)+(THETA(M,JSR)-THETA(M,JSR-1))*DELTA            JET2 031
      THG=THG/RAD                                                       JET2 032
   30 CONTINUE                                                          JET2 033
      SNTH=SIN(THG)                                                     JET2 034
      CSTH=COS(THG)                                                     JET2 035
      DO 38 N=1,NP                                                      JET2 036
      IF (NFP(N) .EQ. 0) GO TO 38                                       JET2 037
      XIPR=(XPR(N)-XG)*CSTH + (ZPR(N)-ZG)*SNTH                          JET2 038
      ETAR=-(YPR(N)-YG )                                                JET2 039
      ZETAR= (XPR(N)-XG)*SNTH - (ZPR(N)-ZG)*CSTH                        JET2 040
      RPR=SQRT(ETAR**2 + ZETAR**2)                                      JET2 041
      IF (XIPR+DSR) 35,35,36                                            JET2 042
   35 NFP(N)=0                                                          JET2 043
      NCT=NCT+1                                                         JET2 044
      GO TO 38                                                          JET2 045
   36 CONTINUE                                                          JET2 046
      RTEST=ABS(RPR-RG)                                                 JET2 047
      XTEST=ABS(XIPR)                                                   JET2 048
      IF (XTEST .GT. DSR/2.0) GO TO 38                                  JET2 049
      NFP(N)=0                                                          JET2 050
      NCT=NCT+1                                                         JET2 051
      IF (RTEST .GE. DSR) GO TO 38                                      JET2 052
      FSIGN=1.0                                                         JET2 053
      IF (XIPR .LT. 0.0) FSIGN=-1.0                                     JET2 054
      XIPRP=FSIGN*(DSR/2.0-XTEST)                                       JET2 055
      XPR(N)=XPR(N)+XIPRP*CSTH                                          JET2 056
      ZPR(N)=ZPR(N)+XIPRP*SNTH                                          JET2 057
   38 CONTINUE                                                          JET2 058
      IF (NCT .LT. NP) GO TO 20                                         JET2 059
      RETURN                                                            JET2 060
      END                                                               JET2 061
```

```
      SUBROUTINE VRING (RGAMR,XIPR,RPR,UGAM,VGAM)                        JET3 001
C                                                                        JET3 002
C     SUBROUTINE TO COMPUTE VELOCITY INDUCED BY A SINGLE VORTEX RING     JET3 003
C                                                                        JET3 004
C          RGAMR = RING RADIUS/REFERENCE RADIUS                          JET3 005
C          XIPR  = AXIAL DISTANCE TO FIELD POINT/REFERENCE RADIUS        JET3 006
C          RPR   = RADIAL DISTANCE TO FIELD POINT/REFERENCE RADIUS       JET3 007
C          UGAM  = AXIAL VELOCITY/GAMMA                                  JET3 008
C          VGAM  = RADIAL VELOCITY/GAMMA                                 JET3 009
C                                                                        JET3 010
      PI=3.1415926                                                       JET3 011
      DENM=XIPR**2 + (RPR-RGAMR)**2                                      JET3 012
      DENP=XIPR**2 + (RPR+RGAMR)**2                                      JET3 013
      AK2=4.0*RPR*RGAMR/DENP                                             JET3 014
      CALL ELLIPS (AK2,ZK,ZE)                                            JET3 015
      UGAM=(ZK-(1.0+2.0*RGAMR*(RPR-RGAMR)/DENM)*ZE) /SQRT(DENP)/(2.0*PI) JET3 016
      VGAM=0.0                                                           JET3 017
      IF (RPR .LE. 1.0E-05) RETURN                                       JET3 018
      VGAM=-XIPR/RPR/(2.0*PI*SQRT(DENP))*(ZK-(1.+2.*RPR*RGAMR/DENM)*ZE)  JET3 019
      RETURN                                                             JET3 020
      END                                                                JET3 021
```

```
      SUBROUTINE ELLIPS (AKSQ,TK,TE)                                    JET4 001
C                                                                       JET4 002
C                -- TABLE LOOK-UP OF ELLIPTIC INTEGRALS --              JET4 003
C                                                                       JET4 004
      DIMENSION CKK(100),CK(100),CE(100)                                JET4 005
C                                                                       JET4 006
      COMMON MZZZ                                                       JET4 007
C                                                                       JET4 008
C     CKK = ARGUMENT OF ELLIPTIC INTEGRALS                              JET4 009
C                                                                       JET4 010
      DATA CKK/0.00,.01,.02,.03,.04,.05,.06,.07,.08,.09,.10,.11,.12,.13,JET4 011
     1        .14,.15,.16,.17,.18,.19,.20,.21,.22,.23,.24,.25,.26,.27,JET4 012
     2        .28,.29,.30,.31,.32,.33,.34,.35,.36,.37,.38,.39,.40,.41,JET4 013
     3        .42,.43,.44,.45,.46,.47,.48,.49,.50,.51,.52,.53,.54,.55,JET4 014
     4        .56,.57,.58,.59,.60,.61,.62,.63,.64,.65,.66,.67,.68,.69,JET4 015
     5        .70,.71,.72,.73,.74,.75,.76,.77,.78,.79,.80,.81,.82,.83,JET4 016
     6        .84,.85,.86,.87,.88,.89,.90,.91,.92,.93,.94,.95,.96,.97,JET4 017
     7        .98,.99/                                                  JET4 018
C                                                                       JET4 019
C     CK = COMPLETE ELLIPTIC INTEGRALS OF FIRST KIND                    JET4 020
C                                                                       JET4 021
      DATA CK/1.570796,1.574746,1.578740,1.582780,1.586868,1.591003,    JET4 022
     1        1.595188,1.599423,1.603710,1.608049,1.612441,1.616889,    JET4 023
     2        1.621393,1.625955,1.630576,1.635257,1.640000,1.644806,    JET4 024
     3        1.649678,1.654617,1.659624,1.664701,1.669850,1.675073,    JET4 025
     4        1.680373,1.685750,1.691208,1.696749,1.702374,1.708087,    JET4 026
     5        1.713889,1.719785,1.725776,1.731865,1.738055,1.744351,    JET4 027
     6        1.750754,1.757269,1.763898,1.770647,1.777519,1.784519,    JET4 028
     7        1.791650,1.798918,1.806328,1.813884,1.821593,1.829460,    JET4 029
     8        1.837491,1.845694,1.854075,1.862641,1.871400,1.880361,    JET4 030
     9        1.889533,1.898925,1.908547,1.918410,1.928526,1.938908,    JET4 031
     A        1.949568,1.960521,1.971783,1.983371,1.995303,2.007598,    JET4 032
     B        2.020279,2.033369,2.046894,2.060882,2.075363,2.090373,    JET4 033
     C        2.105948,2.122132,2.138970,2.156516,2.174827,2.193971,    JET4 034
     D        2.214022,2.235068,2.257205,2.280549,2.305232,2.331409,    JET4 035
     E        2.359264,2.389016,2.420933,2.455338,2.492635,2.533335,    JET4 036
     F        2.578092,2.627773,2.683551,2.747073,2.820752,2.908337,    JET4 037
     G        3.016112,3.155875,3.354141,3.695637/                      JET4 038
C                                                                       JET4 039
C     CE = COMPLETE ELLIPTIC INTEGRALS OF SECOND KIND                   JET4 040
C                                                                       JET4 041
      DATA CE/1.570796,1.566862,1.562913,1.558948,1.554969,1.550973,    JET4 042
     1        1.546963,1.542936,1.538893,1.534833,1.530758,1.526665,    JET4 043
     2        1.522555,1.518428,1.514284,1.510122,1.505942,1.501743,    JET4 044
     3        1.497526,1.493290,1.489035,1.484761,1.480466,1.476152,    JET4 045
     4        1.471818,1.467462,1.463086,1.458688,1.454269,1.449827,    JET4 046
     5        1.445363,1.440876,1.436366,1.431832,1.427274,1.422691,    JET4 047
     6        1.418083,1.413450,1.408791,1.404105,1.399392,1.394652,    JET4 048
     7        1.389883,1.385086,1.380259,1.375402,1.370515,1.365596,    JET4 049
     8        1.360645,1.355661,1.350644,1.345592,1.340505,1.335382,    JET4 050
     9        1.330223,1.325024,1.319788,1.314511,1.309192,1.303832,    JET4 051
     A        1.298428,1.292979,1.287484,1.281942,1.276350,1.270707,    JET4 052
     B        1.265013,1.259263,1.253458,1.247595,1.241671,1.235684,    JET4 053
     C        1.229632,1.223512,1.217321,1.211056,1.204714,1.198290,    JET4 054
     D        1.191781,1.185183,1.178490,1.171697,1.164798,1.157787,    JET4 055
     E        1.150656,1.143396,1.135998,1.128451,1.120742,1.112856,    JET4 056
     F        1.104775,1.096478,1.087938,1.079121,1.069986,1.060474,    JET4 057
     G        1.050502,1.039947,1.028595,1.015994/                      JET4 058
C                                                                       JET4 059
```

```
      IF (MZZZ) 73,30,3                                                 JET4 060
    3 IF(AKSQ-.99)20,20,21                                              JET4 061
   21 PARA=0.25*(1.0-AKSQ)                                              JET4 062
  700 TEST = 1.00E-07                                                   JET4 063
      IF(PARA-TEST)701,702,702                                          JET4 064
  701 PARA=TEST                                                         JET4 065
  702 ZLP=ALOG(4./PARA)                                                 JET4 066
      TK=ZLP*0.5*(1.+PARA)-PARA                                         JET4 067
      TE=1.0+(ZLP*PARA)-PARA                                            JET4 068
      GO TO 30                                                          JET4 069
   20 JA=100.0*AKSQ                                                     JET4 070
      JA=1+JA                                                           JET4 071
      IF(CKK(JA)-AKSQ)22,23,22                                          JET4 072
   23 TK=CK(JA)                                                         JET4 073
      TE=CE(JA)                                                         JET4 074
      GO TO 30                                                          JET4 075
   22 CON=(AKSQ-CKK(JA))/(CKK(JA+1)-CKK(JA))                            JET4 076
      TK=CK(JA)+CON*(CK(JA+1)-CK(JA))                                   JET4 077
      TE=CE(JA)+CON*(CE(JA+1)-CE(JA))                                   JET4 078
      GO TO 30                                                          JET4 079
   73 IF(AKSQ-.01)721,721,720                                           JET4 080
  721 PARA=.25*AKSQ                                                     JET4 081
      GO TO 700                                                         JET4 082
  720 AKSQ=1.-AKSQ                                                      JET4 083
      GO TO 20                                                          JET4 084
   30 CONTINUE                                                          JET4 085
      RETURN                                                            JET4 086
      END                                                               JET4 087
```

SAMPLE CASE

In this section a sample case is described to illustrate the use of the computer programs presented in this report. The case involves an engine wake-wing-flap interference determination. The configuration comprises a swept-wing with flap and one engine mounted underneath the wing panel. Both the wing-flap and jet wake flow model programs are used in accordance with the interference determination procedure described in a previous section.

For the illustrative sample case, the chosen airframe configuration is the semispan swept wing-flap wind tunnel model of reference 5. A 1.02 pressure ratio ducted fan was pylon mounted under the semiwing at mid-span. The wing was cambered with zero dihedral and had no taper. Figure 22(a) shows the configuration in planform and elevation. Figure 22(b) is a section normal to the leading and trailing edges of the wing and flaps. Figure 22(c) shows how the deflected triple slotted flaps, denoted type I with $\delta = 30^{\circ}$ in reference 5, are idealized to a single flap with camber. The flap component deflection angles in the plane normal to the hingeline are 10°, 20°, and 30° for the leading, middle, and aft flap components, respectively. The idealized flap deflection angle required in the input to the wing-flap program must also be specified normal to the hingeline and measures 21.5° in figure 22(c). The wing and idealized flap root chords and other streamwise lengths are related to the lengths perpendicular to the wing and flap leading and trailing edges through the cosine of the sweep angle. The basic wing chord is the chord of the original wing before the trailing edge flaps were attached. In the normal direction, this chord is 5.5 feet, so the (streamwise) basic wing chord for this sample case with a wing sweep angle of 30° is 6.35 feet.

The parameters required by the wing-flap program will now be described. On the wing, a 4 chordwise by 20 spanwise vortex lattice is laid out with equal spanwise spacings. Since the idealized flap chord is longer than the wing chord, 5 chordwise vortices are specified for the flap and the spanwise layout is taken the same as on the wing. Consequently, mean surface angles due to camber and twist are required at four chordwise stations on the wing and 5 chordwise stations over the flap semispan. On the wing, the angles are input as tangents; on the idealized flap the angles are input in radians. These quantities are determined as follows.

The chordwise locations of the control points are given by the midpoint of the 3/4 chord of the area elements in the chordal planes of the wing and idealized flap. The wing airfoil section was specified as NACA 63_2-416 (modified) normal to the wing leading and trailing edge. The mean surface slopes in the streamwise direction are therefore obtained from the slopes associated with the $a = 1.0$ mean line by a scaling procedure:

$$\text{wing mean surface slope} = \tan \alpha_\ell = \left.\frac{d\left(\frac{y_c}{c}\right)}{d\left(\frac{x}{c}\right)}\right|_{c_{\ell_i} = 1.0} c_{\ell_i} \cos \psi \qquad (29)$$

For this case, $c_{\ell_i} = 0.4$ and the cosine factor accounts for the sweep. The chord c is the basic wing chord. Slopes $d(y_c/c)/d(x/c)\big|_{c_{\ell_i} = 1.0}$ for the $a = 1.0$ line are obtained from reference 15, at control point stations x/c based on the basic wing chord ($c = 6.35$ feet). On the flap, the segment characteristics were not specified precisely. Consequently, it is assumed that each segment has no camber. The surface slopes are then given by the difference in slope between the segment mean line and the idealized flap chord line in planes normal to the hingeline. To obtain the slopes in the streamwise direction, the normal slopes are multiplied by cos ψ. To complete the input specifications, the coordinates of a series of points on the geometric engine centerline are required. The necessary information is available in figure 22. A sufficient number of points on the extension to the engine centerline were chosen to generate a good theoretical representation of the flow field from the engine inlet to a point one wing chord length aft of the trailing edge.

The user is now prepared to run the wing-flap program for zero angle of attack without externally induced perturbation velocities. The input deck for this reference (power-off) calculation is shown in figure 21. A data set containing the coordinates of the wing and flap control points is generated (KCP = 7) for use by the jet wake program (KIN = 7). Downwash and sidewash perturbation velocities induced by wing flap vorticity at the specified points along the engine centerline are included in the output shown in figure 23(a). Curves of these induced velocities are shown in figure 17(b).

Details of the jet wake to be included in the sample calculation will now be set up and the induced velocity field determined. Based on the reference area (S_{REF} = 136.8 ft^2) used in reference 5, the fan thrust coefficient under consideration is C_μ = 0.91. From equation (17) the corresponding fan exit velocity ratio based on the fan exit flow area is 4.7. For this configuration which has a large centerbody, the flow was assumed to fill the entire area within the duct exit outer diameter. With this correction, the velocity ratio becomes 3.46. From figure 5, the length of the initial region, ℓ_c, is 13.6 R_o and the radius, R, of the wake boundary at the end of the initial region is 1.97 R_o. If we assume the total length of the jet to be 150 R_o, the final radius of the boundary is approximately 9.5 R_o as obtained from figure 4. The engine has no incidence with respect to the wing root chord. Thus, assuming no downwash or sidewash effect, the shape of the jet is shown in the following sketch.

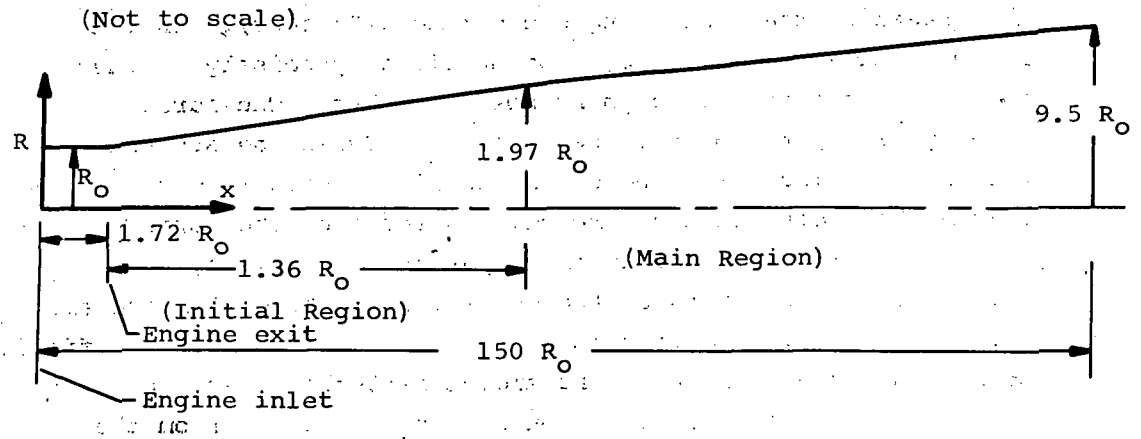

Deflection of the engine wake due to wing-flap induced downwash and sidewash is calculated in the following manner. The wash velocities computed by the wing-flap program with no power effects are shown in figure 17(b). The results of figure 17(b) were obtained from the computer output of figure 23(a). The points along the wake selected for computing the wake deflection are the fan inlet (x/R_o = 0), the fan exit (1.72), a point below the center of the second flap segment (8.5), the end of the initial region (15.3), and a point 150 R_o downstream of the fan exit. Note that the initial region extends considerably downstream of the flap trailing edge.

At the first two points, the wake is of constant radius equal to R_o and is undeflected. At the third point, from figure 17(b), the induced downwash is about +0.2V and the sidewash is about -0.15V (outboard under this left wing panel). At this point, from equation (27), $\bar{V}_j/V$ is 2.64 and, from figure 5, R is about 1.5 R_o. When the wash velocities are combined with $\bar{V}_j$ in accordance with equation (28) (with $\alpha = 0$), the wake deflection angles are $\varepsilon_z = -4.5°$ and $\varepsilon_y = -3.3°$. The coordinates of the wake at this point are obtained by laying out a straight line from the engine exit ($x/R_o = 1.72$) to the third point with slopes in the vertical and horizontal planes equal to the average of the slopes at the second and third points (or -2.25° and -1.65°, respectively).

The fourth point ($x/R_o = 15.3$) is downstream of the region in which wash velocities were calculated. Since the important part of the wake between $x/R_o = 8.5$ and 15.3 is that part near the aft flap segment, the slopes of the wake at $x/R_o = 15.3$ are taken as the values at $x/R_o = 8.5$, which values also occur just downstream of the aft flap segment. Thus, the average values of slopes for the wake centerline segment between 8.5 and 15.3 are the values at either end.

At the last point, the wake is assumed to reach the free stream direction, so its slopes are zero. The resulting wake characteristics are shown in the following table.

x_{CL}/R_o	y_{CL}/R_o	z_{CL}/R_o	R/R_o	θ(deg.)
0	0	0	1.0	0
1.72	0	0	1.0	0
8.5	-0.2	-0.3	1.5	-4.5
15.3	-0.6	-0.8	1.97	-4.5
150.0	-3.0	-5.0	9.5	0

Note that the coordinates are all relative to a system fixed in the jet inlet (fig. 9(a)).

The input deck for this wake calculation is shown in figure 25(a). The wing and flap control points are input via a data set generated by the wing-flap program and the induced velocity field is output in another data set (KOUT = 8) for subsequent use by the wing-flap program (KEI = 8).

The wing-flap program is now rerun to obtain the wing-flap loading including the effect of the wake-induced velocities. The input is shown in figure 21(b). The aerodynamic parameters in the output, figure 23(b), reflect the effects of the jet wake interfering on the wing-flap system. The total lift and moment coefficients in the output must be incremented by the appropriate contribution due to engine thrust

$$\left.\begin{aligned} C_{L_{\substack{\text{Wing-flap}\\+\\\text{thrust}}}} &= C_{L_{\text{Wing-flap}}} + C_{\mu} \sin \alpha \\ C_{m_{\substack{\text{Wing-flap}\\+\\\text{thrust}}}} &= C_{m_{\text{Wing-flap}}} + C_{\mu} \frac{Z_{\text{engine}}\, C_L}{C_{\text{ave}}} \end{aligned}\right\} \tag{30}$$

where Z_{engine} is the vertical coordinate of the engine centerline. For this case, the angle of attack is zero. There is no increment in lift but the pitching moment is increased (Z_{engine} = 2.07 ft from figure 22(b)).

CONCLUDING REMARKS

Analytical methods have been developed to predict the loading distribution on an externally-blown jet-augmented wing-flap configuration with a high-bypass-ratio turbofan engine. Two potential flow models were developed. The first is a nonplanar lifting surface method capable of representing a wing of arbitrary sweep, taper, dihedral, camber, and twist with a large, multiply-slotted, partial or full span flap which can have large deflection angles. The second is a model of the jet wake of a turbofan engine which represents the mass flow, momentum, and spreading rate of a turbulent, coflowing jet and which has the capability to follow a curved centerline. These models are used in sequence to first define the flow field beneath the wing-flap in the absence of an engine to locate the jet wake centerline, then predict the flow field induced by the jet on the wing-flap, and finally calculate the loading on the wing-flap in the presence of the jet wake. The methods yield lift and pitching moment coefficients for the case of symmetry about the vertical plane through the root chord. More than one engine

per semispan can be treated, with the provision that if the engine wakes overlap, their mutual interference is neglected and their effects are considered additive.

Some data are available on lift and pitching moment on wing-flap combinations with externally blown flaps. With few exceptions, these data do not include any direct measurements of the flow at the engine exit or the nature of the engine wake spreading. Such data would be useful in checking computed values of engine exit velocities and in understanding the spreading and deflection of the wake under the wing. Comparisons between predicted and measured lift and pitching moment indicate that the method is satisfactory for predicting lift on externally blown jet-augmented unswept and swept wings with flap deflection angles up to 30 to 40 degrees. In this range, the pitching moment is well predicted for unswept wings but underpredicted somewhat (not sufficiently negative) for swept wings. For flap deflections in excess of 40 degrees, with or without power, the method begins to overpredict lift, due primarily to the onset of flow separation on the flap segments, with overpredictions of 10 to 15 percent at a flap angle of 60 degrees. The pitching moments are considerably underpredicted at large flap angles.

The lift that is obtained through wake-wing-flap interaction is sensitive to the position of the wake relative to the wing chord. Calculations made with and without wake deflection due to the wing-induced downwash and V sin α upwash indicate significant improvements in the accuracy of prediction with inclusion of the wash effects. Since the jet augmentation can be modified by changing the location and incidence of the engine relative to the local wing chord, the prediction method offers a means of systematically investigating the influence of these two variables on jet augmentation.

The single most important factor in increasing the reliability and utility of the prediction method is the wake position determination. A systematic investigation could be done using existing overall force and moment data to evaluate the degree of detail required in the wake description, to examine the final velocity field beneath and aft of the wing, and to determine the sensitivity of the predicted load distributions to wake position. Such an investigation would provide considerable insight into the adequacy of the wake flow model. This work would benefit greatly,

however, by direct flow field measurements made with an EBF model, where care is taken to measure engine thrust and exit velocity profiles and possibly load distributions on the flaps as well as the flow field.

Nielsen Engineering & Research, Inc.
Mountain View, California
February 1972

APPENDIX A

ARRANGEMENT OF VORTICES ON THE WING-FLAP

Calculations were made for a variety of wing-flap configurations to provide guidance to the user of the program on the arrangement of the vortices on the wing-flap. The spanwise and chordwise number of vortices and the vortex spacing on the wing and flap were varied to determine the effect on the predicted aerodynamic forces and moments. As a brief summary of the results to be presented, the following conditions were investigated:

- Nominal aspect ratio 3, 5, and 7 untapered wings with zero and 30-degree sweep and a flap chord approximately half the total wing-flap chord.
- Aspect ratio 3.2 untapered wing with 30-degree sweep and a flap chord approximately one quarter that of the wing-flap chord.
- Aspect ratio 3.2 untapered wing with 30-degree sweep and a part span flap (64 percent) with a chord approximately half the total wing-flap chord.
- Aspect ratio 3.2 untapered wing with 30-degree sweep and a flap chord approximately half the total wing-flap chord and engine wake interaction.

At the end of this appendix some guidelines are given for the vortex layout, based on the calculations made.

Configurations

The major part of the work was conducted using the 30-degree swept wing with triple slotted flap (Flap I) of reference 5. This wing is not tapered and has a combined flap chord of about 58 percent of the combined wing-flap with flap undeflected. The aspect ratio is 3.2. The higher aspect ratio cases were obtained by extending the span an appropriate amount. The unswept configurations have the same flap and camber arrangements. The part span flap configuration was obtained from the 3.2 aspect ratio swept wing-flap by reducing the flap length to the inner 64 percent of the wing span. The smaller flap chord configuration was obtained from the 3.2 aspect ratio swept wing-flap by extending the wing chord and shortening the flap chord so that the flap reduced to a single flap segment

having a chord one-fourth of the total root chord. This flap is uncambered. All moments are taken about a center located at an X station corresponding to the 62 percent root chord.

Wings with Large Flaps

The first set of results, listed in the table below, are those of the basic, aspect ratio 3.2, swept wing with flap deflection angles of 10/20/30 degrees at an angle of attack of 10 degrees.

VORTEX LATTICE		C_L	C_m	C_{D_i}/C_L^2	C_m/C_L
NCW MSW	NCF MSF				
4 x 8	5 x 8	3.915	-1.056	0.0400	-0.269
4 x 8	8 x 8	4.037	-1.018	0.0402	-0.252
4 x 8	10 x 8	4.053	-1.004	0.0402	-0.248
7 x 8	8 x 8	4.038	-1.028	0.0402	-0.255
7 x 8	10 x 8	4.054	1.014	0.0402	-0.250
4 x 14	5 x 14	3.857	-1.022	0.0410	-0.265
4 x 14	8 x 14	3.977	-0.984	0.0410	-0.248
4 x 14	10 x 14	3.993	-0.970	0.0414	-0.243
7 x 14	8 x 14	3.979	-0.994	0.0414	-0.250
4 x 20	5 x 20	3.831	-1.004	0.0416	-0.262
4 x 10	5 x 12	3.903	-1.049	0.0403	-0.268

Loading Results for an aspect ratio 3.2 swept wing-flap at $\alpha = 10°$.

The chordwise numbers of vortices (wing/flap) of 4/5 and 7/8 represent approximately equal chordwise lengths of the area elements over both wing and flap. The 4/8 and 4/10 arrangements represent attempts to get a higher density of elements on the flap. The spanwise numbers considered are 8, 14 and 20 elements, all of equal spanwise width. For 20 spanwise elements, the larger number of chordwise elements cannot be run because of size limitations in the program. The final case is one in which an 8-spanwise element arrangement is modified by dividing each of the two elements around the wing mid-semispan into halves and each of the four elements around the flap mid-semispan into halves. The objective is to determine the effect of locally increasing the spanwise density of elements in the region on which an engine wake would impinge.

APPENDIX A

The results for C_L, C_m, and the span load distribution are shown in figure A-1 for $\alpha = 10°$. The spanwise variations indicate that the calculation has essentially converged with 14 elements. The chordwise variations indicate that 4 elements are sufficient on the wing, but that 7 or 8 elements are required on the flap. Figure A-1(b) shows that the flap span load distribution has converged with 5 chordwise flap elements, but the wing load distribution has not. Thus the additional chordwise elements are required on the flap to cause the proper interference to be felt on the wing.

Similar results are obtained for the same parameters at $\alpha = 0$. There are considerably larger changes as a result of increasing the flap chordwise elements from 5 to 8, because the flap is the primary source of lift in this case, both directly and by its interference on the wing. The calculated values are shown in the table below.

VORTEX LATTICE		C_L	C_m	C_{D_i}/C_L^2	C_m/C_L
NCW MSW	NCF MSF				
4 x 8	5 x 8	2.699	-1.227	0.0389	-0.4544
4 x 8	10 x 8	2.852	-1.170	0.0390	-0.4103
7 x 8	8 x 8	2.836	-1.195	0.0390	-0.4212
4 x 14	5 x 14	2.657	-1.197	0.0400	-0.4504
4 x 14	10 x 14	2.809	-1.140	0.0402	0.4060
7 x 14	8 x 14	2.793	-1.165	0.0401	-0.4171
4 x 20	5 x 20	2.639	-1.182	0.0404	-0.4478
4 x 10	5 x 12	2.690	-1.220	0.0392	-0.4530

Loading results for an aspect ratio 3.2 swept wing-flap at $\alpha = 0°$.

Finally, it can be seen with these results (comparing 4 x 8, 5 x 8 with 4 x 10, 5 x 12) that if one starts with a uniform spanwise arrangement and divides certain elements to obtain a locally denser arrangement spanwise, the predicted loading is essentially unchanged from that of the original uniform arrangement. Thus, to improve convergence by increasing the spanwise number of vortices, one must distribute the increase over the entire span. Conversely, one may judge the convergence of a spanwise arrangement which is locally more dense from the closest uniform spanwise arrangement.

If the aspect ratio of the basic wing just discussed is increased, retaining the sweep, taper, and flap characteristics, a very similar pattern occurs. Results for aspect ratios of 5 and 7 at wing angles of attack of 10° are presented in the tables below and in figures A-3 and A-4. These results indicate that spanwise convergence is obtained with

VORTEX LATTICE		C_L	C_m	C_{D_i}/C_L^2	C_m/C_L
NCW MSW	NCF MSF				
4 x 8	5 x 8	4.556	-3.973	0.0259	-0.872
7 x 8	8 x 8	4.700	-4.037	0.0260	-0.857
4 x 14	5 x 14	4.499	-3.899	0.0268	-0.866
7 x 14	8 x 14	4.642	-3.962	0.0269	-0.854
4 x 20	5 x 20	4.473	-3.861	0.0272	-0.862

Loading results for an aspect ratio 5 swept wing-flap at $\alpha = 10°$.

VORTEX LATTICE		C_L	C_m	C_{D_i}/C_L^2	C_m/C_L
NCW MSW	NCF MSF				
4 x 8	5 x 8	4.963	-7.698	0.0188	-1.55
4 x 8	8 x 8				
7 x 8	8 x 8	5.121	-7.882	0.0188	-1.54
4 x 14	5 x 14	4.906	-7.577	0.0196	-1.55
4 x 14	8 x 14				
7 x 14	8 x 14	5.062	-7.758	0.0197	-1.54
4 x 20	5 x 20	4.881	-7.520	0.0199	-1.54

Loading results for an aspect ratio 7 swept wing-flap at $\alpha = 10°$.

14 elements and that the chordwise density must be higher on the (large) flap than on the wing to obtain the proper flap-wing interference effects.

The effect of increasing the flap deflection to 20/40/60 degrees with the basic aspect ratio 3.2 swept wing is shown in the table below and in figure A-5. The calculations were

APPENDIX A

ANGLE OF ATTACK (deg.)	VORTEX LATTICE		C_L	C_m	C_{D_i}/C_L^2	C_m/C_L
	NCW MSW	NCF MSF				
0	4 x 14	5 x 14	4.702	-1.639	0.039	-0.348
0	4 x 14	10 x 14	4.856	-1.590	0.039	-0.327
0	7 x 14	8 x 14	4.849	-1.617	0.039	-0.334
10	4 x 14	5 x 14	5.601	-1.336	0.041	-0.238
10	4 x 14	10 x 14	5.730	-1.293	0.041	-0.226
10	7 x 14	8 x 14	5.726	-1.319	0.041	-0.230

Loading results for an aspect ratio 3.2 swept wing-flap with large flap deflection.

made with 14 spanwise elements and various combinations of chordwise elements, since the previous calculations indicated convergence with 14 elements. As was the case for the smaller flap deflection, four spanwise elements on the wing are sufficient, but a denser arrangement must be used on the flap.

The characteristics of wings of zero sweep angle which are otherwise identical to the 3.2 aspect ratio swept wing-flap configuration are shown in figures A-6, A-7, and A-8 and the tables below for both 0° and 10° angle of attack.

VORTEX LATTICE		C_L	C_m	C_{D_i}/C_L^2	C_m/C_L
NCW MSW	NCF MSF				
4 x 8	5 x 8	3.050	1.841	0.043	0.603
4 x 8	8 x 8	3.184	2.028	0.043	0.636
7 x 8	8 x 8	3.188	2.021	0.043	0.633
4 x 14	5 x 14	3.000	1.810	0.044	0.603
4 x 14	8 x 14	3.133	1.994	0.044	0.636
7 x 14	8 x 14	3.137	1.987	0.044	0.633
4 x 20	5 x 20	2.981	1.797	0.044	0.602

Loading results for an aspect ratio 2.8 unswept wing-flap at $\alpha = 0°$.

VORTEX LATTICE		C_L	C_m	C_{D_i}/C_L^2	C_m/C_L
NCW MSW	NCF MSF				
4 x 8	5 x 8	3.640	2.343	0.028	0.657
4 x 14	5 x 14	3.592	2.358	0.029	0.656
4 x 20	5 x 20	3.571	2.344	0.029	0.657

Loading results for an aspect ratio 4.4 unswept wing-flap at $\alpha = 0°$.

VORTEX LATTICE		C_L	C_m	C_{D_i}/C_L^2	C_m/C_L
NCW MSW	NCF MSF				
4 x 8	5 x 8	4.032	2.777	0.020	0.688
4 x 14	5 x 14	3.988	2.742	0.021	0.687
4 x 20	5 x 20	3.968	2.727	0.021	0.687

Loading results for an aspect ratio 6.1 unswept wing-flap at $\alpha = 0°$.

VORTEX LATTICE		C_L	C_m	C_{D_i}/C_L^2	C_m/C_L
NCW MSW	NCF MSF				
4 x 8	5 x 8	4.238	3.374	0.045	0.795
4 x 8	8 x 8	4.357	3.547	0.045	0.815
7 x 8	8 x 8	4.361	3.541	0.045	0.812
4 x 14	5 x 14	4.175	3.324	0.046	0.796
4 x 14	8 x 14	4.290	3.494	0.046	0.814
7 x 14	8 x 14	4.295	3.489	0.046	0.813
4 x 20	5 x 20	4.147	3.303	0.046	0.797

Loading results for an aspect ratio 2.8 unswept wing-flap at $\alpha = 10°$.

APPENDIX A

VORTEX LATTICE		C_L	C_m	C_{D_i}/C_L^2	C_m/C_L
NCW MSW	NCF MSF				
4 x 8	5 x 8	5.080	4.198	0.029	0.825
4 x 14	5 x 14	5.018	4.145	0.029	0.825
4 x 20	5 x 20	4.990	4.122	0.029	0.825

Loading results for an aspect ratio 4.4 unswept wing-flap at $\alpha = 10°$.

VORTEX LATTICE		C_L	C_m	C_{D_i}/C_L^2	C_m/C_L
NCW MSW	NCF MSF				
4 x 8	5 x 8	5.650	4.766	0.021	0.843
4 x 14	5 x 14	5.593	4.712	0.021	0.843
4 x 20	5 x 20	5.566	4.689	0.021	0.842

Loading results for an aspect ratio 6.1 unswept wing-flap at $\alpha = 10°$.

The results for zero sweep are similar to those for 30-degree sweep in terms of convergence. The gross force and moment parameters essentially converge to within 1 percent with 14 spanwise elements. The (large) flap requires a denser chordwise spacing than the wing to effect convergence, as is indicated by the span load distributions.

Wings with Small Flaps

A series of calculations was made with an aspect ratio 3.2, 30 degrees swept, untapered wing having a smaller flap system than the one considered in the previous section. The flap considered here is a single, full span flap segment having a chord equal to 25 percent of the combined wing-flap chord with flaps up. The flap deflection is 21.5°, which is the mean deflection angle for the 10/20/30 degrees flap considered previously. Calculations were made for angles of attack of 0 and 10 degrees. All cases were run with 14 spanwise vortices. The results are shown in the table below and in figure A-9.

ANGLE OF ATTACK (deg.)	VORTEX LATTICE		C_L	C_m	C_{D_i}/C_L	C_m/C_L
	NCW MSW	NCF MSF				
0	7 x 14	2 x 14	0.838	-0.309	0.073	-0.369
0	4 x 14	5 x 14	0.839	-0.305	0.073	-0.364
0	4 x 14	8 x 14	0.840	-0.305	0.073	-0.363
10	7 x 14	2 x 14	1.544	-0.237	0.073	-0.153
10	4 x 14	5 x 14	1.545	-0.233	0.073	-0.151
10	4 x 14	8 x 14	1.546	-0.233	0.073	-0.151

Loading results for an aspect ratio 3.2 swept wing with small flap.

The tabular results and those presented in figure A-9 indicate no essential differences in computed loads between the three cases for each angle of attack. The case with 7 chordwise elements on the wing and 2 on the flap represents essentially the same element chordwise length on both flap and wing, whereas the other two represent denser spacings on the flap. For this size flap, the uniform spacing along the entire wing-flap chord is sufficient to obtain the proper wing-flap interference.

It should be noted that as the flap chord decreases relative to the wing chord, the case of a wing alone is approached. In this case, one can use the more extensive calculation presented in reference 10 as a guide to the selection of the vortex-lattice arrangement.

Wings with Part Span Flaps

The method is capable of treating a partial span flap which protrudes from the wing trailing edge. In order to investigate the effect on the load distribution of the positions of the trailing legs of the horseshoe vortices relative to the flap tip, some calculations were run for the basic 30 degree swept, aspect ratio 3.2 wing with the 58 percent chord triple slotted flap. The flap however was considered to extend only from the root chord to the 64 percent semispan station. The spanwise area element arrangements of the two vortex configurations are the following:

APPENDIX A

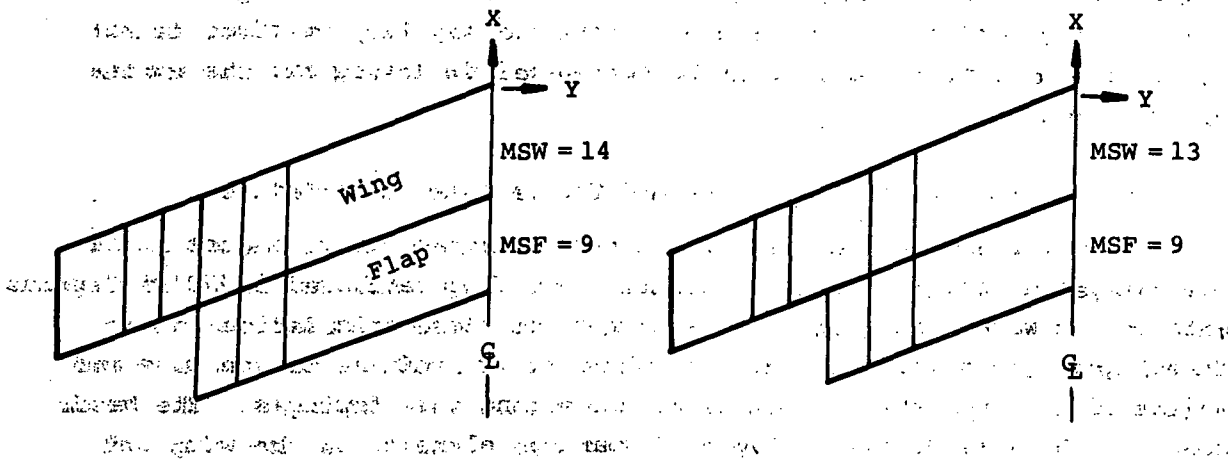

The layout on the wing is basically a 5 x 14 arrangement. The flap has 8 chordwise elements and the same spanwise element size as the wing. Since the flap span is only 64 percent of the wing span, the flap has 9 spanwise elements. In the case on the left above, the Y = constant plane at the flap tip contains trailing legs of both wing and flap vortices. The wing vortex trailing legs lie in the Z = 0 plane, while the flap vortex trailing legs lie in the plane of the flap. In the case on the right, the two spanwise elements on the wing near the 64 percent semispan station have been combined into one element so that no wing vortex legs lie in the same Y plane as the flap tip chord. Thus, the wing element arrangement is a 5 x 13 and the flap arrangement, as before, is an 8 x 9.

The computed results for the span load distribution at $\alpha = 0$ are shown in figure A-10. There is a slight difference in wing loading just outboard of the flap. The influence on the overall loading of this difference is small, however, as shown in the following table

VORTEX LATTICE		C_L	C_m	C_{D_i}/C_L^2	C_m/C_L
NCW MSW	NCF MSF				
5 x 14	8 x 9	1.757	-0.159	0.061	-0.0904
5 x 13	8 x 9	1.771	-0.162	0.059	-0.0913

Loading results for a low aspect ratio swept wing-flap with part span flap at $\alpha = 0°$.

Thus, the coincidence between any Y-plane containing the wing vortex trailing legs and the Y-plane containing the tip flap vortices is not important and should not have to be considered in laying out the vortex arrangement.

Wings with Large Flaps and Engine Wake Augmentation

Calculations were made for the basic 30 degree swept, aspect ratio 3.2 untapered wing with the 58 percent chord flap deflected 10/20/30 degrees with engine wake impingement. The purpose of these calculations is to investigate the sensitivity of the wake-induced loadings to the size and layout of the area elements on which the engine wake impinges. The basic case is a lattice layout employing 8 spanwise elements on the wing and flap, 4 chordwise elements on the wing and 5 chordwise elements on the flap. This arrangement was perturbed by dividing sets of elements spanwise into halves near the mid-semispan location, under which the engine wake centerline is assumed to lie, in accordance with the following sketches. The first case is the uniform spanwise arrangement, the second has 2 additional elements on the wing and 4 on the flap, and the third case has 5 additional on the flap. The engine thrust coefficient (for one engine) was taken to

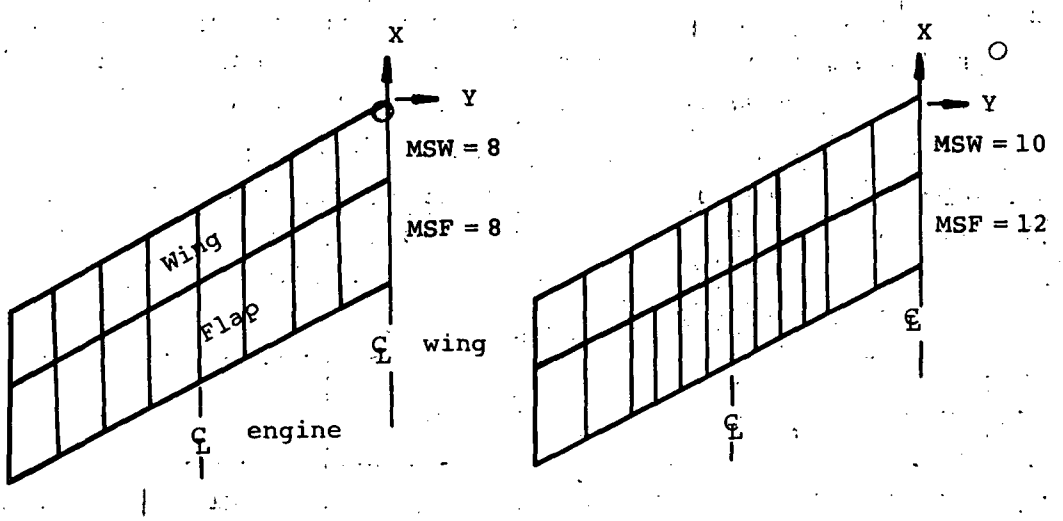

APPENDIX A

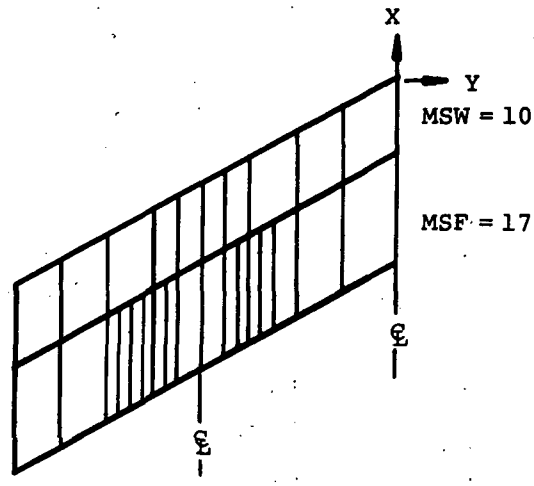

be 0.9, a relatively high thrust level. The force and moment results for $\alpha = 10°$ are given in the following table.

LATTICE ARRANGEMENT		C_μ	C_L	C_m	C_{D_i}/C_L^2	C_m/C_L
NCW MSW	NCF MSF					
4 x 8	5 x 8	0	3.915	-1.056	0.040	-0.269
4 x 10	5 x 12	0	3.903	-1.049	0.040	-0.268
4 x 10	8 x 12	0	4.025	-1.011	0.041	-0.251
4 x 10	8 x 17	0	4.021	-1.007	0.041	-0.250
4 x 8	5 x 8	0.9	5.853	-2.869	0.037	-0.490
4 x 10	5 x 12	0.9	5.567	-2.744	0.029	-0.493
4 x 10	8 x 12	0.9	5.675	-2.640	0.040	-0.465
4 x 10	8 x 17	0.9	5.726	-2.718	0.040	-0.473

Loading results for an aspect ratio 3.2 swept wing-flap at $\alpha = 10°$ with engine wake inpingement.

The forces and moments for $C_\mu = 0.9$ do not include the direct contribution of engine thrust. The tabulated results indicate a considerably larger effect in going from 5 to 8 chordwise elements on the flap than in increasing the spanwise number on the flap from 12 to 17 without wake augmentation, as was the case in previous calculations. With wake augmentation, increases in both spanwise and chordwise number on the flap cause comparable changes

in lift and moment. With wake augmentation, it would not appear necessary to employ any greater a number of elements chordwise and spanwise than is necessary to achieve convergence without wake augmentation, insofar as lift is concerned. The moment is more sensitive to spanwise number, at least for swept wings, and might require a locally denser arrangement on the flap.

The span loading distributions for these cases are shown in figure A-11. Figure A-11(a) shows a comparison of the four lattice arrangements for $C_\mu = 0$. As was indicated previously, the lattice variation has essentially no influence on the flap loading, but the larger chordwise number shows slightly higher induced loadings on the wing. For the case of engine thrust, figure A-11(b), the span loading results are again very similar on the flap. The major effect on the wing is caused by increased chordwise number of vortices, with little effect due to adding spanwise vortices. The effect of engine wake augmentation for the largest number of vortices is shown in figure A-11(c). The flap loading is greatly increased in the region of direct impingement and slightly increased both inboard and outboard of the impingement region. The wing loading is increased over the entire span, with the greatest increments occurring somewhat outboard of the 50 percent semispan station due to wing sweep.

Recommended Procedure for Vortex Arrangement

The following comments are offered with respect to selecting a vortex arrangement for a wing-flap configuration based on the results of the calculations described above and the results of reference 10.

Spanwise number.- Convergence on the four gross aerodynamic properties examined (C_L, C_m, C_{D_i}/C_L^2, C_m/C_L) to within about one percent was obtained using 14 equally spaced elements on the semispan for nominal aspect ratios from 3 to 7 and sweep angles of 0 and 30 degrees and untapered planforms. The results of reference 10 indicate faster convergence as the taper ratio decreases. Thus, it is suggested that the spanwise number not exceed 14 equally spaced elements. It is noted that if an unequal spanwise spacing is employed to create a locally denser spacing, the degree of convergence should be assessed by the nearest equally spaced arrangement.

Chordwise number.- The choice of chordwise arrangement depends principally on the flap size. For a flap whose chord is one-quarter or less than that of the combined wing-flap, the wing-flap mutual interference and

the gross loading characteristics are adequately predicted by an equal spacing on the wing and flap. The convergence then depends on the total number of elements on the wing-flap. The results of reference 10 for a wing alone indicate very small differences between 4 and 6 elements. There should, of course, always be at least one row on the flap. If more chordwise definition of the flap loading is desired, additional elements can be placed on the flap without affecting the gross loading.

For a flap whose chord is greater than one-quarter that of the combined wing-flap, it is necessary to have more chordwise elements on the flap than on the wing to properly model the wing-flap mutual interference. It is suggested that twice as many elements be used on the flaps as on the wing.

The wing-flap aspect ratio, sweep, taper, and flap deflection angle appear to have little influence on convergence and generally need not be considered.

Other considerations.- One consideration that deserves comment is the effect on calculated loadings of the element arrangement in the region(s) of engine wake impingement. Small vertical and/or lateral changes in the engine wake centerline can cause the wake to "cover" or "uncover" area elements which can produce unrealistic discrete changes in wake-induced loading. Calculated results indicate, however, that if a sufficient number of uniformly spaced elements both chordwise and spanwise are used to achieve convergence on engine-off characteristics, the element sizes will be sufficiently small that the results will not be unduly influenced by changes in wake centerline location, at least for wings of low sweep. At larger sweep angles, the pitching moment appears sensitive to the spanwise number on the flap, and it may be desirable to have a locally denser spanwise arrangement in the region of wake impingement on the flap.

Finally, the end effects due to part-span flaps do not appear to be sensitive to the precise arrangement of area elements in the spanwise region of the flap tip.

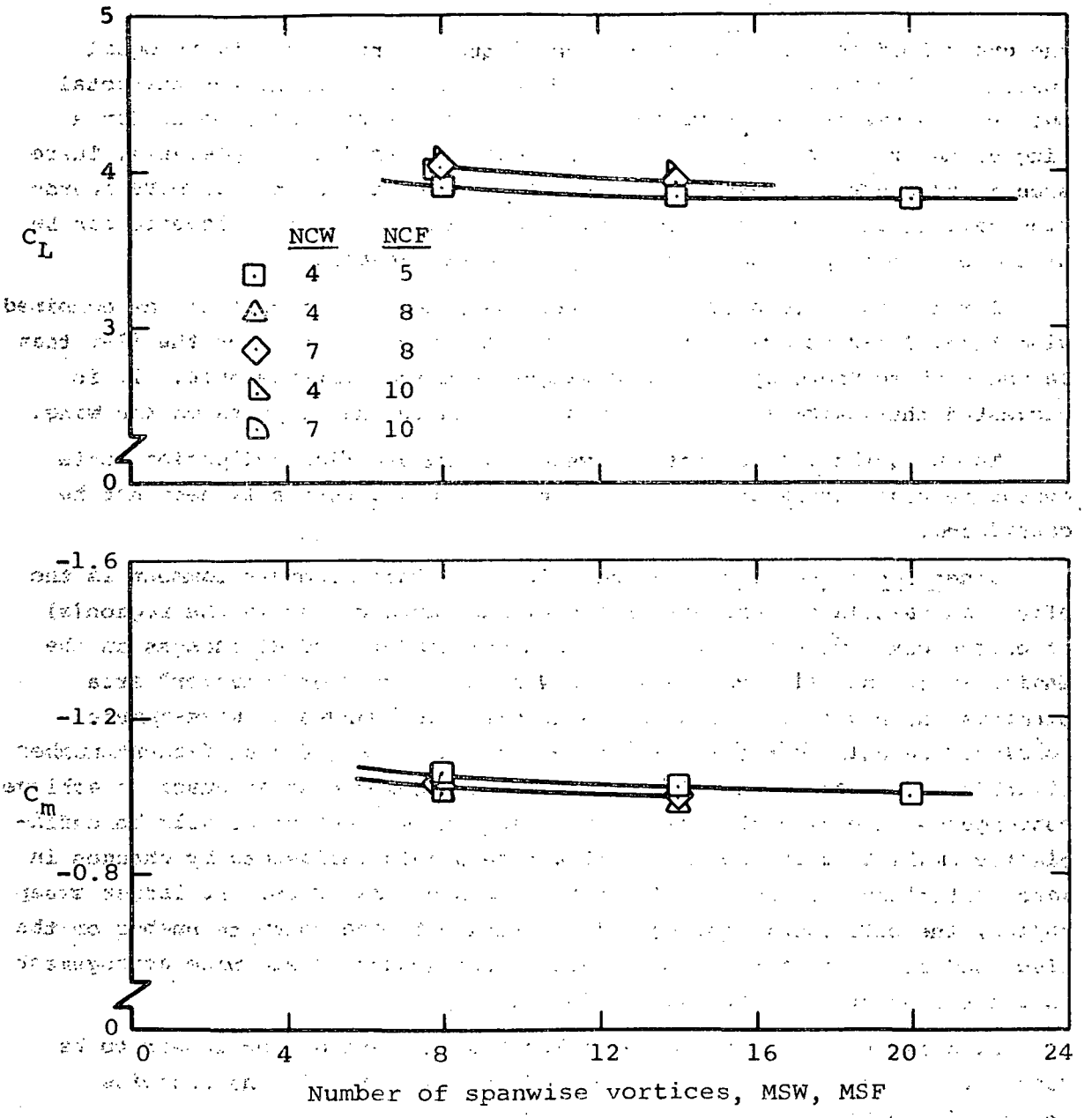

(a) Variation of lift and pitching-moment coefficients with vortex arrangement

Figure A-1.- Predicted load characteristics of a 30° swept, aspect ratio 3.2 untapered wing with a large, triple slotted flap at $\alpha = 10^{\circ}$.

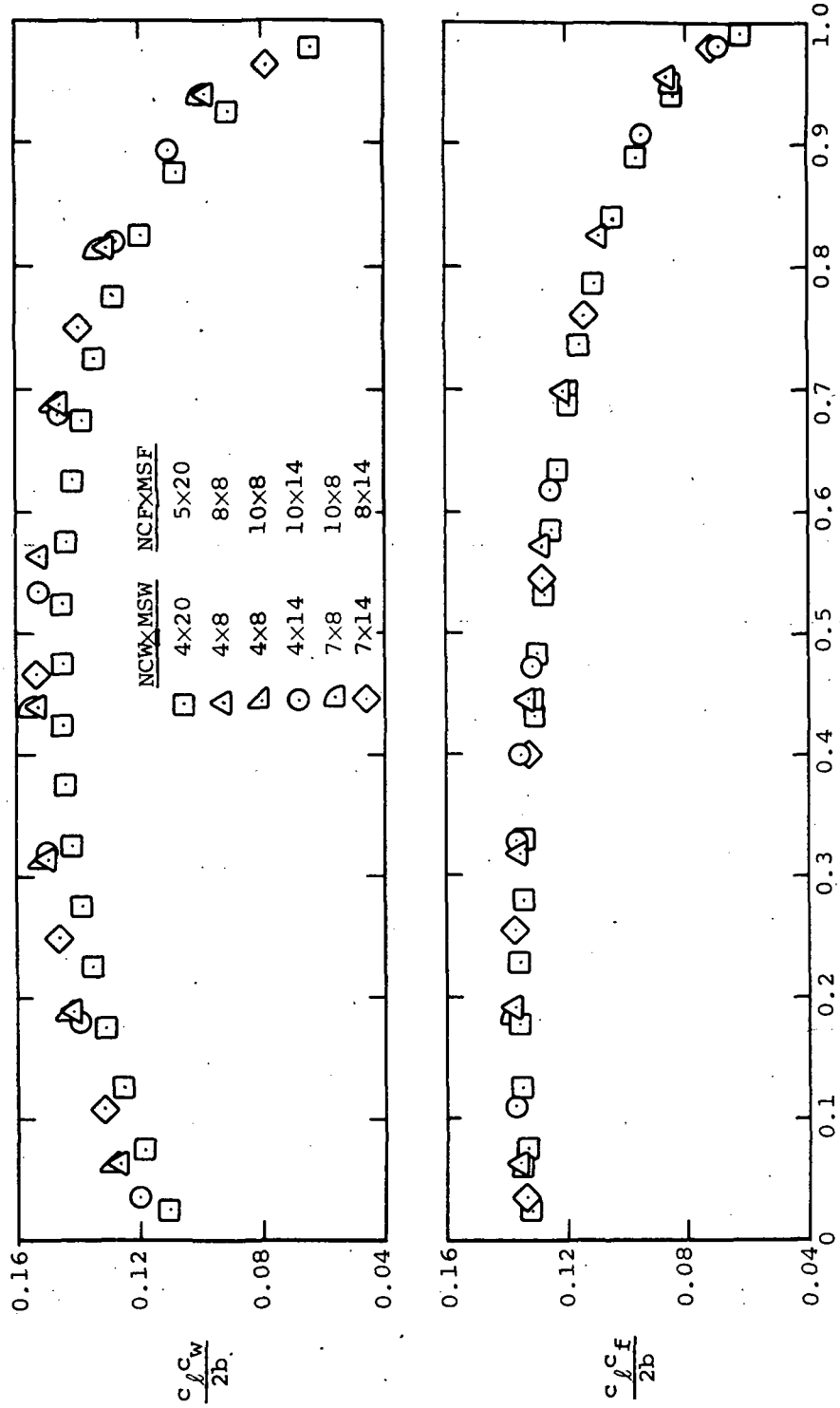

(b) Variation of span load distribution with vortex arrangement.

Figure A-1.- Concluded.

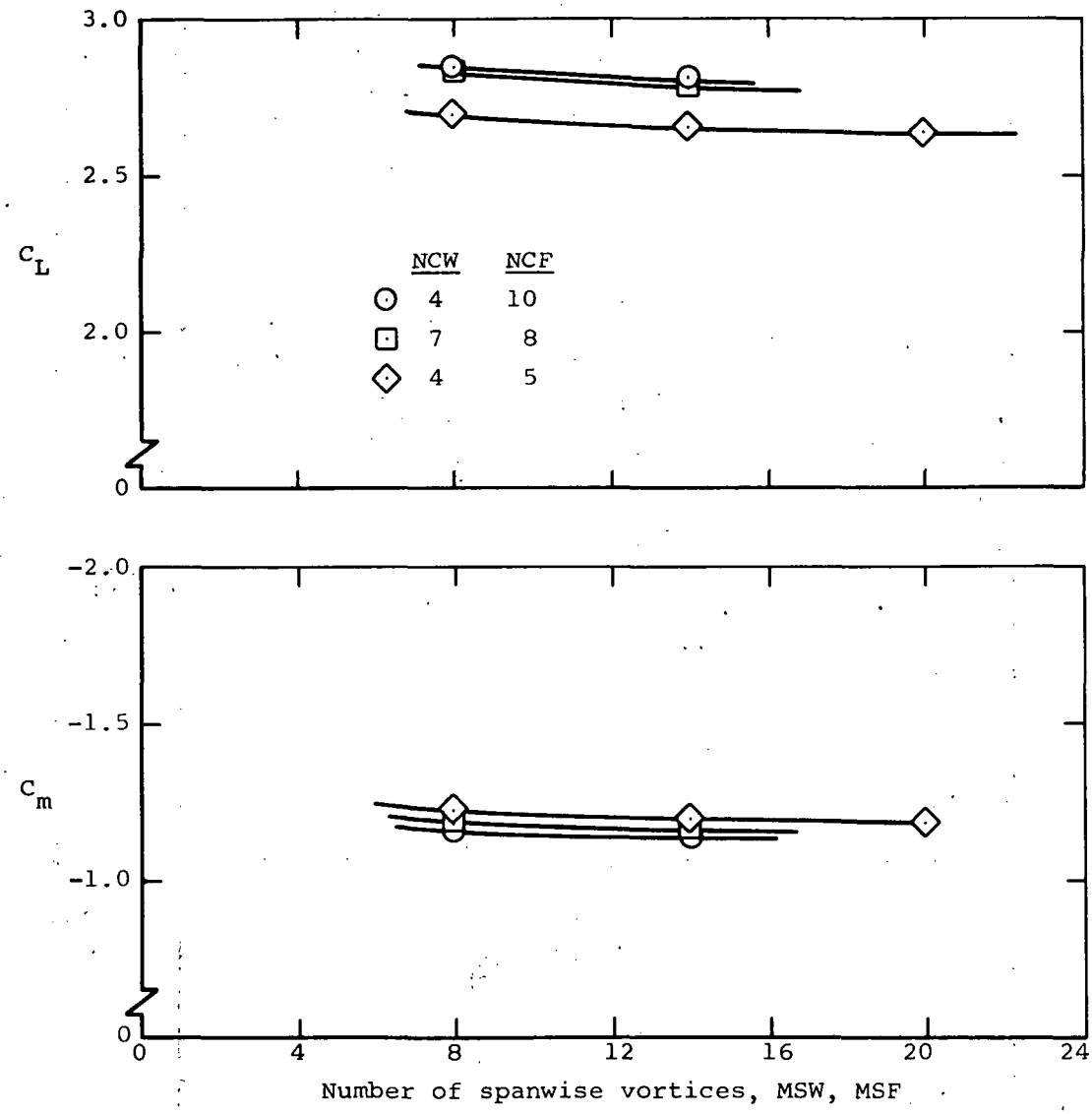

(a) Variation of lift and pitching-moment coefficients with vortex arrangement.

Figure A-2.- Predicted load characteristics of a 30° swept, aspect ratio 3.2 untapered wing with a large, triple slotted flap at $\alpha = 0^{\circ}$.

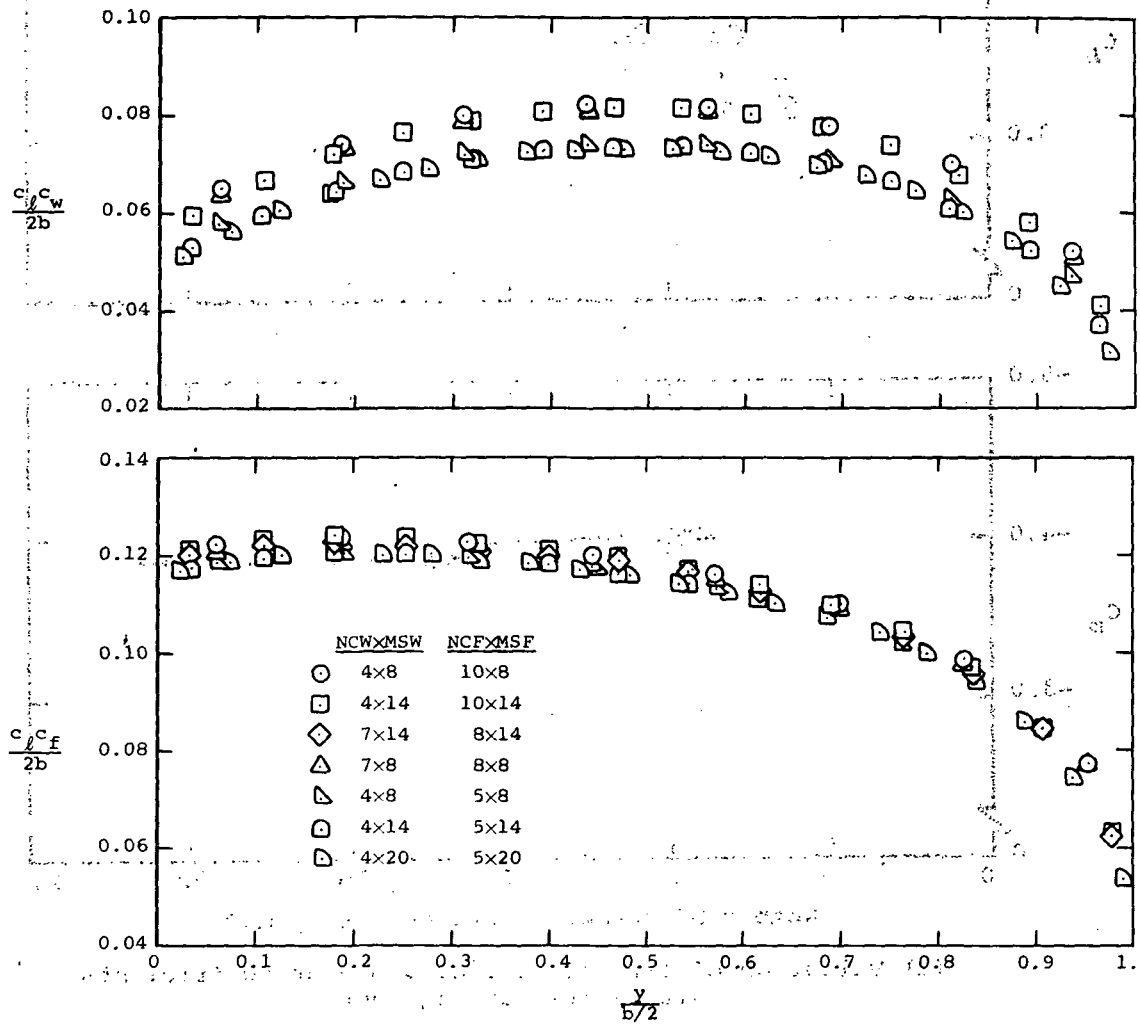

(b) Variation of span load distribution with vortex arrangement.

Figure A-2.- Concluded.

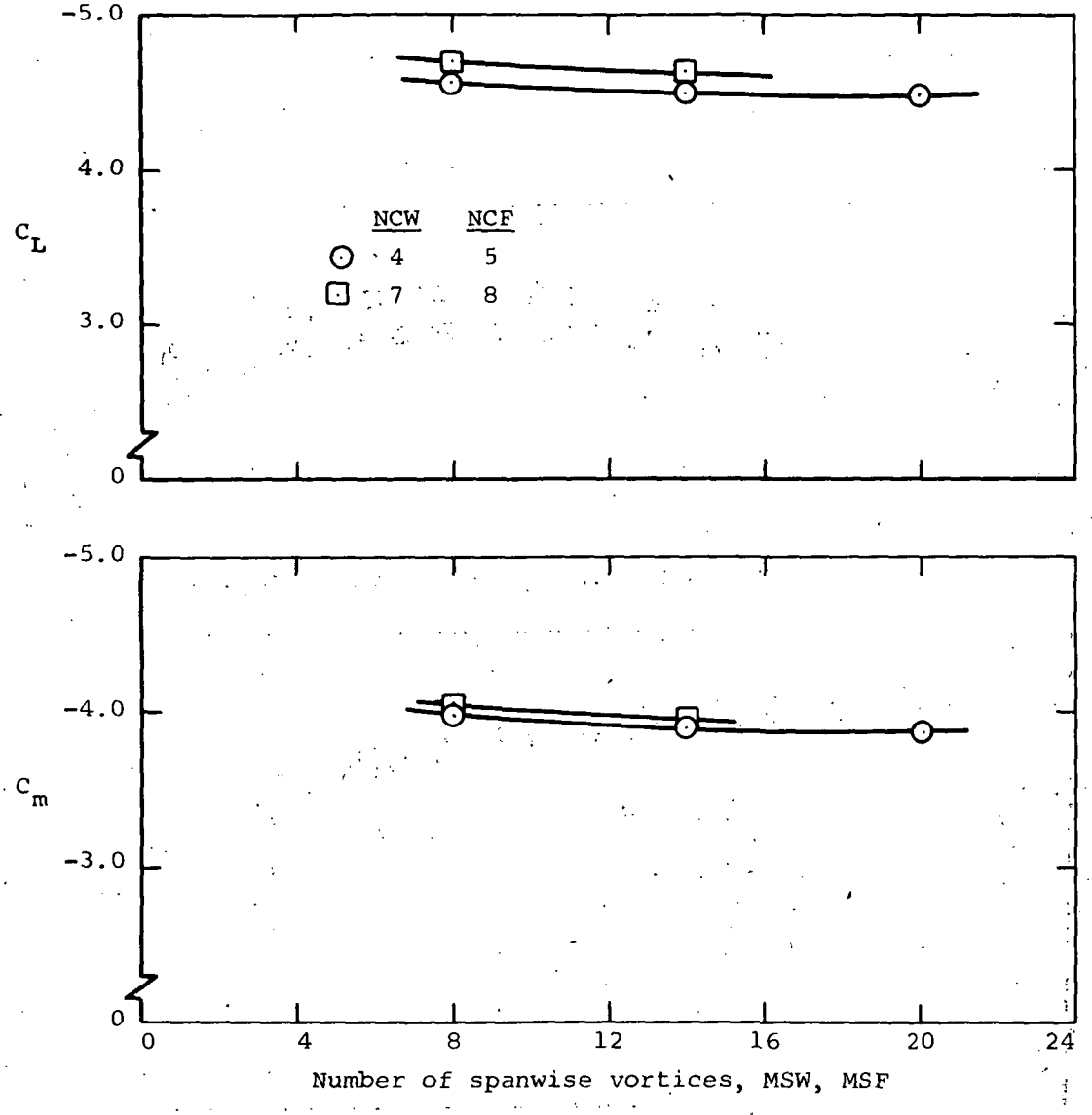

(a) Variation of lift and pitching-moment coefficients with vortex arrangement.

Figure A-3.- Predicted load characteristics of a 30° swept, aspect ratio 5 untapered wing with a large triple slotted flap at $\alpha = 10^{\circ}$.

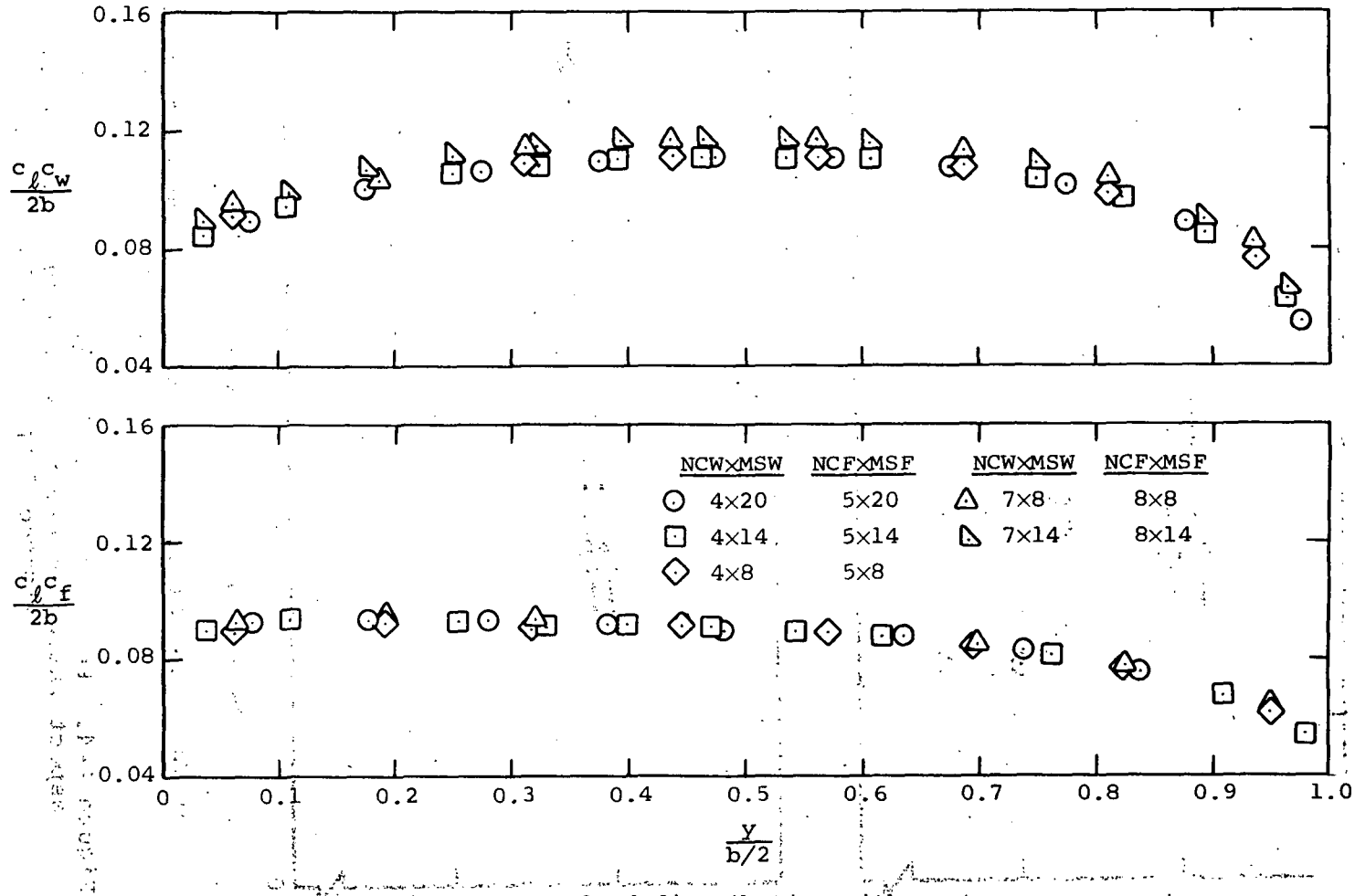

(b) Variation of span load distribution with vortex arrangement.

Figure A-3.- Concluded.

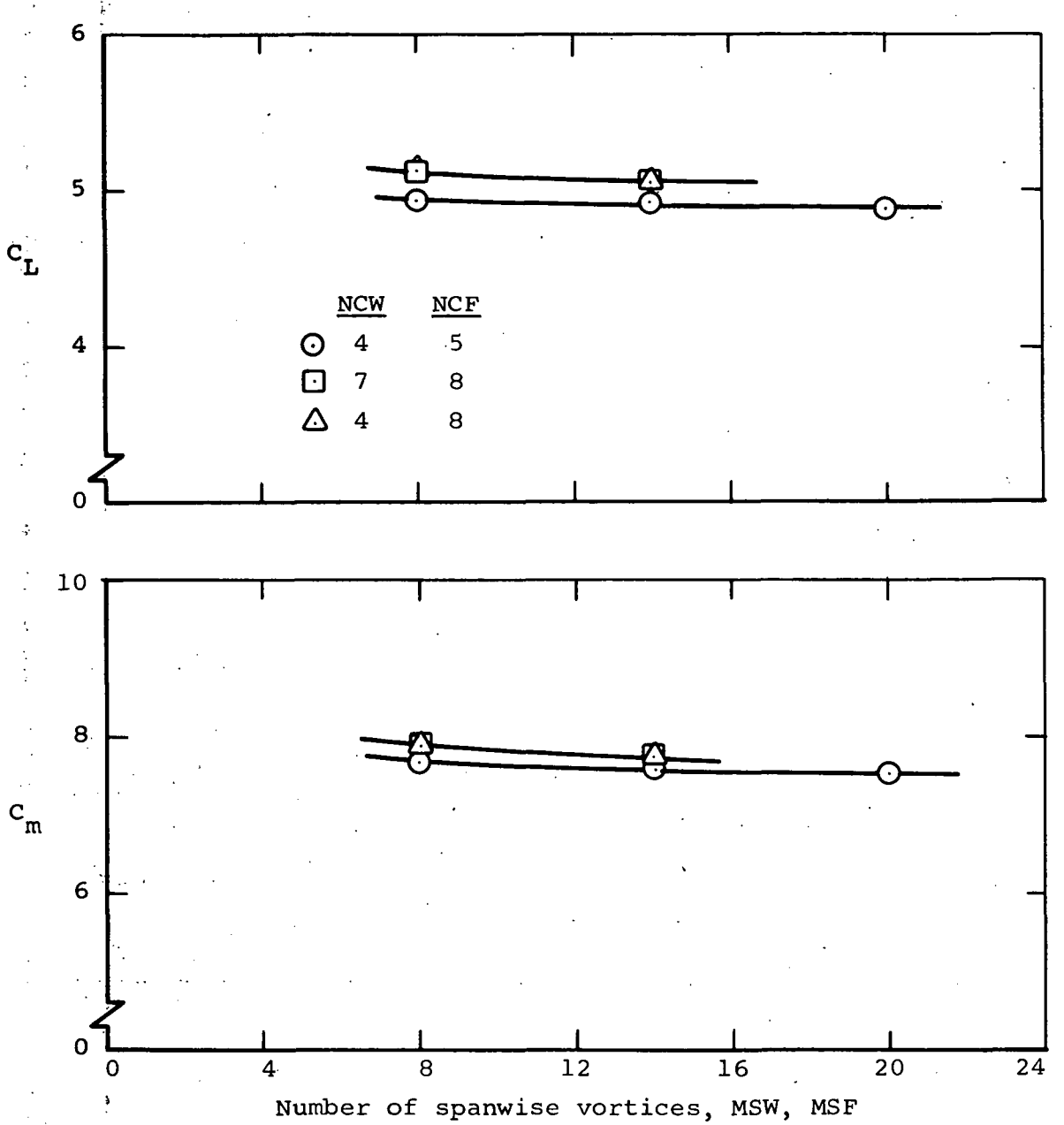

(a) Variation of lift and pitching-moment coefficients with vortex arrangement.

Figure A-4.- Predicted load characteristics of a 30° swept, aspect ratio 7 untapered wing with a large triple slotted flap at $\alpha = 10^{\circ}$.

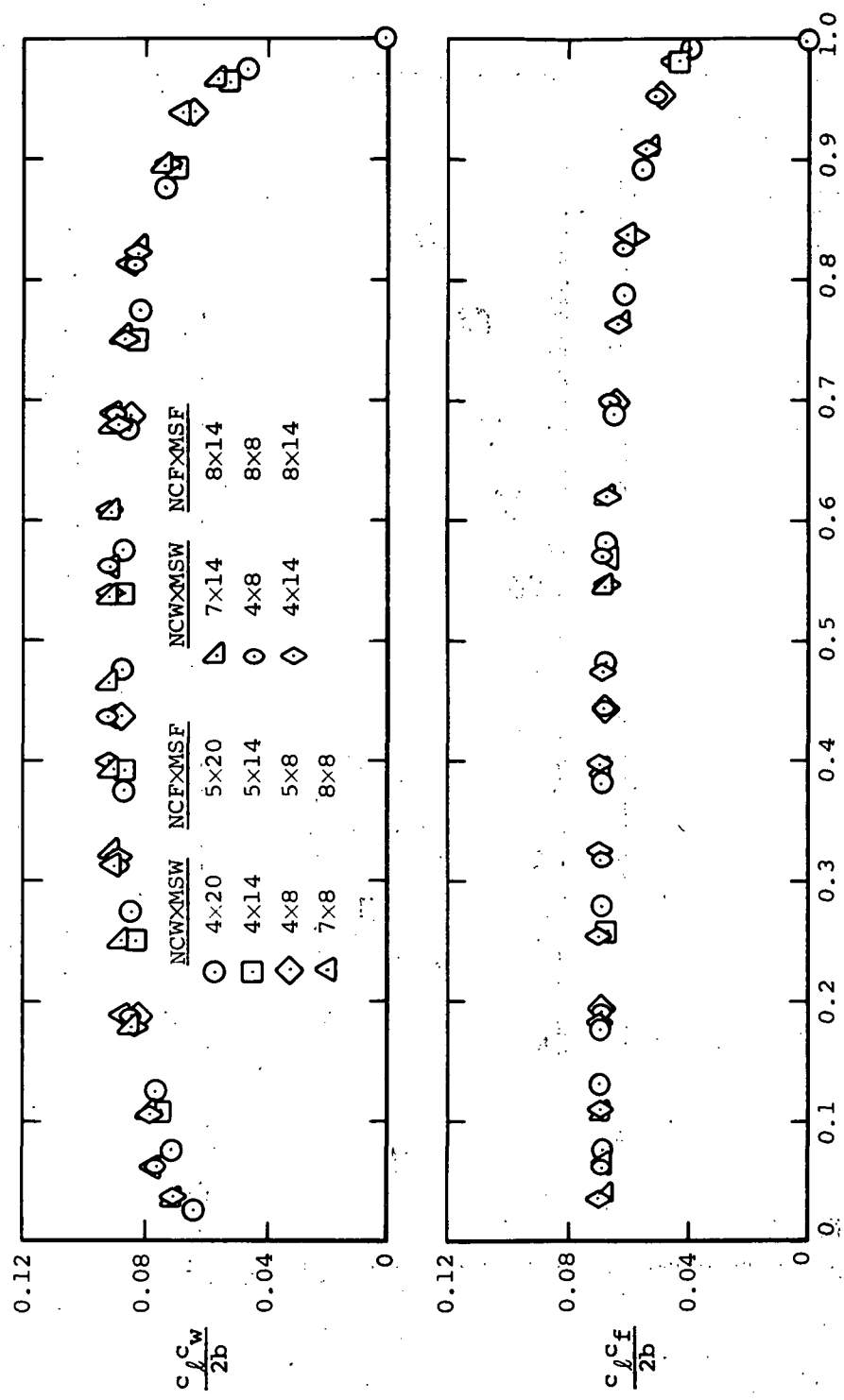

(b) Variation of span load distribution with vortex arrangement.

Figure A-4.- Concluded.

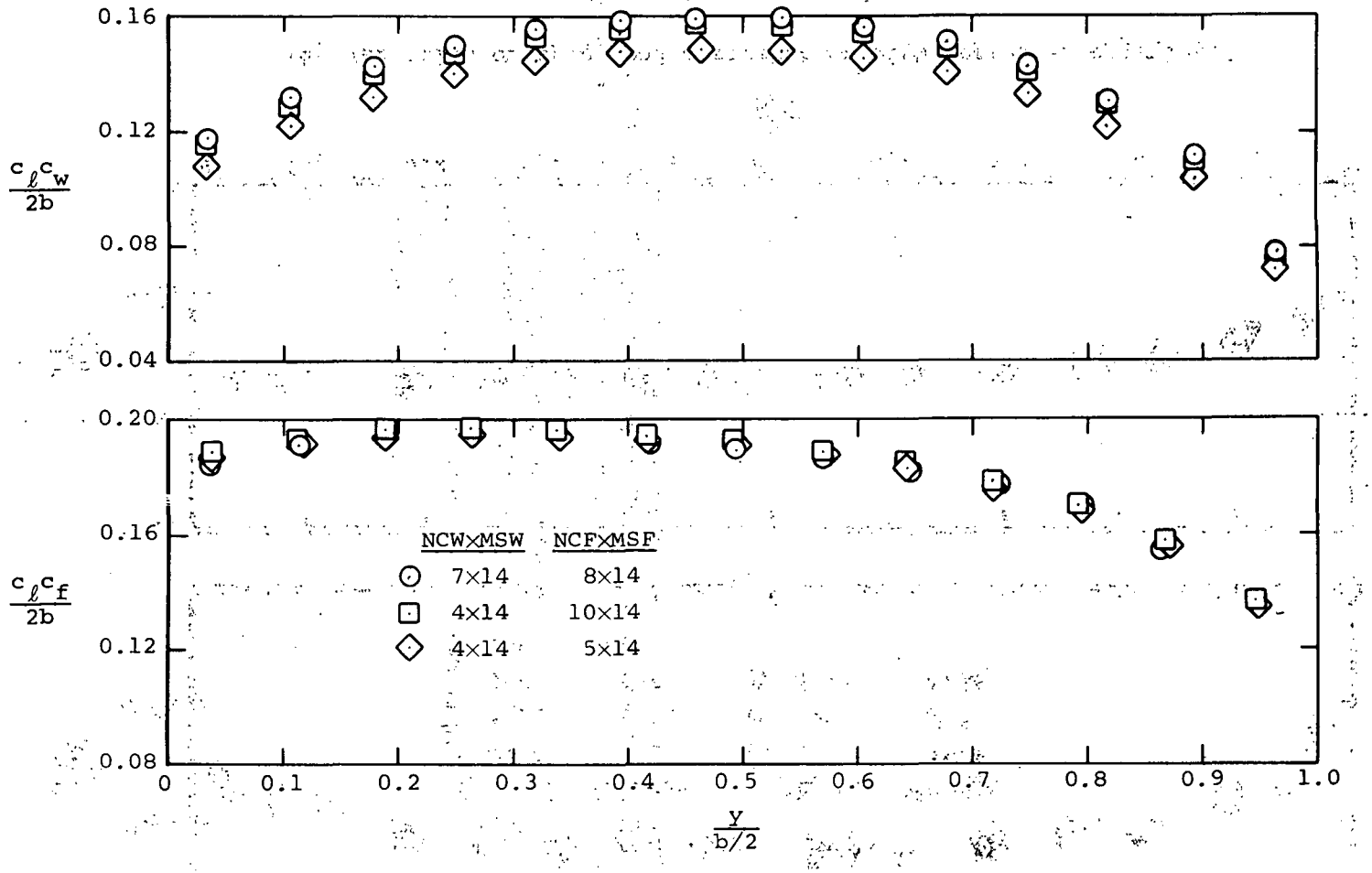

Figure A-5.- Predicted variation of span load distribution with chordwise vortex arrangement for a 30° swept, aspect ratio 3.2 untapered wing with highly deflected triple slotted flap at $\alpha = 0^\circ$.

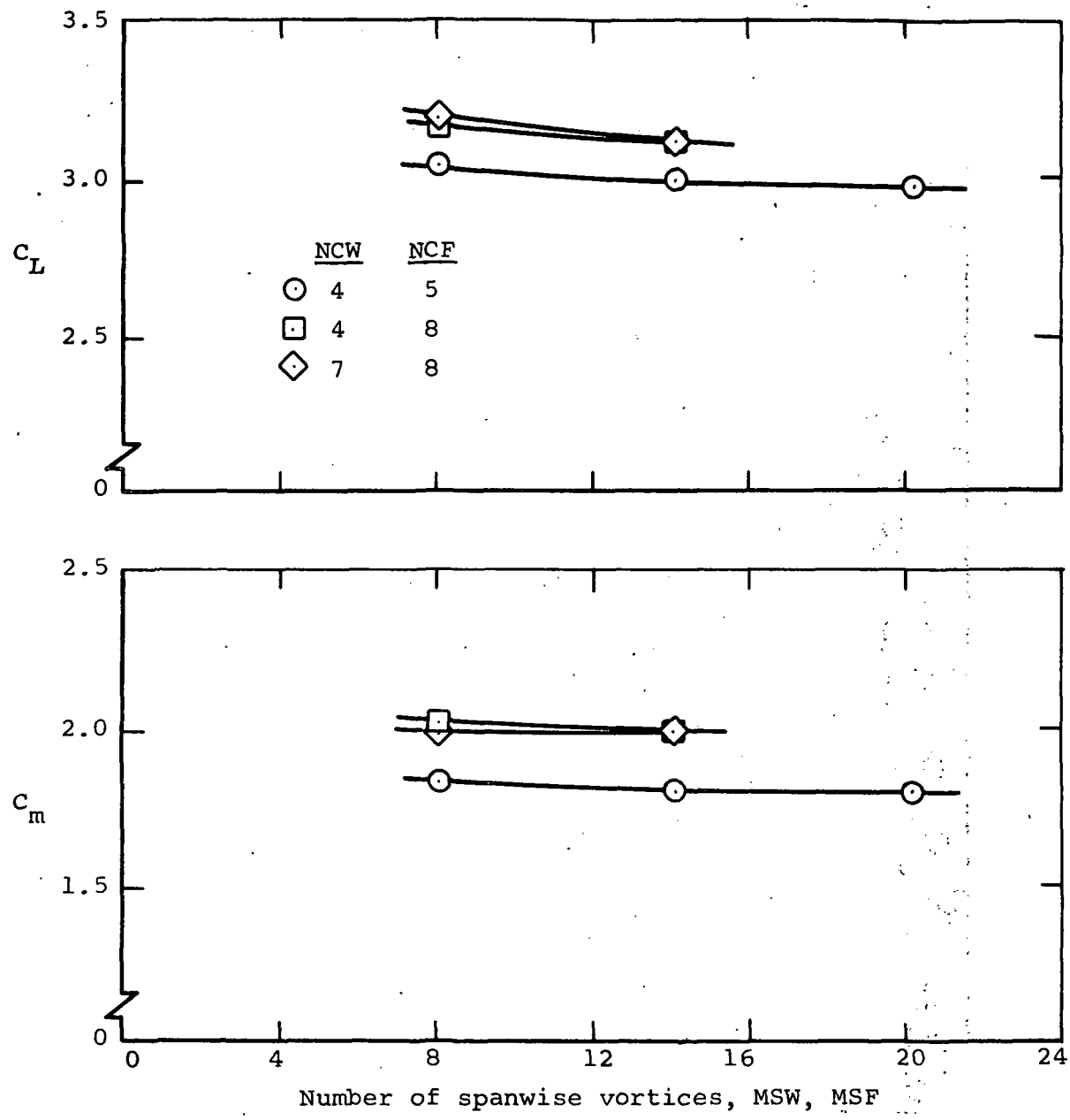

(a) Variation of lift and pitching-moment coefficients with vortex arrangement.

Figure A-6.- Predicted load characteristics of an unswept, aspect ratio 2.8 untapered wing with a large, triple slotted flap at $\alpha = 0^{\circ}$.

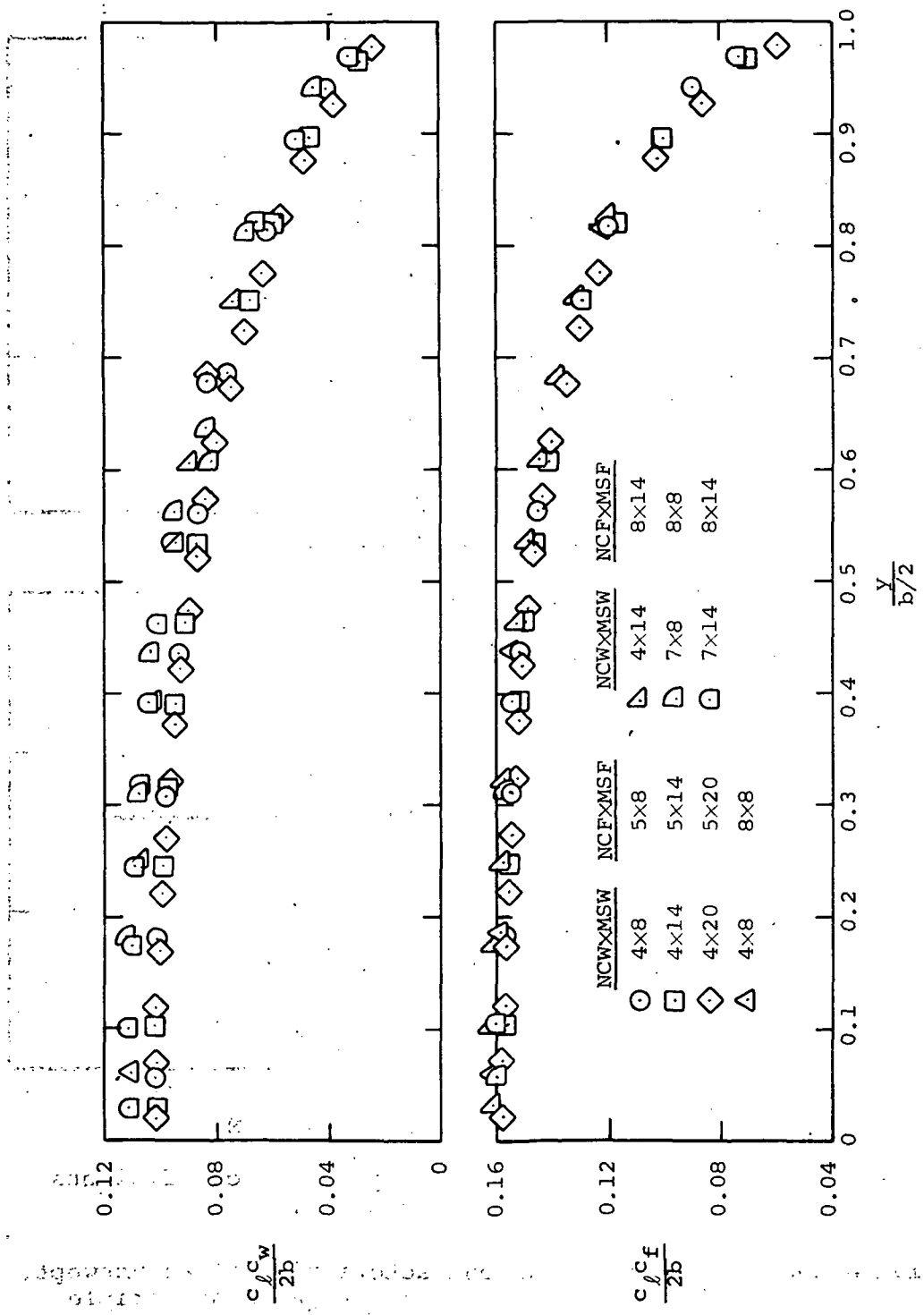

(b) Variation of span load distribution with vortex arrangement.

Figure A-6.- Concluded.

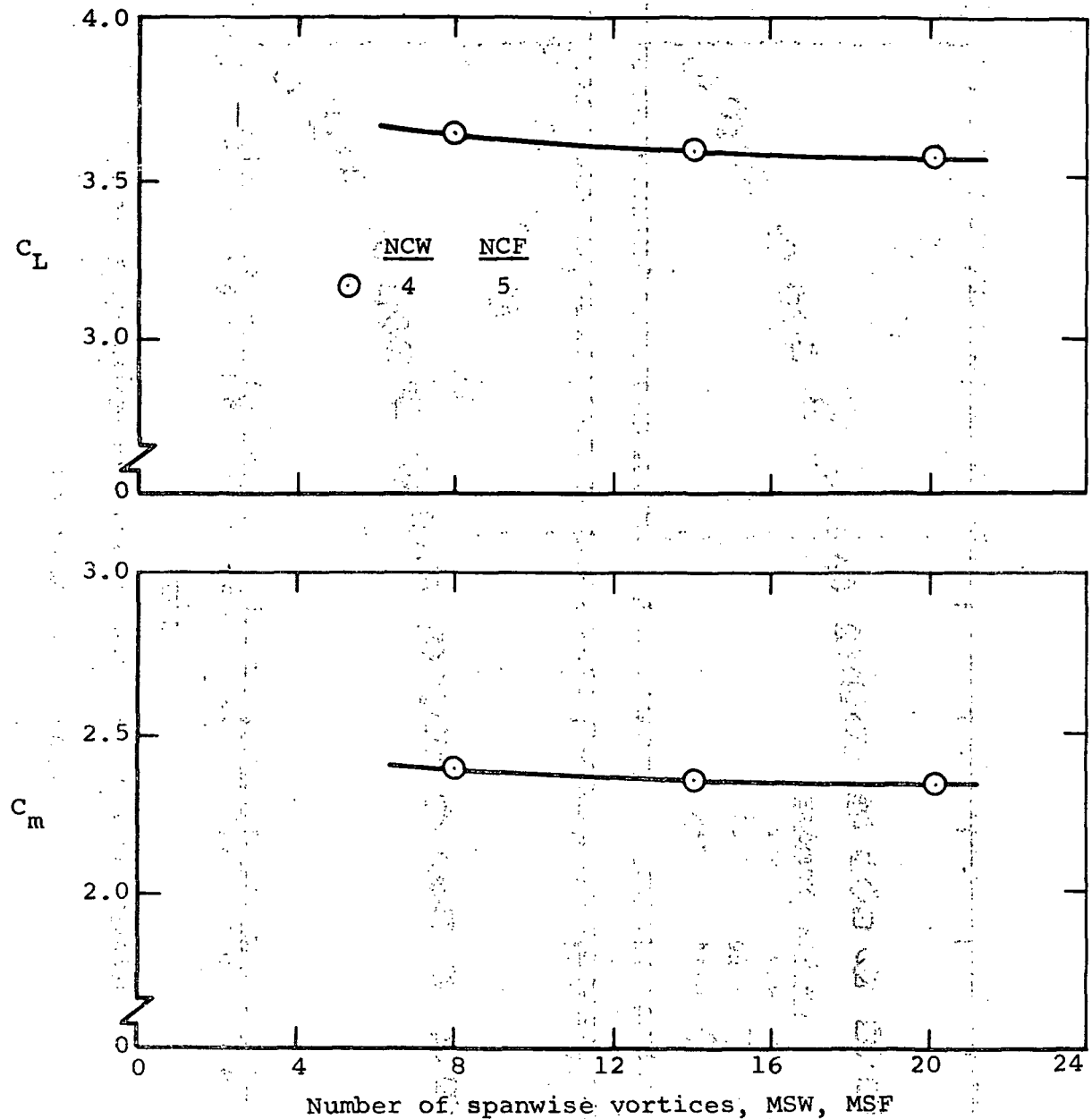

(a) Variation of lift and pitching-moment coefficients with vortex arrangement.

Figure A-7.- Predicted load characteristics of an unswept, aspect ratio 4.4 untapered wing with a large, triple slotted flap at $\alpha = 0^{\circ}$.

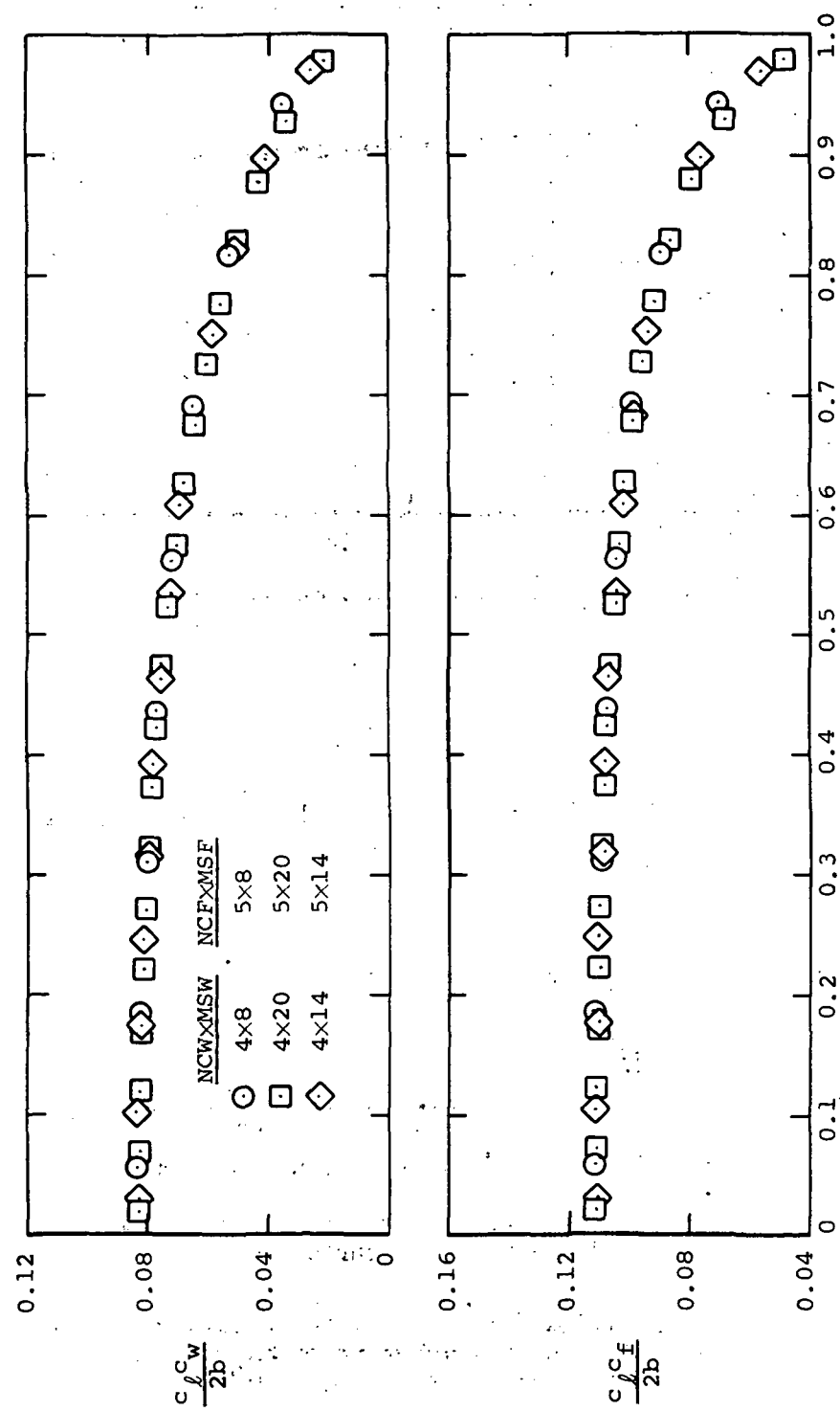

(b) Variation of span load distribution with vortex arrangement.

Figure A-7.- Concluded.

APPENDIX A

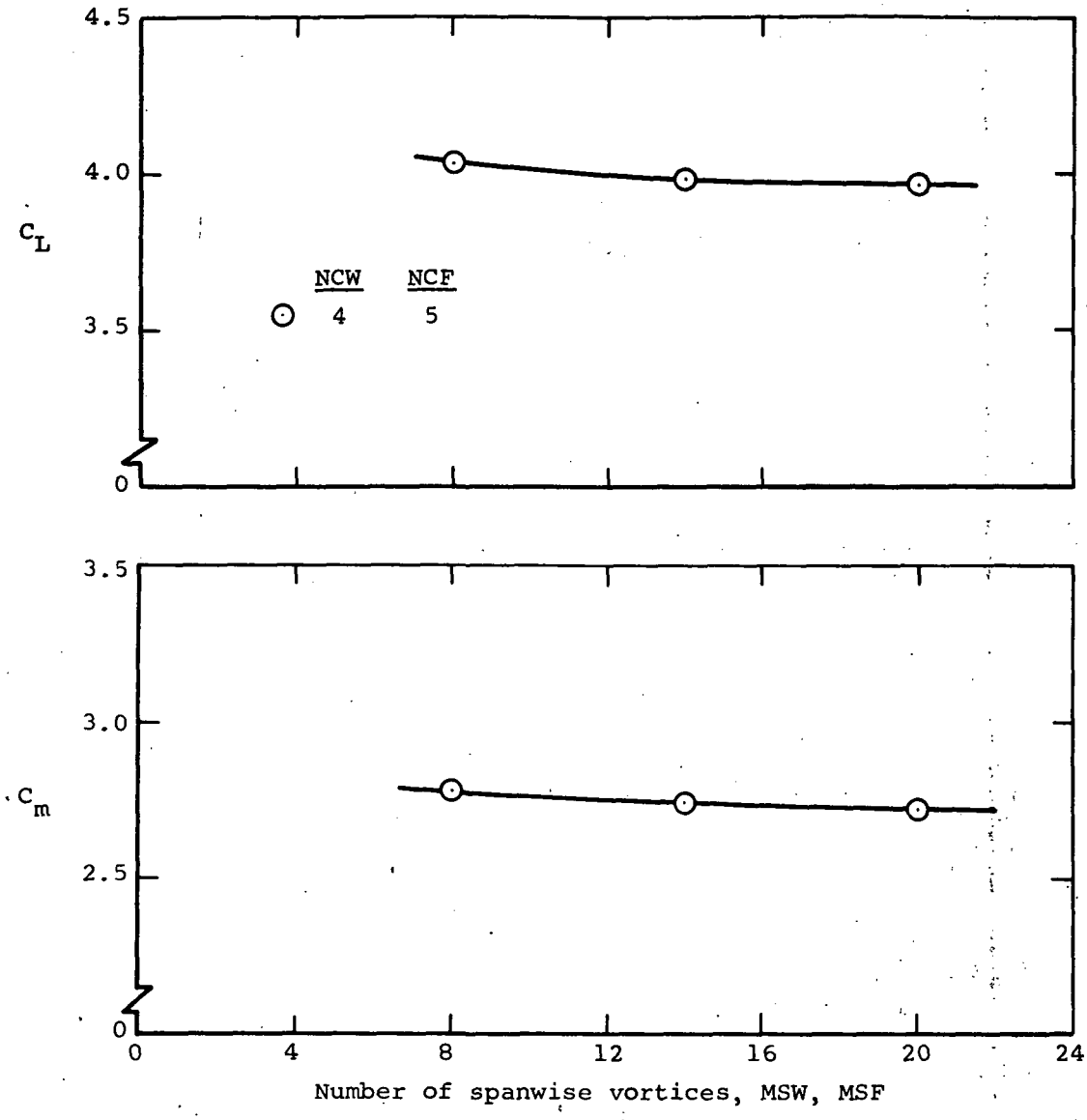

(a) Variation of lift and pitching-moment coefficients with vortex arrangement.

Figure A-8.- Predicted load characteristics of an unswept, aspect ratio 6.1 untapered wing with a large, triple slotted flap at $\alpha = 0^{\circ}$.

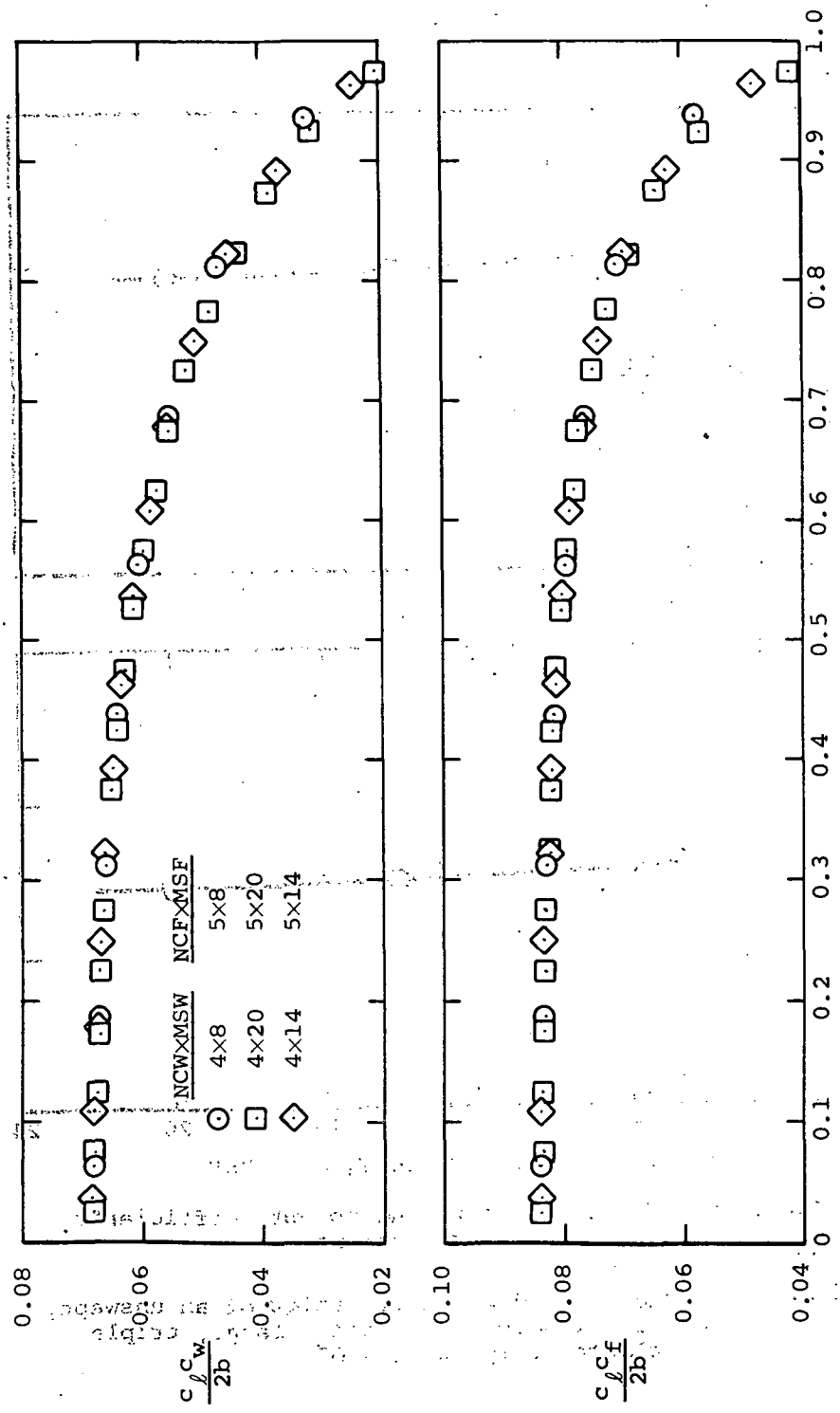

(b) Variation of span load distribution with vortex arrangement.

Figure A-8.- Concluded.

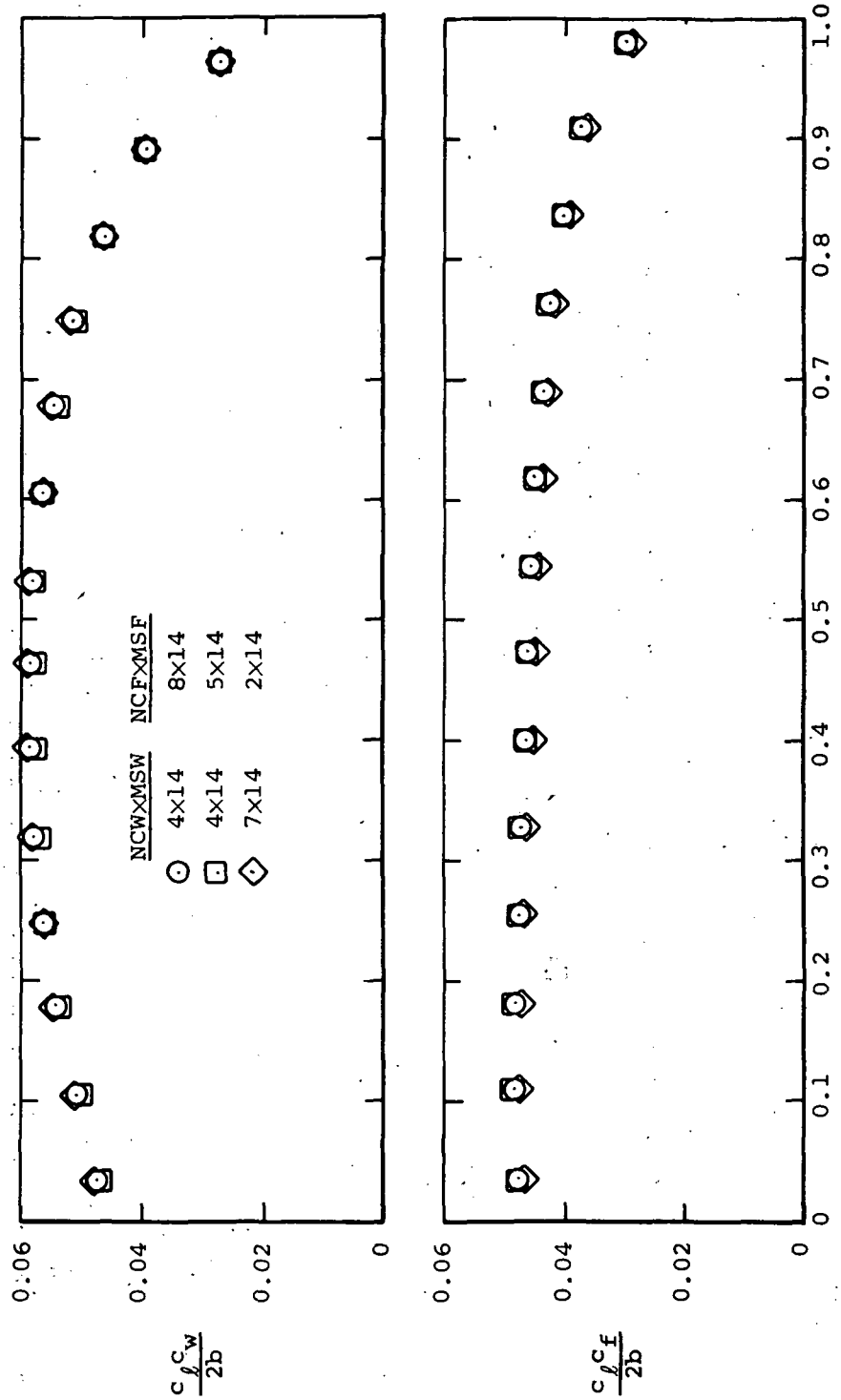

(a) $\alpha = 0^\circ$.

Figure A-9.- Predicted variation of span load distribution with chordwise vortex arrangement for a 30° swept, aspect ratio 3.2 untapered wing with a small single flap.

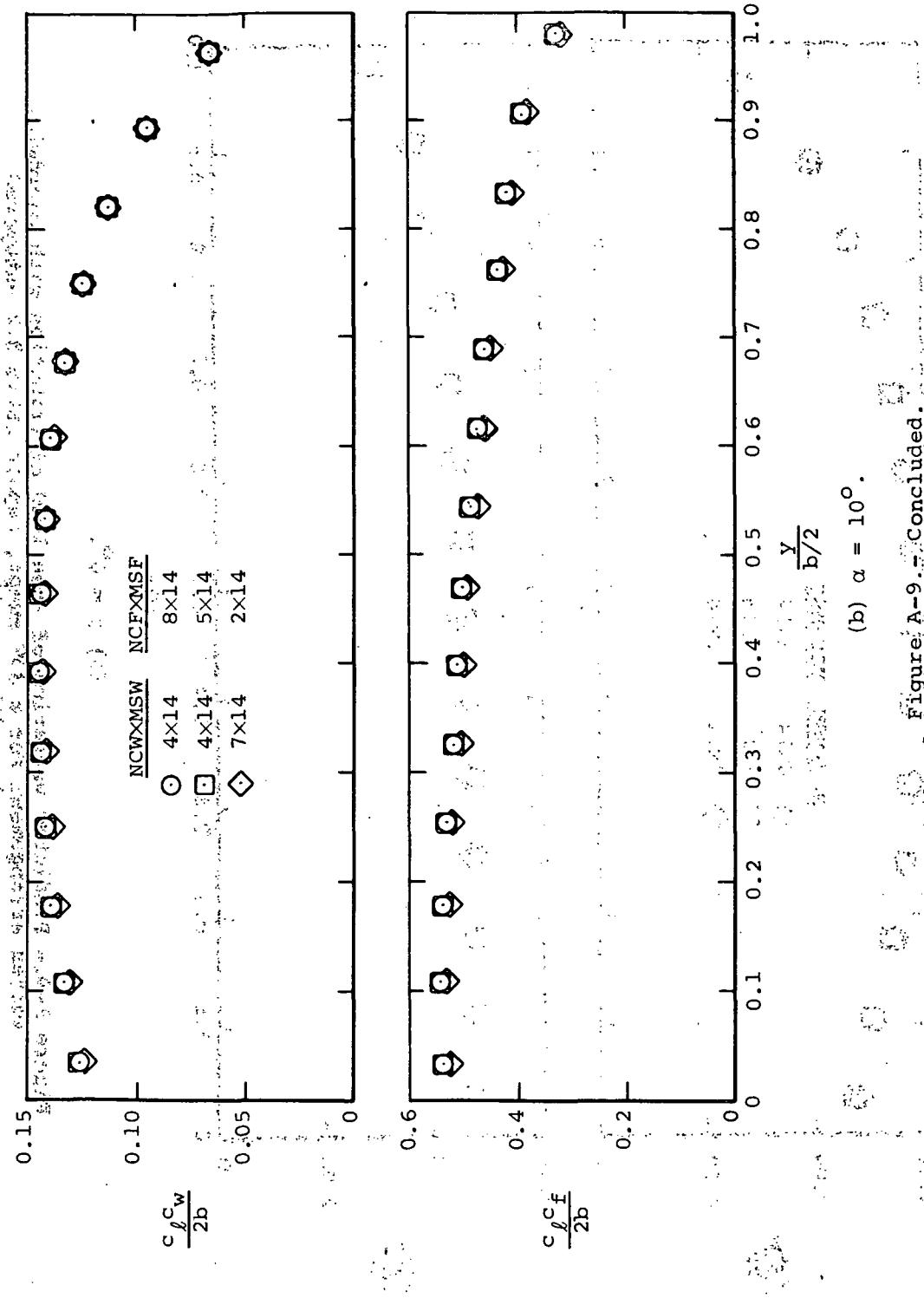

(b) $\alpha = 10^{o}$.

Figure A-9.- Concluded.

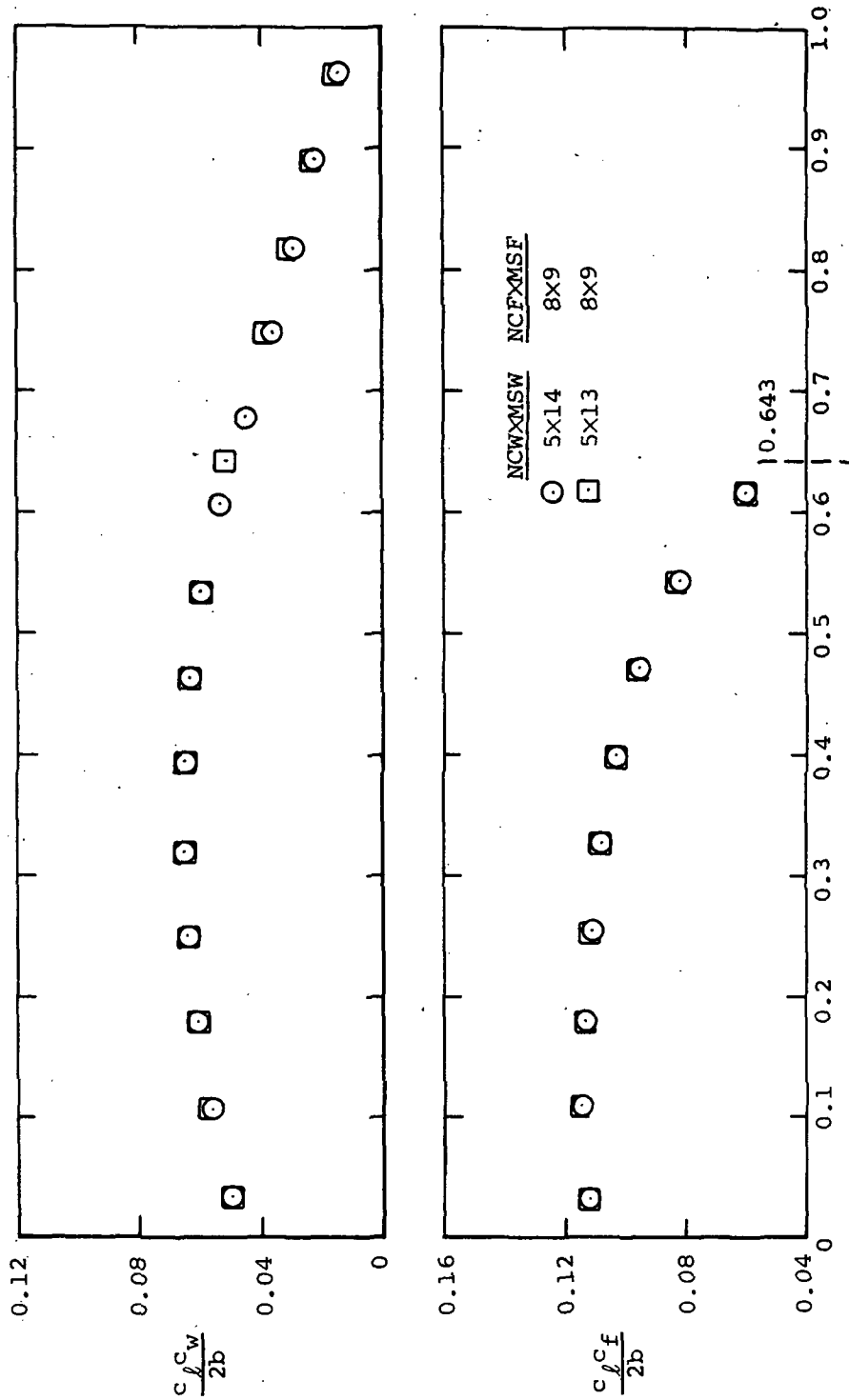

Figure A-10.- Predicted variation of span load distribution with spanwise vortex arrangement for a 30° swept, low-aspect-ratio untapered wing with a part-span flap at $\alpha = 0^{\circ}$.

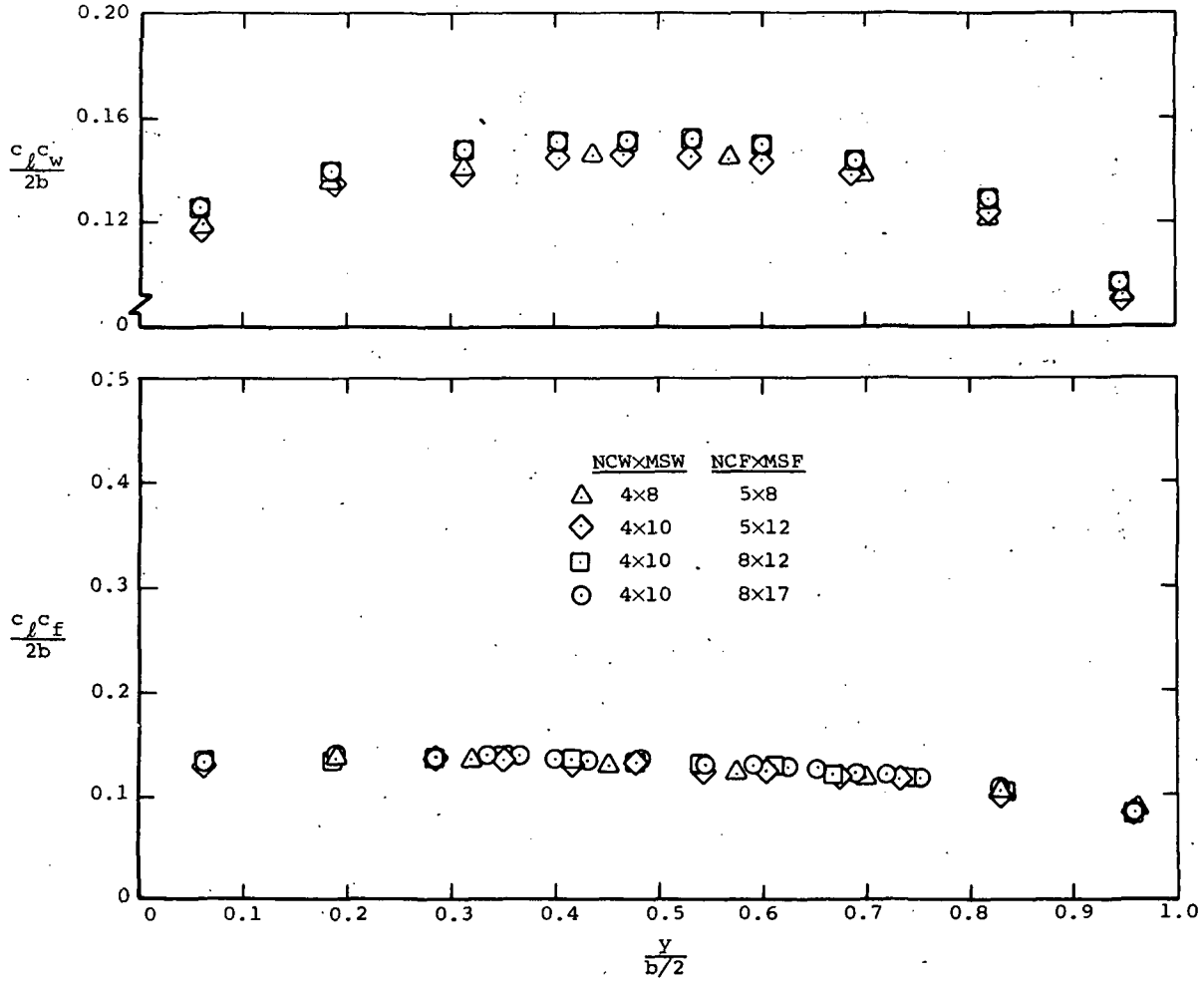

(a) $C_\mu = 0.$

Figure A-11.- Predicted effect of vortex arrangement on spanwise load distribution for a 30° swept, aspect ratio 3.2 untapered wing with large triple slotted flap and engine at mid-semispan for $\alpha = 10^\circ$.

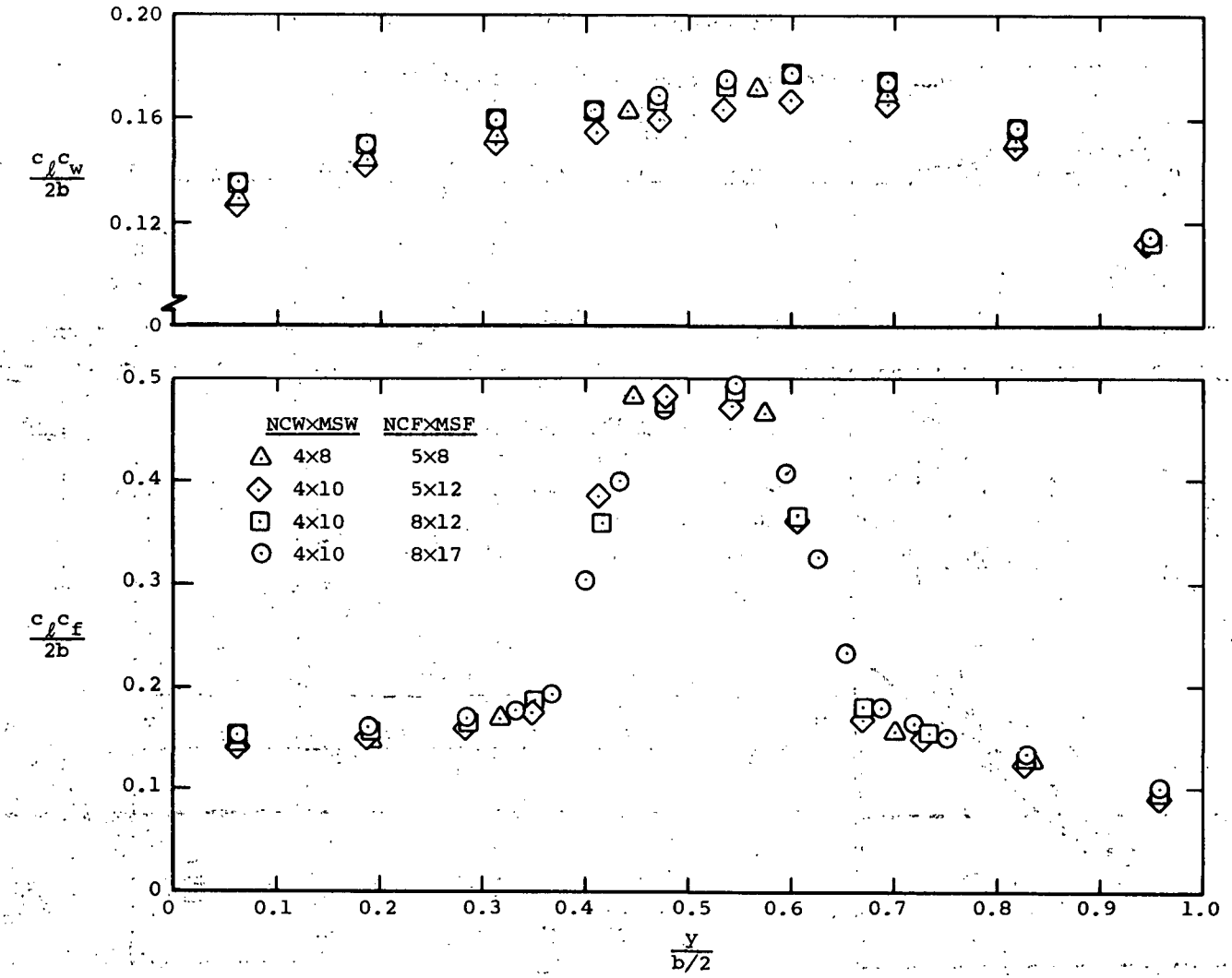

(b) C_μ = 0.9.

Figure A-11.- Continued.

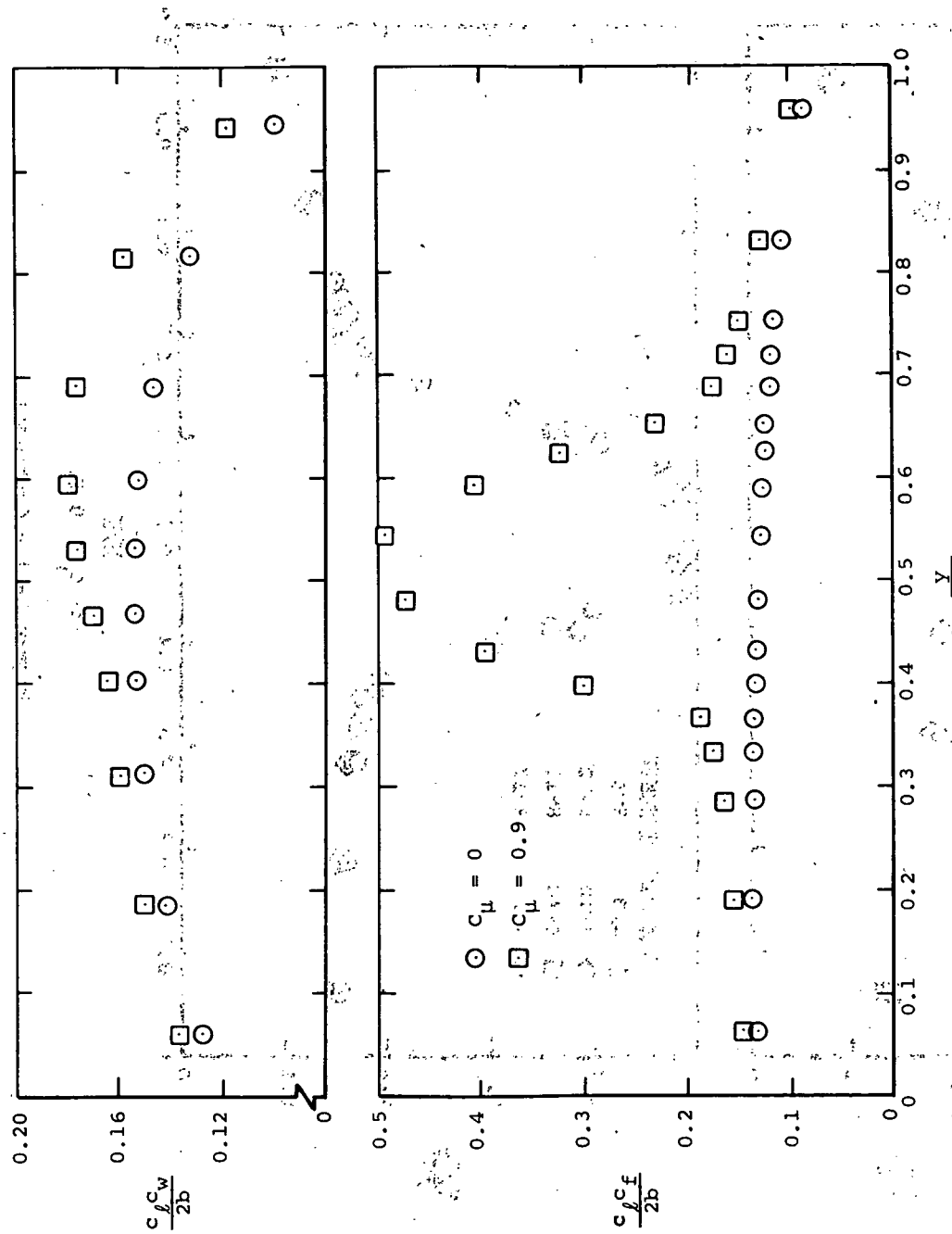

(c) Effect of C_μ for 4x10, 8x17 vortex layout.

Figure A-11.- Concluded.

REFERENCES

1. Campbell, J. P. and Johnson, J. L.: Wind-Tunnel Investigation of an External-Flow Jet-Augmented Slotted Flap Suitable for Application to Airplanes with Pod-Mounted Engines. NACA TN 3898, Dec. 1956.

2. Parlett, L. P., Freeman, D. C., and Smith, C. C.: Wind-Tunnel Investigation of a Jet Transport Airplane Configuration with High Thrust-Weight Ratio and an External-Flow Jet Flap. NASA TN D-6058. Nov. 1970.

3. Parlett, L. P., Greer, H. D., and Henderson, R. L.: Wind-Tunnel Investigation of an External-Flow Jet-Flap Transport Configuration Having Full-Span Triple-Slotted Flaps. NASA TN D-6391. Aug. 1971.

4. Smith, C. C.: Effect of Engine Position and High-Lift Devices on the Aerodynamic Characteristics of an External-Flow Jet-Flap STOL Model. NASA TN D-6222, March 1971.

5. Falarski, M. D. and Aiken, T. N.: Large-Scale Wind-Tunnel Investigation of a Ducted-Fan-Deflected-Slipstream Model with an Auxiliary Wing. NASA TM X-62079, July 1971.

6. Lopez, M. L. and Shen, C. C.: Recent Developments in Jet Flap Theory and Its Application to STOL Aerodynamic Analysis. AIAA Paper 71-578, June 1971.

7. Abramovich, G. N.: Theory of Turbulent Jets. MIT Press, 1963.

8. Mendenhall, M. R., Dillenius, M. F. E., and Spangler, S. B.: Theoretical Investigation of the Aerodynamic Interference Induced by Cruise and Lift Fans on Transport-Type Aircraft. NASA CR-1730, Aug. 1971.

9. Dillenius, M. F. E., Mendenhall, M. R., and Spangler, S. B.: Computer Programs for Calculation of Aerodynamic Interference Between Lifting Surfaces and Lift and Cruise Fans. NASA CR-114332, 1971.

10. Margason, R. J., Lamar, J. E.: Vortex-Lattice Fortran Program for Estimating Subsonic Aerodynamic Characteristics of Complex Planforms. NASA TN D-6142, Feb. 1971.

11. Glauert, H.: The Elements of Airfoil and Airscrew Theory. MacMillan Press, 1943. Chapter 12, pp. 156-160.

12. Küchemann, D. and Weber, J.: Aerodynamics of Propulsion, McGraw-Hill Book Co., Inc., 1953.

13. Carter, A. W.: Pressure Distributions on a Wing Having NACA 4415 Airfoil Sections with Trailing-Edge Flaps Set at 0° and 40°. NASA TM X-2225, June 1971.

14. Falarski, M. D. and Mort, K. W.: Large-Scale Wind-Tunnel Investigation of a Ducted-Fan-Deflected-Slipstream Model with an Auxiliary Wing. NASA TN D-6323, April 1971.

15. Abbott, I. H. and Von Doenhoff, A. E.: Theory of Wing Sections. Dover Publications, 1958, p. 405.

16. Hammond, A. D. and Keffer, B. M.: The Effect at High Subsonic Speed of a Flap-Type Aileron on the Chordwise Pressure Distribution Near Mid-Semispan of a Tapered 35° Sweptback Wing of Aspect Ratio 4 Having NACA 65A006 Airfoil Section. NACA RML 53C23, May 1953.

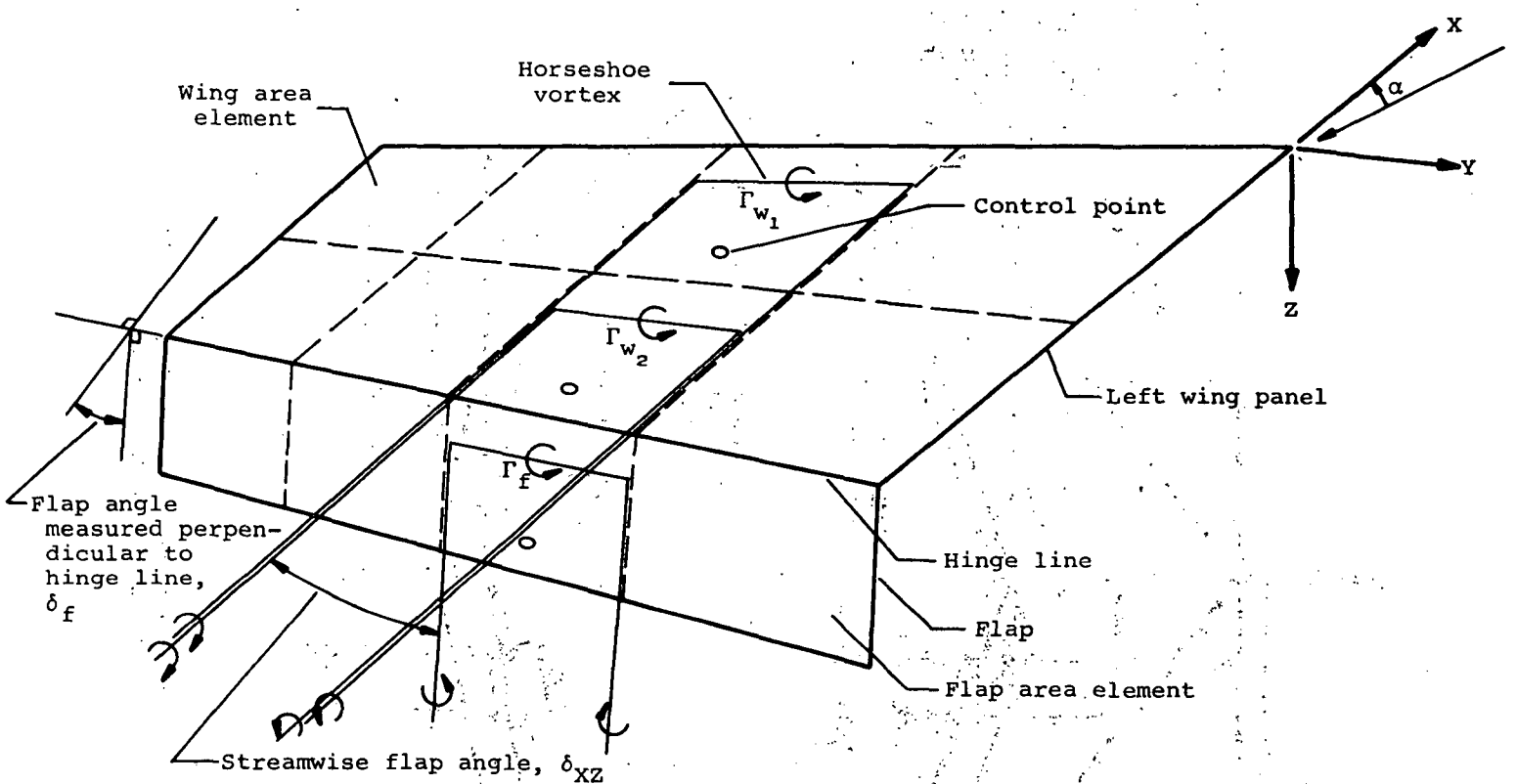

Figure 1.- Vortex-lattice representation of wing-flap system.

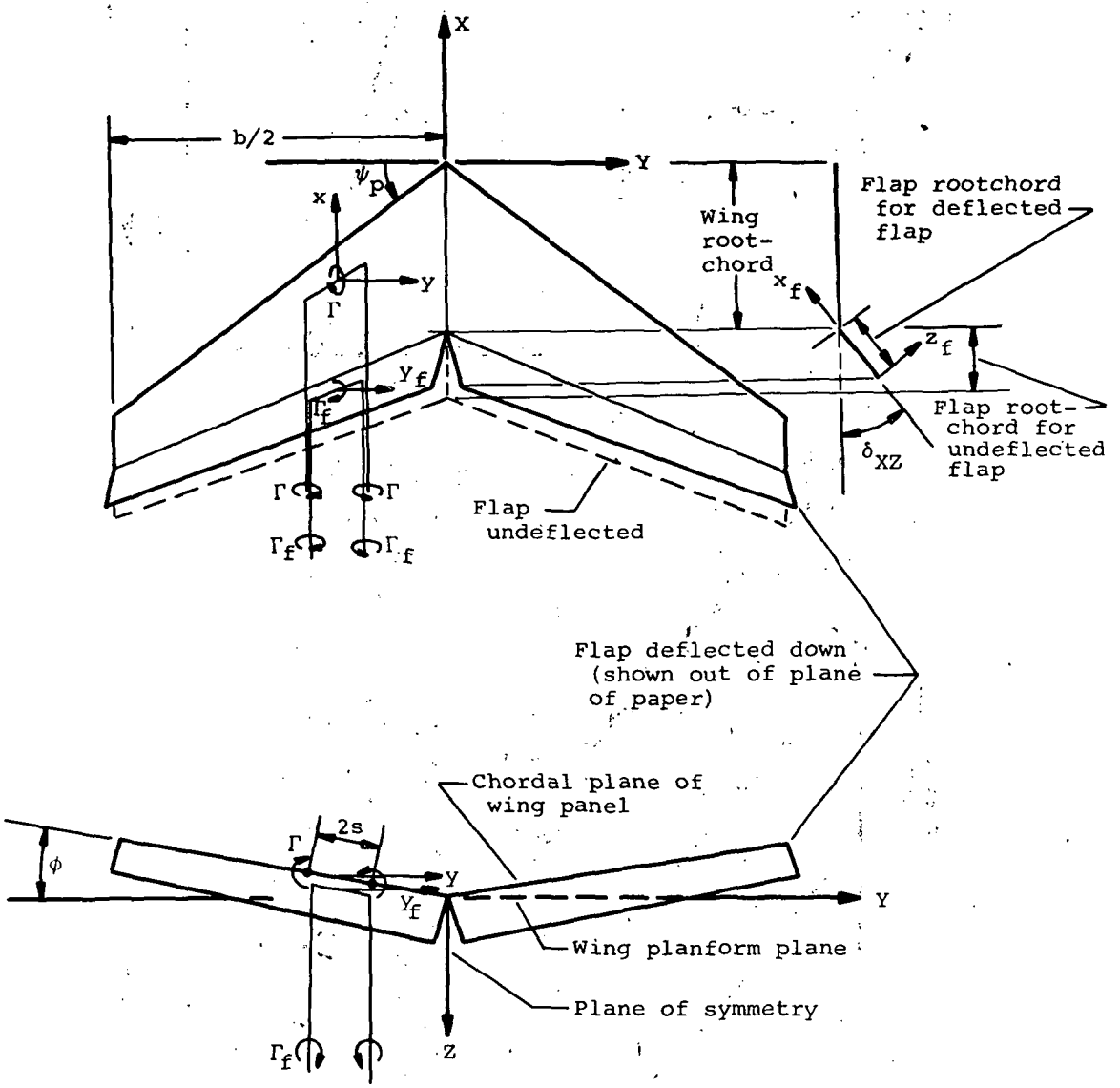

Figure 2.- Coordinate systems for wing-flap and horseshoe vortices.

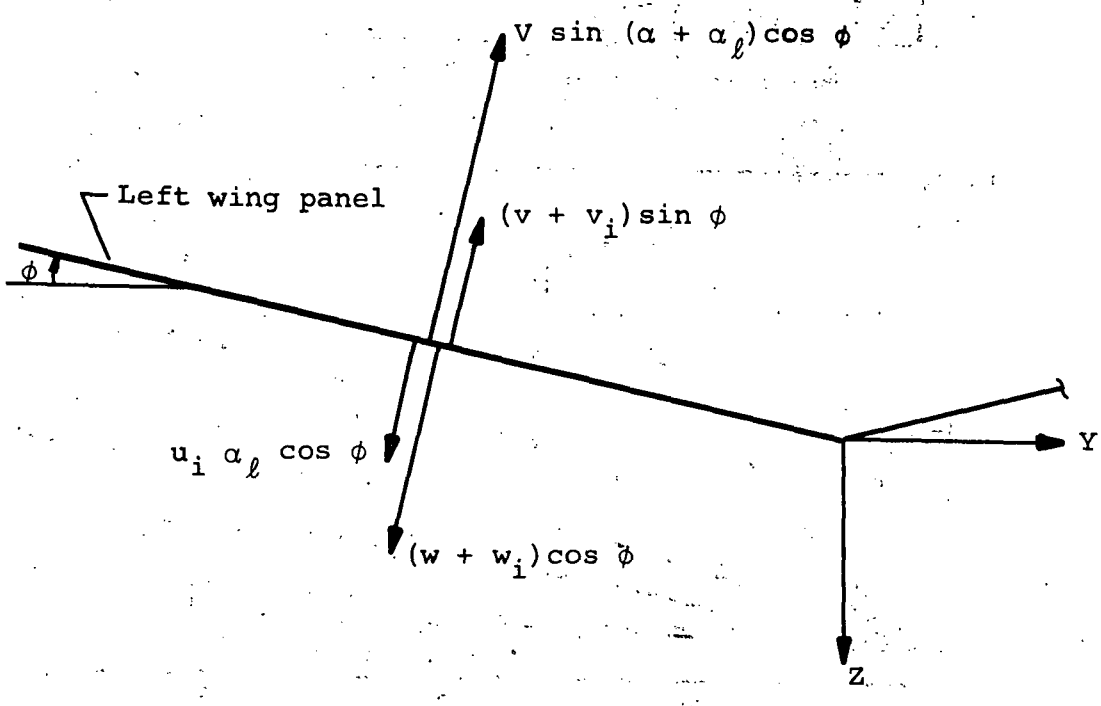

Figure 3.- Wing boundary condition.

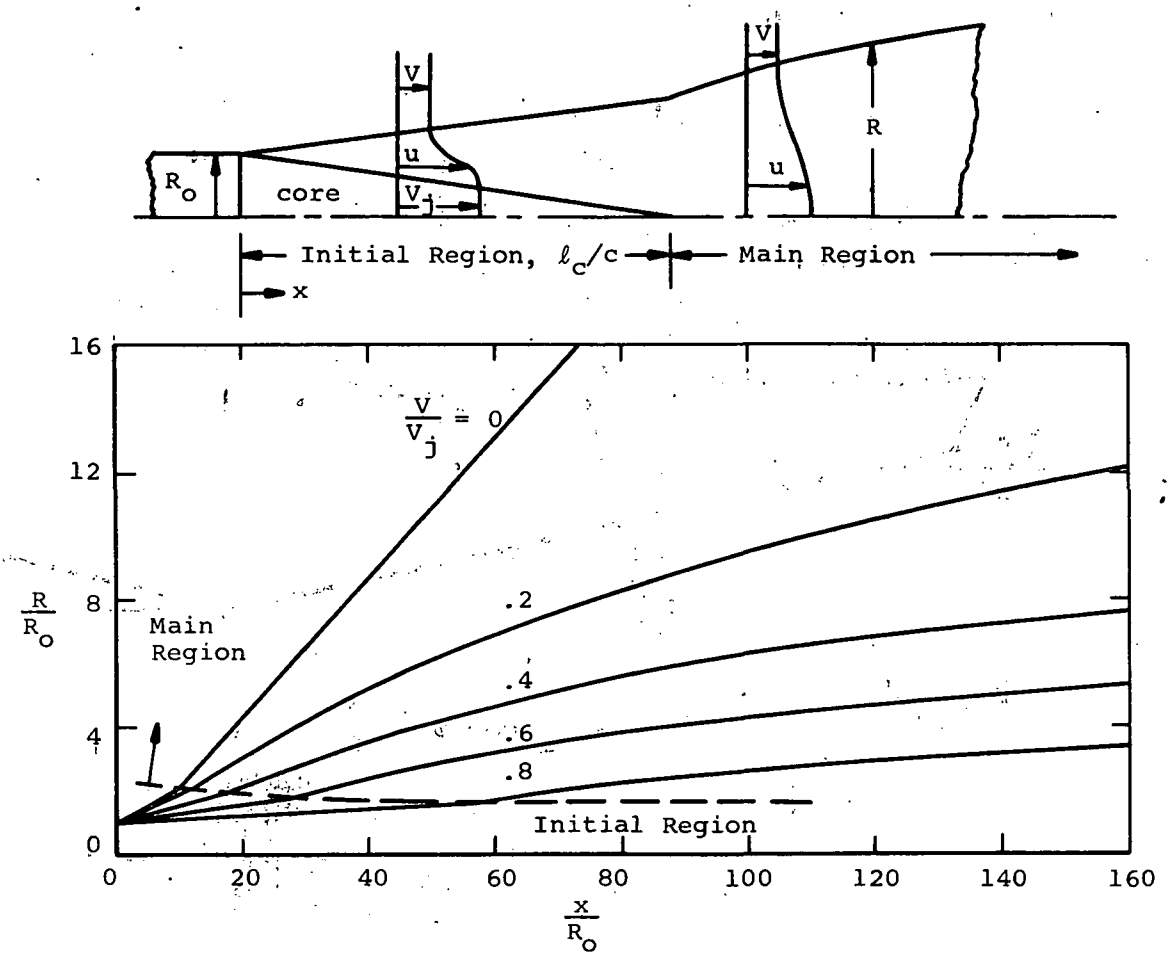

Figure 4.- Analytical spreading rate of an axisymmetric jet in a coflowing stream.

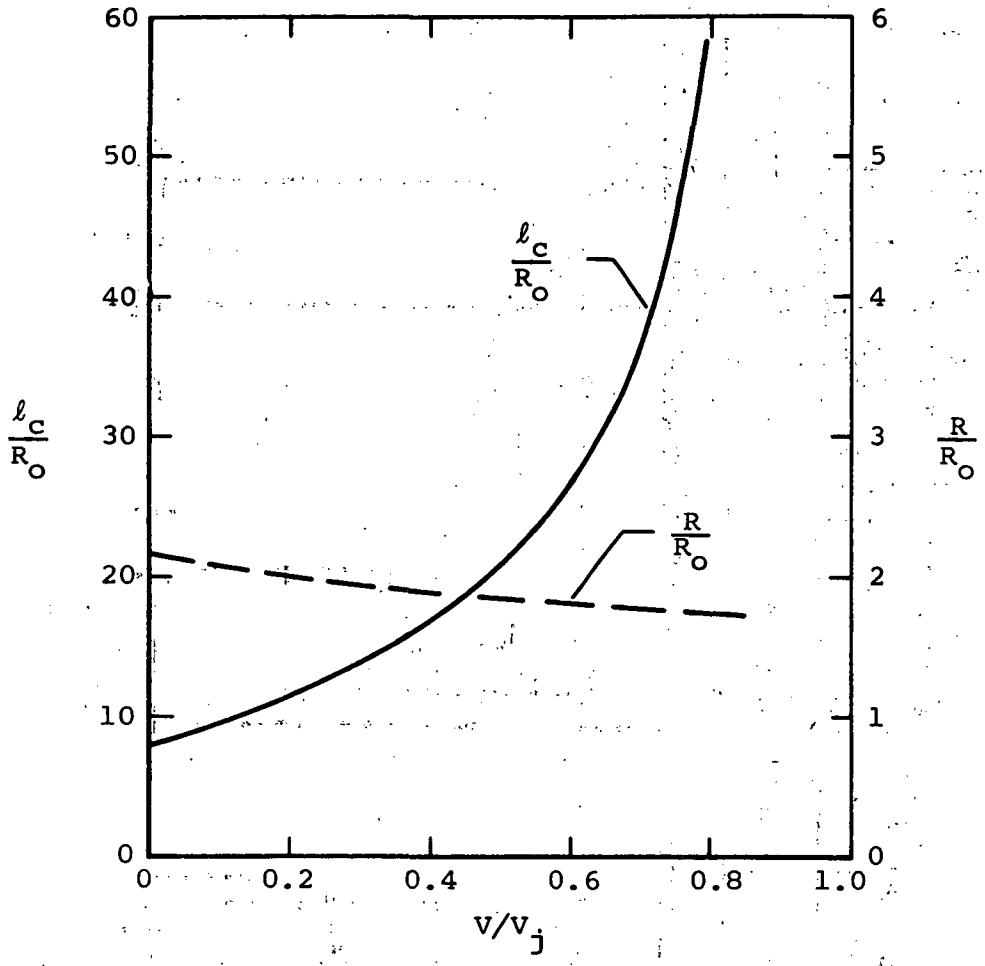

Figure 5.- Characteristics of the initial region of a turbulent jet.

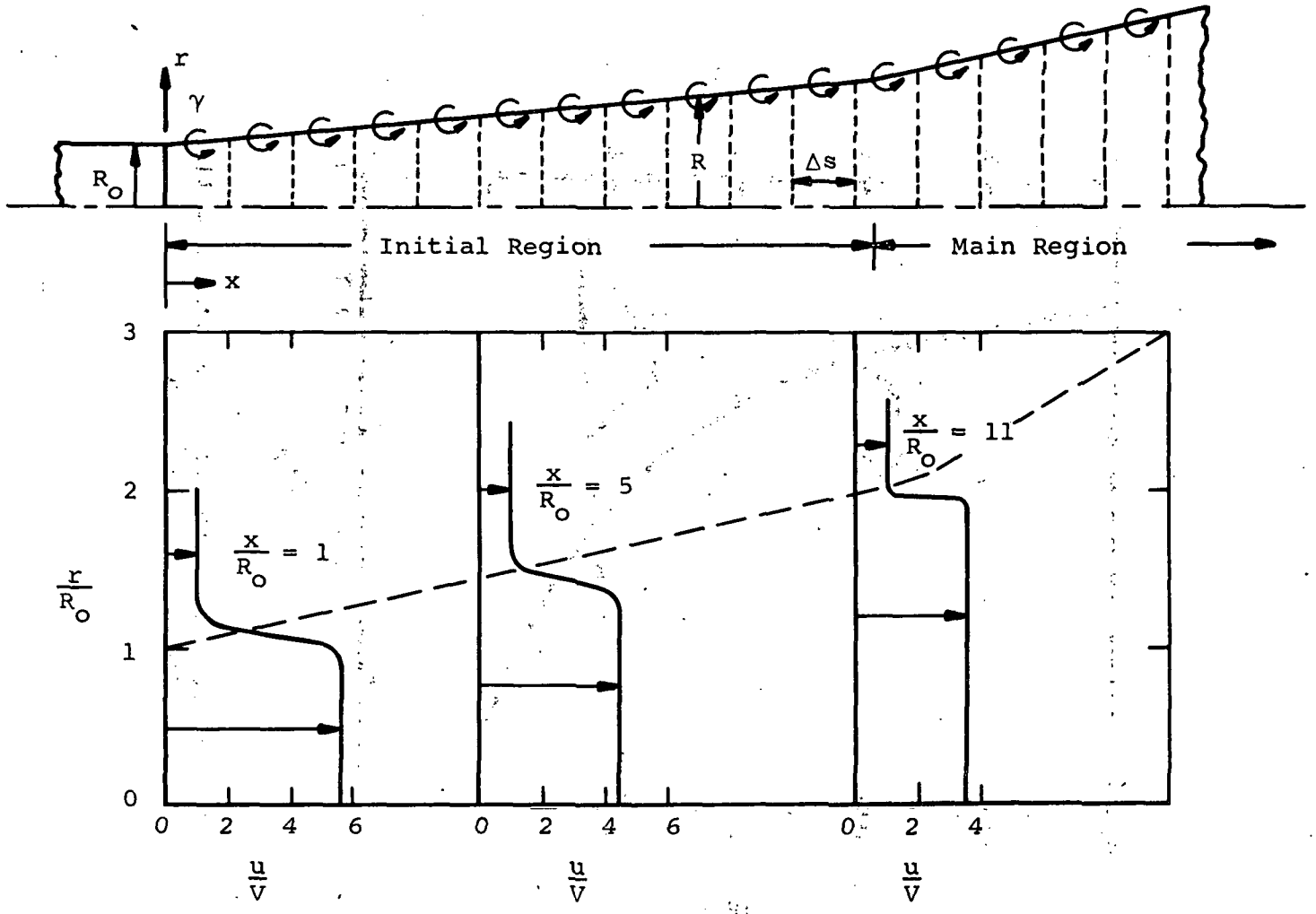

Figure 6.- Vortex ring wake model and velocity profiles for $V_j/V = 6$.

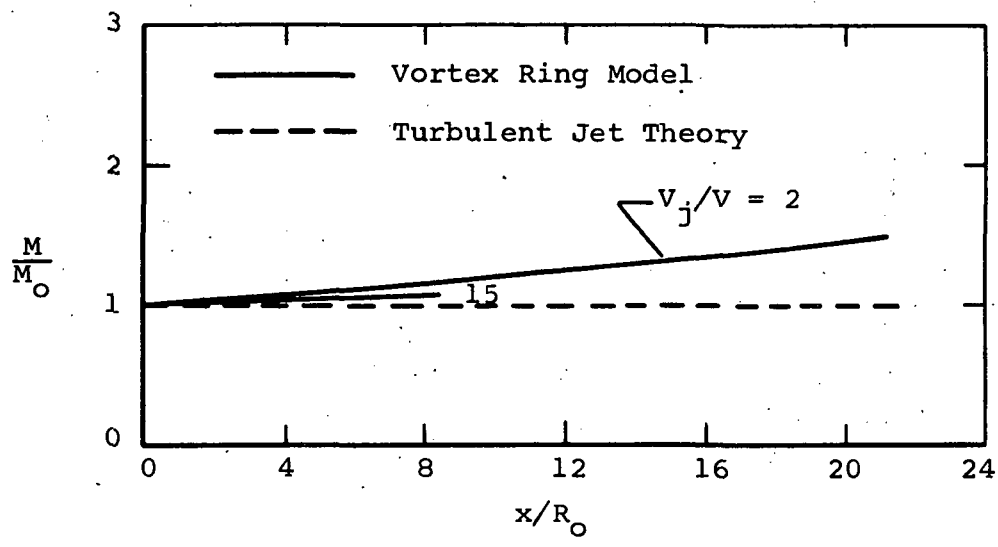

Figure 7.- Momentum in the initial region of an axisymmetric turbulent jet wake.

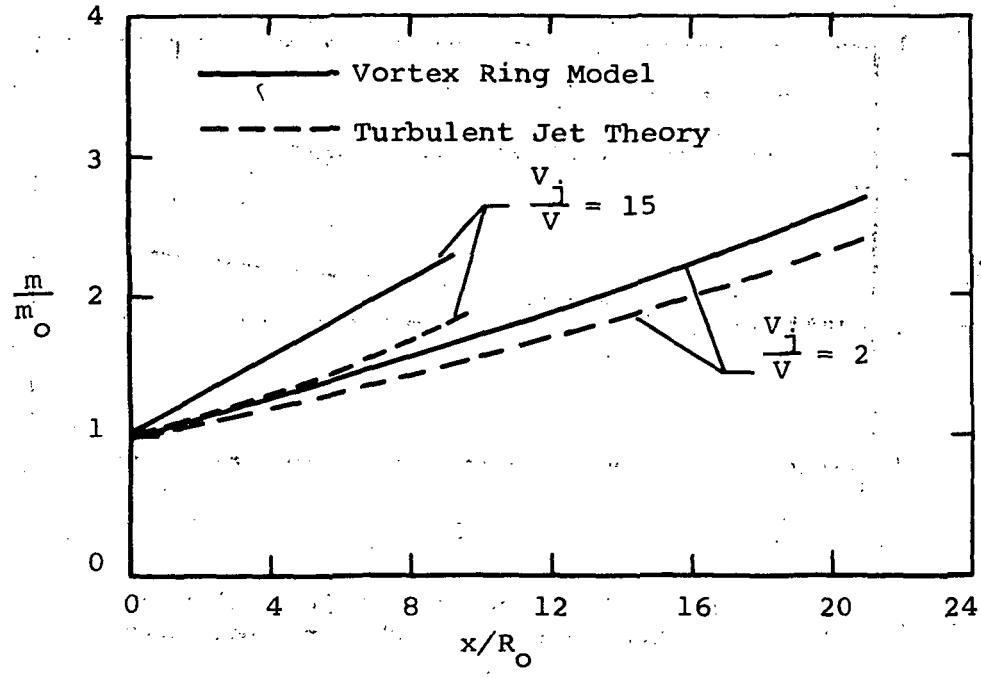

Figure 8.- Mass flow in the initial region of an axisymmetric turbulent jet wake.

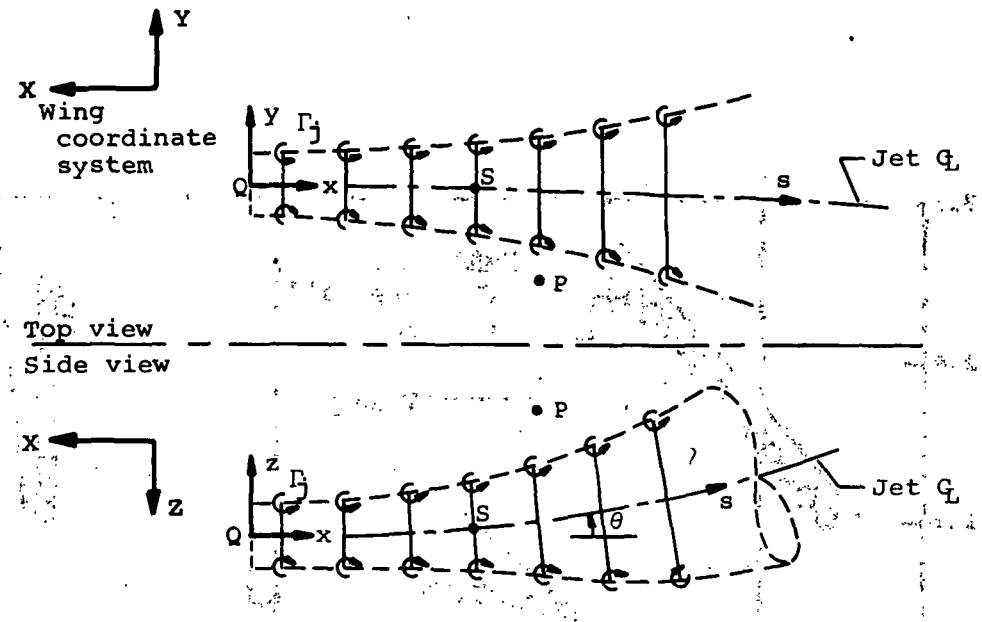

(a) Jet coordinate system.

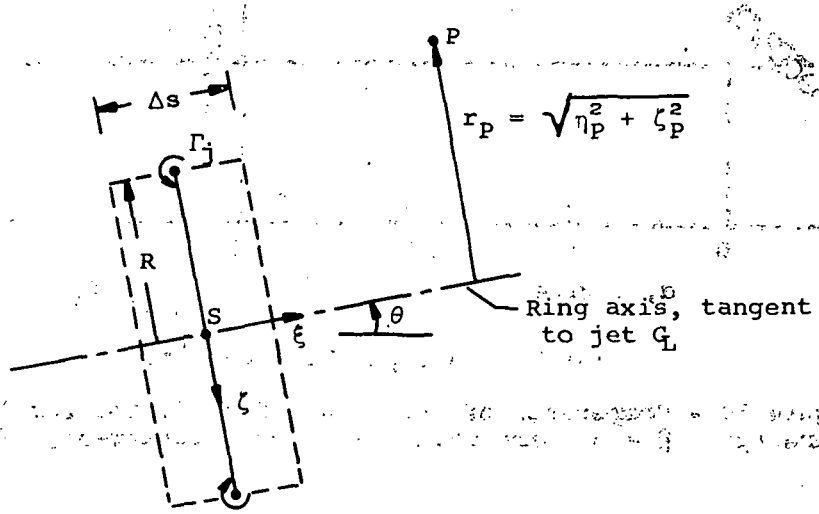

(b) Ring coordinate system.

Figure 9.- Jet wake nomenclature.

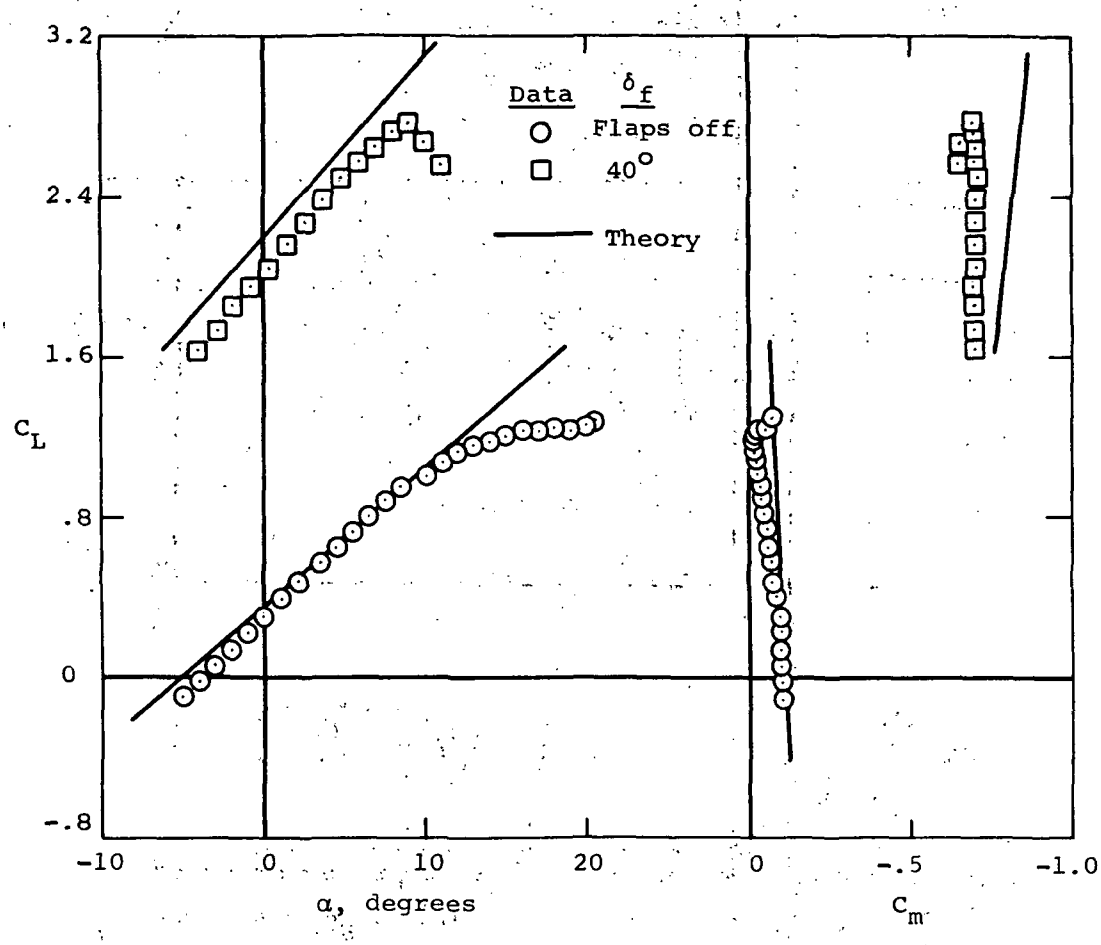

(a) Lift and pitching moment.

Figure 10.- Comparison of measured and predicted results on an unswept $AR = 6$ wing with a slotted trailing-edge flap.

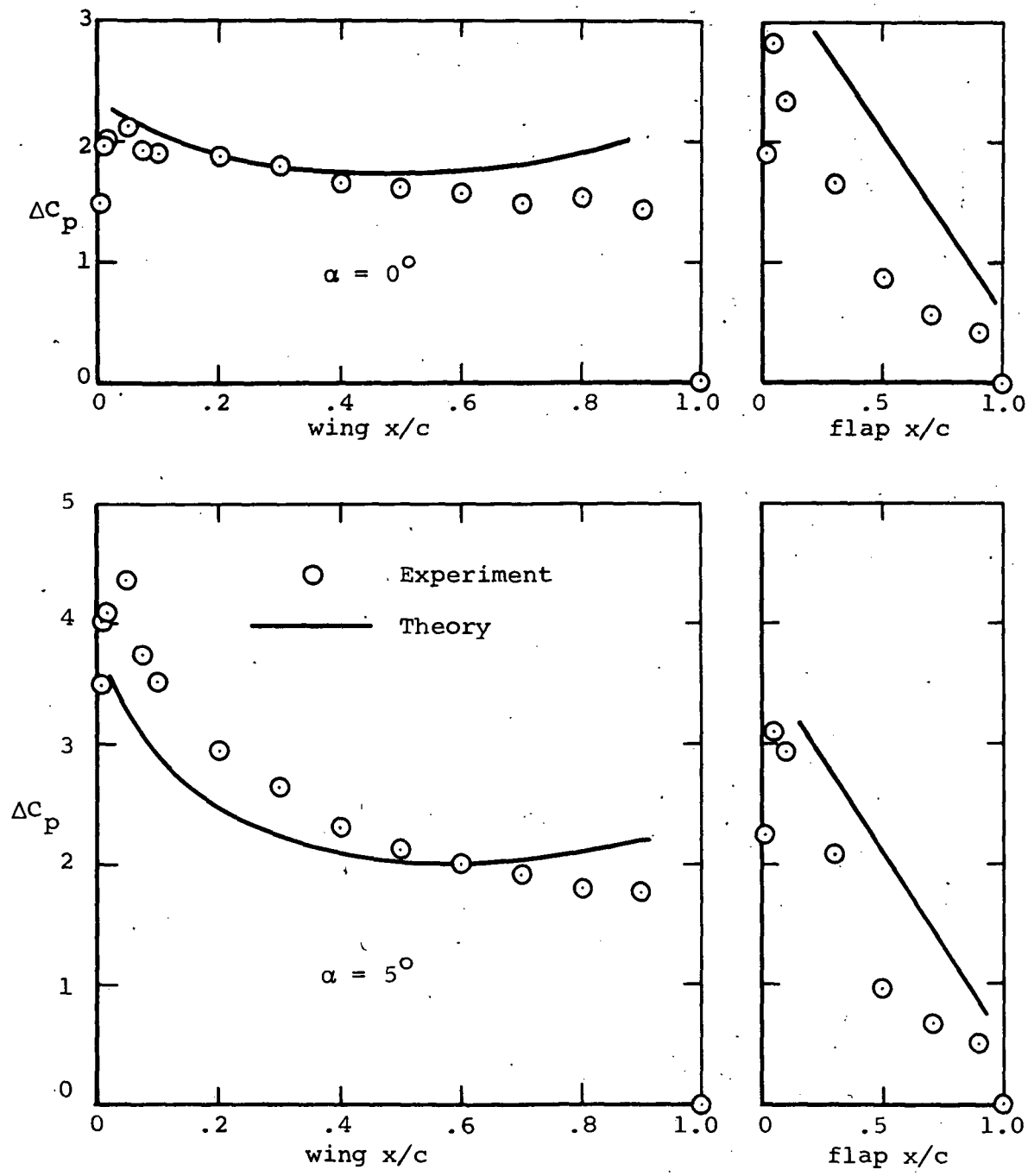

(b) Chordwise loading distribution, $\delta_f = 40^\circ$

Figure 10.- Concluded.

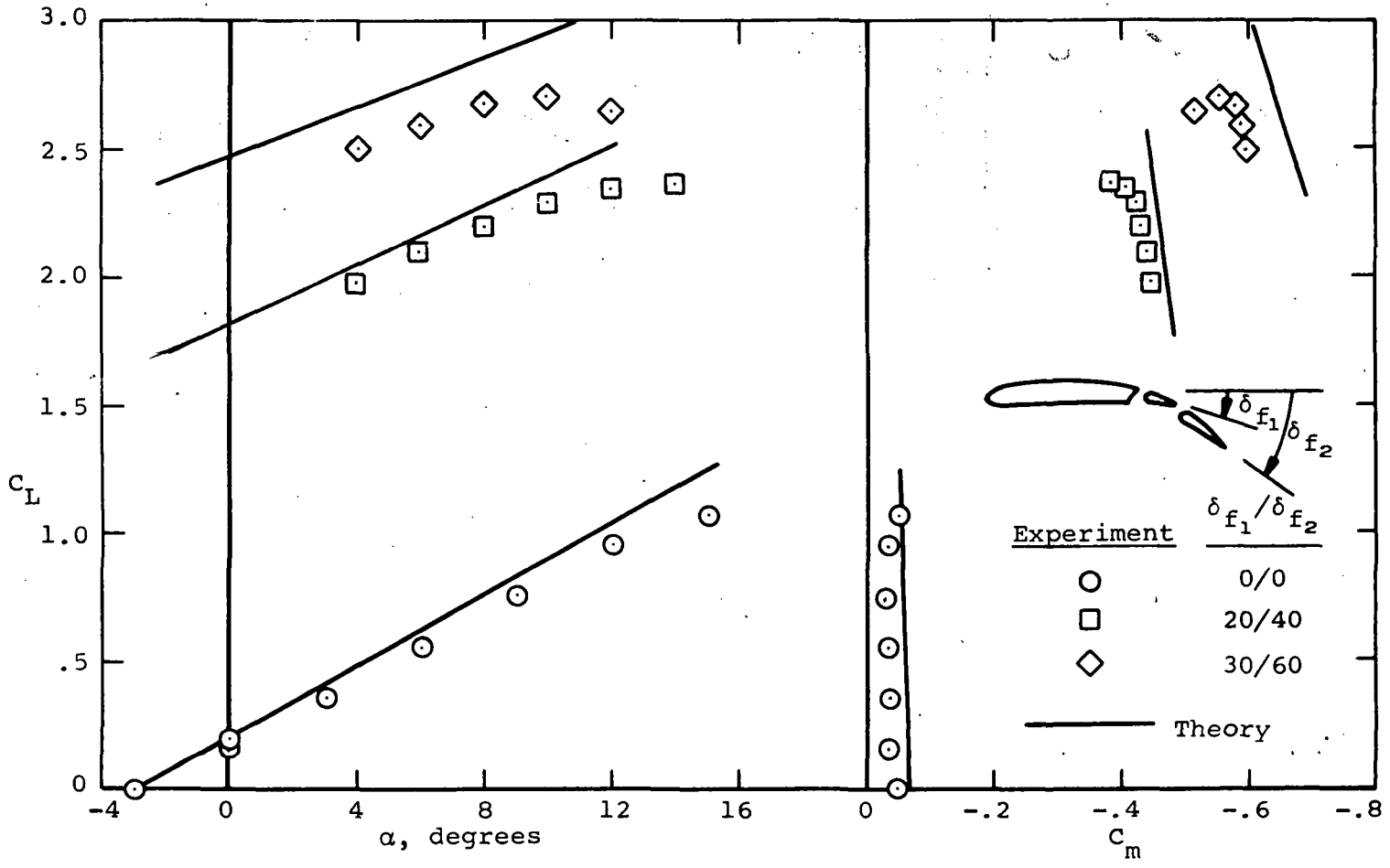

Figure 11.- Comparison of measured and predicted characteristics on an unswept wing model with double-slotted trailing-edge flaps.

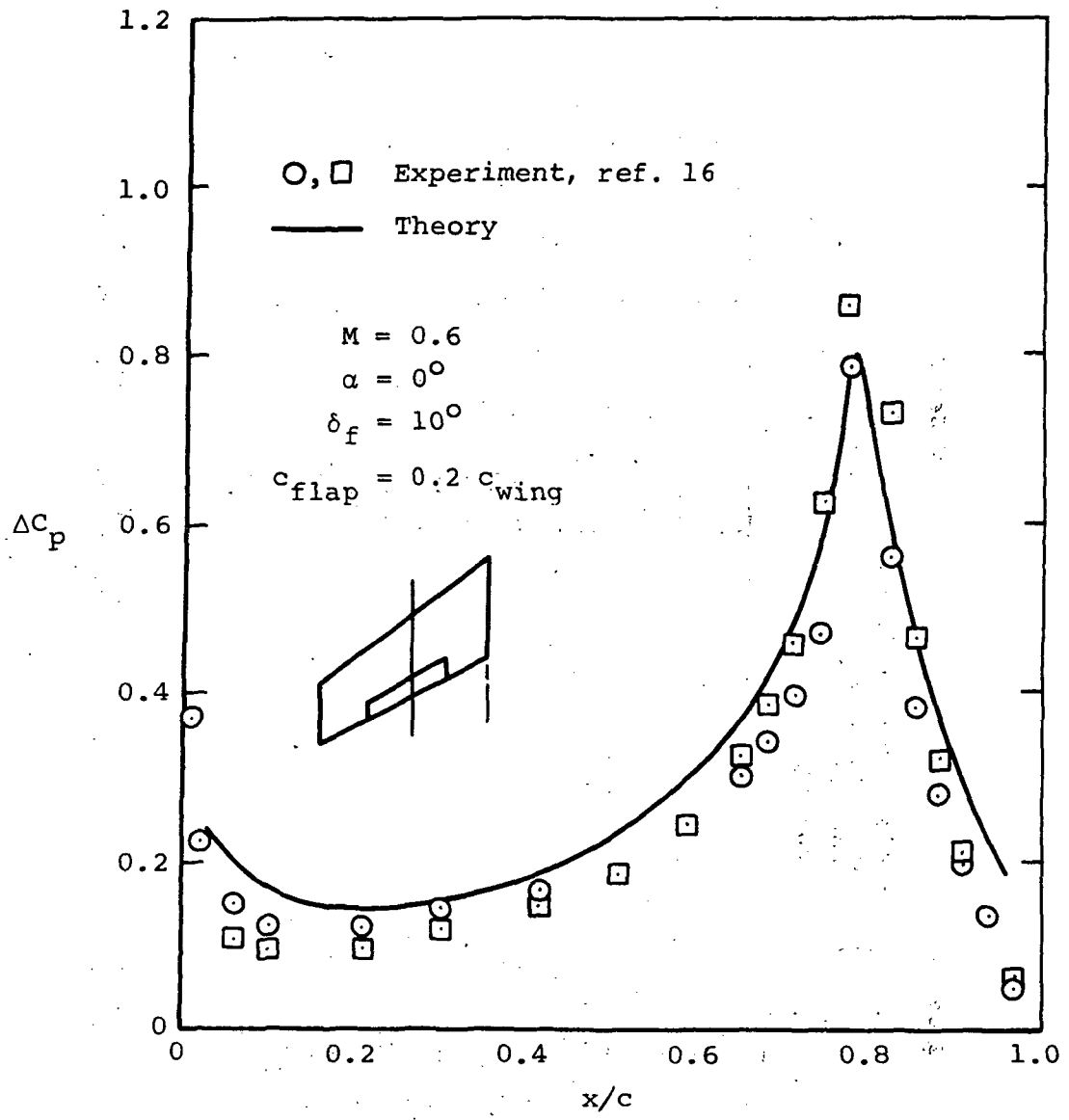

Figure 12.- Pressure distribution at $\eta = 0.46$ on a 35^o swept wing with deflected partial span flap.

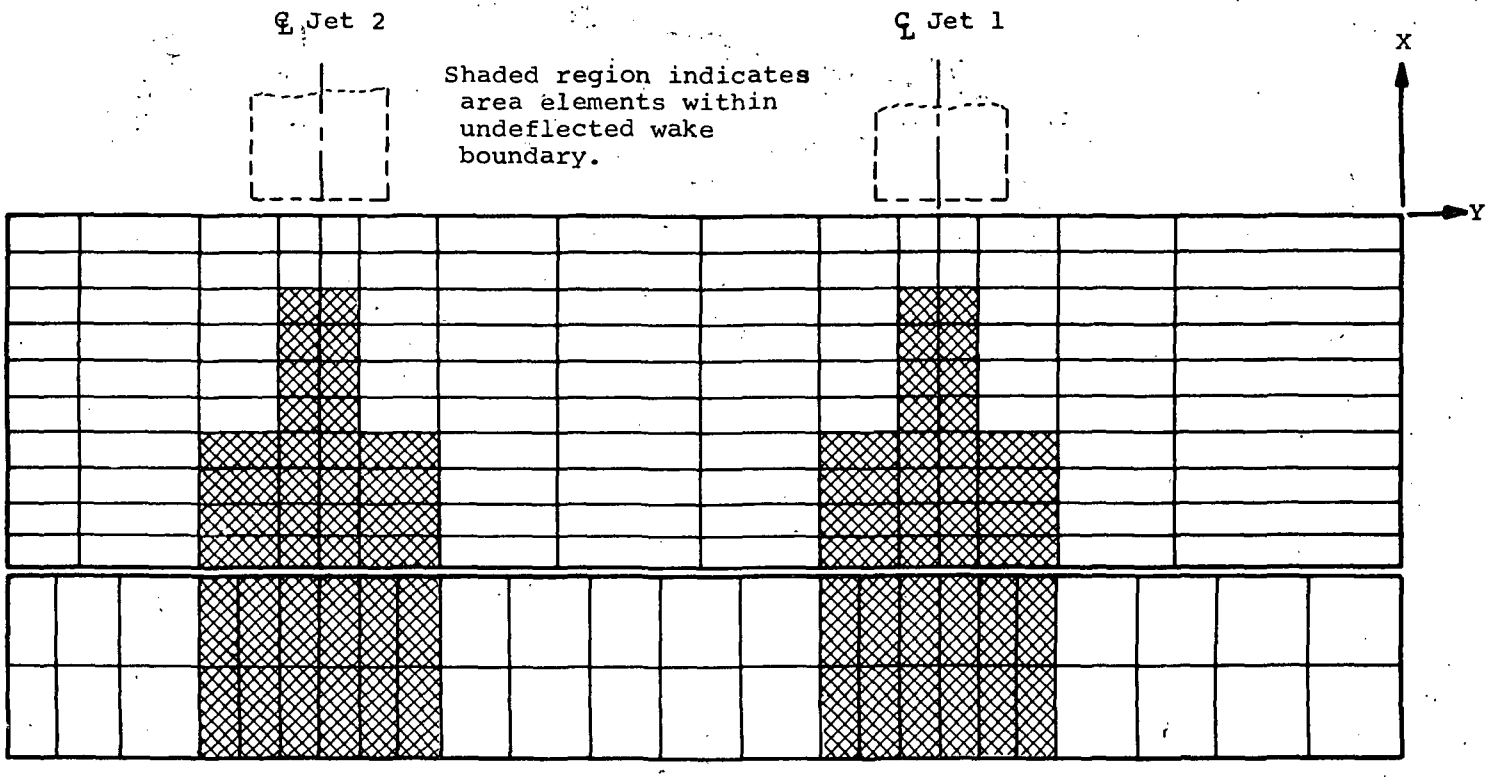

Figure 13.- Vortex-lattice network on an unswept wing with a slotted trailing-edge flap and two engines per semispan.

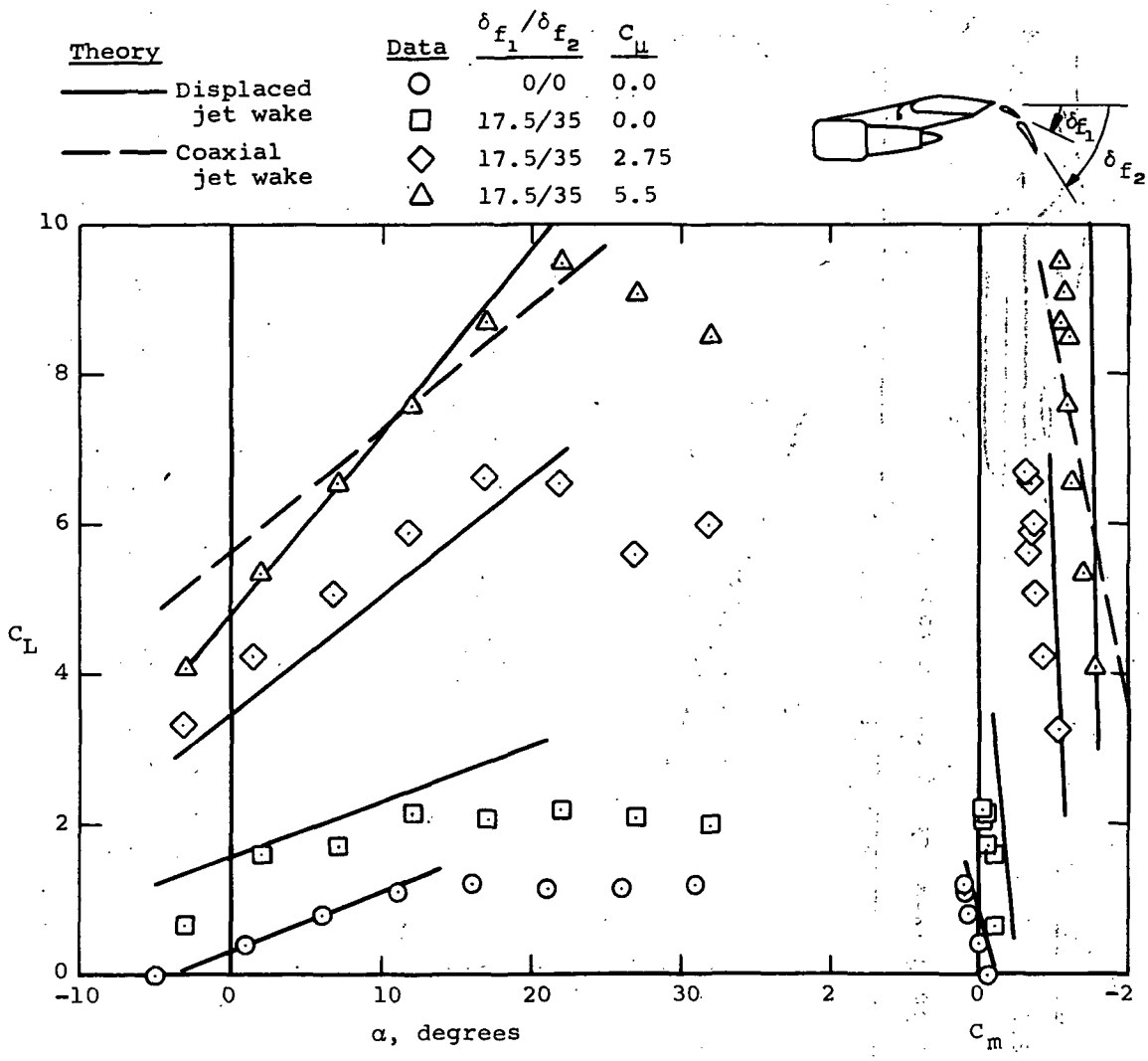

Figure 14.- Comparison of measured and predicted characteristics of an unswept wing with double-slotted trailing-edge flaps, slotted leading-edge slat, and four turbofan engines.

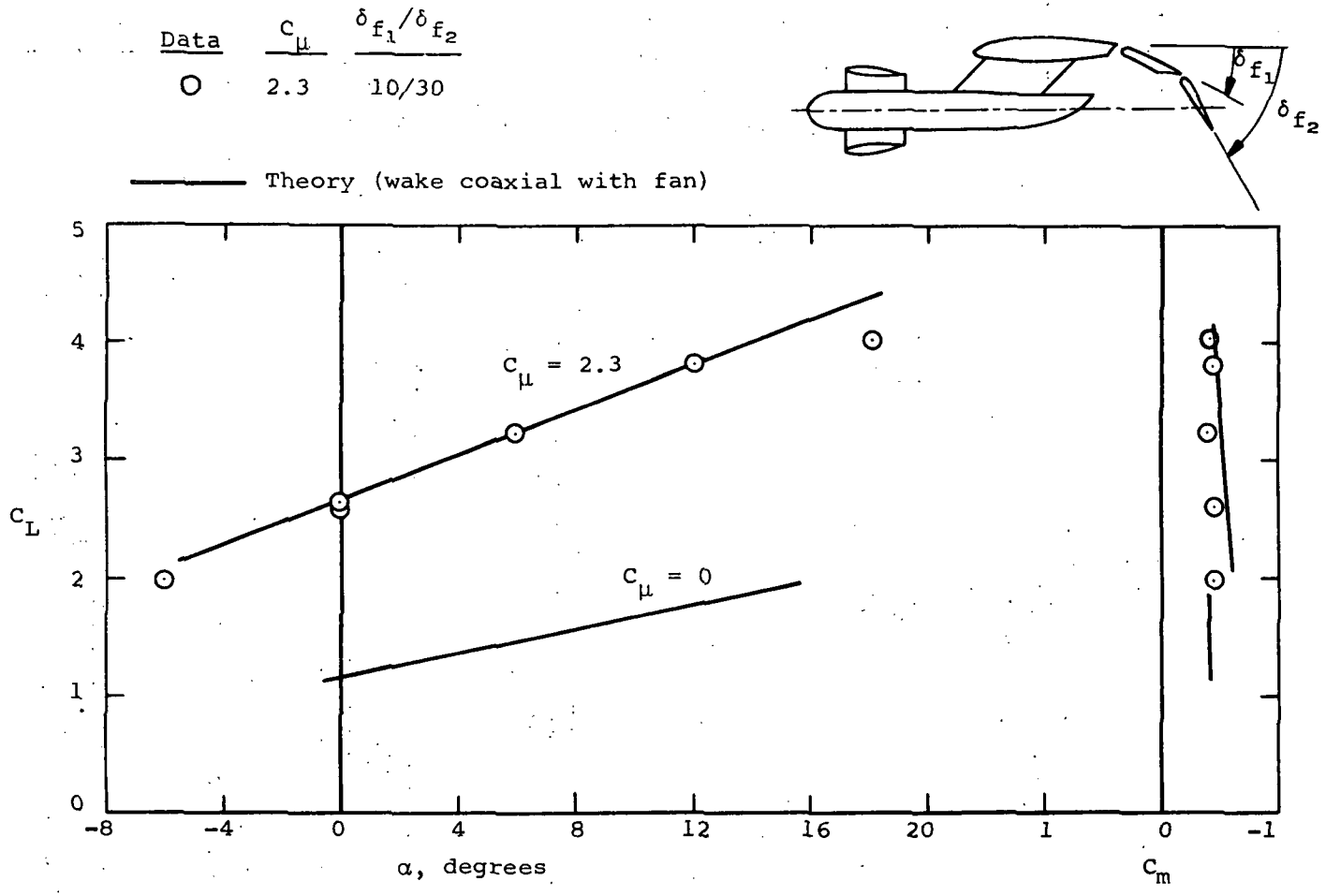

(a) *Comparison of predicted and measured lift and moment.*

Figure 15.- Characteristics of an unswept wing with externally-blown double-slotted trailing-edge flaps deflected 10/30°.

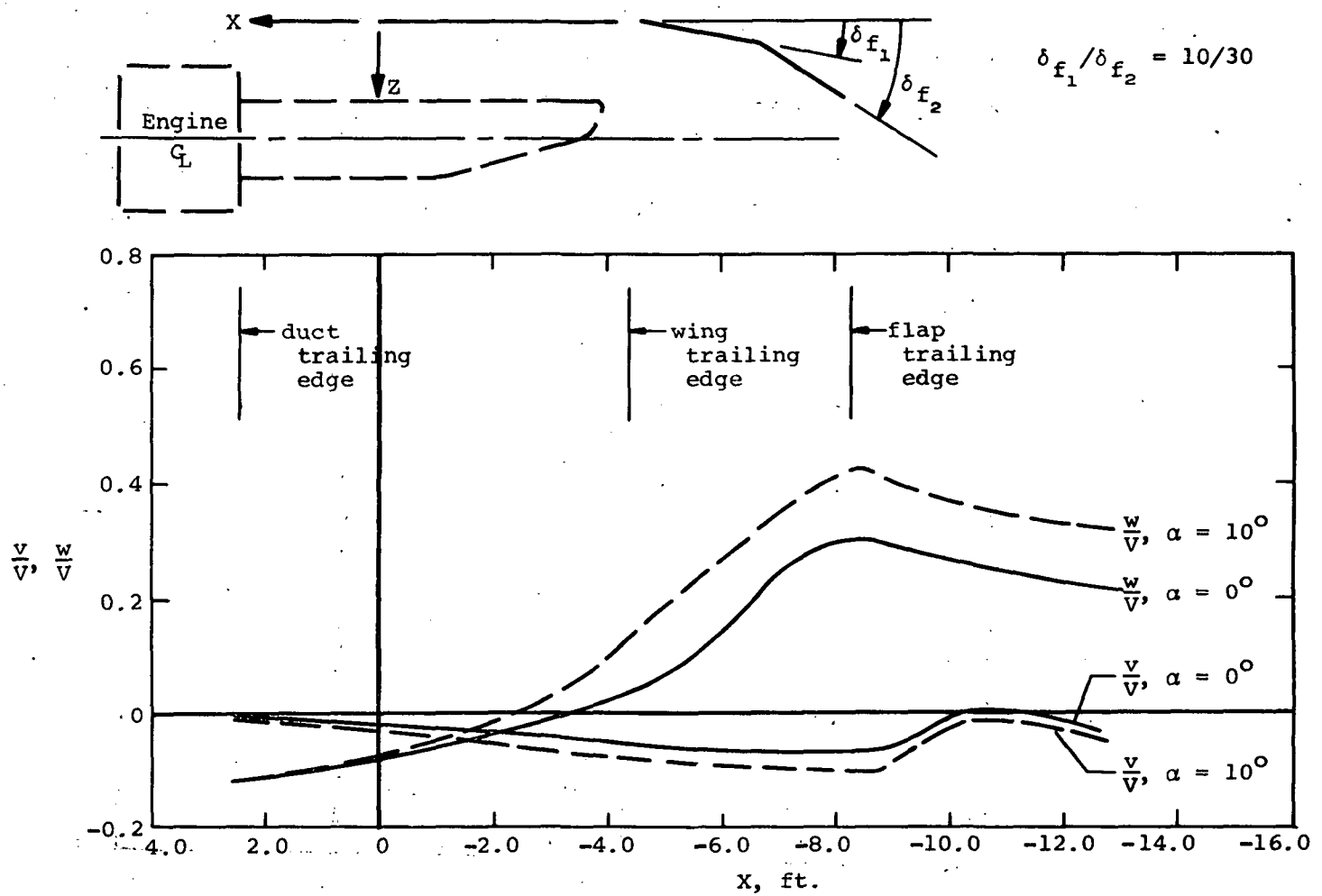

(b) Predicted downwash distribution induced by wing-flap in uniform flow along the engine centerline.

Figure 15.- Concluded.

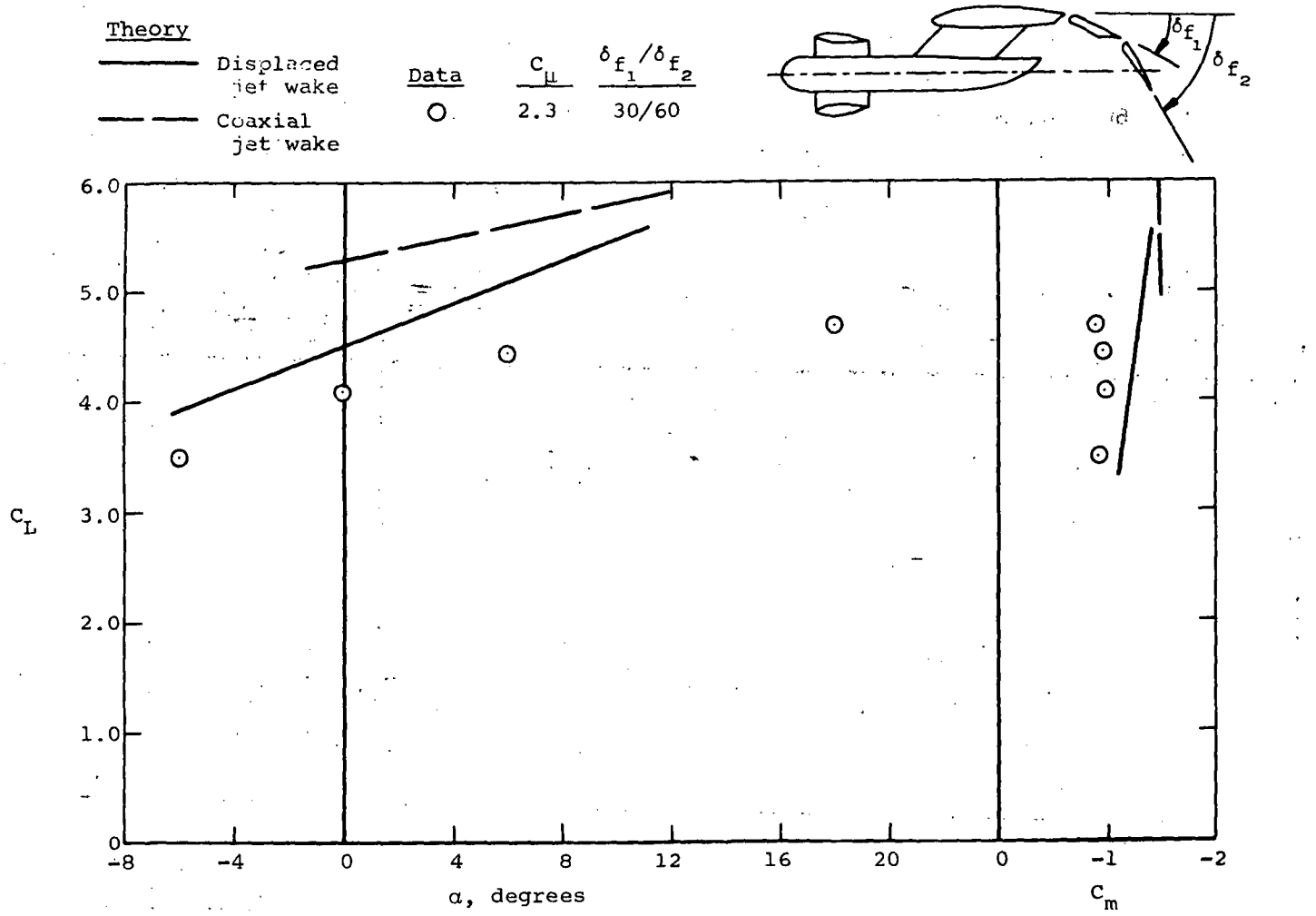

(a) Comparison of predicted and measured lift and moment.

Figure 16.- Characteristics of an unswept wing with externally-blown, double-slotted trailing-edge flaps deflected 30/60°.

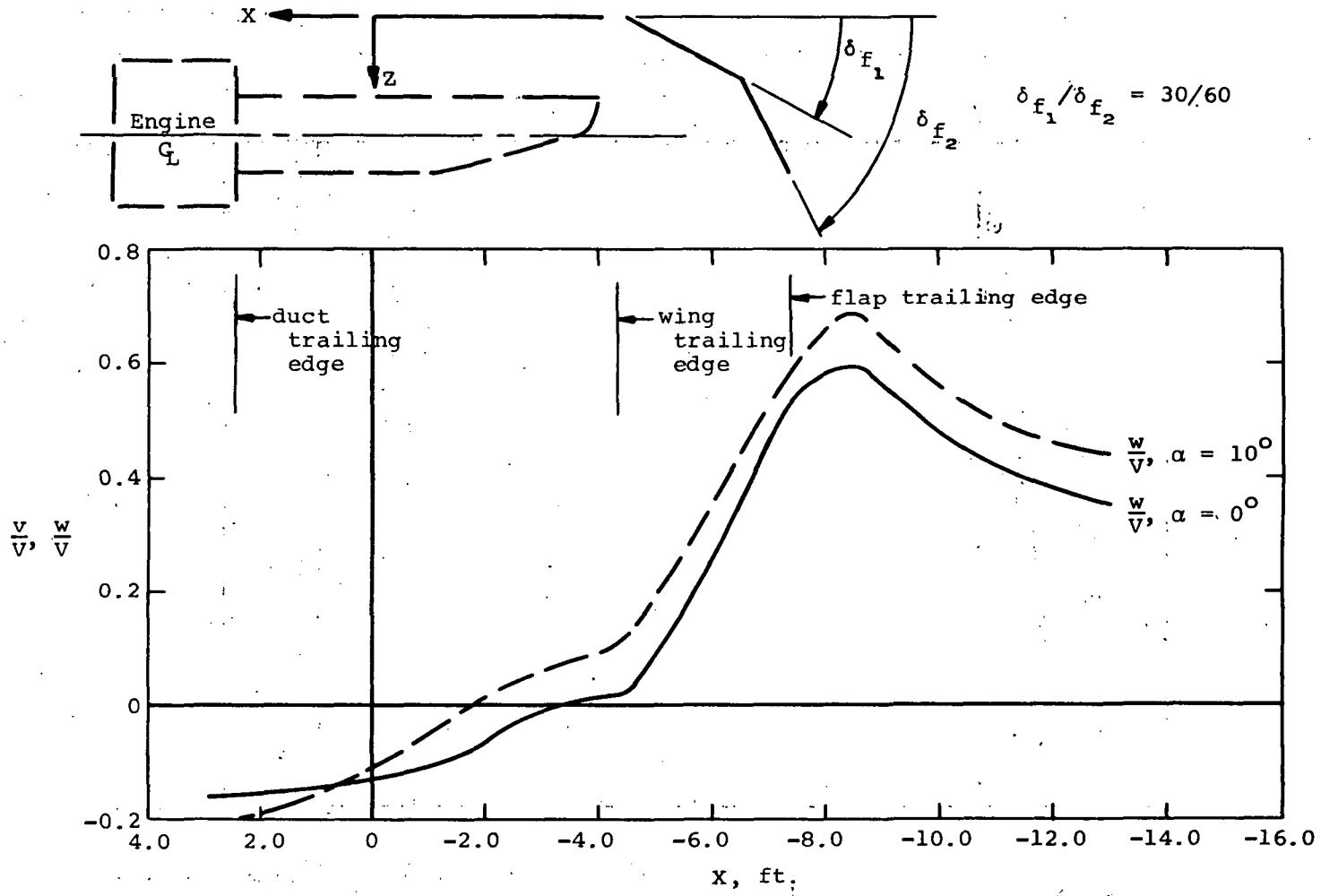

(b) Predicted downwash distribution induced by wing-flap in uniform flow along the engine centerline.

Figure 16.- Concluded.

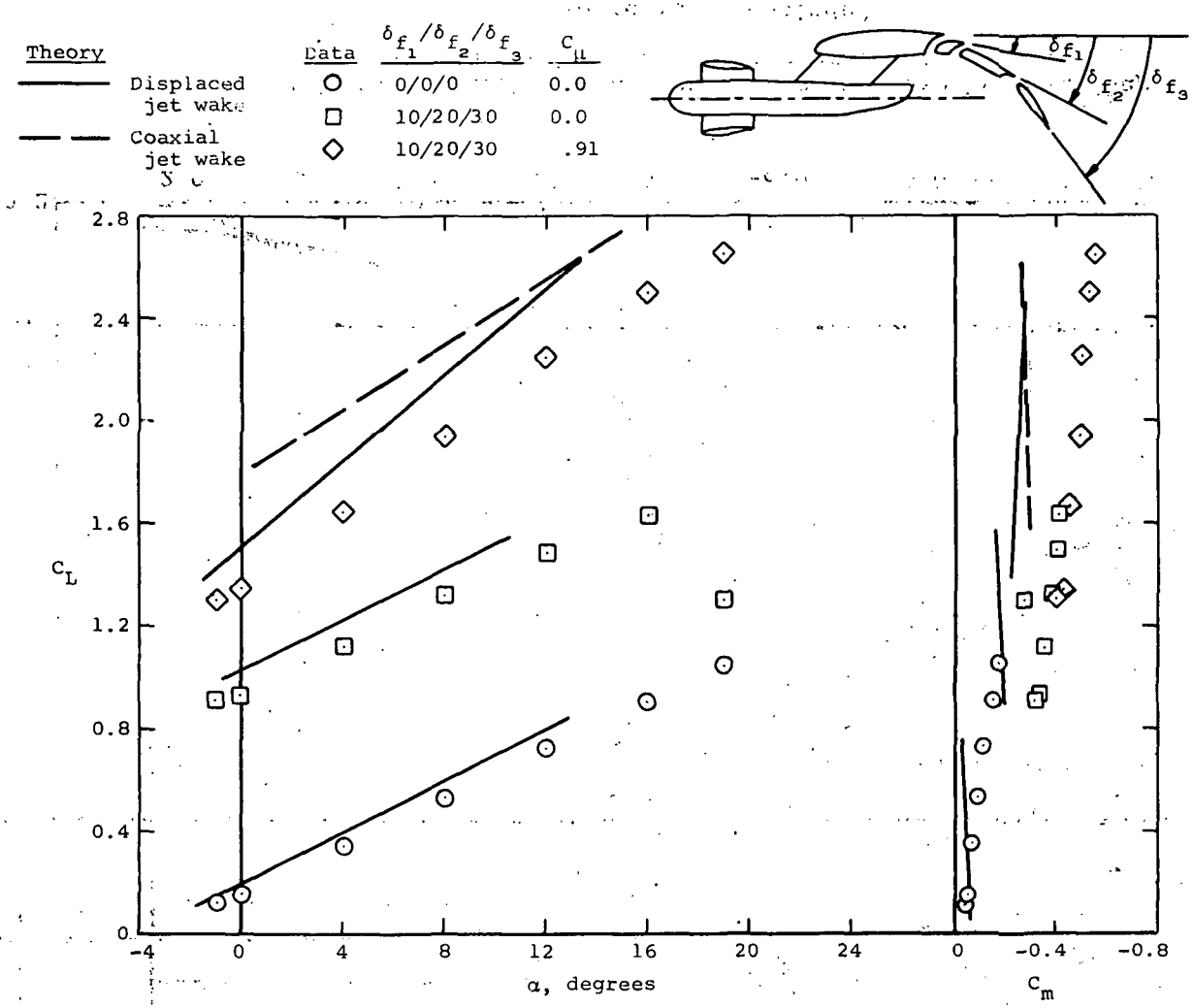

(a) Comparison of predicted and measured lift and moment.

Figure 17.- Characteristics of a 30° swept wing with externally-blown, triple-slotted trailing-edge flaps.

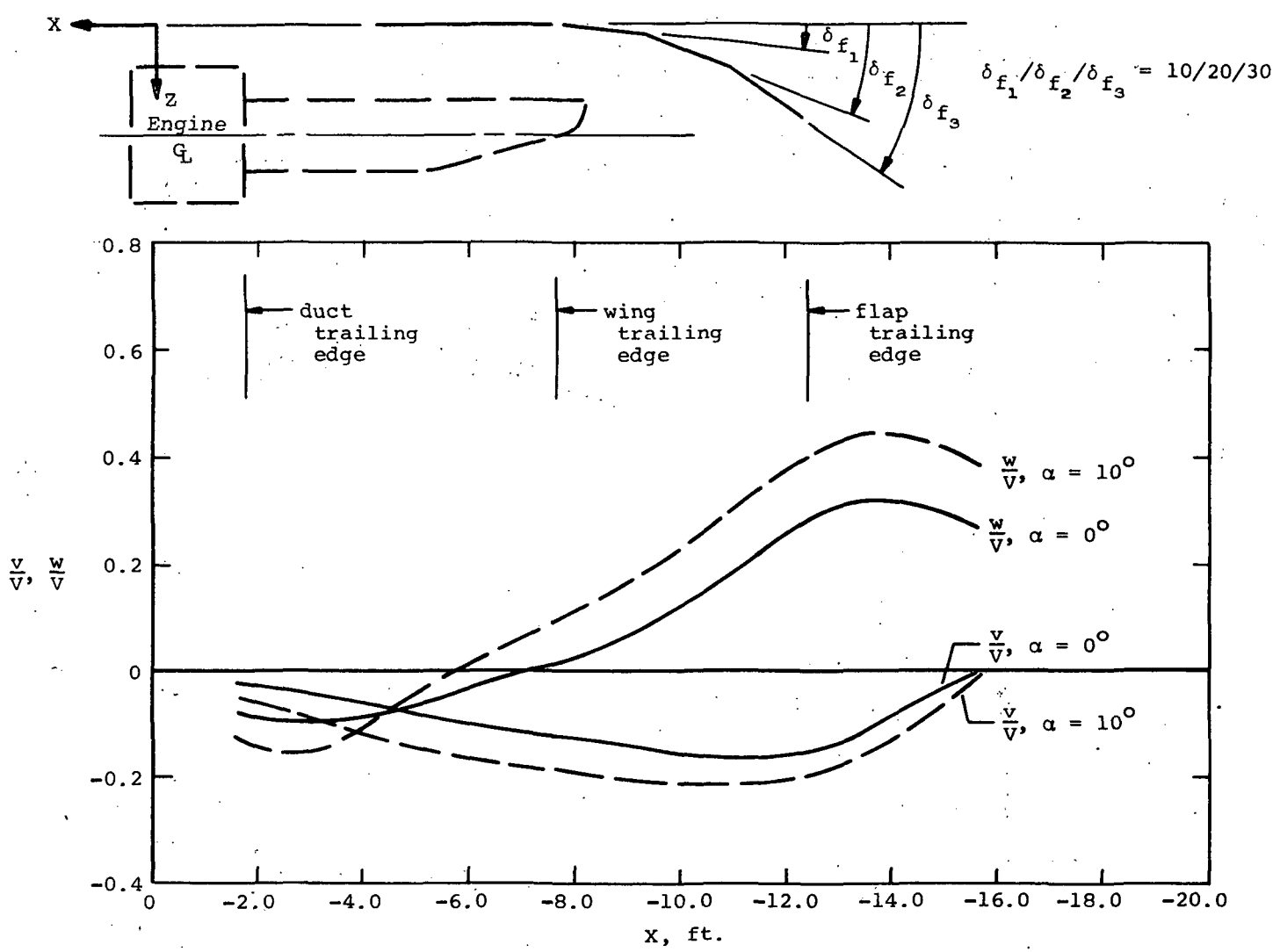

(b) Predicted downwash distribution induced by wing-flap in uniform flow along the engine centerline.

Figure 17.- Concluded.

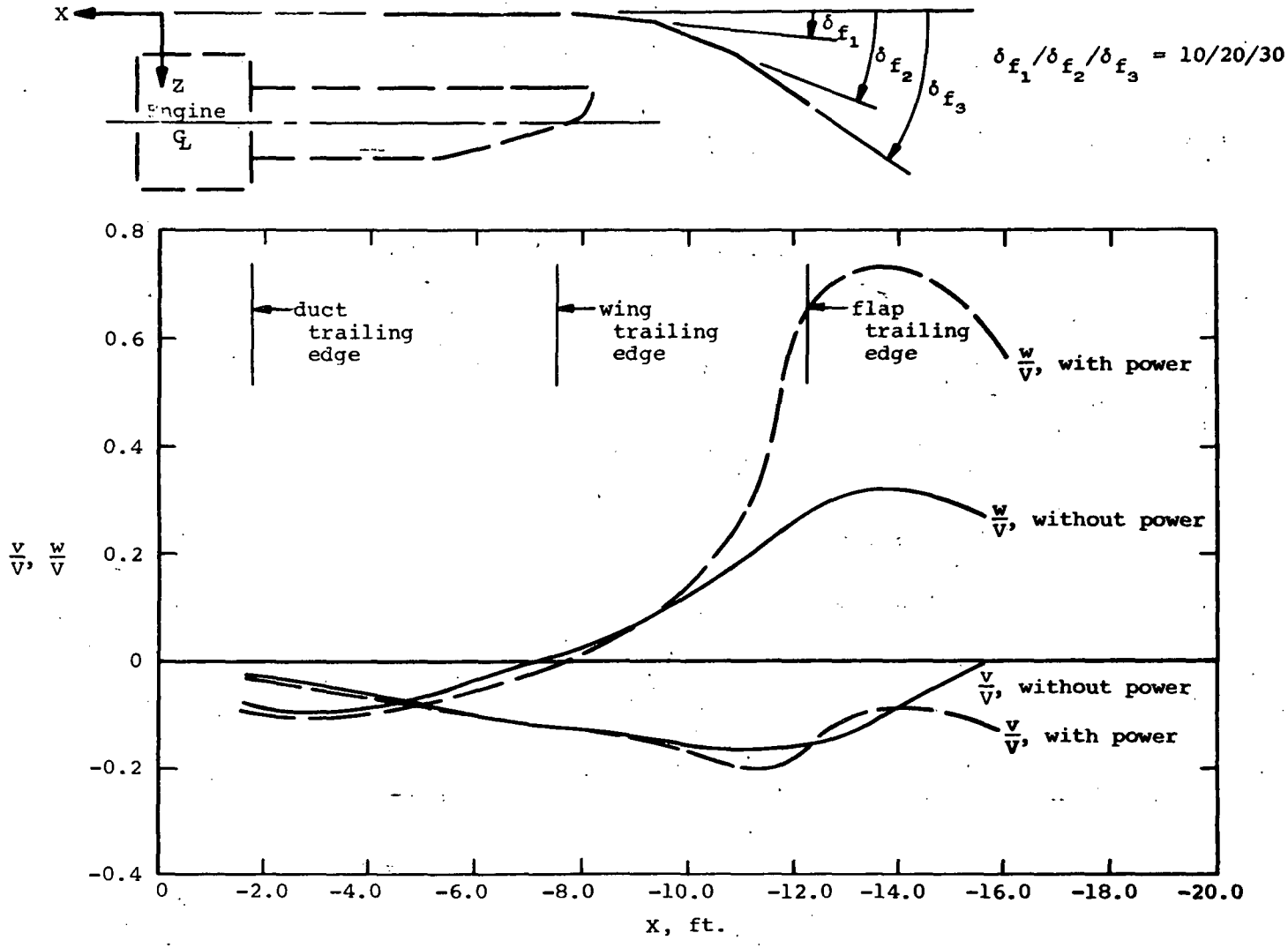

Figure 18.- Comparison of predicted wing-flap-induced down- and sidewash distributions along the engine centerline with and without jet wake interference for a 30° swept wing with triple slotted flaps at $\alpha = 0°$.

Item No. 1: Format (20A4), any alphabetic or numeric information
(1 card)

Column No.	1-80
Program Variable	TALK
Data	

Item No. 2: Format (2F5.1,3I5), decimal point required in first two variables
(1 card)

Column No.	5	10	15	20	25
Program Variable	ALPHLC	DELLC	MMM	MFLAP	MFSPEC
Data					

Item No. 3: Format (8F10.5), decimal point required
(1 card)

Column No.	10	20	30	40	50
Program Variable	PSIWLE	PSIWTE	CRW	SSPAN	PHID
Data					

Item No. 4: Format (8F10.5), decimal point required
(1 card)

Column No.	10	20	30	40	50	60
Program Variable	PSIFLE	PSIFTE	CRF	FSSPAN	XF	ZF
Data						

Note: If MFLAP = 0 (see item 2), insert blank card for this item.

Item No. 5: Format (7I5)
(1 card)

Column No.	5	10	15	20
Program Variable	NCW	MSW	NCF	MSF
Data				

Item No. 6: Format (8F10.5), decimal point required
(≥ 1 card)

(1)

Column No.	10	20	30	40	50	60	70	80
Program Variable	Y(1)	Y(2)	Y(3)	Y(4)	Y(5)	Y(6)	Y(7)	Y(8)
Data	0.0							

(2)

Column No.	10	20	30	40	50	60	70	80
Program Variable	Y(9)	Y(10)	Y(11)	...	Y(IMAX)			
Data								

Figure 19.- Input format for wing-flap program.

Item No. 7 (option): Format (8F10.5), decimal point required
(≥ 1 card)

(1)

Column No.	10	20	30	40	50	60	70	80
Program Variable	YF(1)	YF(2)	YF(3)	YF(4)	YF(5)	YF(6)	YF(7)	YF(8)
Data								

Note: These quantities are read in when MFLAP = 1 (see item 2); if MFLAP = 0 omit this item.

(2)

Column No.	10	20	30	40	50	60	70	80
Program Variable	YF(9)	YF(10)	YF(11)	...	YF(IFMAX)			
Data								

Item No. 8: Format (8F10.5), decimal point required
(1 card)

Column No.	10	20	30	40	50	60	70	80
Program Variable	XM	YM	ZM					
Data								

Item No. 9 (option): Format (8F10.5), decimal point required
(MSW cards)

(1)

Column No.	10	20	30	40
Program Variable	ALPHAL(1)	ALPHAL(2)	...	ALPHAL(NCW)
Data				

Note: These quantities are read in when ALPHLC = 1.0 (see item 2); if ALPHLC = 0.0, omit this item.
Number of data bits per card = number of chordwise wing vortices = NCW

(2)

Column No.	10	20	30	40
Program Variable	ALPHAL(NCW+1)	ALPHAL(NCW+2)	...	ALPHAL(2NCW)
Data				

(MSW)

Column No.	10	20	30	40
Program Variable	ALPHAL M-(NCW-1)	ALPHAL M-(NCW-2)	...	ALPHAL(MSW*NCW=M)

Figure 19.- Continued.

Item No. 10 (option): Format (8F10.5), decimal point required
(MSF cards)

(1)

Column No.	10	20	30	40
Program Variable	DELL(1)	DELL(2)	...	DELL(NCF)
Data				

Note: These quantities are read in when DELLC = 1.0 in item 2; if DELLC = 0.0, omit this item.

(2)

Column No.	10	20	30	40
Program Variable	DELL(NCF+1)	DELL(NCF+2)	...	DELL(2NCF)
Data				

(MSF)

Column No.	10	20	30	40
Program Variable	DELL MF-(NCF-1)	DELL MF-(NCF-2)	...	DELL(MSF*NCF=MF)
Data				

Item No. 11 (option): Format (3F10.3), decimal point required
(MMM cards)

(1)

Column No.	10	20	30
Program Variable	PMX(1)	PMY(1)	PMZ(1)
Data			

(2)

Column No.	10	20	30
Program Variable	PMX(2)	PMY(2)	PMZ(2)
Data			

(MMM)

Column No.	10	20	30
Program Variable	PMX(MMM)	PMY(MMM)	PMZ(MMM)
Data			

Figure 19.- Continued.

Item No. 12: Format (1F10.5, 2I10, F10.5), decimal point required in first variable.
(1 card)

Column No.	10	20	30	40
Program Variable	DELD	KEI	KCP	NRHS
Data				

Item No. 13: Format (F10.5)

Column No.	10
Program Variable	ALPHAD
Data	

Item No. 14 (option): Format (3E13.6)
(≥ 1 card)

(1)

Column No.	13	26	39
Program Variable	UEI(1)	VEI(1)	WEI(1)
Data			

Note: These quantities are read in via cards as shown here when KEI = 5 (see item 12); if KEI = 0 or KEI = 8, omit this item.

(2)

Column No.	13	26	39
Program Variable	UEI(2)	VEI(2)	WEI(2)
Data			

(M)

Column No.	13	26	39
Program Variable	UEI(M)	VEI(M)	WEI(M)
Data			

Note: If MFLAP = 0 (see item 2) this is the last card in this item; if MFLAP = 1, more cards follow.

(M+1)

Column No.	13	26	39
Program Variable	UEI(M+1)	VEI(M+1)	WEI(M+1)
Data			

(M+2)

Column No.	13	26	39
Program Variable	UEI(M+2)	VEI(M+2)	WEI(M+2)
Data			

(M+MF)

Column No.	13	26	39
Program Variable	UEI(M+MF)	VEI(M+MF)	WEI(M+MF)
Data			

Figure 19.- Concluded.

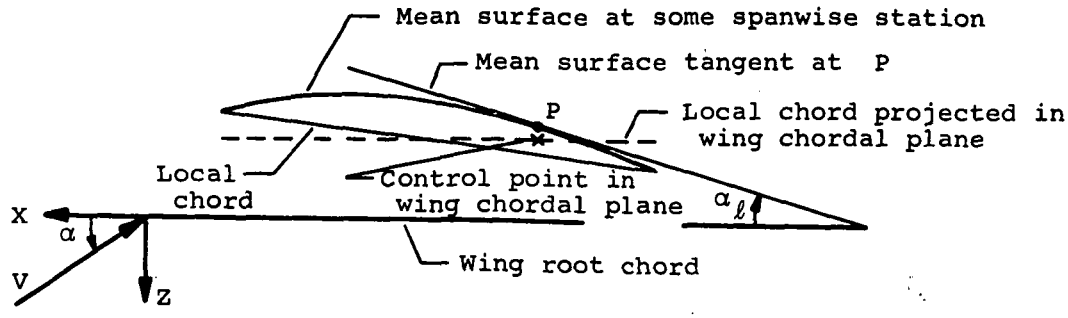

(a) Mean surface detail for a wing with camber, twist, and dihedral.

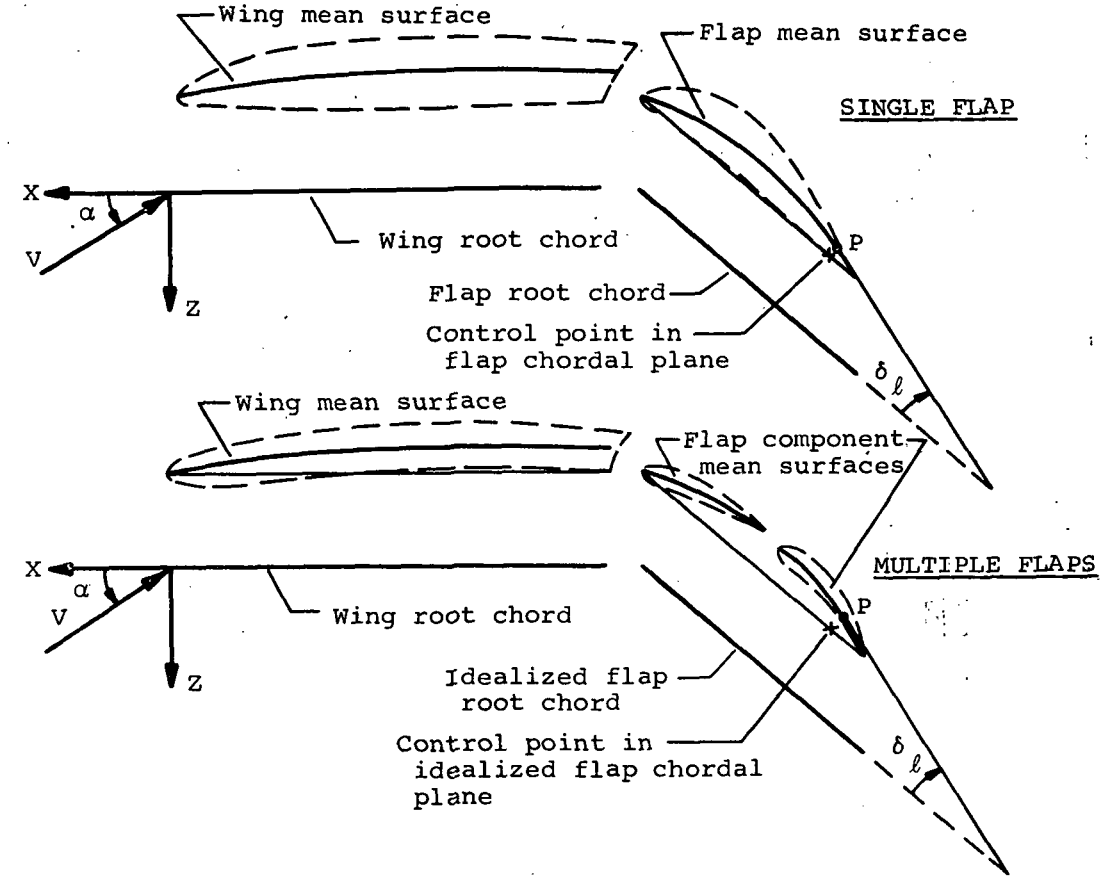

(b) Mean surface detail for wing-flap combinations shown for a rectangular-untwisted wing with dihedral.

Figure 20.- Definitions of local angles α_ℓ and δ_ℓ.

```
SWEPT WING, FLAP I (NASA TMX 62079) FLAP ANGLE = 10/20/30,ALPHA= 0,  NO JET
 1.0  1.0      8      1      .1
30.0          30.0          3.75        14.50        0.0
30.0          30.0          5.575       14.50       -4.00        -0.0683
  4   20       5    20
 0.0           0.725        1.450        2.175        2.900        3.625        4.350        5.075
 5.800         6.525        7.250        7.975        8.700        9.425       10.150       10.875
11.600        12.325       13.050       13.775       14.500
 0.0           0.725        1.450        2.175        2.900        3.625        4.350        5.075
 5.800         6.525        7.250        7.975        8.700        9.425       10.150       10.875
11.600        12.325       13.050       13.775       14.500
-6.56          0.0          0.0
-0.0568       -0.0295      -0.0104       0.0065
-0.0568       -0.0295      -0.0104       0.0065
-0.0568       -0.0295      -0.0104       0.0065
-0.0568       -0.0295      -0.0104       0.0065
-0.0568       -0.0295      -0.0104       0.0065
-0.0568       -0.0295      -0.0104       0.0065
-0.0568       -0.0295      -0.0104       0.0065
-0.0568       -0.0295      -0.0104       0.0065
-0.0568       -0.0295      -0.0104       0.0065
-0.0568       -0.0295      -0.0104       0.0065
-0.0568       -0.0295      -0.0104       0.0065
-0.0568       -0.0295      -0.0104       0.0065
-0.0568       -0.0295      -0.0104       0.0065
-0.0568       -0.0295      -0.0104       0.0065
-.0568        -.0295       -.0104        .0065
-.0568        -.0295       -.0104        .0065
-.0568        -.0295       -.0104        .0065
-.0568        -.0295       -.0104        .0065
-.0568        -.0295       -.0104        .0065
-.0568        -.0295       -.0104        .0065
-0.1736       -0.02265     -0.02265      0.1285       0.1285
-0.1736       -0.02265     -0.02265      0.1285       0.1285
-0.1736       -0.02265     -0.02265      0.1285       0.1285
-0.1736       -0.02265     -0.02265      0.1285       0.1285
-0.1736       -0.02265     -0.02265      0.1285       0.1285
-0.1736       -0.02265     -0.02265      0.1285       0.1285
-0.1736       -0.02265     -0.02265      0.1285       0.1285
-0.1736       -0.02265     -0.02265      0.1285       0.1285
-0.1736       -0.02265     -0.02265      0.1285       0.1285
-0.1736       -0.02265     -0.02265      0.1285       0.1285
-0.1736       -0.02265     -0.02265      0.1285       0.1285
-0.1736       -0.02265     -0.02265      0.1285       0.1285
-0.1736       -0.02265     -0.02265      0.1285       0.1285
-0.1736       -0.02265     -0.02265      0.1285       0.1285
-0.1736       -0.02265     -0.02265      0.1285       0.1285
-0.1736       -0.02265     -0.02265      0.1285       0.1285
-0.1736       -0.02265     -0.02265      0.1285       0.1285
-0.1736       -0.02265     -0.02265      0.1285       0.1285
-0.1736       -0.02265     -0.02265      0.1285       0.1285
-0.1736       -0.02265     -0.02265      0.1285       0.1285
- .70         -7.25         2.07
-3.70         -7.25         2.07
-5.70         -7.25         2.07
-7.70         -7.25         2.07
-9.70         -7.25         2.07
-11.70        -7.25         2.07
-13.70        -7.25         2.07
-15.70        -7.25         2.07
 21.5                 0          7              1
  0.0
```

Figure 21(a).- Input deck for wing-flap program, power off.

```
SWEPT WING, FLAP I (NASA TMX 62079) FLAP ANGLE = 10/20/30,ALPHA= 0, C(MU)=0.9
 1.0  1.0     8    1    1
 30.0        30.0        3.75       14.50       0.0
 30.0        30.0        5.575      14.50      -4.00      -0.0683
   4   20     5   20
  0.0         0.725       1.450      2.175      2.900      3.625      4.350      5.075
  5.800       6.525       7.250      7.975      8.700      9.425     10.150     10.875
 11.600      12.325      13.050     13.775     14.500
  0.0         0.725       1.450      2.175      2.900      3.625      4.350      5.075
  5.800       6.525       7.250      7.975      8.700      9.425     10.150     10.875
 11.600      12.325      13.050     13.775     14.500
 -6.56        0.0         0.0
 -0.0568     -0.0295     -0.0104     0.0065
 -0.0568     -0.0295     -0.0104     0.0065
 -0.0568     -0.0295     -0.0104     0.0065
 -0.0568     -0.0295     -0.0104     0.0065
 -0.0568     -0.0295     -0.0104     0.0065
 -0.0568     -0.0295     -0.0104     0.0065
 -0.0568     -0.0295     -0.0104     0.0065
 -0.0568     -0.0295     -0.0104     0.0065
 -0.0568     -0.0295     -0.0104     0.0065
 -0.0568     -0.0295     -0.0104     0.0065
 -0.0568     -0.0295     -0.0104     0.0065
 -0.0568     -0.0295     -0.0104     0.0065
 -0.0568     -0.0295     -0.0104     0.0065
 -.0568      -.0295      -.0104      .0065
 -.0568      -.0295      -.0104      .0065
 -.0568      -.0295      -.0104      .0065
 -.0568      -.0295      -.0104      .0065
 -.0568      -.0295      -.0104      .0065
 -.0568      -.0295      -.0104      .0065
 -0.1736     -0.02265    -0.02265    0.1285     0.1285
 -0.1736     -0.02265    -0.02265    0.1285     0.1285
 -0.1736     -0.02265    -0.02265    0.1285     0.1285
 -0.1736     -0.02265    -0.02265    0.1285     0.1285
 -0.1736     -0.02265    -0.02265    0.1285     0.1285
 -0.1736     -0.02265    -0.02265    0.1285     0.1285
 -0.1736     -0.02265    -0.02265    0.1285     0.1285
 -0.1736     -0.02265    -0.02265    0.1285     0.1285
 -0.1736     -0.02265    -0.02265    0.1285     0.1285
 -0.1736     -0.02265    -0.02265    0.1285     0.1285
 -0.1736     -0.02265    -0.02265    0.1285     0.1285
 -0.1736     -0.02265    -0.02265    0.1285     0.1285
 -0.1736     -0.02265    -0.02265    0.1285     0.1285
 -0.1736     -0.02265    -0.02265    0.1285     0.1285
 -0.1736     -0.02265    -0.02265    0.1285     0.1285
 -0.1736     -0.02265    -0.02265    0.1285     0.1285
 -0.1736     -0.02265    -0.02265    0.1285     0.1285
 -0.1736     -0.02265    -0.02265    0.1285     0.1285
 -1.70       -7.25        2.07
 -3.70       -7.25        2.07
 -5.70       -7.25        2.07
 -7.70       -7.25        2.07
 -9.70       -7.25        2.07
-11.70       -7.25        2.07
-13.70       -7.25        2.07
-15.70       -7.25        2.07
 21.5                 8          0          1
  0.0
```

Figure 21(b).- Input deck for wing-flap program, power on.

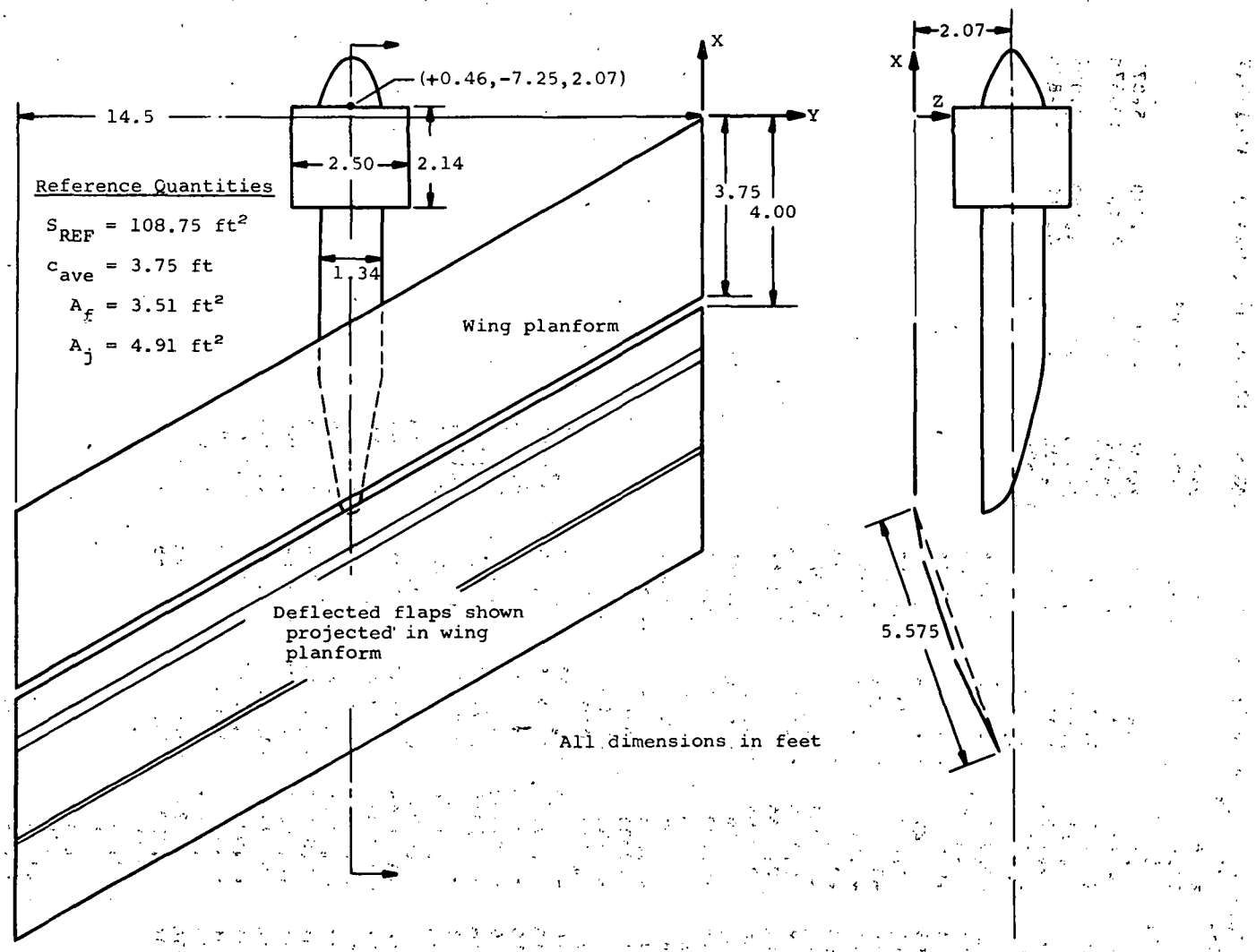

(a) Planform and elevation.

Figure 22.- Swept-wing-flaps I (10/20/30°) configuration of reference 5.

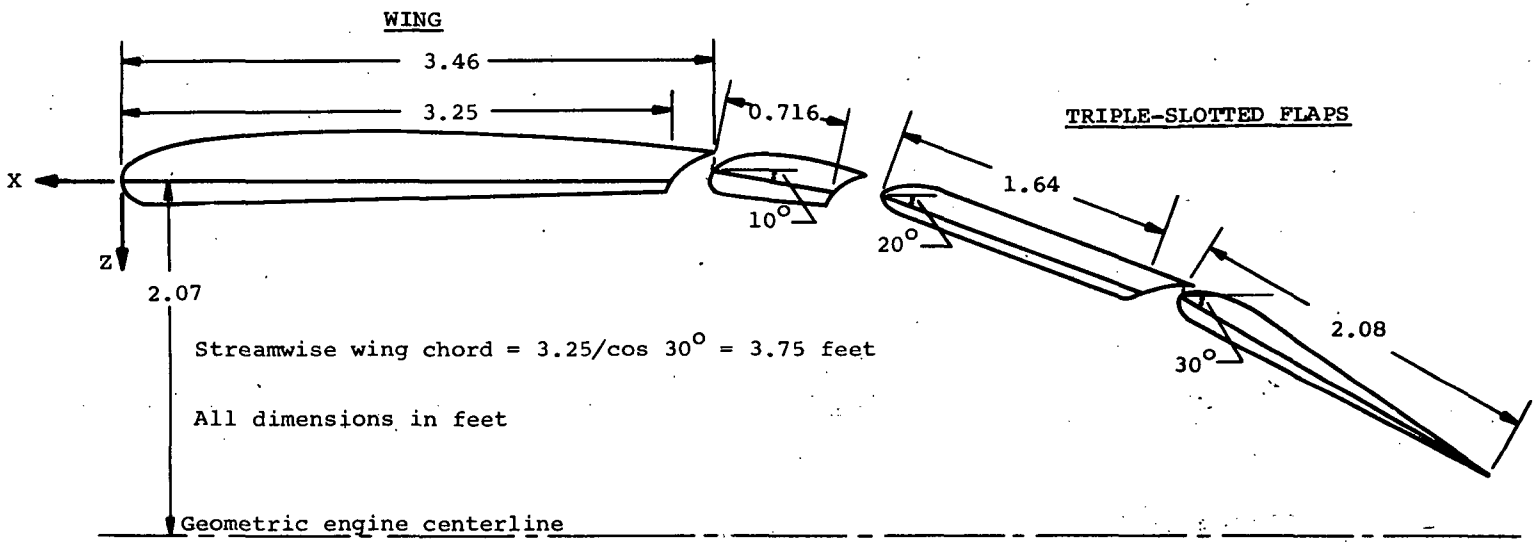

(b) Section normal to wing leading and trailing edges.

Figure 22.- Continued.

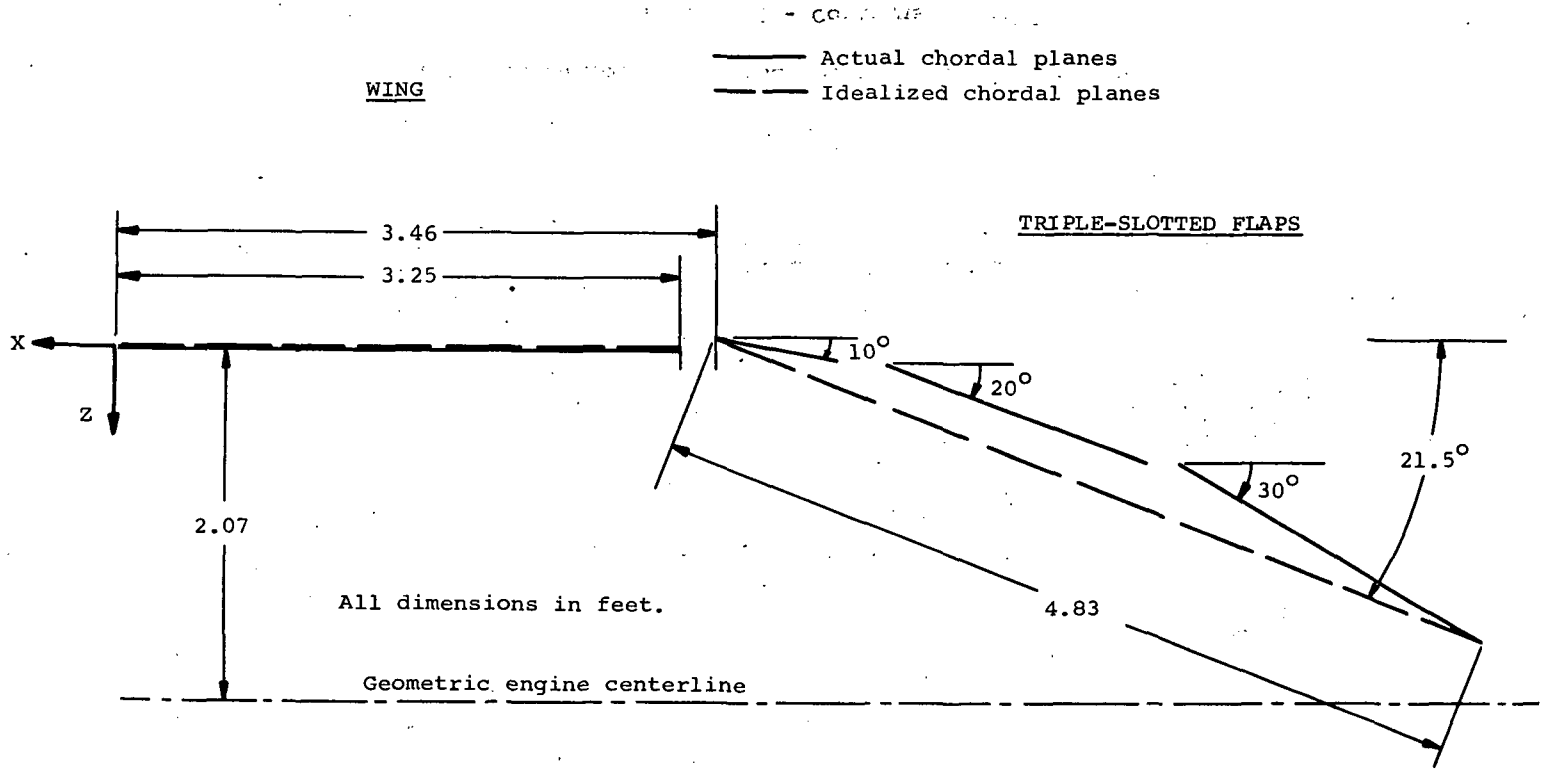

(c) Chordal plane layout in a section normal to wing leading and trailing edges.

Figure 22.- Concluded.

```
SWEPT WING, FLAP 1 (NASA TMX 62079) FLAP ANGLE = 10/20/30,ALPHA= 0,  NO JET

                              GEOMETRY DATA

                          WING              FLAP

 LE SWEEP,DEG.          30.0000           30.0000
 TE SWEEP,DEG.          30.0000           30.0000
 DIHEDRAL,DEG.           0.0000
 CHORD AT WING ROOT      3.7500            5.5750
 SEMISPAN               14.5000           14.5000

 CHORDWISE VORTICES           4                 5
 SPANWISE VORTICES           20                20

 COORDS. OF ROOTCHORD NOSE OF FLAP EXTENDED TO PLANE OF SYMMETRY
                                   X                      Z
                               -4.0000                -0.0683

 UNDEFLECTED FLAP INBOARD SPAN          0.0000
 UNDEFLECTED FLAP OUTBOARD SPAN        14.5000



                                   X          Y          Z
 PITCHING MOMENT CENTER         -6.5600     0.0000     0.0000


 FLAP ANGLE,DELD,DEG.                     21.5000
 CALC. STREAMWISE FLAP ANGLE,DLXD,DEG.    18.8354



                    FLOW CONDITIONS FOR CASE    1

 ANGLE OF ATTACK,ALPHA ,DEG.              0.0000
```

Figure 23(a).- Output from wing-flap program, power off.

J	X	Y	Z	MEAN SURFACE SLOPE	J/V	V/V	W/V
		CONTROL POINT COORDINATES AND SLOPES			EXTERNALLY INDUCED VELOCITIES		
WING CONTROL POINTS							
1	-0.9124	-0.3625	-0.0000	-0.0568	0.00000	0.00000	0.00000
2	-1.8499	-0.3625	-0.0000	-0.0295	0.00000	0.00000	0.00000
3	-2.7874	-0.3625	-0.0000	-0.0104	0.00000	0.00000	0.00000
4	-3.7249	-0.3625	-0.0000	0.0065	0.00000	0.00000	0.00000
5	-1.3310	-1.0875	-0.0000	-0.0568	0.00000	0.00000	0.00000
6	-2.2685	-1.0875	-0.0000	-0.0295	0.00000	0.00000	0.00000
7	-3.2060	-1.0875	-0.0000	-0.0104	0.00000	0.00000	0.00000
8	-4.1435	-1.0875	-0.0000	0.0065	0.00000	0.00000	0.00000
9	-1.7496	-1.8125	-0.0000	-0.0568	0.00000	0.00000	0.00000
10	-2.6871	-1.8125	-0.0000	-0.0295	0.00000	0.00000	0.00000
11	-3.6246	-1.8125	-0.0000	-0.0104	0.00000	0.00000	0.00000
12	-4.5621	-1.8125	-0.0000	0.0065	0.00000	0.00000	0.00000
13	-2.1681	-2.5375	-0.0000	-0.0568	0.00000	0.00000	0.00000
14	-3.1056	-2.5375	-0.0000	-0.0295	0.00000	0.00000	0.00000
15	-4.0431	-2.5375	-0.0000	-0.0104	0.00000	0.00000	0.00000
16	-4.9806	-2.5375	-0.0000	0.0065	0.00000	0.00000	0.00000
17	-2.5867	-3.2625	-0.0000	-0.0568	0.00000	0.00000	0.00000
18	-3.5242	-3.2625	-0.0000	-0.0295	0.00000	0.00000	0.00000
19	-4.4617	-3.2625	-0.0000	-0.0104	0.00000	0.00000	0.00000
20	-5.3992	-3.2625	-0.0000	0.0065	0.00000	0.00000	0.00000
21	-3.0053	-3.9875	-0.0000	-0.0568	0.00000	0.00000	0.00000
22	-3.9428	-3.9875	-0.0000	-0.0295	0.00000	0.00000	0.00000
23	-4.8803	-3.9875	-0.0000	-0.0104	0.00000	0.00000	0.00000
24	-5.8178	-3.9875	-0.0000	0.0065	0.00000	0.00000	0.00000
25	-3.4239	-4.7125	-0.0000	-0.0568	0.00000	0.00000	0.00000
26	-4.3614	-4.7125	-0.0000	-0.0295	0.00000	0.00000	0.00000
27	-5.2989	-4.7125	-0.0000	-0.0104	0.00000	0.00000	0.00000
28	-6.2364	-4.7125	-0.0000	0.0065	0.00000	0.00000	0.00000
29	-3.8425	-5.4375	-0.0000	-0.0568	0.00000	0.00000	0.00000
30	-4.7800	-5.4375	-0.0000	-0.0295	0.00000	0.00000	0.00000
31	-5.7175	-5.4375	-0.0000	-0.0104	0.00000	0.00000	0.00000
32	-6.6550	-5.4375	-0.0000	0.0065	0.00000	0.00000	0.00000
33	-4.2610	-6.1625	-0.0000	-0.0568	0.00000	0.00000	0.00000
34	-5.1985	-6.1625	-0.0000	-0.0295	0.00000	0.00000	0.00000
35	-6.1360	-6.1625	-0.0000	-0.0104	0.00000	0.00000	0.00000
36	-7.0735	-6.1625	-0.0000	0.0065	0.00000	0.00000	0.00000
37	-4.6796	-6.8875	-0.0000	-0.0568	0.00000	0.00000	0.00000
38	-5.6171	-6.8875	-0.0000	-0.0295	0.00000	0.00000	0.00000
39	-6.5546	-6.8875	-0.0000	-0.0104	0.00000	0.00000	0.00000
40	-7.4921	-6.8875	-0.0000	0.0065	0.00000	0.00000	0.00000
41	-5.0982	-7.6125	-0.0000	-0.0568	0.00000	0.00000	0.00000
42	-6.0357	-7.6125	-0.0000	-0.0295	0.00000	0.00000	0.00000
43	-6.9732	-7.6125	-0.0000	-0.0104	0.00000	0.00000	0.00000
44	-7.9107	-7.6125	-0.0000	0.0065	0.00000	0.00000	0.00000
45	-5.5168	-8.3375	-0.0000	-0.0568	0.00000	0.00000	0.00000
46	-6.4543	-8.3375	-0.0000	-0.0295	0.00000	0.00000	0.00000
47	-7.3918	-8.3375	-0.0000	-0.0104	0.00000	0.00000	0.00000
48	-8.3293	-8.3375	-0.0000	0.0065	0.00000	0.00000	0.00000
49	-5.9354	-9.0625	-0.0000	-0.0568	0.00000	0.00000	0.00000
50	-6.8729	-9.0625	-0.0000	-0.0295	0.00000	0.00000	0.00000
51	-7.8104	-9.0625	-0.0000	-0.0104	0.00000	0.00000	0.00000
52	-8.7479	-9.0625	-0.0000	0.0065	0.00000	0.00000	0.00000
53	-6.3539	-9.7875	-0.0000	-0.0568	0.00000	0.00000	0.00000
54	-7.2914	-9.7875	-0.0000	-0.0295	0.00000	0.00000	0.00000
55	-8.2289	-9.7875	-0.0000	-0.0104	0.00000	0.00000	0.00000
56	-9.1664	-9.7875	-0.0000	0.0065	0.00000	0.00000	0.00000

Figure 23(a).- Continued.

57	-6.7725	-10.5125	-0.0000	-0.0568	0.00000	0.00000	0.00000
58	-7.7100	-10.5125	-0.0000	-0.0295	0.00000	0.00000	0.00000
59	-8.6475	-10.5125	-0.0000	-0.0104	0.00000	0.00000	0.00000
60	-9.5850	-10.5125	-0.0000	0.0065	0.00000	0.00000	0.00000
61	-7.1911	-11.2375	-0.0000	-0.0568	0.00000	0.00000	0.00000
62	-8.1286	-11.2375	-0.0000	-0.0295	0.00000	0.00000	0.00000
63	-9.0661	-11.2375	-0.0000	-0.0104	0.00000	0.00000	0.00000
64	-10.0036	-11.2375	-0.0000	0.0065	0.00000	0.00000	0.00000
65	-7.6097	-11.9625	-0.0000	-0.0568	0.00000	0.00000	0.00000
66	-8.5472	-11.9625	-0.0000	-0.0295	0.00000	0.00000	0.00000
67	-9.4847	-11.9625	-0.0000	-0.0104	0.00000	0.00000	0.00000
68	-10.4222	-11.9625	-0.0000	0.0065	0.00000	0.00000	0.00000
69	-8.0282	-12.6875	-0.0000	-0.0568	0.00000	0.00000	0.00000
70	-8.9657	-12.6875	-0.0000	-0.0295	0.00000	0.00000	0.00000
71	-9.9032	-12.6875	-0.0000	-0.0104	0.00000	0.00000	0.00000
72	-10.8407	-12.6875	-0.0000	0.0065	0.00000	0.00000	0.00000
73	-8.4468	-13.4125	-0.0000	-0.0568	0.00000	0.00000	0.00000
74	-9.3843	-13.4125	-0.0000	-0.0295	0.00000	0.00000	0.00000
75	-10.3218	-13.4125	-0.0000	-0.0104	0.00000	0.00000	0.00000
76	-11.2593	-13.4125	-0.0000	0.0065	0.00000	0.00000	0.00000
77	-8.8654	-14.1375	-0.0000	-0.0568	0.00000	0.00000	0.00000
78	-9.8029	-14.1375	-0.0000	-0.0295	0.00000	0.00000	0.00000
79	-10.7404	-14.1375	-0.0000	-0.0104	0.00000	0.00000	0.00000
80	-11.6779	-14.1375	-0.0000	0.0065	0.00000	0.00000	0.00000
FLAP CONTROL POINTS							
81	-5.0008	-0.3625	0.2017	-0.1736	0.00000	0.00000	0.00000
82	-6.0560	-0.3625	0.5617	-0.0226	0.00000	0.00000	0.00000
83	-7.1113	-0.3625	0.9217	-0.0226	0.00000	0.00000	0.00000
84	-8.1666	-0.3625	1.2817	0.1285	0.00000	0.00000	0.00000
85	-9.2219	-0.3625	1.6417	0.1285	0.00000	0.00000	0.00000
86	-5.4193	-1.0875	0.2017	-0.1736	0.00000	0.00000	0.00000
87	-6.4746	-1.0875	0.5617	-0.0226	0.00000	0.00000	0.00000
88	-7.5299	-1.0875	0.9217	-0.0226	0.00000	0.00000	0.00000
89	-8.5852	-1.0875	1.2817	0.1285	0.00000	0.00000	0.00000
90	-9.6405	-1.0875	1.6417	0.1285	0.00000	0.00000	0.00000
91	-5.8379	-1.8125	0.2017	-0.1736	0.00000	0.00000	0.00000
92	-6.8932	-1.8125	0.5617	-0.0226	0.00000	0.00000	0.00000
93	-7.9485	-1.8125	0.9217	-0.0226	0.00000	0.00000	0.00000
94	-9.0038	-1.8125	1.2817	0.1285	0.00000	0.00000	0.00000
95	-10.0590	-1.8125	1.6417	0.1285	0.00000	0.00000	0.00000
96	-6.2565	-2.5375	0.2017	-0.1736	0.00000	0.00000	0.00000
97	-7.3118	-2.5375	0.5617	-0.0226	0.00000	0.00000	0.00000
98	-8.3671	-2.5375	0.9217	-0.0226	0.00000	0.00000	0.00000
99	-9.4223	-2.5375	1.2817	0.1285	0.00000	0.00000	0.00000
100	-10.4776	-2.5375	1.6417	0.1285	0.00000	0.00000	0.00000
101	-6.6751	-3.2625	0.2017	-0.1736	0.00000	0.00000	0.00000
102	-7.7304	-3.2625	0.5617	-0.0226	0.00000	0.00000	0.00000
103	-8.7856	-3.2625	0.9217	-0.0226	0.00000	0.00000	0.00000
104	-9.8409	-3.2625	1.2817	0.1285	0.00000	0.00000	0.00000
105	-10.8962	-3.2625	1.6417	0.1285	0.00000	0.00000	0.00000
106	-7.0936	-3.9875	0.2017	-0.1736	0.00000	0.00000	0.00000
107	-8.1489	-3.9875	0.5617	-0.0226	0.00000	0.00000	0.00000
108	-9.2042	-3.9875	0.9217	-0.0226	0.00000	0.00000	0.00000
109	-10.2595	-3.9875	1.2817	0.1285	0.00000	0.00000	0.00000
110	-11.3148	-3.9875	1.6417	0.1285	0.00000	0.00000	0.00000
111	-7.5122	-4.7125	0.2017	-0.1736	0.00000	0.00000	0.00000
112	-8.5675	-4.7125	0.5617	-0.0226	0.00000	0.00000	0.00000
113	-9.6228	-4.7125	0.9217	-0.0226	0.00000	0.00000	0.00000
114	-10.6781	-4.7125	1.2817	0.1285	0.00000	0.00000	0.00000
115	-11.7334	-4.7125	1.6417	0.1285	0.00000	0.00000	0.00000
116	-7.9308	-5.4375	0.2017	-0.1736	0.00000	0.00000	0.00000
117	-8.9861	-5.4375	0.5617	-0.0226	0.00000	0.00000	0.00000

Figure 23(a).- Continued

118	-10.0414	-5.4375	0.9217	-0.0226	0.00000	0.00000	0.00000
119	-11.0967	-5.4375	1.2817	0.1285	0.00000	0.00000	0.00000
120	-12.1519	-5.4375	1.6417	0.1285	0.00000	0.00000	0.00000
121	-8.3494	-6.1625	0.2017	-0.1736	0.00000	0.00000	0.00000
122	-9.4047	-6.1625	0.5617	-0.0226	0.00000	0.00000	0.00000
123	-10.4600	-6.1625	0.9217	-0.0226	0.00000	0.00000	0.00000
124	-11.5152	-6.1625	1.2817	0.1285	0.00000	0.00000	0.00000
125	-12.5705	-6.1625	1.6417	0.1285	0.00000	0.00000	0.00000
126	-8.7680	-6.8875	0.2017	-0.1736	0.00000	0.00000	0.00000
127	-9.8232	-6.8875	0.5617	-0.0226	0.00000	0.00000	0.00000
128	-10.8785	-6.8875	0.9217	-0.0226	0.00000	0.00000	0.00000
129	-11.9338	-6.8875	1.2817	0.1285	0.00000	0.00000	0.00000
130	-12.9891	-6.8875	1.6417	0.1285	0.00000	0.00000	0.00000
131	-9.1865	-7.6125	0.2017	-0.1736	0.00000	0.00000	0.00000
132	-10.2418	-7.6125	0.5617	-0.0226	0.00000	0.00000	0.00000
133	-11.2971	-7.6125	0.9217	-0.0226	0.00000	0.00000	0.00000
134	-12.3524	-7.6125	1.2817	0.1285	0.00000	0.00000	0.00000
135	-13.4077	-7.6125	1.6417	0.1285	0.00000	0.00000	0.00000
136	-9.6051	-8.3375	0.2017	-0.1736	0.00000	0.00000	0.00000
137	-10.6604	-8.3375	0.5617	-0.0226	0.00000	0.00000	0.00000
138	-11.7157	-8.3375	0.9217	-0.0226	0.00000	0.00000	0.00000
139	-12.7710	-8.3375	1.2817	0.1285	0.00000	0.00000	0.00000
140	-13.8263	-8.3375	1.6417	0.1285	0.00000	0.00000	0.00000
141	-10.0237	-9.0625	0.2017	-0.1736	0.00000	0.00000	0.00000
142	-11.0790	-9.0625	0.5617	-0.0226	0.00000	0.00000	0.00000
143	-12.1343	-9.0625	0.9217	-0.0226	0.00000	0.00000	0.00000
144	-13.1896	-9.0625	1.2817	0.1285	0.00000	0.00000	0.00000
145	-14.2448	-9.0625	1.6417	0.1285	0.00000	0.00000	0.00000
146	-10.4423	-9.7875	0.2017	-0.1736	0.00000	0.00000	0.00000
147	-11.4976	-9.7875	0.5617	-0.0226	0.00000	0.00000	0.00000
148	-12.5528	-9.7875	0.9217	-0.0226	0.00000	0.00000	0.00000
149	-13.6081	-9.7875	1.2817	0.1285	0.00000	0.00000	0.00000
150	-14.6634	-9.7875	1.6417	0.1285	0.00000	0.00000	0.00000
151	-10.8609	-10.5125	0.2017	-0.1736	0.00000	0.00000	0.00000
152	-11.9161	-10.5125	0.5617	-0.0226	0.00000	0.00000	0.00000
153	-12.9714	-10.5125	0.9217	-0.0226	0.00000	0.00000	0.00000
154	-14.0267	-10.5125	1.2817	0.1285	0.00000	0.00000	0.00000
155	-15.0820	-10.5125	1.6417	0.1285	0.00000	0.00000	0.00000
156	-11.2794	-11.2375	0.2017	-0.1736	0.00000	0.00000	0.00000
157	-12.3347	-11.2375	0.5617	-0.0226	0.00000	0.00000	0.00000
158	-13.3900	-11.2375	0.9217	-0.0226	0.00000	0.00000	0.00000
159	-14.4453	-11.2375	1.2817	0.1285	0.00000	0.00000	0.00000
160	-15.5006	-11.2375	1.6417	0.1285	0.00000	0.00000	0.00000
161	-11.6980	-11.9625	0.2017	-0.1736	0.00000	0.00000	0.00000
162	-12.7533	-11.9625	0.5617	-0.0226	0.00000	0.00000	0.00000
163	-13.8086	-11.9625	0.9217	-0.0226	0.00000	0.00000	0.00000
164	-14.8639	-11.9625	1.2817	0.1285	0.00000	0.00000	0.00000
165	-15.9191	-11.9625	1.6417	0.1285	0.00000	0.00000	0.00000
166	-12.1166	-12.6875	0.2017	-0.1736	0.00000	0.00000	0.00000
167	-13.1719	-12.6875	0.5617	-0.0226	0.00000	0.00000	0.00000
168	-14.2272	-12.6875	0.9217	-0.0226	0.00000	0.00000	0.00000
169	-15.2824	-12.6875	1.2817	0.1285	0.00000	0.00000	0.00000
170	-16.3377	-12.6875	1.6417	0.1285	0.00000	0.00000	0.00000
171	-12.5352	-13.4125	0.2017	-0.1736	0.00000	0.00000	0.00000
172	-13.5905	-13.4125	0.5617	-0.0226	0.00000	0.00000	0.00000
173	-14.6457	-13.4125	0.9217	-0.0226	0.00000	0.00000	0.00000
174	-15.7010	-13.4125	1.2817	0.1285	0.00000	0.00000	0.00000
175	-16.7563	-13.4125	1.6417	0.1285	0.00000	0.00000	0.00000
176	-12.9537	-14.1375	0.2017	-0.1736	0.00000	0.00000	0.00000
177	-14.0090	-14.1375	0.5617	-0.0226	0.00000	0.00000	0.00000
178	-15.0643	-14.1375	0.9217	-0.0226	0.00000	0.00000	0.00000
179	-16.1196	-14.1375	1.2817	0.1285	0.00000	0.00000	0.00000
180	-17.1749	-14.1375	1.6417	0.1285	0.00000	0.00000	0.00000

Figure 23(a).- Continued.

HORSESHOE VORTEX CHARACTERISTICS

J WING	BOUNDLEG MIDPOINT COORDINATES X VORTICES	Y	Z	SWEEP,DEG.	SEMIWIDTH	VORTEX STRENGTHS,GAMMA/V ALPHAD= 0.0000,DELD= 21.5000
1	-0.4437	-0.3625	-0.0000	30.0000	0.3625	0.3633
2	-1.3812	-0.3625	-0.0000	30.0000	0.3625	0.3524
3	-2.3187	-0.3625	-0.0000	30.0000	0.3625	0.3746
4	-3.2562	-0.3625	-0.0000	30.0000	0.3625	0.3911
5	-0.8622	-1.0875	-0.0000	30.0000	0.3625	0.4342
6	-1.7997	-1.0875	-0.0000	30.0000	0.3625	0.3779
7	-2.7372	-1.0875	-0.0000	30.0000	0.3625	0.3929
8	-3.6747	-1.0875	-0.0000	30.0000	0.3625	0.4120
9	-1.2808	-1.8125	-0.0000	30.0000	0.3625	0.4930
10	-2.2183	-1.8125	-0.0000	30.0000	0.3625	0.4043
11	-3.1558	-1.8125	-0.0000	30.0000	0.3625	0.4125
12	-4.0933	-1.8125	-0.0000	30.0000	0.3625	0.4290
13	-1.6994	-2.5375	-0.0000	30.0000	0.3625	0.5429
14	-2.6369	-2.5375	-0.0000	30.0000	0.3625	0.4276
15	-3.5744	-2.5375	-0.0000	30.0000	0.3625	0.4289
16	-4.5119	-2.5375	-0.0000	30.0000	0.3625	0.4405
17	-2.1180	-3.2625	-0.0000	30.0000	0.3625	0.5851
18	-3.0555	-3.2625	-0.0000	30.0000	0.3625	0.4471
19	-3.9930	-3.2625	-0.0000	30.0000	0.3625	0.4415
20	-4.9305	-3.2625	-0.0000	30.0000	0.3625	0.4480
21	-2.5366	-3.9875	-0.0000	30.0000	0.3625	0.6205
22	-3.4741	-3.9875	-0.0000	30.0000	0.3625	0.4626
23	-4.4116	-3.9875	-0.0000	30.0000	0.3625	0.4506
24	-5.3491	-3.9875	-0.0000	30.0000	0.3625	0.4526
25	-2.9551	-4.7125	-0.0000	30.0000	0.3625	0.6494
26	-3.8926	-4.7125	-0.0000	30.0000	0.3625	0.4745
27	-4.8301	-4.7125	-0.0000	30.0000	0.3625	0.4568
28	-5.7676	-4.7125	-0.0000	30.0000	0.3625	0.4549
29	-3.3737	-5.4375	-0.0000	30.0000	0.3625	0.6723
30	-4.3112	-5.4375	-0.0000	30.0000	0.3625	0.4831
31	-5.2487	-5.4375	-0.0000	30.0000	0.3625	0.4604
32	-6.1862	-5.4375	-0.0000	30.0000	0.3625	0.4552
33	-3.7923	-6.1625	-0.0000	30.0000	0.3625	0.6896
34	-4.7298	-6.1625	-0.0000	30.0000	0.3625	0.4885
35	-5.6673	-6.1625	-0.0000	30.0000	0.3625	0.4616
36	-6.6048	-6.1625	-0.0000	30.0000	0.3625	0.4537
37	-4.2109	-6.8875	-0.0000	30.0000	0.3625	0.7014
38	-5.1484	-6.8875	-0.0000	30.0000	0.3625	0.4911
39	-6.0859	-6.8875	-0.0000	30.0000	0.3625	0.4606
40	-7.0234	-6.8875	-0.0000	30.0000	0.3625	0.4504
41	-4.6295	-7.6125	-0.0000	30.0000	0.3625	0.7079
42	-5.5670	-7.6125	-0.0000	30.0000	0.3625	0.4906
43	-6.5045	-7.6125	-0.0000	30.0000	0.3625	0.4572
44	-7.4420	-7.6125	-0.0000	30.0000	0.3625	0.4452
45	-5.0480	-8.3375	-0.0000	30.0000	0.3625	0.7090
46	-5.9855	-8.3375	-0.0000	30.0000	0.3625	0.4871
47	-6.9230	-8.3375	-0.0000	30.0000	0.3625	0.4512
48	-7.8605	-8.3375	-0.0000	30.0000	0.3625	0.4380
49	-5.4666	-9.0625	-0.0000	30.0000	0.3625	0.7045
50	-6.4041	-9.0625	-0.0000	30.0000	0.3625	0.4802
51	-7.3416	-9.0625	-0.0000	30.0000	0.3625	0.4424
52	-8.2791	-9.0625	-0.0000	30.0000	0.3625	0.4282
53	-5.8852	-9.7875	-0.0000	30.0000	0.3625	0.6940
54	-6.8227	-9.7875	-0.0000	30.0000	0.3625	0.4694
55	-7.7602	-9.7875	-0.0000	30.0000	0.3625	0.4301
56	-8.6977	-9.7875	-0.0000	30.0000	0.3625	0.4152
57	-6.3038	-10.5125	-0.0000	30.0000	0.3625	0.6765
58	-7.2413	-10.5125	-0.0000	30.0000	0.3625	0.4540
59	-8.1788	-10.5125	-0.0000	30.0000	0.3625	0.4133
60	-9.1163	-10.5125	-0.0000	30.0000	0.3625	0.3982

Figure 23(a).- Continued

61	-6.7223	-11.2375	-0.0000	30.0000	0.3625	0.6508
62	-7.6596	-11.2375	-0.0000	30.0000	0.3625	0.4325
63	-8.5973	-11.2375	-0.0000	30.0000	0.3625	0.3908
64	-9.5348	-11.2375	-0.0000	30.0000	0.3625	0.3759
65	-7.1409	-11.9625	-0.0000	30.0000	0.3625	0.6145
66	-8.0784	-11.9625	-0.0000	30.0000	0.3625	0.4027
67	-9.0159	-11.9625	-0.0000	30.0000	0.3625	0.3602
68	-9.9534	-11.9625	-0.0000	30.0000	0.3625	0.3464
69	-7.5595	-12.6875	-0.0000	30.0000	0.3625	0.5635
70	-8.4970	-12.6875	-0.0000	30.0000	0.3625	0.3606
71	-9.4345	-12.6875	-0.0000	30.0000	0.3625	0.3179
72	-10.3720	-12.6875	-0.0000	30.0000	0.3625	0.3067
73	-7.9781	-13.4125	-0.0000	30.0000	0.3625	0.4885
74	-8.9156	-13.4125	-0.0000	30.0000	0.3625	0.2977
75	-9.8531	-13.4125	-0.0000	30.0000	0.3625	0.2585
76	-10.7906	-13.4125	-0.0000	30.0000	0.3625	0.2523
77	-8.3967	-14.1375	-0.0000	30.0000	0.3625	0.3610
78	-9.3342	-14.1375	-0.0000	30.0000	0.3625	0.1968
79	-10.2717	-14.1375	-0.0000	30.0000	0.3625	0.1719
80	-11.2092	-14.1375	-0.0000	30.0000	0.3625	0.1722

FLAP VORTICES

81	-4.4731	-0.3625	0.0217	28.2437	0.3687	0.9474
82	-5.5284	-0.3625	0.3817	28.2437	0.3687	0.6556
83	-6.5837	-0.3625	0.7417	28.2437	0.3687	0.6436
84	-7.6390	-0.3625	1.1017	28.2437	0.3687	0.6943
85	-8.6943	-0.3625	1.4617	28.2437	0.3687	0.3728
86	-4.8917	-1.0875	0.0217	28.2437	0.3687	0.9989
87	-5.9470	-1.0875	0.3817	28.2437	0.3687	0.6871
88	-7.0023	-1.0875	0.7417	28.2437	0.3687	0.6492
89	-8.0575	-1.0875	1.1017	28.2437	0.3687	0.6752
90	-9.1128	-1.0875	1.4617	28.2437	0.3687	0.3411
91	-5.3103	-1.8125	0.0217	28.2437	0.3687	1.0225
92	-6.3656	-1.8125	0.3817	28.2437	0.3687	0.9021
93	-7.4208	-1.8125	0.7417	28.2437	0.3687	0.6513
94	-8.4761	-1.8125	1.1017	28.2437	0.3687	0.6661
95	-9.5314	-1.8125	1.4617	28.2437	0.3687	0.3286
96	-5.7286	-2.5375	0.0217	28.2437	0.3687	1.0334
97	-6.7841	-2.5375	0.3817	28.2437	0.3687	0.9070
98	-7.8394	-2.5375	0.7417	28.2437	0.3687	0.6497
99	-8.8947	-2.5375	1.1017	28.2437	0.3687	0.6008
100	-9.9500	-2.5375	1.4617	28.2437	0.3687	0.3229
101	-5.1474	-3.2625	0.0217	28.2437	0.3687	1.0373
102	-7.2027	-3.2625	0.3817	28.2437	0.3687	0.9068
103	-8.2580	-3.2625	0.7417	28.2437	0.3687	0.6463
104	-9.3133	-3.2625	1.1017	28.2437	0.3687	0.6565
105	-10.3686	-3.2625	1.4617	28.2437	0.3687	0.3491
106	-8.5660	-3.9875	0.0217	28.2437	0.3687	1.0368
107	-7.6215	-3.9875	0.3817	28.2437	0.3687	0.9037
108	-8.6768	-3.9875	0.7417	28.2437	0.3687	0.6418
109	-9.7319	-3.9875	1.1017	28.2437	0.3687	0.6525
110	-10.7871	-3.9875	1.4617	28.2437	0.3687	0.3157
111	-6.9846	-4.7125	0.0217	28.2437	0.3687	1.0334
112	-8.0399	-4.7125	0.3817	28.2437	0.3687	0.8988
113	-9.0951	-4.7125	0.7417	28.2437	0.3687	0.6395
114	-10.1504	-4.7125	1.1017	28.2437	0.3687	0.6478
115	-11.2057	-4.7125	1.4617	28.2437	0.3687	0.3122
116	-7.4032	-5.4375	0.0217	28.2437	0.3687	1.0276
117	-8.4584	-5.4375	0.3817	28.2437	0.3687	0.8926
118	-9.5137	-5.4375	0.7417	28.2437	0.3687	0.6303
119	-10.5690	-5.4375	1.1017	28.2437	0.3687	0.6427

Figure 23(a).- Continued.

120	-11.6243	-5.4375	1.4617	28.2437	0.3687	0.3084
121	-7.8217	-6.1625	0.0217	28.2437	0.3687	1.0195
122	-8.8770	-6.1625	0.3817	28.2437	0.3687	0.8849
123	-9.9323	-6.1625	0.7417	28.2437	0.3687	0.6233
124	-10.9876	-6.1625	1.1017	28.2437	0.3687	0.6370
125	-12.0429	-6.1625	1.4617	28.2437	0.3687	0.3042
126	-8.2403	-6.8875	0.0217	28.2437	0.3687	1.0091
127	-9.2956	-6.8875	0.3817	28.2437	0.3687	0.8758
128	-10.3509	-6.8875	0.7417	28.2437	0.3687	0.6151
129	-11.4062	-6.8875	1.1017	28.2437	0.3687	0.6303
130	-12.4615	-6.8875	1.4617	28.2437	0.3687	0.2994
131	-8.6589	-7.6125	0.0217	28.2437	0.3687	0.9961
132	-9.7142	-7.6125	0.3817	28.2437	0.3687	0.8649
133	-10.7695	-7.6125	0.7417	28.2437	0.3687	0.6055
134	-11.8248	-7.6125	1.1017	28.2437	0.3687	0.6225
135	-12.8800	-7.6125	1.4617	28.2437	0.3687	0.2939
136	-9.0775	-8.3375	0.0217	28.2437	0.3687	0.9798
137	-10.1328	-8.3375	0.3817	28.2437	0.3687	0.8517
138	-11.1880	-8.3375	0.7417	28.2437	0.3687	0.5941
139	-12.2433	-8.3375	1.1017	28.2437	0.3687	0.6134
140	-13.2986	-8.3375	1.4617	28.2437	0.3687	0.2875
141	-9.4961	-9.0625	0.0217	28.2437	0.3687	0.9596
142	-10.5513	-9.0625	0.3817	28.2437	0.3687	0.8359
143	-11.6066	-9.0625	0.7417	28.2437	0.3687	0.5805
144	-12.6619	-9.0625	1.1017	28.2437	0.3687	0.6026
145	-13.7172	-9.0625	1.4617	28.2437	0.3687	0.2799
146	-9.9146	-9.7875	0.0217	28.2437	0.3687	0.9342
147	-10.9699	-9.7875	0.3817	28.2437	0.3687	0.8166
148	-12.0252	-9.7875	0.7417	28.2437	0.3687	0.5642
149	-13.0805	-9.7875	1.1017	28.2437	0.3687	0.5894
150	-14.1358	-9.7875	1.4617	28.2437	0.3687	0.2707
151	-10.3332	-10.5125	0.0217	28.2437	0.3687	0.9023
152	-11.3885	-10.5125	0.3817	28.2437	0.3687	0.7929
153	-12.4438	-10.5125	0.7417	28.2437	0.3687	0.5442
154	-13.4991	-10.5125	1.1017	28.2437	0.3687	0.5732
155	-14.5544	-10.5125	1.4617	28.2437	0.3687	0.2594
156	-10.7518	-11.2375	0.0217	28.2437	0.3687	0.8617
157	-11.8071	-11.2375	0.3817	28.2437	0.3687	0.7634
158	-12.8624	-11.2375	0.7417	28.2437	0.3687	0.5193
159	-13.9176	-11.2375	1.1017	28.2437	0.3687	0.5525
160	-14.9729	-11.2375	1.4617	28.2437	0.3687	0.2448
161	-11.1704	-11.9625	0.0217	28.2437	0.3687	0.8090
162	-12.2257	-11.9625	0.3817	28.2437	0.3687	0.7262
163	-13.2809	-11.9625	0.7417	28.2437	0.3687	0.4871
164	-14.3362	-11.9625	1.1017	28.2437	0.3687	0.5248
165	-15.3915	-11.9625	1.4617	28.2437	0.3687	0.2250
166	-11.5889	-12.6875	0.0217	28.2437	0.3687	0.7391
167	-12.6442	-12.6875	0.3817	28.2437	0.3687	0.6772
168	-13.6995	-12.6875	0.7417	28.2437	0.3687	0.4428
169	-14.7548	-12.6875	1.1017	28.2437	0.3687	0.4845
170	-15.8101	-12.6875	1.4617	28.2437	0.3687	0.1962
171	-12.0075	-13.4125	0.0217	28.2437	0.3687	0.6410
172	-13.0628	-13.4125	0.3817	28.2437	0.3687	0.6079
173	-14.1181	-13.4125	0.7417	28.2437	0.3687	0.3746
174	-15.1734	-13.4125	1.1017	28.2437	0.3687	0.4196
175	-16.2287	-13.4125	1.4617	28.2437	0.3687	0.1517
176	-12.4261	-14.1375	0.0217	28.2437	0.3687	0.4821
177	-13.4814	-14.1375	0.3817	28.2437	0.3687	0.4849
178	-14.5367	-14.1375	0.7417	28.2437	0.3687	0.2492
179	-15.5920	-14.1375	1.1017	28.2437	0.3687	0.2987
180	-16.6472	-14.1375	1.4617	28.2437	0.3687	0.0829

Figure 23(a).- Continued

AERODYNAMIC LOADING RESULTS FOR ALPHA = 0.00000 DEG.

WING LIFT COEFFICIENT	FLAP LIFT COEFFICIENT
0.9808	1.6580

TOTAL LIFT COEFFICIENT,CL	PITCHING MOMENT COEFFICIENT,CM
2.6388	-1.1817

REFERENCE QUANTITIES

WING SPAN,B	WING PLANFORM AREA,SREF	WING AVE.CHORD,CAVE
29.0000	108.7500	3.7500

SPANWISE LOAD DISTRIBUTION

STATION	Y/(B/2)	LOCAL CHORD,C	CL*C/CL*CAVE	CL*C/(2*B)
WING				
1	0.0250	3.7500	0.6091	0.0513
2	0.0750	3.7500	0.8848	0.0561
3	0.1250	3.7500	0.9530	0.0604
4	0.1750	3.7500	1.0097	0.0640
5	0.2250	3.7500	1.0556	0.0669
6	0.2750	3.7500	1.0918	0.0692
7	0.3250	3.7500	1.1193	0.0710
8	0.3750	3.7500	1.1390	0.0722
9	0.4250	3.7500	1.1515	0.0730
10	0.4750	3.7500	1.1571	0.0734
11	0.5250	3.7500	1.1557	0.0733
12	0.5750	3.7500	1.1470	0.0727
13	0.6250	3.7500	1.1305	0.0717
14	0.6750	3.7500	1.1045	0.0700
15	0.7250	3.7500	1.0678	0.0677
16	0.7750	3.7500	1.0170	0.0645
17	0.8250	3.7500	0.9476	0.0601
18	0.8750	3.7500	0.8513	0.0540
19	0.9250	3.7500	0.7129	0.0452
20	0.9750	3.7500	0.4951	0.0314
FLAP				
1	0.0254	5.5750	1.0905	0.1169
2	0.0763	5.5750	1.1073	0.1187
3	0.1272	5.5750	1.1186	0.1199
4	0.1780	5.5750	1.1227	0.1204
5	0.2289	5.5750	1.1223	0.1203
6	0.2797	5.5750	1.1186	0.1199
7	0.3306	5.5750	1.1126	0.1193
8	0.3815	5.5750	1.1046	0.1184
9	0.4323	5.5750	1.0947	0.1173
10	0.4832	5.5750	1.0827	0.1161
11	0.5340	5.5750	1.0682	0.1145
12	0.5849	5.5750	1.0507	0.1126
13	0.6358	5.5750	1.0295	0.1104
14	0.6866	5.5750	1.0035	0.1076
15	0.7375	5.5750	0.9713	0.1041
16	0.7883	5.5750	0.9303	0.0997
17	0.8392	5.5750	0.8767	0.0940
18	0.8901	5.5750	0.8029	0.0861
19	0.9409	5.5750	0.6922	0.0742
20	0.9918	5.5750	0.5001	0.0536

CM,WING	CM,FLAP	CD,WING	CD,FLAP	CD	CD/CL*CL
0.26375	-1.44541	-0.07666	0.35821	0.28155	0.04043

Figure 23(a).- Continued

VELOCITIES INDUCED AT SPECIFIED POINTS IN THE VICINITY OF THE WING

N	X	Y	Z	U/V	V/V	W/V
1	-1.7000	-7.2500	2.0700	0.05404	-0.02610	-0.07911
2	-3.7000	-7.2500	2.0700	0.11256	-0.05904	-0.08841
3	-5.7000	-7.2500	2.0700	0.17087	-0.09431	-0.04045
4	-7.7000	-7.2500	2.0700	0.20652	-0.12167	0.01573
5	-9.7000	-7.2500	2.0700	0.23905	-0.15162	0.10427
6	-11.7000	-7.2500	2.0700	0.23202	-0.16010	0.23445
7	-13.7000	-7.2500	2.0700	0.10073	-0.10177	0.32020
8	-15.7000	-7.2500	2.0700	0.05532	-0.00027	0.26956

Figure 23(a).- Concluded.

SWEPT WING, FLAP I (NASA TMX 62079) FLAP ANGLE = 10/20/30,ALPHA= 0, C(MU)=0.9 .

GEOMETRY DATA

	WING	FLAP
LE SWEEP,DEG.	30.0000	30.0000
TE SWEEP,DEG.	30.0000	30.0000
DIHEDRAL,DEG.	0.0000	
CHORD AT WING ROOT	3.7500	5.5750
SEMISPAN	14.5000	14.5000
CHORDWISE VORTICES	4	5
SPANWISE VORTICES	20	20

COORDS. OF ROOTCHORD NOSE OF FLAP EXTENDED TO PLANE OF SYMMETRY

X	Z
-4.0000	-0.0683

UNDEFLECTED FLAP INBOARD SPAN	0.0000
UNDEFLECTED FLAP OUTBOARD SPAN	14.5000

	X	Y	Z
PITCHING MOMENT CENTER	-6.5600	0.0000	0.0000

FLAP ANGLE,DELD,DEG.	21.5000
CALC. STREAMWISE FLAP ANGLE,DLXD,DEG.	18.8364

FLOW CONDITIONS FOR CASE 1

ANGLE OF ATTACK,ALPHA ,DEG. 0.0000

SOURCE OF EXTERNALLY INDUCED VELOCITIES, ALPHA=0 DEGREES , C(MU)=0.9

Figure 23(b).- Output from wing-flap program, with power.

	CONTROL POINT COORDINATES AND SLOPES				EXTERNALLY INDUCED VELOCITIES		
J	X	Y	Z	MEAN SURFACE SLOPE	U/V	V/V	W/V
WING CONTROL POINTS							
1	-0.9124	-0.3625	-0.0000	-0.0568	-0.00204	-0.02287	0.00690
2	-1.8499	-0.3625	-0.0000	-0.0295	-0.00016	-0.02206	0.00664
3	-2.7874	-0.3625	-0.0000	-0.0104	0.00121	-0.02087	0.00625
4	-3.7249	-0.3625	-0.0000	0.0065	0.00209	-0.01954	0.00581
5	-1.3310	-1.0875	-0.0000	-0.0568	-0.00034	-0.02617	0.00882
6	-2.2685	-1.0875	-0.0000	-0.0295	0.00165	-0.02457	0.00826
7	-3.2060	-1.0875	-0.0000	-0.0104	0.00287	-0.02272	0.00759
8	-4.1435	-1.0875	-0.0000	0.0065	0.00349	-0.02096	0.00692
9	-1.7496	-1.8125	-0.0000	-0.0568	0.00223	-0.02953	0.01128
10	-2.6871	-1.8125	-0.0000	-0.0295	0.00402	-0.02687	0.01023
11	-3.6246	-1.8125	-0.0000	-0.0104	0.00480	-0.02432	0.00917
12	-4.5621	-1.8125	-0.0000	0.0065	0.00497	-0.02219	0.00823
13	-2.1681	-2.5375	-0.0000	-0.0568	0.00574	-0.03245	0.01430
14	-3.1056	-2.5375	-0.0000	-0.0295	0.00680	-0.02863	0.01253
15	-4.0431	-2.5375	-0.0000	-0.0104	0.00680	-0.02553	0.01101
16	-4.9806	-2.5375	-0.0000	0.0065	0.00636	-0.02321	0.00977
17	-2.5867	-3.2625	-0.0000	-0.0568	0.00998	-0.03424	0.01777
18	-3.5242	-3.2625	-0.0000	-0.0295	0.00963	-0.02953	0.01513
19	-4.4617	-3.2625	-0.0000	-0.0104	0.00857	-0.02626	0.01314
20	-5.3992	-3.2625	-0.0000	0.0065	0.00745	-0.02410	0.01164
21	-3.0053	-3.9875	-0.0000	-0.0568	0.01416	-0.03421	0.02147
22	-3.9428	-3.9875	-0.0000	-0.0295	0.01191	-0.02943	0.01804
23	-4.8803	-3.9875	-0.0000	-0.0104	0.00972	-0.02661	0.01569
24	-5.8178	-3.9875	-0.0000	0.0065	0.00803	-0.02502	0.01402
25	-3.4239	-4.7125	-0.0000	-0.0568	0.01709	-0.03221	0.02521
26	-4.3614	-4.7125	-0.0000	-0.0295	0.01299	-0.02853	0.02136
27	-5.2989	-4.7125	-0.0000	-0.0104	0.00993	-0.02684	0.01896
28	-6.2364	-4.7125	-0.0000	0.0065	0.00790	-0.02624	0.01736
29	-3.8425	-5.4375	-0.0000	-0.0568	0.01769	-0.02886	0.02905
30	-4.7800	-5.4375	-0.0000	-0.0295	0.01243	-0.02729	0.02559
31	-5.7175	-5.4375	-0.0000	-0.0104	0.00899	-0.02721	0.02369
32	-6.6550	-5.4375	-0.0000	0.0065	0.00694	-0.02788	0.02260
33	-4.2610	-6.1625	-0.0000	-0.0568	0.01568	-0.02522	0.03404
34	-5.1985	-6.1625	-0.0000	-0.0295	0.01020	-0.02582	0.03204
35	-6.1360	-6.1625	-0.0000	-0.0104	0.00692	-0.02719	0.03146
36	-7.0735	-6.1625	-0.0000	0.0065	0.00517	-0.02895	0.03155
37	-4.6796	-6.8875	-0.0000	-0.0568	0.01195	-0.01994	0.04232
38	-5.6171	-6.8875	-0.0000	-0.0295	0.00722	-0.02139	0.04234
39	-6.5546	-6.8875	-0.0000	-0.0104	0.00428	-0.02308	0.04347
40	-7.4921	-6.8875	-0.0000	0.0065	0.00305	-0.02501	0.04513
41	-5.0982	-7.6125	-0.0000	-0.0568	0.00859	-0.00759	0.05124
42	-6.0357	-7.6125	-0.0000	-0.0295	0.00459	-0.00849	0.05234
43	-6.9732	-7.6125	-0.0000	-0.0104	0.00246	-0.00938	0.05436
44	-7.9107	-7.6125	-0.0000	0.0065	0.00148	-0.01052	0.05688
45	-5.5168	-8.3375	-0.0000	-0.0568	0.00620	0.00972	0.05135
46	-6.4543	-8.3375	-0.0000	-0.0295	0.00326	0.00941	0.05238
47	-7.3918	-8.3375	-0.0000	-0.0104	0.00155	0.00925	0.05420
48	-8.3293	-8.3375	-0.0000	0.0065	0.00093	0.00885	0.05659
49	-5.9354	-9.0625	-0.0000	-0.0568	0.00459	0.02205	0.04268
50	-6.8729	-9.0625	-0.0000	-0.0295	0.00243	0.02189	0.04334
51	-7.8104	-9.0625	-0.0000	-0.0104	0.00116	0.02195	0.04464
52	-8.7479	-9.0625	-0.0000	0.0065	0.00080	0.02181	0.04652
53	-6.3539	-9.7875	-0.0000	-0.0568	0.00336	0.02699	0.03236
54	-7.2914	-9.7875	-0.0000	-0.0295	0.00187	0.02679	0.03276
55	-8.2289	-9.7875	-0.0000	-0.0104	0.00092	0.02679	0.03367
56	-9.1664	-9.7875	-0.0000	0.0065	0.00065	0.02665	0.03508
57	-6.7725	-10.5125	-0.0000	-0.0568	0.00239	0.02746	0.02399

Figure 23(b).- Continued.

58	-7.7100	-10.5125	-0.0000	-0.0295	0.00134	0.02719	0.02428
59	-8.6475	-10.5125	-0.0000	-0.0104	0.00068	0.02712	0.02496
60	-9.5850	-10.5125	-0.0000	0.0065	0.00046	0.02698	0.02599
61	-7.1911	-11.2375	-0.0000	-0.0568	0.00162	0.02602	0.01796
62	-8.1286	-11.2375	-0.0000	-0.0295	0.00092	0.02574	0.01819
63	-9.0661	-11.2375	-0.0000	-0.0104	0.00047	0.02563	0.01871
64	-10.0036	-11.2375	-0.0000	0.0065	0.00031	0.02553	0.01945
65	-7.6097	-11.9625	-0.0000	-0.0568	0.00103	0.02398	0.01371
66	-8.5472	-11.9625	-0.0000	-0.0295	0.00058	0.02373	0.01392
67	-9.4847	-11.9625	-0.0000	-0.0104	0.00031	0.02361	0.01430
68	-10.4222	-11.9625	-0.0000	0.0065	0.00022	0.02353	0.01481
69	-8.0282	-12.6875	-0.0000	-0.0568	0.00060	0.02187	0.01070
70	-8.9657	-12.6875	-0.0000	-0.0295	0.00034	0.02165	0.01086
71	-9.9032	-12.6875	-0.0000	-0.0104	0.00019	0.02154	0.01113
72	-10.8407	-12.6875	-0.0000	0.0065	0.00016	0.02147	0.01147
73	-8.4468	-13.4125	-0.0000	-0.0568	0.00030	0.01989	0.00850
74	-9.3843	-13.4125	-0.0000	-0.0295	0.00016	0.01971	0.00863
75	-10.3218	-13.4125	-0.0000	-0.0104	0.00011	0.01961	0.00882
76	-11.2593	-13.4125	-0.0000	0.0065	0.00013	0.01954	0.00904
77	-8.8654	-14.1375	-0.0000	-0.0568	0.00008	0.01811	0.00687
78	-9.8029	-14.1375	-0.0000	-0.0295	0.00004	0.01796	0.00696
79	-10.7404	-14.1375	-0.0000	-0.0104	0.00005	0.01786	0.00708
80	-11.6779	-14.1375	-0.0000	0.0065	0.00012	0.01778	0.00722
FLAP CONTROL POINTS							
81	-5.0008	-0.3625	0.2017	-0.1736	0.00281	-0.01811	0.00480
82	-6.0560	-0.3625	0.5617	-0.0226	0.00315	-0.01723	0.00365
83	-7.1113	-0.3625	0.9217	-0.0226	0.00330	-0.01636	0.00259
84	-8.1666	-0.3625	1.2817	0.1285	0.00336	-0.01549	0.00163
85	-9.2219	-0.3625	1.6417	0.1285	0.00333	-0.01460	0.00078
86	-5.4193	-1.0875	0.2017	-0.1736	0.00388	-0.01926	0.00564
87	-6.4746	-1.0875	0.5617	-0.0226	0.00403	-0.01832	0.00425
88	-7.5299	-1.0875	0.9217	-0.0226	0.00407	-0.01742	0.00299
89	-8.5852	-1.0875	1.2817	0.1285	0.00405	-0.01649	0.00184
90	-9.6405	-1.0875	1.6417	0.1285	0.00397	-0.01548	0.00084
91	-5.8379	-1.8125	0.2017	-0.1736	0.00492	-0.02038	0.00663
92	-6.8932	-1.8125	0.5617	-0.0226	0.00488	-0.01951	0.00498
93	-7.9485	-1.8125	0.9217	-0.0226	0.00484	-0.01865	0.00346
94	-9.0038	-1.8125	1.2817	0.1285	0.00481	-0.01765	0.00206
95	-10.0590	-1.8125	1.6417	0.1285	0.00469	-0.01645	0.00085
96	-6.2565	-2.5375	0.2017	-0.1736	0.00584	-0.02155	0.00785
97	-7.3118	-2.5375	0.5617	-0.0226	0.00567	-0.02093	0.00588
98	-8.3671	-2.5375	0.9217	-0.0226	0.00565	-0.02018	0.00401
99	-9.4223	-2.5375	1.2817	0.1285	0.00570	-0.01904	0.00226
100	-10.4776	-2.5375	1.6417	0.1285	0.00555	-0.01749	0.00077
101	-6.6751	-3.2625	0.2017	-0.1736	0.00653	-0.02293	0.00942
102	-7.7304	-3.2625	0.5617	-0.0226	0.00636	-0.02279	0.00706
103	-8.7856	-3.2625	0.9217	-0.0226	0.00657	-0.02222	0.00466
104	-9.8409	-3.2625	1.2817	0.1285	0.00686	-0.02076	0.00235
105	-10.8962	-3.2625	1.6417	0.1285	0.00661	-0.01850	0.00045
106	-7.0936	-3.9875	0.2017	-0.1736	0.00689	-0.02480	0.01158
107	-8.1489	-3.9875	0.5617	-0.0226	0.00698	-0.02551	0.00872
108	-9.2042	-3.9875	0.9217	-0.0226	0.00780	-0.02523	0.00547
109	-10.2595	-3.9875	1.2817	0.1285	0.00859	-0.02286	0.00209
110	-11.3148	-3.9875	1.6417	0.1285	0.00783	-0.01923	-0.00043
111	-7.5122	-4.7125	0.2017	-0.1736	0.00685	-0.02756	0.01490
112	-8.5675	-4.7125	0.5617	-0.0226	0.00756	-0.02983	0.01143
113	-9.6228	-4.7125	0.9217	-0.0226	0.00991	-0.03006	0.00659
114	-10.6781	-4.7125	1.2817	0.1285	0.01128	-0.02511	0.00069
115	-11.7334	-4.7125	1.6417	0.1285	0.00866	-0.01945	-0.00274
116	-7.9308	-5.4375	0.2017	-0.1736	0.00628	-0.03152	0.02076
117	-8.9861	-5.4375	0.5617	-0.0226	0.00819	-0.03699	0.01699

Figure 23(b).- Continued.

118	-10.0414	-5.4375	0.9217	-0.0226	0.01445	-0.03852	0.00868
119	-11.0967	-5.4375	1.2817	0.1285	0.01276	-0.02736	-0.00403
120	-12.1519	-5.4375	1.6417	0.1285	0.00803	-0.02036	-0.00872
121	-8.3494	-6.1625	0.2017	-0.1736	0.00504	-0.03552	0.03206
122	-9.4047	-6.1625	0.5617	-0.0226	0.00806	-0.04730	0.03082
123	-10.4600	-6.1625	0.9217	-0.0226	0.02889	-0.04845	0.00865
124	-11.5152	-6.1625	1.2817	0.1285	-1.50771	-0.00280	0.07772
125	-12.5705	-6.1625	1.6417	0.1285	-1.50105	-0.00451	0.08834
126	-8.7680	-6.8875	0.2017	-0.1736	0.00282	-0.03301	0.05091
127	-9.8232	-6.8875	0.5617	-0.0226	0.00713	-0.05166	0.06325
128	-10.8785	-6.8875	0.9217	-0.0226	-1.58238	-0.02323	0.07702
129	-11.9338	-6.8875	1.2817	0.1285	-1.53258	-0.02271	0.08143
130	-12.9891	-6.8875	1.6417	0.1285	-1.47985	-0.02160	0.08638
131	-9.1865	-7.6125	0.2017	-0.1736	0.00196	-0.01503	0.06770
132	-10.2418	-7.6125	0.5617	-0.0226	-0.50867	-0.03051	0.09550
133	-11.2971	-7.6125	0.9217	-0.0226	-1.56507	-0.04142	0.07416
134	-12.3524	-7.6125	1.2817	0.1285	-1.51100	-0.04038	0.07962
135	-13.4077	-7.6125	1.6417	0.1285	-1.45871	-0.03809	0.08454
136	-9.6051	-8.3375	0.2017	-0.1736	0.00215	0.00950	0.06667
137	-10.6604	-8.3375	0.5617	-0.0226	0.01152	0.00575	0.07908
138	-11.7157	-8.3375	0.9217	-0.0226	-1.54339	-0.06042	0.07241
139	-12.7710	-8.3375	1.2817	0.1285	-1.48896	-0.05752	0.07802
140	-13.8263	-8.3375	1.6417	0.1285	-1.43717	-0.05378	0.08267
141	-10.0237	-9.0625	0.2017	-0.1736	0.00208	0.02404	0.05257
142	-11.0790	-9.0625	0.5617	-0.0226	0.00320	0.02735	0.06068
143	-12.1343	-9.0625	0.9217	-0.0226	0.00349	0.03323	0.07110
144	-13.1896	-9.0625	1.2817	0.1285	-1.46025	-0.07486	0.07482
145	-14.2448	-9.0625	1.6417	0.1285	-1.41626	-0.06878	0.08096
146	-10.4423	-9.7875	0.2017	-0.1736	0.00114	0.02873	0.03824
147	-11.4976	-9.7875	0.5617	-0.0226	0.00134	0.03365	0.04188
148	-12.5528	-9.7875	0.9217	-0.0226	0.00086	0.04044	0.04548
149	-13.6081	-9.7875	1.2817	0.1285	0.00004	0.05018	0.04830
150	-14.6634	-9.7875	1.6417	0.1285	0.00040	0.06263	0.04854
151	-10.8609	-10.5125	0.2017	-0.1736	0.00053	0.02874	0.02756
152	-11.9161	-10.5125	0.5617	-0.0226	0.00049	0.03288	0.02864
153	-12.9714	-10.5125	0.9217	-0.0226	0.00031	0.03794	0.02915
154	-14.0267	-10.5125	1.2817	0.1285	0.00004	0.04417	0.02864
155	-15.0820	-10.5125	1.6417	0.1285	-0.00026	0.05159	0.02652
156	-11.2794	-11.2375	0.2017	-0.1736	0.00029	0.02691	0.02013
157	-12.3347	-11.2375	0.5617	-0.0226	0.00023	0.02997	0.02003
158	-13.3900	-11.2375	0.9217	-0.0226	0.00020	0.03345	0.01940
159	-14.4453	-11.2375	1.2817	0.1285	0.00027	0.03738	0.01799
160	-15.5006	-11.2375	1.6417	0.1285	0.00060	0.04165	0.01547
161	-11.6980	-11.9625	0.2017	-0.1736	0.00021	0.02457	0.01500
162	-12.7533	-11.9625	0.5617	-0.0226	0.00021	0.02675	0.01441
163	-13.8086	-11.9625	0.9217	-0.0226	0.00031	0.02911	0.01341
164	-14.8639	-11.9625	1.2817	0.1285	0.00058	0.03160	0.01184
165	-15.9191	-11.9625	1.6417	0.1285	0.00117	0.03404	0.00949
166	-12.1166	-12.6875	0.2017	-0.1736	0.00021	0.02223	0.01141
167	-13.1719	-12.6875	0.5617	-0.0226	0.00028	0.02377	0.01064
168	-14.2272	-12.6875	0.9217	-0.0226	0.00046	0.02536	0.00957
169	-15.2824	-12.6875	1.2817	0.1285	0.00083	0.02691	0.00807
170	-16.3377	-12.6875	1.6417	0.1285	0.00148	0.02822	0.00602
171	-12.5352	-13.4125	0.2017	-0.1736	0.00023	0.02008	0.00883
172	-13.5905	-13.4125	0.5617	-0.0226	0.00035	0.02115	0.00804
173	-14.6457	-13.4125	0.9217	-0.0226	0.00060	0.02221	0.00700
174	-15.7010	-13.4125	1.2817	0.1285	0.00099	0.02313	0.00565
175	-16.7563	-13.4125	1.6417	0.1285	0.00155	0.02375	0.00394
176	-12.9537	-14.1375	0.2017	-0.1736	0.00025	0.01815	0.00695
177	-14.0090	-14.1375	0.5617	-0.0226	0.00041	0.01889	0.00618
178	-15.0643	-14.1375	0.9217	-0.0226	0.00067	0.01957	0.00523
179	-16.1196	-14.1375	1.2817	0.1285	0.00102	0.02008	0.00405
180	-17.1749	-14.1375	1.6417	0.1285	0.00145	0.02031	0.00265

Figure 23(b).- Continued.

HORSESHOE VORTEX CHARACTERISTICS

J	BOUNDLEG MIDPOINT COORDINATES X	Y	Z	SWEEP,DEG.	SEMIWIDTH	VORTEX STRENGTHS,GAMMA/V ALPHAD= 0.0000,DELD= 21.5000
WING	VORTICES					
1	-0.4437	-0.3625	-0.0000	30.0000	0.3625	0.3972
2	-1.3812	-0.3625	-0.0000	30.0000	0.3625	0.3797
3	-2.3187	-0.3625	-0.0000	30.0000	0.3625	0.4027
4	-3.2562	-0.3625	-0.0000	30.0000	0.3625	0.4191
5	-0.8622	-1.0875	-0.0000	30.0000	0.3625	0.4717
6	-1.7997	-1.0875	-0.0000	30.0000	0.3625	0.4068
7	-2.7372	-1.0875	-0.0000	30.0000	0.3625	0.4226
8	-3.6747	-1.0875	-0.0000	30.0000	0.3625	0.4417
9	-1.2808	-1.8125	-0.0000	30.0000	0.3625	0.5320
10	-2.2183	-1.8125	-0.0000	30.0000	0.3625	0.4351
11	-3.1558	-1.8125	-0.0000	30.0000	0.3625	0.4444
12	-4.0933	-1.8125	-0.0000	30.0000	0.3625	0.4612
13	-1.6994	-2.5375	-0.0000	30.0000	0.3625	0.5818
14	-2.6369	-2.5375	-0.0000	30.0000	0.3625	0.4604
15	-3.5744	-2.5375	-0.0000	30.0000	0.3625	0.4635
16	-4.5119	-2.5375	-0.0000	30.0000	0.3625	0.4760
17	-2.1180	-3.2625	-0.0000	30.0000	0.3625	0.6230
18	-3.0555	-3.2625	-0.0000	30.0000	0.3625	0.4819
19	-3.9930	-3.2625	-0.0000	30.0000	0.3625	0.4791
20	-4.9305	-3.2625	-0.0000	30.0000	0.3625	0.4873
21	-2.5366	-3.9875	-0.0000	30.0000	0.3625	0.6565
22	-3.4741	-3.9875	-0.0000	30.0000	0.3625	0.4993
23	-4.4116	-3.9875	-0.0000	30.0000	0.3625	0.4915
24	-5.3491	-3.9875	-0.0000	30.0000	0.3625	0.4964
25	-2.9551	-4.7125	-0.0000	30.0000	0.3625	0.6831
26	-3.8926	-4.7125	-0.0000	30.0000	0.3625	0.5126
27	-4.8301	-4.7125	-0.0000	30.0000	0.3625	0.5010
28	-5.7676	-4.7125	-0.0000	30.0000	0.3625	0.5040
29	-3.3737	-5.4375	-0.0000	30.0000	0.3625	0.7028
30	-4.3112	-5.4375	-0.0000	30.0000	0.3625	0.5216
31	-5.2487	-5.4375	-0.0000	30.0000	0.3625	0.5076
32	-6.1862	-5.4375	-0.0000	30.0000	0.3625	0.5103
33	-3.7923	-6.1625	-0.0000	30.0000	0.3625	0.7147
34	-4.7298	-6.1625	-0.0000	30.0000	0.3625	0.5263
35	-5.6673	-6.1625	-0.0000	30.0000	0.3625	0.5118
36	-6.6048	-6.1625	-0.0000	30.0000	0.3625	0.5158
37	-4.2109	-6.8875	-0.0000	30.0000	0.3625	0.7179
38	-5.1484	-6.8875	-0.0000	30.0000	0.3625	0.5282
39	-6.0859	-6.8875	-0.0000	30.0000	0.3625	0.5146
40	-7.0234	-6.8875	-0.0000	30.0000	0.3625	0.5209
41	-4.6295	-7.6125	-0.0000	30.0000	0.3625	0.7172
42	-5.5670	-7.6125	-0.0000	30.0000	0.3625	0.5303
43	-6.5045	-7.6125	-0.0000	30.0000	0.3625	0.5174
44	-7.4420	-7.6125	-0.0000	30.0000	0.3625	0.5256
45	-5.0480	-8.3375	-0.0000	30.0000	0.3625	0.7234
46	-5.9855	-8.3375	-0.0000	30.0000	0.3625	0.5334
47	-6.9230	-8.3375	-0.0000	30.0000	0.3625	0.5194
48	-7.8605	-8.3375	-0.0000	30.0000	0.3625	0.5277
49	-5.4666	-9.0625	-0.0000	30.0000	0.3625	0.7372
50	-6.4041	-9.0625	-0.0000	30.0000	0.3625	0.5355
51	-7.3416	-9.0625	-0.0000	30.0000	0.3625	0.5176
52	-8.2791	-9.0625	-0.0000	30.0000	0.3625	0.5230
53	-5.8852	-9.7875	-0.0000	30.0000	0.3625	0.7496
54	-6.8227	-9.7875	-0.0000	30.0000	0.3625	0.5330
55	-7.7602	-9.7875	-0.0000	30.0000	0.3625	0.5091
56	-8.6977	-9.7875	-0.0000	30.0000	0.3625	0.5095
57	-6.3038	-10.5125	-0.0000	30.0000	0.3625	0.7528
58	-7.2413	-10.5125	-0.0000	30.0000	0.3625	0.5231
59	-8.1788	-10.5125	-0.0000	30.0000	0.3625	0.4921
60	-9.1163	-10.5125	-0.0000	30.0000	0.3625	0.4867

Figure 23(b).- Continued.

61	-6.7223	-11.2375	-0.0000	30.0000	0.3625	0.7422
62	-7.6598	-11.2375	-0.0000	30.0000	0.3625	0.5034
63	-8.5973	-11.2375	-0.0000	30.0000	0.3625	0.4654
64	-9.5348	-11.2375	-0.0000	30.0000	0.3625	0.4551
65	-7.1409	-11.9625	-0.0000	30.0000	0.3625	0.7144
66	-8.0784	-11.9625	-0.0000	30.0000	0.3625	0.4715
67	-9.0159	-11.9625	-0.0000	30.0000	0.3625	0.4274
68	-9.9534	-11.9625	-0.0000	30.0000	0.3625	0.4140
69	-7.5595	-12.6875	-0.0000	30.0000	0.3625	0.6646
70	-8.4970	-12.6875	-0.0000	30.0000	0.3625	0.4230
71	-9.4345	-12.6875	-0.0000	30.0000	0.3625	0.3749
72	-10.3720	-12.6875	-0.0000	30.0000	0.3625	0.3616
73	-7.9781	-13.4125	-0.0000	30.0000	0.3625	0.5827
74	-8.9156	-13.4125	-0.0000	30.0000	0.3625	0.3487
75	-9.8531	-13.4125	-0.0000	30.0000	0.3625	0.3023
76	-10.7906	-13.4125	-0.0000	30.0000	0.3625	0.2934
77	-8.3967	-14.1375	-0.0000	30.0000	0.3625	0.4346
78	-9.3342	-14.1375	-0.0000	30.0000	0.3625	0.2290
79	-10.2717	-14.1375	-0.0000	30.0000	0.3625	0.1992
80	-11.2092	-14.1375	-0.0000	30.0000	0.3625	0.1977
FLAP VORTICES						
81	-4.4731	-0.3625	0.0217	28.2437	0.3687	0.9979
82	-5.5284	-0.3625	0.3817	28.2437	0.3687	0.9073
83	-6.5837	-0.3625	0.7417	28.2437	0.3687	0.6989
84	-7.6390	-0.3625	1.1017	28.2437	0.3687	0.7477
85	-8.6943	-0.3625	1.4617	28.2437	0.3687	0.4152
86	-4.8917	-1.0875	0.0217	28.2437	0.3687	1.0549
87	-5.9470	-1.0875	0.3817	28.2437	0.3687	0.9446
88	-7.0023	-1.0875	0.7417	28.2437	0.3687	0.7087
89	-8.0575	-1.0875	1.1017	28.2437	0.3687	0.7315
90	-9.1128	-1.0875	1.4617	28.2437	0.3687	0.3844
91	-5.3103	-1.8125	0.0217	28.2437	0.3687	1.0843
92	-6.3656	-1.8125	0.3817	28.2437	0.3687	0.9663
93	-7.4208	-1.8125	0.7417	28.2437	0.3687	0.7181
94	-8.4761	-1.8125	1.1017	28.2437	0.3687	0.7296
95	-9.5314	-1.8125	1.4617	28.2437	0.3687	0.3777
96	-5.7288	-2.5375	0.0217	28.2437	0.3687	1.1027
97	-6.7841	-2.5375	0.3817	28.2437	0.3687	0.9803
98	-7.8394	-2.5375	0.7417	28.2437	0.3687	0.7279
99	-8.8947	-2.5375	1.1017	28.2437	0.3687	0.7370
100	-9.9500	-2.5375	1.4617	28.2437	0.3687	0.3832
101	-6.1474	-3.2625	0.0217	28.2437	0.3687	1.1166
102	-7.2027	-3.2625	0.3817	28.2437	0.3687	0.9933
103	-8.2580	-3.2625	0.7417	28.2437	0.3687	0.7424
104	-9.3133	-3.2625	1.1017	28.2437	0.3687	0.7542
105	-10.3686	-3.2625	1.4617	28.2437	0.3687	0.3983
106	-6.5660	-3.9875	0.0217	28.2437	0.3687	1.1295
107	-7.6213	-3.9875	0.3817	28.2437	0.3687	1.0097
108	-8.6766	-3.9875	0.7417	28.2437	0.3687	0.7666
109	-9.7319	-3.9875	1.1017	28.2437	0.3687	0.7869
110	-10.7871	-3.9875	1.4617	28.2437	0.3687	0.4265
111	-6.9846	-4.7125	0.0217	28.2437	0.3687	1.1436
112	-8.0399	-4.7125	0.3817	28.2437	0.3687	1.0334
113	-9.0951	-4.7125	0.7417	28.2437	0.3687	0.8093
114	-10.1504	-4.7125	1.1017	28.2437	0.3687	0.8519
115	-11.2057	-4.7125	1.4617	28.2437	0.3687	0.4747
116	-7.4032	-5.4375	0.0217	28.2437	0.3687	1.1604
117	-8.4584	-5.4375	0.3817	28.2437	0.3687	1.0692
118	-9.5137	-5.4375	0.7417	28.2437	0.3687	0.8898
119	-10.5690	-5.4375	1.1017	28.2437	0.3687	1.0064
120	-11.6243	-5.4375	1.4617	28.2437	0.3687	0.5436

Figure 23(b).- Continued.

121	-7.8217	-6.1625	0.0217	28.2437	0.3687	1.1803
122	-8.8770	-6.1625	0.3817	28.2437	0.3687	1.1222
123	-9.9323	-6.1625	0.7417	28.2437	0.3687	1.0592
124	-10.9876	-6.1625	1.1017	28.2437	0.3687	1.6162
125	-12.0429	-6.1625	1.4617	28.2437	0.3687	0.5664
126	-8.2403	-6.8875	0.0217	28.2437	0.3687	1.2036
127	-9.2956	-6.8875	0.3817	28.2437	0.3687	1.1985
128	-10.3509	-6.8875	0.7417	28.2437	0.3687	1.5425
129	-11.4062	-6.8875	1.1017	28.2437	0.3687	1.3521
130	-12.4615	-6.8875	1.4617	28.2437	0.3687	0.5397
131	-8.6589	-7.6125	0.0217	28.2437	0.3687	1.2299
132	-9.7142	-7.6125	0.3817	28.2437	0.3687	1.3553
133	-10.7695	-7.6125	0.7417	28.2437	0.3687	1.4855
134	-11.8248	-7.6125	1.1017	28.2437	0.3687	1.3001
135	-12.8800	-7.6125	1.4617	28.2437	0.3687	0.5214
136	-9.0775	-8.3375	0.0217	28.2437	0.3687	1.2387
137	-10.1328	-8.3375	0.3817	28.2437	0.3687	1.2353
138	-11.1880	-8.3375	0.7417	28.2437	0.3687	1.4990
139	-12.2433	-8.3375	1.1017	28.2437	0.3687	1.2767
140	-13.2986	-8.3375	1.4617	28.2437	0.3687	0.5047
141	-9.4961	-9.0625	0.0217	28.2437	0.3687	1.2186
142	-10.5513	-9.0625	0.3817	28.2437	0.3687	1.1664
143	-11.6066	-9.0625	0.7417	28.2437	0.3687	1.0220
144	-12.6619	-9.0625	1.1017	28.2437	0.3687	1.5150
145	-13.7172	-9.0625	1.4617	28.2437	0.3687	0.4587
146	-9.9146	-9.7875	0.0217	28.2437	0.3687	1.1748
147	-10.9699	-9.7875	0.3817	28.2437	0.3687	1.0844
148	-12.0252	-9.7875	0.7417	28.2437	0.3687	0.8740
149	-13.0805	-9.7875	1.1017	28.2437	0.3687	0.8951
150	-14.1358	-9.7875	1.4617	28.2437	0.3687	0.4028
151	-10.3332	-10.5125	0.0217	28.2437	0.3687	1.1131
152	-11.3885	-10.5125	0.3817	28.2437	0.3687	1.0065
153	-12.4438	-10.5125	0.7417	28.2437	0.3687	0.7567
154	-13.4991	-10.5125	1.1017	28.2437	0.3687	0.7470
155	-14.5544	-10.5125	1.4617	28.2437	0.3687	0.3531
156	-10.7518	-11.2375	0.0217	28.2437	0.3687	1.0387
157	-11.8071	-11.2375	0.3817	28.2437	0.3687	0.9309
158	-12.8624	-11.2375	0.7417	28.2437	0.3687	0.6711
159	-13.9176	-11.2375	1.1017	28.2437	0.3687	0.6716
160	-14.9729	-11.2375	1.4617	28.2437	0.3687	0.3136
161	-11.1704	-11.9625	0.0217	28.2437	0.3687	0.9528
162	-12.2257	-11.9625	0.3817	28.2437	0.3687	0.8566
163	-13.2809	-11.9625	0.7417	28.2437	0.3687	0.6000
164	-14.3362	-11.9625	1.1017	28.2437	0.3687	0.6126
165	-15.3915	-11.9625	1.4617	28.2437	0.3687	0.2768
166	-11.5889	-12.6875	0.0217	28.2437	0.3687	0.8520
167	-12.6442	-12.6875	0.3817	28.2437	0.3687	0.7785
168	-13.6995	-12.6875	0.7417	28.2437	0.3687	0.5285
169	-14.7548	-12.6875	1.1017	28.2437	0.3687	0.5505
170	-15.8101	-12.6875	1.4617	28.2437	0.3687	0.2352
171	-12.0075	-13.4125	0.0217	28.2437	0.3687	0.7251
172	-13.0628	-13.4125	0.3817	28.2437	0.3687	0.6858
173	-14.1181	-13.4125	0.7417	28.2437	0.3687	0.4385
174	-15.1734	-13.4125	1.1017	28.2437	0.3687	0.4671
175	-16.2287	-13.4125	1.4617	28.2437	0.3687	0.1791
176	-12.4261	-14.1375	0.0217	28.2437	0.3687	0.5375
177	-13.4814	-14.1375	0.3817	28.2437	0.3687	0.5415
178	-14.5367	-14.1375	0.7417	28.2437	0.3687	0.2892
179	-15.5920	-14.1375	1.1017	28.2437	0.3687	0.3257
180	-16.6472	-14.1375	1.4617	28.2437	0.3687	0.0978

Figure 23(b).- Continued.

AERODYNAMIC LOADING RESULTS FOR ALPHA = 0.00000 DEG.

WING LIFT COEFFICIENT	FLAP LIFT COEFFICIENT
1.0918	2.7312
TOTAL LIFT COEFFICIENT,CL	**PITCHING MOMENT COEFFICIENT,CM**
3.8230	-2.5953

REFERENCE QUANTITIES

WING SPAN,B	WING PLANFORM AREA,SREF	WING AVE.CHORD,CAVE
29.0000	108.7500	3.7500

SPANWISE LOAD DISTRIBUTION

STATION	Y/(B/2)	LOCAL CHORD,C	CL*C/CL*CAVE	CL*C/(2*B)
WING				
1	0.0250	3.7500	0.7816	0.0552
2	0.0750	3.7500	0.8508	0.0601
3	0.1250	3.7500	0.9122	0.0644
4	0.1750	3.7500	0.9627	0.0680
5	0.2250	3.7500	1.0033	0.0708
6	0.2750	3.7500	1.0361	0.0731
7	0.3250	3.7500	1.0625	0.0750
8	0.3750	3.7500	1.0832	0.0765
9	0.4250	3.7500	1.0984	0.0775
10	0.4750	3.7500	1.1104	0.0784
11	0.5250	3.7500	1.1253	0.0794
12	0.5750	3.7500	1.1439	0.0807
13	0.6250	3.7500	1.1572	0.0817
14	0.6750	3.7500	1.1559	0.0816
15	0.7250	3.7500	1.1351	0.0801
16	0.7750	3.7500	1.0922	0.0771
17	0.8250	3.7500	1.0239	0.0723
18	0.8750	3.7500	0.9240	0.0652
19	0.9250	3.7500	0.7793	0.0550
20	0.9750	3.7500	0.5621	0.0397
FLAP				
1	0.0254	5.5750	0.7107	0.1255
2	0.0763	5.5750	0.7245	0.1279
3	0.1272	5.5750	0.7374	0.1302
4	0.1780	5.5750	0.7494	0.1323
5	0.2289	5.5750	0.7639	0.1349
6	0.2797	5.5750	0.7853	0.1387
7	0.3306	5.5750	0.8205	0.1449
8	0.3815	5.5750	0.8842	0.1561
9	0.4323	5.5750	1.6382	0.2893
10	0.4832	5.5750	2.0706	0.3656
11	0.5340	5.5750	2.1649	0.3823
12	0.5849	5.5750	1.9969	0.3526
13	0.6358	5.5750	1.5580	0.2751
14	0.6866	5.5750	0.8656	0.1529
15	0.7375	5.5750	0.7772	0.1372
16	0.7883	5.5750	0.7084	0.1251
17	0.8392	5.5750	0.6437	0.1137
18	0.8901	5.5750	0.5733	0.1012
19	0.9409	5.5750	0.4838	0.0854
20	0.9918	5.5750	0.3437	0.0607

CM,WING	CM,FLAP	CD,WING	CD,FLAP	CD	CD/CL*CL
0.25150	-2.84678	-0.08432	0.65771	0.57339	0.03923

Figure 23(b).- Continued.

VELOCITIES INDUCED AT SPECIFIED POINTS IN THE VICINITY OF THE WING

N	X	Y	Z	U/V	V/V	W/V
1	-1.7000	-7.2500	2.0700	0.06080	-0.02753	-0.09245
2	-3.7000	-7.2500	2.0700	0.12594	-0.06215	-0.10663
3	-5.7000	-7.2500	2.0700	0.19800	-0.09940	-0.06224
4	-7.7000	-7.2500	2.0700	0.26257	-0.12752	-0.00573
5	-9.7000	-7.2500	2.0700	0.37937	-0.16295	0.11820
6	-11.7000	-7.2500	2.0700	0.47324	-0.19667	0.47547
7	-13.7000	-7.2500	2.0700	0.25392	-0.08860	0.73498
8	-15.7000	-7.2500	2.0700	0.16644	-0.12091	0.61595

Figure 23(b).- Concluded.

Item 1: Format (20A4), any alphabetic or numeric information
(1 card)

Column No.	1-80
Program Variable	TITLE
Data	

Item 2: Format (6I5, F10.5), decimal point required for last variable
(1 card)

Column No.	5	10	15	20	25	30	40
Program Variable	NJET	NP	NCYL	NPRNT	KIN	KOUT	DS
Data							

Item 3: Format (5F10.5), decimal point required
(1 + NCYL ,cards)

Column No.	10	20	30	40	50
Program Variable	GAMVJ(J)	RJET(J)	XQ(J)	YQ(J)	ZQ(J)
Data					

Column No.	10	20	30	40	50
Program Variable	XCLR(J,1)	YCLR(J,1)	ZCLR(J,1)	RGR(J,1)	THETA(J,1)
Data					

Column No.	10	20	30	40	50
Program Variable	XCLR(J,N)	YCLR(J,N)	ZCLR(J,N)	RGR(J,N)	THETA(J,N)
Data					

where N = 1,2,...,NCYL

Note: Item 3 is repeated for each jet; J = 1,2,...,NJET

If KIN > 6, Item 4 is omitted; but, if KIN = 5, include the following cards.

Item 4: Format (3F10.5), decimal point required
(NP cards)

Column No.	10	20	30
Program Variable	XP(N)	YP(N)	ZP(N)
Data			

where N = 1,2,...,NP

Figure 24.- Input format for jet-wake program.

```
SOURCE OF EXTERNALLY INDUCED VELOCITIES,   ALPHA=0 DEGREES ,  C(MU)=0.9
   1  180     5     1     7     8    0.125
  2.46        1.25        0.46       -7.25        2.07
   0.0         0.0         0.0         1.0         0.0
  1.72         0.0         0.0         1.0         0.0
   8.5        -0.2        -0.3         1.5        -4.5
  15.3        -0.6        -0.8        1.97        -4.5
 150.0        -3.0        -5.0         9.5         0.0
SOURCE OF EXTERNALLY INDUCED VELOCITIES,   ALPHA=10 DEGREES ,  C(MU)=0.9
   1  180     5     0     7     8    0.125
  2.46        1.25        0.46       -7.25        2.07
   0.0         0.0         0.0         1.0         0.0
 -1.72         0.0         0.0         1.0         0.0
   8.5        -0.32       -0.10        1.5        -1.4
  15.3        -0.88       -0.26        1.97       -1.4
 150.0        -4.0        -2.0         9.5         0.0
```

(a) Input for single jet case, including use of data sets and optional output.

```
UNSWEPT WING  (NASA TN D-6222)  FLAP ANGLE = 17.5/35 , ALPHA = 0 , C(MU) = 5.5
   2   20     4     0     5     6    0.17
  4.61        1.70        6.96      -11.64        2.5
   0.0         0.0         0.0         1.0         3.0
  2.68         0.0         0.14        1.0         3.0
  13.4         0.0         0.70        2.0         3.0
 150.0         0.0         4.0        12.0         0.0
  4.61        1.70        6.96       -27.22        2.5
   0.0         0.0         0.0         1.0         3.0
  2.68         0.0         0.14        1.0         3.0
  13.4         0.0         0.70        2.0         3.0
 150.0         0.0         4.0        12.0         0.0
 -0.760      -2.82         0.0
 -1.773      -2.82         0.0
 -2.786      -2.82         0.0
 -3.799      -2.82         0.0
 -4.812      -2.82         0.0
 -5.825      -2.82         0.0
 -6.838      -2.82         0.0
 -7.851      -2.82         0.0
 -8.864      -2.82         0.0
 -9.877      -2.82         0.0
-10.722     -28.720        1.565
-11.950     -28.720        2.426
-10.722     -29.720        1.565
-11.950     -29.720        2.462
-10.722     -31.22         1.565
-11.950     -31.22         2.426
-10.722     -33.02         1.565
-11.950     -33.02         2.426
-10.722     -34.41         1.565
-11.950     -34.41         2.426
```

(b) Input for multiple jet case, including use of conventional input and output.

Figure 25.- Sample input to jet-wake program.

SOURCE OF EXTERNALLY INDUCED VELOCITIES. ALPHA=0 DEGREES , C(MU)=0.9

D(S)	KIN	KOUT
0.1250	7	8

(1) JET PARAMETERS D(S/R) = 0.1000

X/R	Y/R	Z/R	S/R	THETA	RGAM/R	R	XQ	YQ	ZQ	GAMMA/V
0.00	0.00	0.00	0.00	0.00	1.00	1.2500	0.460	-7.250	2.070	2.460
1.72	0.00	0.00	1.72	0.00	1.00					
8.50	-0.20	-0.30	8.51	-4.50	1.50					
15.30	-0.60	-0.80	15.34	-4.50	1.97					
150.00	-3.00	-5.00	150.13	0.00	9.90					

VELOCITIES INDUCED BY JET 1 - JET COORDINATE SYSTEM

N	XP/R	YP/R	ZP/R	U/V	V/V	W/V
1	1.098	5.510	1.656	2.0391E-03	-2.2873E-02	-6.8959E-03
2	1.848	5.510	1.656	1.6129E-04	-2.2063E-02	-6.6390E-03
3	2.598	5.510	1.656	-1.2063E-03	-2.0865E-02	-6.2502E-03
4	3.348	5.510	1.656	-2.0918E-03	-1.9542E-02	-5.8060E-03
5	1.433	4.930	1.656	3.3611E-04	-2.6174E-02	-8.8246E-03
6	2.183	4.930	1.656	-1.6543E-03	-2.4567E-02	-8.2609E-03
7	2.933	4.930	1.656	-2.8705E-03	-2.2720E-02	-7.5919E-03
8	3.683	4.930	1.656	-3.4909E-03	-2.0955E-02	-6.9228E-03
9	1.768	4.350	1.656	-2.2277E-03	-2.9530E-02	-1.1285E-02
10	2.518	4.350	1.656	-4.0104E-03	-2.6866E-02	-1.0226E-02
11	3.268	4.350	1.656	-4.7980E-03	-2.4324E-02	-9.1722E-03
12	4.018	4.350	1.656	-4.9669E-03	-2.2187E-02	-8.2301E-03
13	2.103	3.770	1.656	-5.7426E-03	-3.2453E-02	-1.4298E-02
14	2.853	3.770	1.656	-6.7992E-03	-2.8628E-02	-1.2527E-02
15	3.603	3.770	1.656	-6.7986E-03	-2.5527E-02	-1.1007E-02
16	4.353	3.770	1.656	-6.3568E-03	-2.3215E-02	-9.7701E-03
17	2.437	3.190	1.656	-9.9766E-03	-3.4238E-02	-1.7766E-02
18	3.187	3.190	1.656	-9.6276E-03	-2.9529E-02	-1.5133E-02
19	3.937	3.190	1.656	-8.5661E-03	-2.6259E-02	-1.3138E-02
20	4.687	3.190	1.656	-7.4462E-03	-2.4102E-02	-1.1636E-02
21	2.772	2.610	1.656	-1.4162E-02	-3.4213E-02	-2.1474E-02
22	3.522	2.610	1.656	-1.1909E-02	-2.9434E-02	-1.8037E-02
23	4.272	2.610	1.656	-9.7224E-03	-2.6609E-02	-1.5686E-02
24	5.022	2.610	1.656	-8.0289E-03	-2.5023E-02	-1.4022E-02
25	3.107	2.030	1.656	-1.7094E-02	-3.2205E-02	-2.5207E-02
26	3.857	2.030	1.656	-1.2992E-02	-2.8529E-02	-2.1361E-02
27	4.607	2.030	1.656	-9.9278E-03	-2.6835E-02	-1.8959E-02
28	5.357	2.030	1.656	-7.8992E-03	-2.6241E-02	-1.7361E-02
29	3.442	1.450	1.656	-1.7690E-02	-2.8865E-02	-2.9049E-02
30	4.192	1.450	1.656	-1.2427E-02	-2.7294E-02	-2.5588E-02
31	4.942	1.450	1.656	-8.9887E-03	-2.7209E-02	-2.3691E-02
32	5.692	1.450	1.656	-6.9391E-03	-2.7883E-02	-2.2602E-02
33	3.777	0.870	1.656	-1.5676E-02	-2.5218E-02	-3.4042E-02
34	4.527	0.870	1.656	-1.0204E-02	-2.5816E-02	-3.2043E-02
35	5.277	0.870	1.656	-6.9242E-03	-2.7186E-02	-3.1457E-02
36	6.027	0.870	1.656	-5.1680E-03	-2.8949E-02	-3.1548E-02
37	4.112	0.290	1.656	-1.1953E-02	-1.9936E-02	-4.2320E-02
38	4.862	0.290	1.656	-7.2162E-03	-2.1387E-02	-4.2341E-02
39	5.612	0.290	1.656	-4.2772E-03	-2.3080E-02	-4.3470E-02
40	6.362	0.290	1.656	-3.0488E-03	-2.5006E-02	-4.5128E-02
41	4.447	-0.290	1.656	-8.5923E-03	-7.5891E-03	-5.1245E-02
42	5.197	-0.290	1.656	-4.5946E-03	-8.4872E-03	-5.2345E-02
43	5.947	-0.290	1.656	-2.4600E-03	-9.3811E-03	-5.4356E-02
44	6.697	-0.290	1.656	-1.4756E-03	-1.0521E-02	-5.6877E-02
45	4.781	-0.870	1.656	-6.2014E-03	9.7228E-03	-5.1351E-02
46	5.531	-0.870	1.656	-3.2631E-03	9.4125E-03	-5.2381E-02
47	6.281	-0.870	1.656	-1.5477E-03	9.2532E-03	-5.4199E-02
48	7.031	-0.870	1.656	-9.3422E-04	8.8547E-03	-5.6587E-02
49	5.116	-1.450	1.656	-4.5941E-03	2.2050E-02	-4.2681E-02
50	5.866	-1.450	1.656	-2.4343E-03	2.1894E-02	-4.3339E-02
51	6.616	-1.450	1.656	-1.1601E-03	2.1951E-02	-4.4643E-02
52	7.366	-1.450	1.656	-7.9592E-04	2.1814E-02	-4.6523E-02
53	5.451	-2.030	1.656	-3.3636E-03	2.6992E-02	-3.2358E-02
54	6.201	-2.030	1.656	-1.8660E-03	2.6787E-02	-3.2760E-02
55	6.951	-2.030	1.656	-9.2253E-04	2.6788E-02	-3.3675E-02
56	7.701	-2.030	1.656	-6.4568E-04	2.6648E-02	-3.5081E-02
57	5.786	-2.610	1.656	-2.3922E-03	2.7463E-02	-2.3991E-02
58	6.536	-2.610	1.656	-1.3437E-03	2.7193E-02	-2.4275E-02
59	7.286	-2.610	1.656	-8.8351E-04	2.7117E-02	-2.4957E-02
60	8.036	-2.610	1.656	-4.6196E-04	2.6977E-02	-2.5994E-02

Figure 26.- Output from jet-wake program (single jet).

61	6.121	-3.190	1.656	-1.6225E-03	2.6023E-02	-1.7957E-02
62	6.871	-3.190	1.656	-9.1544E-04	2.5745E-02	-1.8194E-02
63	7.621	-3.190	1.656	-4.6646E-04	2.5635E-02	-1.8711E-02
64	8.371	-3.190	1.656	-3.1326E-04	2.5526E-02	-1.9451E-02
65	6.456	-3.770	1.656	-1.0345E-03	2.3978E-02	-1.3715E-02
66	7.206	-3.770	1.656	-5.8306E-04	2.3725E-02	-1.3917E-02
67	7.956	-3.770	1.656	-3.0549E-04	2.3612E-02	-1.4299E-02
68	8.706	-3.770	1.656	-2.1843E-04	2.3529E-02	-1.4807E-02
69	5.791	-4.350	1.656	-6.0354E-04	2.1869E-02	-1.0699E-02
70	7.541	-4.350	1.656	-3.3750E-04	2.1653E-02	-1.0863E-02
71	8.291	-4.350	1.656	-1.8943E-04	2.1545E-02	-1.1135E-02
72	9.041	-4.350	1.656	-1.6152E-04	2.1471E-02	-1.1474E-02
73	7.125	-4.930	1.656	-2.9580E-04	1.9894E-02	-8.5041E-03
74	7.875	-4.930	1.656	-1.6419E-04	1.9712E-02	-8.6298E-03
75	8.625	-4.930	1.656	-1.0761E-04	1.9608E-02	-8.8172E-03
76	9.375	-4.930	1.656	-1.3317E-04	1.9537E-02	-9.0374E-03
77	7.460	-5.510	1.656	-8.2246E-05	1.8110E-02	-6.8692E-03
78	8.210	-5.510	1.656	-4.3353E-05	1.7955E-02	-6.9604E-03
79	8.960	-5.510	1.656	-5.2318E-05	1.7856E-02	-7.0848E-03
80	9.710	-5.510	1.656	-1.1593E-04	1.7781E-02	-7.2225E-03
81	4.369	5.510	1.495	-2.8080E-03	-1.8110E-02	-4.7958E-03
82	5.213	5.510	1.207	-3.1461E-03	-1.7225E-02	-3.6463E-03
83	6.057	5.510	0.919	-3.3042E-03	-1.6356E-02	-2.5892E-03
84	6.901	5.510	0.631	-3.3582E-03	-1.5489E-02	-1.6321E-03
85	7.746	5.510	0.343	-3.3298E-03	-1.4602E-02	-7.8299E-04
86	4.703	4.930	1.495	-3.8775E-03	-1.9255E-02	-5.6355E-03
87	5.548	4.930	1.207	-4.0286E-03	-1.8322E-02	-4.2517E-03
88	6.392	4.930	0.919	-4.0669E-03	-1.7424E-02	-2.9886E-03
89	7.236	4.930	0.631	-4.0519E-03	-1.6491E-02	-1.8434E-03
90	8.080	4.930	0.343	-3.9665E-03	-1.5482E-02	-8.3637E-04
91	5.038	4.350	1.495	-4.9215E-03	-2.0375E-02	-6.6343E-03
92	5.883	4.350	1.207	-4.8828E-03	-1.9513E-02	-4.9812E-03
93	6.727	4.350	0.919	-4.8429E-03	-1.8652E-02	-3.4563E-03
94	7.571	4.350	0.631	-4.8107E-03	-1.7648E-02	-2.0620E-03
95	8.415	4.350	0.343	-4.6880E-03	-1.6449E-02	-8.4976E-04
96	5.373	3.770	1.495	-5.8376E-03	-2.1546E-02	-7.8549E-03
97	6.217	3.770	1.207	-5.6671E-03	-2.0927E-02	-5.8846E-03
98	7.062	3.770	0.919	-5.6542E-03	-2.0176E-02	-4.0064E-03
99	7.906	3.770	0.631	-5.6989E-03	-1.9040E-02	-2.2584E-03
100	8.750	3.770	0.343	-5.5467E-03	-1.7486E-02	-7.6624E-04
101	5.708	3.190	1.495	-6.5278E-03	-2.2930E-02	-9.4189E-03
102	6.552	3.190	1.207	-6.3629E-03	-2.2787E-02	-7.0580E-03
103	7.397	3.190	0.919	-6.5698E-03	-2.2224E-02	-4.6648E-03
104	8.241	3.190	0.631	-6.8583E-03	-2.0758E-02	-2.3503E-03
105	9.085	3.190	0.343	-6.6089E-03	-1.8500E-02	-4.5091E-04
106	6.043	2.610	1.495	-6.8913E-03	-2.4803E-02	-1.1578E-02
107	6.887	2.610	1.207	-6.9777E-03	-2.5506E-02	-8.7166E-03
108	7.731	2.610	0.919	-7.7992E-03	-2.5225E-02	-5.4740E-03
109	8.576	2.610	0.631	-8.5949E-03	-2.2858E-02	-2.0925E-03
110	9.420	2.610	0.343	-7.8285E-03	-1.9229E-02	4.3320E-04
111	6.378	2.030	1.495	-6.8482E-03	-2.7563E-02	-1.4899E-02
112	7.222	2.030	1.207	-7.5598E-03	-2.9827E-02	-1.1431E-02
113	8.066	2.030	0.919	-9.9061E-03	-3.0059E-02	-6.5894E-03
114	8.910	2.030	0.631	-1.1276E-02	-2.5106E-02	-6.9166E-04
115	9.755	2.030	0.343	-8.6615E-03	-1.9451E-02	2.7377E-03
116	6.713	1.450	1.495	-6.2836E-03	-3.1524E-02	-2.0762E-02
117	7.557	1.450	1.207	-8.1902E-03	-3.6987E-02	-1.6993E-02
118	8.401	1.450	0.919	-1.4448E-02	-3.8520E-02	-8.6848E-03
119	9.245	1.450	0.631	-1.2757E-02	-2.7359E-02	4.0333E-03
120	10.090	1.450	0.343	-8.0256E-03	-2.0358E-02	8.7195E-03

Figure 26.- Continued.

121	7.048	0.870	1.495	-5.0402E-03	-3.5520E-02	-3.2064E-02
122	7.892	0.870	1.207	-3.0614E-03	-4.7297E-02	-3.0816E-02
123	8.736	0.870	0.919	-2.8888E-02	-4.8448E-02	-8.6527E-03
124	9.585	0.870	0.632	1.5077E 00	-2.7968E-03	-7.7724E-02
125	10.424	0.870	0.343	1.5011E 00	-4.5142E-03	-8.8344E-02
126	7.382	0.290	1.495	-2.8240E-03	-3.3011E-02	-5.0909E-02
127	8.202	0.290	1.208	-7.1290E-03	-5.1663E-02	-6.3253E-02
128	9.071	0.290	0.919	1.5824E 00	-2.3233E-02	-7.7019E-02
129	9.915	0.290	0.631	1.5326E 00	-2.2715E-02	-8.1433E-02
130	10.759	0.290	0.343	1.4798E 00	-2.1599E-02	-8.6376E-02
131	7.717	-0.290	1.495	-1.9642E-03	-1.5031E-02	-6.7699E-02
132	8.608	-0.290	1.203	5.0867E-01	-3.0515E-02	-9.5502E-02
133	9.406	-0.290	0.919	1.5651E 00	-4.1419E-02	-7.4156E-02
134	10.250	-0.290	0.631	1.5110E 00	-4.0377E-02	-7.9623E-02
135	11.094	-0.290	0.343	1.4587E 00	-3.8089E-02	-8.4539E-02
136	8.052	-0.870	1.495	-2.1478E-03	9.5024E-03	-6.6667E-02
137	8.896	-0.870	1.207	-1.1516E-02	5.7506E-03	-7.9075E-02
138	9.741	-0.870	0.919	1.5434E 00	-6.0416E-02	-7.2407E-02
139	10.585	-0.870	0.631	1.4890E 00	-5.7518E-02	-7.8022E-02
140	11.429	-0.870	0.343	1.4372E 00	-5.3784E-02	-8.2672E-02
141	8.387	-1.450	1.495	-2.0813E-03	2.4040E-02	-5.2569E-02
142	9.231	-1.450	1.207	-3.2005E-03	2.7353E-02	-6.0675E-02
143	10.075	-1.450	0.919	-3.4866E-03	3.3227E-02	-7.1103E-02
144	10.967	-1.450	0.627	1.4602E 00	-7.4860E-02	-7.4821E-02
145	11.764	-1.450	0.343	1.4163E 00	-6.8781E-02	-8.0958E-02
146	8.722	-2.030	1.495	-1.1425E-03	2.8734E-02	-3.8241E-02
147	9.566	-2.030	1.207	-1.3384E-03	3.3651E-02	-4.1883E-02
148	10.410	-2.030	0.919	-8.6345E-04	4.0440E-02	-4.5477E-02
149	11.255	-2.030	0.631	-3.5204E-05	5.0177E-02	-4.8295E-02
150	12.099	-2.030	0.343	-4.0137E-04	6.2633E-02	-4.8540E-02
151	9.057	-2.610	1.495	-5.3472E-04	2.8738E-02	-2.7564E-02
152	9.901	-2.610	1.207	-4.8953E-04	3.2879E-02	-2.8639E-02
153	10.745	-2.610	0.919	-3.0809E-04	3.7937E-02	-2.9148E-02
154	11.589	-2.610	0.631	-3.5176E-05	4.4174E-02	-2.8644E-02
155	12.434	-2.610	0.343	2.5759E-04	5.1593E-02	-2.6521E-02
156	9.392	-3.190	1.495	-2.9058E-04	2.6913E-02	-2.0132E-02
157	10.236	-3.190	1.207	-2.2924E-04	2.9968E-02	-2.0028E-02
158	11.080	-3.190	0.919	-1.9707E-04	3.3448E-02	-1.9400E-02
159	11.924	-3.190	0.631	-2.6732E-04	3.7377E-02	-1.7986E-02
160	12.768	-3.190	0.343	-6.0065E-04	4.1655E-02	-1.5466E-02
161	9.726	-3.770	1.495	-2.1072E-04	2.4570E-02	-1.5002E-02
162	10.571	-3.770	1.207	-2.1352E-04	2.6747E-02	-1.4411E-02
163	11.415	-3.770	0.919	-3.0621E-04	2.9109E-02	-1.3410E-02
164	12.259	-3.770	0.631	-5.7661E-04	3.1600E-02	-1.1836E-02
165	13.103	-3.770	0.343	-1.1697E-03	3.4045E-02	-9.4877E-03
166	10.061	-4.350	1.495	-2.0687E-04	2.2231E-02	-1.1407E-02
167	10.905	-4.350	1.207	-2.7738E-04	2.3770E-02	-1.0644E-02
168	11.750	-4.350	0.919	-4.6391E-04	2.5361E-02	-9.5650E-03
169	12.594	-4.350	0.631	-8.3280E-04	2.6913E-02	-8.0655E-03
170	13.439	-4.350	0.343	-1.4799E-03	2.8223E-02	-6.0230E-03
171	10.396	-4.930	1.495	-2.2703E-04	2.0077E-02	-8.8339E-03
172	11.240	-4.930	1.207	-3.5444E-04	2.1154E-02	-8.0350E-03
173	12.085	-4.930	0.919	-5.9540E-04	2.2206E-02	-6.9952E-03
174	12.929	-4.930	0.631	-9.8509E-04	2.3133E-02	-5.6485E-03
175	13.773	-4.930	0.343	-1.5463E-03	2.3750E-02	-3.9366E-03
176	10.731	-5.510	1.495	-2.5058E-04	1.8152E-02	-6.9515E-03
177	11.575	-5.510	1.207	-4.1415E-04	1.8895E-02	-6.1800E-03
178	12.419	-5.510	0.919	-6.6881E-04	1.9569E-02	-5.2258E-03
179	13.264	-5.510	0.631	-1.0230E-03	2.0084E-02	-4.0535E-03
180	14.108	-5.510	0.343	-1.4529E-03	2.0308E-02	-2.6486E-03

Figure 26.- Continued.

WING COORDINATE SYSTEM N	XW	YW	ZW	U/V	V/V	W/V
1	-0.912	-0.362	-0.000	-2.0391E-03	-2.2873E-02	6.8959E-03
2	-1.850	-0.362	-0.000	-1.6129E-04	-2.2063E-02	6.6390E-03
3	-2.787	-0.362	-0.000	1.2063E-03	-2.0865E-02	6.2502E-03
4	-3.725	-0.362	-0.000	2.0918E-03	-1.9542E-02	5.8060E-03
5	-1.331	-1.087	-0.000	-3.3611E-04	-2.6174E-02	8.8246E-03
6	-2.268	-1.087	-0.000	1.6543E-03	-2.4567E-02	8.2609E-03
7	-3.206	-1.087	-0.000	2.8705E-03	-2.2720E-02	7.5919E-03
8	-4.143	-1.087	-0.000	3.4909E-03	-2.0955E-02	6.9228E-03
9	-1.750	-1.813	-0.000	2.2277E-03	-2.9530E-02	1.1285E-02
10	-2.687	-1.813	-0.000	4.0164E-03	-2.6866E-02	1.0226E-02
11	-3.625	-1.813	-0.000	4.7980E-03	-2.4324E-02	9.1722E-03
12	-4.562	-1.813	-0.000	4.9669E-03	-2.2187E-02	8.2301E-03
13	-2.168	-2.537	-0.000	5.7426E-03	-3.2453E-02	1.4298E-02
14	-3.106	-2.537	-0.000	6.7992E-03	-2.8628E-02	1.2527E-02
15	-4.043	-2.537	-0.000	6.7986E-03	-2.5527E-02	1.1007E-02
16	-4.981	-2.537	-0.000	6.3568E-03	-2.3215E-02	9.7701E-03
17	-2.587	-3.262	-0.000	9.9766E-03	-3.4238E-02	1.7766E-02
18	-3.524	-3.262	-0.000	9.6276E-03	-2.9529E-02	1.5133E-02
19	-4.462	-3.262	-0.000	8.5661E-03	-2.6259E-02	1.3138E-02
20	-5.399	-3.262	-0.000	7.4462E-03	-2.4102E-02	1.1636E-02
21	-3.005	-3.987	-0.000	1.4162E-02	-3.4213E-02	2.1474E-02
22	-3.943	-3.987	-0.000	1.1909E-02	-2.9434E-02	1.8037E-02
23	-4.880	-3.987	-0.000	9.7224E-03	-2.6609E-02	1.5686E-02
24	-5.818	-3.987	-0.000	8.0289E-03	-2.5023E-02	1.4022E-02
25	-3.424	-4.712	-0.000	1.7094E-02	-3.2205E-02	2.5207E-02
26	-4.361	-4.712	-0.000	1.2992E-02	-2.8529E-02	2.1361E-02
27	-5.299	-4.712	-0.000	9.9278E-03	-2.6835E-02	1.8959E-02
28	-6.236	-4.712	-0.000	7.8992E-03	-2.6241E-02	1.7361E-02
29	-3.842	-5.438	-0.000	1.7690E-02	-2.8865E-02	2.9049E-02
30	-4.780	-5.438	-0.000	1.2427E-02	-2.7294E-02	2.5588E-02
31	-5.717	-5.438	-0.000	8.9887E-03	-2.7209E-02	2.3691E-02
32	-6.655	-5.438	-0.000	6.9391E-03	-2.7883E-02	2.2602E-02
33	-4.261	-6.162	-0.000	1.5676E-02	-2.5218E-02	3.4042E-02
34	-5.199	-6.162	-0.000	1.0204E-02	-2.5816E-02	3.2043E-02
35	-6.136	-6.162	-0.000	6.9242E-03	-2.7186E-02	3.1457E-02
36	-7.074	-6.162	-0.000	5.1680E-03	-2.8949E-02	3.1548E-02
37	-4.680	-6.887	-0.000	1.1953E-02	-1.9936E-02	4.2320E-02
38	-5.617	-6.887	-0.000	7.2162E-03	-2.1387E-02	4.2341E-02
39	-6.555	-6.887	-0.000	4.2772E-03	-2.3080E-02	4.3470E-02
40	-7.492	-6.887	-0.000	3.0488E-03	-2.5006E-02	4.5128E-02
41	-5.098	-7.612	-0.000	8.5923E-03	-7.5891E-03	5.1245E-02
42	-6.036	-7.612	-0.000	4.5946E-03	-8.4872E-03	5.2345E-02
43	-6.973	-7.612	-0.000	2.4600E-03	-9.3811E-03	5.4356E-02
44	-7.911	-7.612	-0.000	1.4756E-03	-1.0521E-02	5.6877E-02
45	-5.517	-8.337	-0.000	6.2014E-03	9.7228E-03	5.1351E-02
46	-6.454	-8.337	-0.000	3.2631E-03	9.4125E-03	5.2381E-02
47	-7.392	-8.337	-0.000	1.5477E-03	9.2532E-03	5.4199E-02
48	-8.329	-8.337	-0.000	9.3422E-04	8.8547E-03	5.6587E-02
49	-5.935	-9.062	-0.000	4.5941E-03	2.2050E-02	4.2681E-02
50	-6.873	-9.062	-0.000	2.4343E-03	2.1894E-02	4.3339E-02
51	-7.810	-9.062	-0.000	1.1601E-03	2.1951E-02	4.4643E-02
52	-8.748	-9.062	-0.000	7.9592E-04	2.1814E-02	4.6523E-02
53	-6.354	-9.787	-0.000	3.3636E-03	2.6992E-02	3.2358E-02
54	-7.291	-9.787	-0.000	1.8660E-03	2.6787E-02	3.2760E-02
55	-8.229	-9.787	-0.000	9.2253E-04	2.6788E-02	3.3675E-02
56	-9.166	-9.787	-0.000	6.4568E-04	2.6648E-02	3.5081E-02
57	-6.773	-10.512	-0.000	2.3922E-03	2.7463E-02	2.3991E-02
58	-7.710	-10.512	-0.000	1.3437E-03	2.7193E-02	2.4275E-02

Figure 26.- Continued.

59	-8.648	-10.512	-0.000	6.8351E-04	2.7117E-02	2.4957E-02
60	-9.585	-10.512	-0.000	4.6196E-04	2.6977E-02	2.5994E-02
61	-7.191	-11.237	-0.000	1.6225E-03	2.6023E-02	1.7957E-02
62	-8.129	-11.237	-0.000	9.1544E-04	2.5745E-02	1.8194E-02
63	-9.066	-11.237	-0.000	4.6646E-04	2.5635E-02	1.8711E-02
64	-10.004	-11.237	-0.000	3.1326E-04	2.5526E-02	1.9451E-02
65	-7.610	-11.962	-0.000	1.0345E-03	2.3978E-02	1.3719E-02
66	-8.547	-11.962	-0.000	5.8306E-04	2.3725E-02	1.3917E-02
67	-9.485	-11.962	-0.000	3.0549E-04	2.3612E-02	1.4299E-02
68	-10.422	-11.962	-0.000	2.1843E-04	2.3529E-02	1.4807E-02
69	-8.028	-12.687	-0.000	6.0354E-04	2.1869E-02	1.0699E-02
70	-8.966	-12.687	-0.000	3.3750E-04	2.1653E-02	1.0863E-02
71	-9.903	-12.687	-0.000	1.8943E-04	2.1545E-02	1.1135E-02
72	-10.841	-12.687	-0.000	1.6152E-04	2.1471E-02	1.1474E-02
73	-8.447	-13.412	-0.000	2.9580E-04	1.9894E-02	8.5041E-03
74	-9.384	-13.412	-0.000	1.6419E-04	1.9712E-02	8.6298E-03
75	-10.322	-13.412	-0.000	1.0761E-04	1.9608E-02	8.8172E-03
76	-11.259	-13.412	-0.000	1.3317E-04	1.9537E-02	9.0374E-03
77	-8.865	-14.137	-0.000	8.2246E-05	1.8110E-02	6.8692E-03
78	-9.803	-14.137	-0.000	4.3353E-05	1.7955E-02	6.9604E-03
79	-10.740	-14.137	-0.000	5.2318E-05	1.7856E-02	7.0848E-03
80	-11.678	-14.137	-0.000	1.1593E-04	1.7781E-02	7.2225E-03
81	-5.001	-0.362	0.202	2.8080E-03	-1.8110E-02	4.7958E-03
82	-6.056	-0.362	0.562	3.1461E-03	-1.7225E-02	3.6463E-03
83	-7.111	-0.362	0.922	3.3042E-03	-1.6356E-02	2.5892E-03
84	-8.167	-0.362	1.282	3.3562E-03	-1.5489E-02	1.6321E-03
85	-9.222	-0.362	1.642	3.3298E-03	-1.4602E-02	7.8299E-04
86	-5.419	-1.087	0.202	3.8775E-03	-1.9255E-02	5.6355E-03
87	-6.475	-1.087	0.562	4.0286E-03	-1.8322E-02	4.2517E-03
88	-7.530	-1.087	0.922	4.0669E-03	-1.7424E-02	2.9886E-03
89	-8.585	-1.087	1.282	4.0519E-03	-1.6491E-02	1.8434E-03
90	-9.640	-1.087	1.642	3.9665E-03	-1.5482E-02	8.3637E-04
91	-5.838	-1.813	0.202	4.9215E-03	-2.0375E-02	6.6343E-03
92	-6.893	-1.813	0.562	4.8828E-03	-1.9513E-02	4.9812E-03
93	-7.948	-1.813	0.922	4.9429E-03	-1.8652E-02	3.4563E-03
94	-9.004	-1.813	1.282	4.8107E-03	-1.7648E-02	2.0620E-03
95	-10.059	-1.813	1.642	4.6880E-03	-1.6449E-02	8.4976E-04
96	-6.256	-2.537	0.202	5.8376E-03	-2.1546E-02	7.8549E-03
97	-7.312	-2.537	0.562	5.6671E-03	-2.0927E-02	5.8846E-03
98	-8.367	-2.537	0.922	5.6542E-03	-2.0176E-02	4.0064E-03
99	-9.422	-2.537	1.282	5.6989E-03	-1.9040E-02	2.2584E-03
100	-10.478	-2.537	1.642	5.5467E-03	-1.7486E-02	7.6624E-04
101	-6.675	-3.262	0.202	6.5278E-03	-2.2930E-02	9.4189E-03
102	-7.730	-3.262	0.562	6.3629E-03	-2.2787E-02	7.0580E-03
103	-8.786	-3.262	0.922	6.5698E-03	-2.2224E-02	4.6648E-03
104	-9.841	-3.262	1.282	6.8583E-03	-2.0758E-02	2.3503E-03
105	-10.896	-3.262	1.642	6.6089E-03	-1.8500E-02	4.5091E-04
106	-7.094	-3.987	0.202	6.8913E-03	-2.4803E-02	1.1578E-02
107	-8.149	-3.987	0.562	6.9777E-03	-2.5506E-02	8.7166E-03
108	-9.204	-3.987	0.922	7.7992E-03	-2.5225E-02	5.4740E-03
109	-10.259	-3.987	1.282	8.5949E-03	-2.2858E-02	2.0925E-03
110	-11.315	-3.987	1.642	7.8285E-03	-1.9229E-02	-4.3320E-04
111	-7.512	-4.712	0.202	6.8482E-03	-2.7563E-02	1.4899E-02
112	-8.568	-4.712	0.562	7.5598E-03	-2.9827E-02	1.1431E-02
113	-9.623	-4.712	0.922	9.9061E-03	-3.0059E-02	6.5894E-03
114	-10.678	-4.712	1.282	1.1276E-02	-2.5106E-02	6.9186E-04
115	-11.733	-4.712	1.642	8.6615E-03	-1.9451E-02	-2.7377E-03
116	-7.931	-5.438	0.202	6.2836E-03	-3.1524E-02	2.0762E-02
117	-8.986	-5.438	0.562	8.1902E-03	-3.6987E-02	1.6993E-02
118	-10.041	-5.438	0.922	1.4448E-02	-3.8520E-02	8.6848E-03
119	-11.097	-5.438	1.282	1.2757E-02	-2.7359E-02	-4.0333E-03

Figure 26.- Continued.

120	-12.152	-5.438	1.642	8.0256E-03	-2.0358E-02	-8.7195E-03
121	-8.349	-6.162	0.202	5.0402E-03	-3.5520E-02	3.2064E-02
122	-9.405	-6.162	0.562	8.0614E-03	-4.7297E-02	3.0816E-02
123	-10.460	-6.162	0.922	2.8888E-02	-4.8448E-02	8.6527E-03
124	-11.515	-6.162	1.282	-1.5077E 00	-2.7968E-03	7.7724E-02
125	-12.571	-6.162	1.642	-1.5011E 00	-4.5142E-03	8.8344E-02
126	-8.768	-6.887	0.202	2.8240E-03	-3.3011E-02	5.0909E-02
127	-9.823	-6.887	0.562	7.1290E-03	-5.1663E-02	6.3253E-02
128	-10.879	-6.887	0.922	-1.5824E 00	-2.3233E-02	7.7019E-02
129	-11.934	-6.887	1.282	-1.5326E 00	-2.2715E-02	8.1433E-02
130	-12.989	-6.887	1.642	-1.4798E 00	-2.1599E-02	8.6376E-02
131	-9.187	-7.612	0.202	1.9642E-03	-1.5031E-02	6.7699E-02
132	-10.242	-7.612	0.562	-5.0867E-01	-3.0515E-02	9.5502E-02
133	-11.297	-7.612	0.922	-1.5651E 00	-4.1419E-02	7.4156E-02
134	-12.352	-7.612	1.282	-1.5110E 00	-4.0377E-02	7.9623E-02
135	-13.408	-7.612	1.642	-1.4587E 00	-3.8089E-02	8.4539E-02
136	-9.605	-8.337	0.202	2.1478E-03	9.5024E-03	6.6667E-02
137	-10.660	-8.337	0.562	1.1516E-02	5.7506E-03	7.9075E-02
138	-11.716	-8.337	0.922	-1.5434E 00	-6.0416E-02	7.2407E-02
139	-12.771	-8.337	1.282	-1.4890E 00	-5.7518E-02	7.8022E-02
140	-13.826	-8.337	1.642	-1.4372E 00	-5.3784E-02	8.2672E-02
141	-10.024	-9.063	0.202	2.0813E-03	2.4040E-02	5.2569E-02
142	-11.079	-9.063	0.562	3.2005E-03	2.7353E-02	6.0675E-02
143	-12.134	-9.063	0.922	3.4866E-03	3.3227E-02	7.1103E-02
144	-13.190	-9.063	1.282	-1.4602E 00	-7.4860E-02	7.4821E-02
145	-14.245	-9.063	1.642	-1.4163E 00	-6.8781E-02	8.0958E-02
146	-10.442	-9.787	0.202	1.1425E-03	2.8734E-02	3.8241E-02
147	-11.498	-9.787	0.562	1.3384E-03	3.3651E-02	4.1883E-02
148	-12.553	-9.787	0.922	8.6345E-04	4.0440E-02	4.5477E-02
149	-13.608	-9.787	1.282	3.5204E-05	5.0177E-02	4.8295E-02
150	-14.663	-9.787	1.642	4.0137E-04	6.2633E-02	4.8540E-02
151	-10.861	-10.512	0.202	5.3472E-04	2.8738E-02	2.7564E-02
152	-11.916	-10.512	0.562	4.8953E-04	3.2879E-02	2.8639E-02
153	-12.971	-10.512	0.922	3.0809E-04	3.7937E-02	2.9148E-02
154	-14.027	-10.512	1.282	3.5176E-05	4.4174E-02	2.8644E-02
155	-15.082	-10.512	1.642	-2.5759E-04	5.1593E-02	2.6521E-02
156	-11.279	-11.237	0.202	2.9058E-04	2.6913E-02	2.0132E-02
157	-12.335	-11.237	0.562	2.2924E-04	2.9968E-02	2.0028E-02
158	-13.390	-11.237	0.922	1.9707E-04	3.3448E-02	1.9400E-02
159	-14.445	-11.237	1.282	2.6732E-04	3.7377E-02	1.7986E-02
160	-15.501	-11.237	1.642	6.0065E-04	4.1655E-02	1.5466E-02
161	-11.698	-11.962	0.202	2.1072E-04	2.4570E-02	1.5002E-02
162	-12.753	-11.962	0.562	2.1352E-04	2.6747E-02	1.4411E-02
163	-13.809	-11.962	0.922	3.0621E-04	2.9109E-02	1.3410E-02
164	-14.864	-11.962	1.282	5.7661E-04	3.1600E-02	1.1836E-02
165	-15.919	-11.962	1.642	1.1697E-03	3.4045E-02	9.4877E-03
166	-12.117	-12.687	0.202	2.0687E-04	2.2231E-02	1.1407E-02
167	-13.172	-12.687	0.562	2.7738E-04	2.3770E-02	1.0644E-02
168	-14.227	-12.687	0.922	4.6391E-04	2.5361E-02	9.5650E-03
169	-15.282	-12.687	1.282	8.3280E-04	2.6913E-02	8.0655E-03
170	-16.338	-12.687	1.642	1.4799E-03	2.8223E-02	6.0230E-03
171	-12.535	-13.412	0.202	2.2703E-04	2.0077E-02	8.8339E-03
172	-13.590	-13.412	0.562	3.5444E-04	2.1154E-02	8.0350E-03
173	-14.646	-13.412	0.922	5.9540E-04	2.2206E-02	6.9952E-03
174	-15.701	-13.412	1.282	9.9509E-04	2.3133E-02	5.6485E-03
175	-16.756	-13.412	1.642	1.5463E-03	2.3750E-02	3.9366E-03
176	-12.954	-14.137	0.202	2.5058E-04	1.8152E-02	8.9515E-03
177	-14.009	-14.137	0.562	4.1415E-04	1.8895E-02	6.1800E-03
178	-15.064	-14.137	0.922	6.6881E-04	1.9569E-02	5.2258E-03
179	-16.120	-14.137	1.282	1.0230E-03	2.0084E-02	4.0535E-03
180	-17.175	-14.137	1.642	1.4529E-03	2.0308E-02	2.6486E-03

Figure 26.- Concluded.

*U.S. GOVERNMENT PRINTING OFFICE: 1974-739-157/85

NATIONAL AERONAUTICS AND SPACE ADMINISTRATION
WASHINGTON, D.C. 20546

OFFICIAL BUSINESS
PENALTY FOR PRIVATE USE $300

SPECIAL FOURTH-CLASS RATE BOOK

POSTAGE AND FEES PAID
NATIONAL AERONAUTICS AND SPACE ADMINISTRATION
451

U.S.MAIL

POSTMASTER: If Undeliverable (Section 158 Postal Manual) Do Not Return

"The aeronautical and space activities of the United States shall be conducted so as to contribute . . . to the expansion of human knowledge of phenomena in the atmosphere and space. The Administration shall provide for the widest practicable and appropriate dissemination of information concerning its activities and the results thereof."

—NATIONAL AERONAUTICS AND SPACE ACT OF 1958

NASA SCIENTIFIC AND TECHNICAL PUBLICATIONS

TECHNICAL REPORTS: Scientific and technical information considered important, complete, and a lasting contribution to existing knowledge.

TECHNICAL NOTES: Information less broad in scope but nevertheless of importance as a contribution to existing knowledge.

TECHNICAL MEMORANDUMS: Information receiving limited distribution because of preliminary data, security classification, or other reasons. Also includes conference proceedings with either limited or unlimited distribution.

CONTRACTOR REPORTS: Scientific and technical information generated under a NASA contract or grant and considered an important contribution to existing knowledge.

TECHNICAL TRANSLATIONS: Information published in a foreign language considered to merit NASA distribution in English.

SPECIAL PUBLICATIONS: Information derived from or of value to NASA activities. Publications include final reports of major projects, monographs, data compilations, handbooks, sourcebooks, and special bibliographies.

TECHNOLOGY UTILIZATION PUBLICATIONS: Information on technology used by NASA that may be of particular interest in commercial and other non-aerospace applications. Publications include Tech Briefs, Technology Utilization Reports and Technology Surveys.

Details on the availability of these publications may be obtained from:

SCIENTIFIC AND TECHNICAL INFORMATION OFFICE

NATIONAL AERONAUTICS AND SPACE ADMINISTRATION

Washington, D.C. 20546